10.15774/PPKE.ITK.2021.004

Pázmány Péter Catholic University
Faculty of Information Technology and Bionics

Doctoral Thesis

Computational analysis of nonlinear uncertain systems

Author:
Péter Polcz

Thesis Advisor:
Dr. Gábor Szederkényi, DSc

A thesis submitted in partial fulfilment of the requirements for the degree of Doctor of Philosophy

in the

Roska Tamás Doctoral School of Sciences and Technology

2019

10.15774/PPKE.ITK.2021.004

Acknowledgements

I would like to express my gratitude to my thesis advisor, Prof. Gábor Szederkényi, who coordinated and helped my work tirelessly with endless patience.

I am also grateful to Prof. Balázs Kulcsár for the useful discussions and the opportunity to visit him and collaborate with him in Götheborg several times. Furthermore, I would like to say many thanks to Dr. Péni Tamás, whose suggestions proved to be essential during my work, especially before submitting a manuscript.

I would like to express my appreciation to Prof. Katalin Hangos, Prof. Peter Seiler, Dr. Bernadett Ács, and Dr. Dávid Csercsik for the useful discussions. I thank my doctoral fellows, especially Gergely Szlobodnyik and Gergely Sváb for the good conversations and the stimulating discussions. I say many thanks to my diligent students and my undergraduate friends, who motivated me continuously by their persistent interest in science.

I would like to convey my gratitude to my family for their endless patience and support in various fields of life during the last four years. I am also very grateful to Father Prof. Istán Pákozdi, who helped me in many ways during my doctoral studies.

I am grateful to the Roska Tamás Doctoral School for accepting and supporting me during my road to graduation. I would like to thank Mrs. Dr. Katinka Vida for helping my work with her caring maternal rigor.

I have to recognize that the supporting guardian hand of many others (who are not listed here) proved to be essential in these years. I say many thanks to all of them.

Last but not least, I am very grateful to the reviewers for their constructive comments.

Finally, I gratefully acknowledge the financial support of the following grants

- Ministry of Innovation and Technology through the New National Excellence Program scholarships (ÚNKP-18-3-I-PPKE-9, ÚNKP-19-3-I-PPKE-6, and ÚNKP-20-4-I-PPKE-41),
- European Union, co-financed by the European Social Fund (EFOP-3.6.3-VEKOP-16-2017-00002),
- National Research, Development, and Innovation Office (NKFIH) through grant OTKA-125739,
- Pázmány Péter Catholic University through the projects KAP16-71005-1.1-ITK, KAP17-61005-1.1-ITK, KAP17-63009-3.3-ITK, and KAP18-51005-1.1-ITK.

10.15774/PPKE.ITK.2021.004

Abstract

This thesis investigates optimization-based techniques for robustness and performance analysis of a wide class of nonlinear dynamical systems with parametric uncertainty. The dynamics are described by ordinary differential equations written in a linear fractional representation (LFR). To formulate convex Lyapunov-type stability certificates, Finsler's lemma is used with affine annihilators.

A generic modeling framework is proposed to solve a parameter-dependent linear matrix inequality (PD-LMI) constraint written in a rational (i.e., fraction of polynomials) form. Such a nonlinear parameter-dependent condition is an infinite dimensional problem in the sense that its feasibility should be tested in infinitely many parameter points. The linear fractional transformation (LFT) and Finsler's lemma are used to formulate a sufficient polytopic (i.e., affine) PD-LMI condition. Based on the duality of minimal generators and maximal annihilators, numerical methods are proposed to reduce both the dimension and the conservatism of the obtained sufficient polytopic constraint.

Furthermore, robust stability and dissipativity analysis is addressed for nonlinear rational models. The Lyapunov/storage function candidate is searched as rational function of the state and parameter. The Lyapunov conditions for robust stability as well as the dissipativity constraint are rational scalar inequalities. The proposed relaxation techniques are able to cope with and find a solution for these typically infinite-dimensional problems. In order to perform local analysis, the Lyapunov-type certificates are prescribed only on a compact polytopic subset of the extended state and parameter space. Convex boundary conditions are formulated to expand the unitary level set of the Lyapunov function as much as possible. The size of each boundary (PD-LMI) condition is reduced in an unconventional way. The proposed dissipativity analysis method is able to compute a tight upper-bound for the induced $\mathcal{L}_2$ norm of a nonlinear model or a linear parameter-varying (LPV) system with rational parameter dependence. Convex conditions are proposed to compute a passivating output projection law to a rational LPV system and to check its feedback equivalence to a strictly passive LPV system.

Illustrative examples are used to demonstrate the applicability of the proposed method and compare against existing solutions in the literature. A robust stability domain is computed for a simple disease model and a Lotka-Volterra system with a parameter-varying equilibrium point. A continuous fermentation process model is considered with a stabilizing proportional or integral substrate feedback law. Finally, a 3-dimensional invariant domain is computed for the inverted pendulum balancing system with a simple nonlinear state feedback. To evaluate the proposed $\mathcal{L}_2$-gain computation technique a conservative quasi-LPV model is considered for the pendulum-cart system. Stable dynamic inversion of the pendulum-cart system is presented as an application example of the passivating output projection synthesis.

10.15774/PPKE.ITK.2021.004

Contents

10.15774/PPKE.ITK.2021.004

10.15774/PPKE.ITK.2021.004

10.15774/PPKE.ITK.2021.004

Basic notions, notations and symbols

In this thesis, the following notations are used:

$\mathbb{R}$, $\mathbb{C}$	denote the set of reals and complex values, respectively.
$\mathbb{R}^n$	n-dimensional Euclidean space
I_n	$n \times n$ unit matrix
0_n	$n \times n$ zero matrix
$0_{n\times m}$	$n \times m$ zero matrix
$\mathbf{1}_n$	$n \times n$ matrix, in which all elements are 1
$\mathbf{1}_{n\times m}$	$n \times m$ matrix, in which all elements are 1.
$I, 0, \mathbf{1}$	The dimensions in the subscripts of I_n, 0_n, $0_{n\times m}$, $\mathbf{1}_n$, $\mathbf{1}_{n\times m}$ are suppressed whenever they are obvious or irrelevant, e.g., $\left(\begin{smallmatrix} I_n & 0 \\ 0 & 0_{m_1\times m_2}\end{smallmatrix}\right)$ denotes the same matrix as $\left(\begin{smallmatrix} I_n & 0_{n\times m_2} \\ 0_{m_1\times n} & 0_{m_1\times m_2}\end{smallmatrix}\right)$.
$A^\top$	transpose of matrix $A \in \mathbb{R}^{n\times m}$, therefore, $A^\top \in \mathbb{R}^{m\times n}$
$\mathrm{He}\{A\}$	stands for $A^\top + A$, where $A \in \mathbb{R}^{n\times n}$
$\mathrm{Tr}\{A\}$	denotes the trace of a square matrix $A = \left(\begin{smallmatrix} a_{11} & \dots & a_{1n} \\ \dots & \dots & \dots \\ a_{n1} & \dots & a_{nn}\end{smallmatrix}\right) \in \mathbb{R}^{n\times n}$, $\mathrm{Tr}\{A\} = \sum_{i=1}^n a_{ii}$.
$\mathrm{Ker}(A)$	kernel space of matrix $A \in \mathbb{R}^{n\times m}$, i.e., $\mathrm{Ker}(A) = \{v \in \mathbb{R}^m \mid Av = 0\}$.
$\mathrm{Im}(A)$	image space of matrix $A \in \mathbb{R}^{n\times m}$, i.e., $\mathrm{Im}(A) = \{w \in \mathbb{R}^n \mid \exists v \in \mathbb{R}^m$ such that $w = Av\}$.
$\|A\|_\mathrm{F}$	denotes the Frobenius norm of matrix $A \in \mathbb{R}^{n\times m}$, $\|A\|_\mathrm{F} = \sqrt{\mathrm{Tr}\{A^\top A\}}$. mixed multiplication property
$A \otimes B$	Kronecker tensor product of matrices $A \in \mathbb{R}^{n\times m}$ and B, namely, $$A \otimes B = \left(\begin{smallmatrix} A_{11}B & \dots & A_{1m}B \\ \dots & & \dots \\ A_{n1}B & \dots & A_{nm}B\end{smallmatrix}\right). \quad (1)$$ Let $A \in \mathbb{R}^{n_1\times n_2}$, $B \in \mathbb{R}^{m_1\times m_2}$, $C \in \mathbb{R}^{n_2\times n_3}$, $D \in \mathbb{R}^{m_2\times m_3}$, then, the so-called mixed multiplication property $$(A \otimes B) \cdot (C \otimes D) = (A \cdot C) \otimes (B \cdot D) \quad (2)$$ of the Kronecker tensor product holds.
$\mathrm{diag}(\dots)$	$\mathrm{diag}(A_1, \dots, A_n)$ denotes $\left(\begin{smallmatrix} A_1 & \dots & 0 \\ \dots & \dots & \dots \\ 0 & \dots & A_n\end{smallmatrix}\right)$.
$A \succ 0$	matrix A is positive definite
$A \succeq 0$	matrix A is positive semidefinite
$A \prec 0$	matrix A is negative definite
$A \preceq 0$	matrix A is negative semidefinite

10.15774/PPKE.ITK.2021.004

$A^\dagger$ — left pseudo inverse of the full column-rank matrix $A \in \mathbb{R}^{n\times m}$ $(n \geq m)$, namely, $A^\dagger = (A^\top A)^{-1}A^\top \in \mathbb{R}^{m\times n}$, thus $A^\dagger A = I_m$.

$A^\perp$ — the rows of matrix $A^\perp \in \mathbb{R}^{(n-m)\times n}$ is an orthonormal basis for the kernel space of matrix $A^\top$ (i.e., $A^\perp A = 0_{(n-m)\times m}$), where $A \in \mathbb{R}^{n\times m}$.

$\mathcal{X}^\circ$ — denotes the interior of a compact set $\mathcal{X}$.

$\partial\mathcal{X}$ — $\partial\mathcal{X} = \mathcal{X} \setminus \mathcal{X}^\circ$ denotes the set of boundary points of a compact set $\mathcal{X}$.

$\mathbf{Co}(H)$ — denotes the convex hull of set $H \subset R^n$, e.g., $H = \{v_1, \ldots, v_m\} \subset \mathbb{R}^n$, then $\mathbf{Co}(H) = \{v = \sum_{i=1}^m \alpha_i v_i \in \mathbb{R}^n \,|\, \sum_{i=1}^m \alpha_i = 1\}$. H is said to be the set of vertices of set $\mathbf{Co}(H)$.

polytope — $\mathcal{X} = \mathbf{Co}(\{v_1, \ldots, v_{n_\mathcal{X}}\}) \subset \mathbb{R}^n$ is called a polytope in $\mathbb{R}^n$.
Let $U = (v_1 \ \ldots \ v_{n_\mathcal{X}}) \in \mathbb{R}^{n\times n_\mathcal{X}}$. If $\operatorname{rank} U = n$ (i.e., $\{v_1, \ldots, v_{n_\mathcal{X}}\}$ is a generator system in $\mathbb{R}^n$), $\mathcal{X}$ is compact and is called a full-dimensional polytope in $\mathbb{R}^n$. If $\operatorname{rank} U = r < n$, then $\mathcal{X}$ is an r-dimensional polytopic submanifold in $\mathbb{R}^n$ and is said to be a "compact" polytope in the submanifold $\mathcal{U} = \{v = \sum_{i=1}^{n_\mathcal{X}} \alpha_i v_i \in \mathbb{R}^n \,|\, \alpha_i \in \mathbb{R}\}$ of $\mathbb{R}^n$. Throughout the thesis, polytopes are denoted by calligraphic letters, e.g., $\mathcal{X}$, $\mathcal{P}$, $\mathcal{R}$, $\mathcal{W}$. Note that the kth facets $\mathcal{F}_k$, $k = 1, \ldots, m_\mathcal{X}$ of a full-dimensional polytope $\mathcal{X} \in \mathbb{R}^n$ is an $(n-1)$-dimensional polytopic submanifold in $\mathbb{R}^n$. Integers $n_\mathcal{X}$ and $m_\mathcal{X}$ denote the number of corner points and the number of facets, respectively, of polytope $\mathcal{X}$.

$\mathbf{Ve}(\mathcal{X})$ — denotes the set of vertices of polytope $\mathcal{X}$,
e.g., $\mathbf{Ve}(\mathbf{Co}(v_1, \ldots, v_{n_\mathcal{X}})) = \{v_1, \ldots, v_{n_\mathcal{X}}\}$.

$\bigtimes_{i=1}^{n} H_n$ — is the Cartesian product $H_1 \times \cdots \times H_n$ of sets H_n.

$\mathbf{Gr}(\mathcal{P}, \ldots)$ — denotes a gridding of rectangular set $\mathcal{P} = \bigtimes_{i=1}^{n_p} [\underline{p}_i, \overline{p}_i]$, namely,

$$\mathbf{Gr}(\mathcal{P}, K_1 \times \ldots \times K_{n_p}) = \bigtimes_{i=1}^{n_p} \left\{ \underline{p}_i + (\overline{p}_i - \underline{p}_i)\tfrac{k-1}{K_i-1} \,\middle|\, k = 1, \ldots, K_i \right\}. \quad (3)$$

$x, y, z, p,$ u, v, w (signals) — are multidimensional signals $(x : [0,\infty) \to \mathbb{R}^{n_x}, \ldots, w : [0,\infty) \to \mathbb{R}^{n_w})$. The dimension of the signal values are denoted by n_x, n_y, n_z, n_p, n_u, n_v, n_w, respectively, corresponding to the name of the signal. For simplicity, dimension of signal x is denoted by n when it is possible. Though, the values of signals in time instant t are denoted by $x(t)$, $\ldots$, $w(t)$, the time argument (t) is often suppressed (as it is commonly done in the literature) and only used when it is necessary.

$\frac{\mathrm{d}x}{\mathrm{d}t} = \dot{x}$ — is the time-derivative of signal x.

$x, p, \dot{p} = \varrho,$ w (independent variables) — $x \in \mathbb{R}^{n_x}$, $p \in \mathbb{R}^{n_p}$, or $w \in \mathbb{R}^{n_w}$ is often used as independent variables and not the value of a signal at time t. The context or the element containment relations ("$x \in \mathbb{R}^{n_x}$") will clarify how to interpret symbols x, p, etc. On the other hand, variable $\varrho \in \mathbb{R}^{n_p}$ is used as a replacement for $\dot{p} \in \mathbb{R}^{n_p}$ whenever it should be considered an independent variable.

$\frac{\partial V}{\partial x_i}$ — is the partial derivative of function $V : \mathbb{R}^{n_x} \to \mathbb{R}$ with respect to variable x_i.

10.15774/PPKE.ITK.2021.004

$\frac{\partial V}{\partial x}$, $\frac{\partial V}{\partial p}$ — $\frac{\partial V}{\partial x} : \mathbb{R}^{n_x+n_p} \to \mathbb{R}^{1\times n_x}$, $\frac{\partial V}{\partial p} : \mathbb{R}^{n_x+n_p} \to \mathbb{R}^{1\times n_p}$ denote the gradient row vector of the continuously differentiable function $V : \mathbb{R}^{n_x+n_p} \to \mathbb{R}$ with respect to variables $x = (x_1 \ \dots \ x_{n_x})^\top \in \mathbb{R}^{n_x}$ and $p = (p_1 \ \dots \ p_{n_p}) \in \mathbb{R}^{n_p}$, respectively. The value of function $\frac{\partial V}{\partial x}$ in (x, p) is denoted by $\frac{\partial V}{\partial x}(x, p)$.

∇H — $\nabla H = (\frac{\partial H}{\partial x})^\top : \mathbb{R}^n \to \mathbb{R}^n$ denotes the gradient of function $H : \mathbb{R}^n \to \mathbb{R}$.

$\frac{\partial f}{\partial x}$ — $\frac{\partial f}{\partial x} : \mathbb{R}^{n_x} \to \mathbb{R}^{n_x\times n_x}$, denotes the Jacobian matrix of the continuously differentiable mapping $f : \mathbb{R}^{n_x} \to \mathbb{R}^{n_x}$ with respect to variables $x = (x_1 \ \dots \ x_{n_x})^\top \in \mathbb{R}^{n_x}$.

operations without function arguments — Consider well-defined functions $A, B, C, D : \mathbb{R}^{n_x} \to \mathbb{R}^{m_1\times m_2}$ and constant matrix $E \in \mathbb{R}^{n_x\times m_1}$, then, let $M = \begin{pmatrix} (A+B)C^\top & D \\ x^\top E & 0_{1\times m_2} \\ 0_{m_2\times m_1} & I_{m_2} \end{pmatrix}$ denote that function $M : \mathbb{R}^{n_x} \to \mathbb{R}^{(m_1+m_2+1)\times(m_1+m_2)}$ satisfies

$$M(x) = \begin{pmatrix} (A(x)+B(x))C^\top(x) & D(x) \\ x^\top E & 0_{1\times m_2} \\ 0_{m_2\times m_1} & I_{m_2} \end{pmatrix} \text{ for all } x \in \mathbb{R}^{n_x}. \tag{4}$$

Furthermore, let "$A^\top A \succeq 0$ on $\mathcal{X}$" denote the fact that $A^\top(x)A(x) \succeq 0$ for all $x \in \mathcal{X} \subset \mathbb{R}^{n_x}$. We use this abuse of notations typically in large matrix compositions, where the parameter arguments would significantly increase the size of the equations.

$u \equiv 0$ — Let $u : [0, \infty) \to \mathbb{R}^{n_u}$. Then, $u \equiv 0$ denotes that $u(t) = 0$ for all $t \geq 0$.

$V(t)$=$V(x(t))$ — For simplicity, the composite functions often inherit the name of the outer function, e.g., $V \circ x$ is referred to as V, and $V(t) = V(x(t))$, where $V : \mathbb{R}^n \to \mathbb{R}$ and $x : \mathbb{R} \to \mathbb{R}^n$.

$\check{V}(x, p, \varrho)$ — denotes the value in (x, p, ϱ) of the Lie derivative of the scalar-valued function $V : \mathbb{R}^{n_x+n_p} \to \mathbb{R}$ with respect to $\dot{x} = f(x, p)$ and $\dot{p} = \varrho$, namely, $\check{V}(x, p, \varrho) = \frac{\partial V}{\partial x}(x, p)f(x, p) + \frac{\partial V}{\partial p}(x, p)\varrho$, where ϱ is considered as an independent variable.

well-defined rational functions — Function $f : \mathcal{X} \to \mathbb{R}^{m_1\times m_2}$ is called a *well-defined rational function* on polytope $\mathcal{X}$ if it is Lipschitz continuous in $\mathcal{X} \subseteq \mathbb{R}^{n_x}$ and has a rational (i.e., fraction of polynomials) algebraic form. Namely, $f(x)$ can be given as the following sum:

$$f(x) = f_0 + \sum_{j=1}^{J} \frac{q_{1j}(x)}{q_{2j}(x)} f_j,$$

where $f_0, f_j \in \mathbb{R}^{m_1\times m_2}$ and q_{1j}, q_{2j} are polynomials with $q_{2j}(x) \geq \varepsilon$ for all $j = 1, \dots, J$ and for some $\varepsilon > 0$.

$\pi, \pi_b, \pi_c,$ $\pi_d, \widehat{\pi}_d,$ etc. — are rational vector-valued functions, their dimensions are denoted by m, m_b, m_c, m_d, m'_d, respectively.

$\Pi, \Pi_c, \Pi_d,$ $\widehat{\Pi}_d$, etc. — are rational matrix-valued functions having m, m_c, m_d, m'_d number of rows, respectively.

monic — a polynomial is said to be *monic* if its leading coefficient is 1.

10.15774/PPKE.ITK.2021.004

Abbreviations

CT continuous-time

DT discrete-time

SDP semidefinite program/problem

LMI linear matrix inequality

LF Lyapunov function

SF storage function

PD parameter-dependent

PD-LMI parameter-dependent linear matrix inequality

LFT linear fractional transformation

LFR linear fractional representation

MIMO multiple input multiple output

LTI linear time-invariant

LTV linear time-varying

LPV linear parameter-varying

qLVP quasi-linear parameter-varying

DOA domain of attraction

rDOA robust domain of attraction

RSD robust stability domain

IQC integral quadratic constraints

SOS sum of squares

KYP Kalman-Yakubovich-Popov (lemma, property)

UIO unknown input observer

PS Positivstellensatz

ODE ordinary differential equation

GSS generalized state-space

10.15774/PPKE.ITK.2021.004

Chapter 1

Introduction

All scientific knowledge to which man owes his role as master of the world arose from playful activities.
/Konrad Lorenz/

Dynamical models allow us to understand and effectively influence (control) physical, biological and social processes taking place in the world. In practice, we usually have uncertain and often nonlinear models that are difficult to analyse and control. Fortunately, the availability of complex computational tools and the new theoretical results provide new opportunities for dealing with uncertain nonlinear systems. This thesis presents new numerical methods to perform stability, performance, and passivity analysis of nonlinear uncertain dynamical systems. The three analysis tasks are related to different engineering problems, namely, domain of attraction estimation, disturbance attenuation analysis, and dynamic invertibility, respectively. Nevertheless, these problems connect at the level of the more general theory of dissipativity, which provides a common computational framework for system analysis.

Stability analysis allows to estimate the secure operating domain of a safety-critical system, like a nuclear reactor, but also of a Segway. For instance, a Segway vehicle is in balance if the passenger is standing vertically. When the passenger leans forward, the motor of the Segway tries to balance the vehicle by moving forward with a given velocity. As the power of the Segway's motor is limited, the vehicle will tumble down if the inclination angle is too large. The *domain of attraction* (DOA) determines a safe interval for the inclination angle, from which the motor has enough power to balance the vehicle.

The induced $\mathcal{L}_2$ norm of a dynamical model is one possible quantitative descriptor of the input-output behaviour. This metric is of potential interest when a system operates in an environment where the environmental factors change frequently. For example, the *induced $\mathcal{L}_2$-gain* of a suspension system can quantify the expected vibration of a vehicle in the function of the road's quality. Accordingly, we also call this metric the *disturbance attenuation level*.

The passivity property ensures many advantageous features of a dynamical system. It can be shown that an unknown disturbance input applied to the system can be asymptotically reconstructed if the system can be strictly passivated with a state feedback, so to say, if the system is *feedback strictly passive*. Although the open loop model may be unstable, the feedback strict passivity property guarantees an *asymptotically stable zero dynamics*, which is an essential condition for many *fault detection and isolation* techniques.

The analysis, filtering, and control of nonlinear uncertain models are all challenging tasks in nonlinear systems and control theory. Often, these problems require the solution of nonlinear parameter-dependent algebraic or matrix equality/inequality constraints. To solve these typically non-convex problems, different convex relaxation approaches are available in the literature. Some of these techniques give only an approximate solution of the nonlinear problem. Other approaches formulate convex sufficient conditions to find a (conservative) solution for the nonlinear problem.

1.1 Contributions and layout of the thesis

In this dissertation, I present a new optimization-based numerical methodology to address different nonlinear problems in the field of analysis and filtering of a wide class of nonlinear uncertain systems.

The thesis consists of 9 chapters and an Appendix. The main scientific contributions corresponding to the 3 different thesis points are presented in Chapters 5-8. These four chapters begin with a problem statement, where the goals are formulated, and each chapter ends with a summary, where the conclusions are drawn. The layout of the thesis and the main scientific contributions are described below.

Chapter 1. I review the literature of DOA estimation, induced $\mathcal{L}_2$-gain and passivity techniques. Furthermore, I revise the existing convex linear matrix inequality (LMI) techniques in robust and nonlinear control theory.

Chapter 2. Two motivating nonlinear physical systems are presented here.

Chapter 3. I summarize important notions, definitions, and known results in the field of dissipativity theory of nonlinear systems, semidefinite programming (SDP), linear parameter-varying (LPV) modeling with linear fractional transformation (LFT), and Finsler's lemma. These results and notions will be used throughout the work.

Chapter 4. I present few recent (or still popular) results, which serve as possible reference solutions in the comparative evaluation of my approach.

Chapter 5. I propose efficient computer algebra and numerical methods to model and solve rational parameter-dependent constraints in a convex computational framework. Based on the preliminary results of Trofino and Dezuo (2013), I formulated sufficient Lagrange-type LMIs to solve *infinite-dimensional constraints*. To reduce both the dimension and the conservatism of the LMIs, I introduced the duality of minimal generators and maximal annihilators. The proposed methodology is applied in the next chapters to address different system analysis problems.

Chapter 6. I present an improved computational method to estimate the robust domain of attraction of nonlinear uncertain systems. I illustrate the method on multiple process system models. Finally, I computed a 3-dimensional stability domain for the inverted pendulum balancing system using its dynamically extended rational model.

Chapter 7. I propose a new approach to compute a local upper-estimate of the induced $\mathcal{L}_2$ operator norm of a locally stable nonlinear input-output system. The proposed approach is also applicable for global performance estimation of LPV systems with rational parameter dependence.

Chapter 8. I prove advantageous properties of feedback passive LPV systems. I formulate convex constraints to test feedback passivity of an LPV model, and to

synthesize a structured passivating output to a stable LPV model. I illustrate the applicability of my approach through a hypothetical bench-mark problem.

Chapter 9. I list the theses of my dissertation, and I mention a few possible directions for future research.

Appendix A. I provide a few additional details here.

In the following three sections, we revise some basic results related to DOA estimation, $\mathcal{L}_2$-gain, and passivity techniques. Then, convex LMI relaxation techniques are explored in Section 1.4 to perform analysis and filtering tasks for nonlinear uncertain and LPV systems.

1.2 Domain of attraction estimation

Finding or at least approximating the DOA of a locally stable equilibrium point of a nonlinear dynamical system is an important but also a non-trivial task in model analysis and controller design/evaluation. A (positively) invariant stability domain is often determined as an appropriate level set of a local Lyapunov function.

Numerical approximation of Massera's construction. In the literature, several numerical DOA approximation results are available, which are based on converse Lyapunov theorems [2] such as Massera's construction [1]. Many successor Massera-type approaches [3–8] provide a Lyapunov function in the form of a line integral, which can be numerically approximated along the system's solutions. These approaches often involves discretization of both the state-space (spacial) and the dynamics (temporal).

Iterative solutions of Zubov's equation. It is well-known that the DOA of an asymptotically stable equilibrium point of a nonlinear dynamical system can be precisely determined in theory by solving Zubov's first order nonlinear partial differential equation [9]. There exist several generalizations of Zubov's method, such as [10; 11]. The former is dedicated to determine the *robust* domain of attraction (rDOA) of an uncertain nonlinear system with a bounded perturbation. In this field, a fundamental result is the existence of the so-called maximal Lyapunov functions for a wide class of nonlinear systems and the corresponding (simplified) partial differential equation, which characterizes them [12]. In comparison with Zubov's equation, an iterative procedure is given for approximating the maximal *rational* Lyapunov function. In [13], maximal Lyapunov functions were defined and computed for hybrid (piecewise nonlinear) systems. Although the above mentioned nonlinear (rational) structures are advantageous for DOA computation, they are less attractive from a computational point of view.

The optimization-based approaches, see, e.g., [14–16], consider a preliminarily structured parameterized Lyapunov function candidate, which is defined as a composition of elementary functions and free decision variables. Then, the free variables are meant to be found such that the function satisfies a set of sufficient Lyapunov-type certificates, which are formulated as convex constraints, typically LMIs. Other approaches, like [17; 18], are seeking for a piecewise affine Lyapunov function by solving a linear program.

For nonlinear discrete-time systems, specifically, further approaches exist, e.g., an analytical Lyapunov-like solution is proposed in [19] by introducing the so-called G-functions. For convergence analysis of DT dynamical systems, the authors of [20–22] used the Banach fixed-point principle together with the contraction mapping theorem. At the same time, there exist alternative simulation-guided approaches (which are different from

Massera's construction), for example, the authors of [23; 24] prescribed linear constraints obtained from the execution traces of the dynamics in discrete sample points.

Point-like attractors. Computational Lyapunov function research puts the primary focus on dynamical systems with a single locally stable equilibrium point in the origin. Therefore, the nonzero point-like attractive equilibrium solution are generally translated to the origin to perform DOA estimation. In [5; 6], important results are available on the Lyapunov function construction for dynamical models with multiple (not necessarily point-like) local attractors.

1.3 Induced $\mathcal{L}_2$-gain and passivity techniques

The importance of feedback passivity of a dynamical system has been recognized in the literature [25] due its advantageous properties related to stable zero dynamics (minimum phase property), and internal stability. These system properties give rise to stable input-output linearization of nonlinear (possibly uncertain) systems [25; 26], and provide stable dynamic inversion [27]. Several inversion-based fault diagnosis results are available for minimum phase LPV systems [28–33]. As another advantage of passivity property is that it allows unknown input reconstruction by computing only the first derivative of the output vector.

On the other hand, it is natural in many control problems to involve finite-energy signals in the analysis, and target induced $\mathcal{L}_2$-gain to measure the effect of a disturbance signal on the output of the system. This metric can be quantified for a wide range of dynamical systems, linear or nonlinear problems [34], therefore, the induced $\mathcal{L}_2$-gain analysis is of potential interest for applications, e.g., in transport [35], aerospace [36], or renewable energy industry [37; 38].

In general systems theory, the small-gain theorem and the passivity results have a central role in dynamical analysis and control, with a particular importance in interconnection-based techniques [25; 39–41]. Passivity-based global asymptotic stabilization of a wide class of dynamical (possibly interconnected) systems can be found in [26; 40–44]. Important passivity-based stability conditions for feedback systems are introduced in [45] for linear time-varying (LTV) systems.

As it was observed by Li and Zhao [46], there is a strong relationship between passivity and finite $\mathcal{L}_2$ performance level. Van der Schaft [39, Proposition 4.2.1] showed that strict output passivity implies finite $\mathcal{L}_2$-gain. What is more, passivity and finite $\mathcal{L}_2$-gain property of a dynamical system are both special cases of dissipativity with respect to different supply rate functions [39]. Also, the Lyapunov condition for stability is again a special case of the dissipation inequality with the zero supply rate.

It is not surprising that many $\mathcal{L}_2$-gain and passivity approaches are based on the dissipativity relation, where a so-called storage function is needed to be computed. An alternative formulation of the dissipation inequality for passivity is given by the Kalman-Yakubovich-Popov (KYP) properties [25; 26].

In the general case of nonlinear systems, the dissipativity relation is a nonlinear state- and parameter-dependent inequality constraint, that cannot be solved in a convex computational framework. There exists an extended literature related to optimization-based stability, passivity, and $\mathcal{L}_2$ performance analysis as-well-as robust controller synthesis for a wide class of nonlinear uncertain systems. In the following section, we present in detail the main computational approaches to account for nonlinear analysis and synthesis problems.

1.3.1 Passivating output selection for a stable zero dynamics

Independently of the internal stability of a dynamical system, a fortunate selection of the output can render a stable zero dynamics [25; 26]. The output should be selected such that the number of independent output signals matches the number of independent input signals. Furthermore, the system with the new output should be *feedback passive*, namely, there exists a full state feedback law such that the closed-loop model with the selected output is passive.

In the case of general nonlinear uncertain systems (but even for linear parameter varying models) finding such on output is not trivial. Sepulchre et al. [42] stated that "many passivation attempts are frustrated by the requirements that the system must have a relative degree one and be weakly minimum phase."

A recursive differential geometrical technique is proposed by Sepulchre et al. [41; 42] to compute a passivating state feedback law and output for a special class of nonlinear systems. The nth order dynamic equations should be written as a cascade interconnection of an $(n-r)$th order input-affine model and an rth order integrator chain, where r is the relative degree of the system with respect to a given (initial) output. Their technique was successfully applied by Astolfi et al. [47] on a magnetic suspension system, however, these highly nonlinear structures are less attractive from the computational point of view. In the case of a general nonlinear system, a state transformation mapping should be found to recast the dynamics into the required structured normal form. As an alternative solution, a simple linear output selection technique was proposed by Szederkényi et al. [48] by using a linear quadratic regulator design [49, Section 3.5.4].

Port-Hamiltonian systems. The passivity framework naturally arises in circuit theory [50], and hence in the theory of port-Hamiltonian systems [51]. Arghir [52] introduced important passivity-based techniques for complex power networks modeled by Hamiltonian control systems, e.g., a zero dynamics refinement is presented in [52, Chapter 3] by using an output transformation. Furthermore, specific feedback passivation is addressed in [52, Chapter 4].

Output selection for local stabilization. In the literature (e.g., [41; 42; 46–48; 52–59]), a passivating output selection is principally motivated by local asymptotic stabilization through input-output linearization [27, Section 4.4]. At the same time, a passivating output provides a stable unknown input reconstruction [29]. Moreno [60], e.g., proved strong relationships in the LTI framework between passivity properties and the existence of an unknown input observer. For general input affine nonlinear systems, this strong relationship is not maintained [61].

1.4 LMI approaches

The use of LMI/SDP techniques in control theory has become very popular due to their advantageous properties and the availability of efficient numerical tools to solve LMI problems [62–64].

In the context of linear uncertain systems, important results are available [62–69]. The introduction of LFT to the theory of linear time-invariant (LTI) systems constituted a crucial step in the late '80s [66; 67]. The LFT/LMI methodology "unified many concepts and generalized transfer functions and their state-space realizations to include uncertainty" [67]. However, it is still not straightforward to extend these results to the class of nonlinear parametric models.

LPV modeling serves as an intermediate step, which "fills in the gap" between LTI and nonlinear uncertain systems. This powerful modeling framework was gradually developed by [70–76]. LPV principles are widely used in system analysis and controller design [35; 36; 77], due to their ability to represent a wide class of nonlinear systems, while preserving the advantageous properties of linear structures. Several polytopic results are available in the literature to handle affine or switched LPV models [55; 62; 78–84].

The grid-based approach have gained wide popularity in control applications (see, e.g., [38]) as it provides an easy-to-use methodology, when the polytopic solutions are not applicable. To obtain an *approximate solution* for a general nonlinear problem, the authors of [73–75] suggested to evaluate and solve the emerging nonlinear constraints over a finite set of state and parameter grid points. This approach requires not only a fine enough gridding policy but often results in large and computationally demanding SDP.

Representing rational functions with LFT can be considered as the next step towards a unified framework to cope with general parametric uncertainty [85–88] and nonlinearity [89; 90]. LFT allows to recast a rational nonlinear parameter-dependent model as a feedback interconnection of a LTI system and a static state- and parameter-dependent diagonal block. In this way, the nonlinear and parameter-dependent part of the system equation is separated from the dynamics as an artificial feedback loop. The authors of [85–90] considered a quadratic Lyapunov function, and defined convex conditions for stability analysis and state feedback design for rational nonlinear and LPV systems. Differently from the grid-based approximation, these approaches result in a possibly conservative but *guaranteed* solution for the nonlinear problem.

Low order LFT modeling. The dimension and the accuracy of the derived stability conditions may be prone to LFT factorization. Therefore, in [91] a minimal linear fractional representation (LFR) is suggested for polynomial equations. Furthermore, a Kalman-like numeric n-dimensional order reduction (n-DOR) method [92] and different symbolic low-order LFT modeling techniques [93] are available to yield a *relative-minimal* realization [94] of a rational expression. These symbolic and numeric procedures are implemented in the Enhanced LFR-Toolbox for Matlab [95] and in the Generalized State Space (GSS) Library [96] of the SMAC Toolbox [97].

In the following subsections, we revise a few advanced LMI relaxation techniques from the last two decades related to analysis, filtering, and controller synthesis of nonlinear uncertain systems.

1.4.1 Multiplier approaches with integral quadratic constraints

In parallel with the progressive development of the LFT techniques, an advanced robust analysis and synthesis approach was emerging, that made extensive use of *integral quadratic constraints* (IQC) and the so-called *multipliers* [98; 99].

The IQC-theory is a general framework, which is able to cope with a wide class of nonlinear, uncertain, but also time-delayed models. Starting from the results of Megretski and Rantzer [99], the basic IQC concept has gained a special interest in the robust control theory, and many generalizations/extensions are now available (see, e.g., [100–110]). Moreover, Seiler [111] presented important theoretical results about IQC in relation with the dissipation theory.

Analysis with rate bounded parameters. As IQC approach is based on frequency-domain considerations [106], it formulates frequency-domain conditions for stability. In

order to generate equivalent time-domain LMIs, the well-known KYP lemma [98; 99] is used. In the case of LPV systems, the obtained time-domain LMI conditions are parameter-dependent. To solve the dissipativity relation, Scherer [100] used the full block S-procedure, and formulated convex conditions, in which the bounds of the parameter's derivative are not considered. Compared to [100], the authors of [103; 104] considered dynamic multipliers and used the swapping lemma [102, Section 1.5] to cope with parameter rate bounds during the analysis. Two possible implementations of the IQC-analysis technique is proposed in [112; 113].

Dissipativity relation in the IQC-framework. Seiler [111] showed that a class of IQC multipliers has so-called J-spectral factorization, which allows to formulate IQC stability constraints in the dissipativity framework. However, the IQC approach of [103; 104] with dynamic multipliers do not generate a Lyapunov/storage function directly as the stability criteria are formulated in the frequency-domain. Though, the dynamic multiplier corresponds to a parameter-dependent storage function [112], it is not straightforward to obtain the exact structure of the storage function from the IQC solution. Nevertheless, there exist other multiplier approaches where a storage function is involved naturally in the analysis.

A multiplier approach with quadratic separators and a specific augmented model representation is proposed by Iwasaki and Shibata [114] to check the global stability of LPV/LFT systems. This approach brings about three major advantageous features. First, the time-domain LMI conditions for stability generated by the KYP lemma are already parameter independent. Second, the system model is augmented with the parameter's dynamics, hence, the rate bounds of the parameter signals are taken into account. Finally, the resulting parameter-dependent Lyapunov function can be obtained naturally by considering the linear fractional representation of the system equations.

One drawback of the multiplier approach, in general, is that the finally obtained LMI condition for stability should be tested over a set characterized by infinitely many inequalities [100; 103; 114]. As a possible solution, a so-called D-G scaling is used, e.g., in [105; 114], which may introduced further conservatism into the solution.

1.4.2 Descriptor approach

The theory of LTI descriptor systems can be attributed to Luenberger's name [115], and it dates back to the late '70s. Nonetheless, a general dissipativity theory for descriptor models was founded only in the mid '90s [116; 117], simultaneously with the appearance of the robust control approaches for uncertain LTI descriptor models [118–120]. Finally, the past twenty years of research emerged a novel methodology, which allows efficient dissipativity analysis and controller synthesis for a wide class of liner uncertain and/or parameter-varying systems.

Though it operates on the seemingly narrow class of affine LPV models, the strength of the approach constitutes in the ability to represent any LPV model in the LFR form. The authors of [121–125] used the extension of the bounded real lemma [116] to test stability and compute an upper bound on the $\mathcal{L}_2$-gain for this class of LTI and LPV descriptor systems. Masubuchi et al. [123; 125] formulated nonlinear parameter-dependent LMI (PD-LMI) conditions, which can be solved by a specific LMI relaxation technique proposed by the same author [126; 127]. The nonlinearity in these PD-LMIs is in the form of products of two multi-affine parameter-dependent terms.

In this methodology, as in the case of the IQC theory, the proposed PD-LMI constraint

is the KYP reformulation of a frequency-domain stability criterion in the form of an IQC. Therefore, a major drawback of this approach is the concealed structure of the storage function.

1.4.3 Polynomial approaches

Compared to the methods reviewed so far, a relatively different line of research is related to the polynomial techniques and the sum of square (SOS) approach, see, e.g. [128; 129]. For rational or polynomial parameter-dependent nonlinear models, the SOS method can account for DOA estimation [15; 130–135], system analysis [136–139], and controller synthesis [14; 140–149].

A dissipativity-based synthesis method is proposed in [148; 149], by measuring of the passivity indices with SOS constraints. Pirkelmann et al. [147] used SOS approach to computationally check the central assumption (strict dissipativity) of the model predictive control methods presented in [151; 152]. Wu and Prajna [141] proposed SOS-based analysis and synthesis methods for a class of LPV models. In [136–139], homogeneous polynomial solutions are investigated for the robust stability analysis of autonomous LPV systems. It is worth remarking that [139] gives necessary and sufficient conditions for the robust stability of rational autonomous LPV systems.

The main mathematical apparatus behind the SOS techniques is the *positive locus theorem* or, as it is commonly called, the *Positivstellensatz* (PS), which was introduced by Stengle [153]. PS is considered an important result in the real algebraic geometry. A detailed description of PS can be found in [14]. Using PS, one can formulate sophisticated set containment constraints related to the specific level sets of different multivariate scalar functions. The SOS techniques give a computational framework to solve PS conditions. [143; 144], As the PS constraints should be satisfied on the whole extended state and parameter space, the obtained solutions may be conservative. Chesi [133] and Yang and Wu [145] introduced polynomial Lagrange multipliers into the scalar inequality constraints to reduce the conservatism of the solution.

Though the SOS algorithm is promising [14; 15] and its expansion to rational systems is possible, it is computationally heavy and may require bilinear [133] or iterative LMI algorithms to obtain a disturbance attenuation level [146].

1.4.4 Polytopic approach with Finsler's lemma and affine annihilators

The most closely related results for stability and dissipativity analysis of rational parameter-dependent nonlinear systems are presented in [16; 149; 150; 154–159], where Finsler's lemma [160] is borrowed to address DOA computation, performance estimation, and dissipativity-based robust nonlinear controller design.

For DOA estimation, an LMI approach is presented in [154] together with Finsler's lemma to construct polynomial Lyapunov functions for discrete-time nonlinear systems with parametric uncertainties. Trofino and Dezuo [16] considered rational state- and parameter-dependent Lyapunov functions and used affine annihilators to generate sufficient LMI conditions ensuring local stability for uncertain rational continuous-time (CT) systems. The Lyapunov conditions are required to be fulfilled only within a bounded polytopic subset of the state-space, therefore, it is enough to check the feasibility of the obtained LMIs only in the corner points of the polytope. Trofino and Dezuo [16] primarily focus on the fundamental theory of DOA computation using Finsler's lemma. Therefore, there is a room for the further study of the automatic generation of the set of

rational functions contained in the Lyapunov function and that of the corresponding annihilator. Based on [16], finite-time stability of nonlinear quadratic systems is addressed in [161] by using polynomial Lyapunov functions.

Induced $\mathcal{L}_2$-gain and passivity with Finsler's lemma. Coutinho et al. [155; 156] performed induced $\mathcal{L}_2$ norm estimation and robust nonlinear controller synthesis for rational uncertain nonlinear systems. By the introduction of an admissible disturbance set, the authors of [155; 156] gave a local interpretation of the computed upper bound for the induced $\mathcal{L}_2$ norm. Following the concepts of [16; 156], a passivity-based static/dynamic output feedback controller design is proposed in [149; 150] for rational nonlinear models. Uncertainty or time-varying parameter dependency are not considered in the system equations, and no systematic design is proposed in [149; 150] to compute rational parameter-dependent storage functions.

As a Lagrange multiplier approach, Finsler's lemma with affine annihilators is an efficient relaxation technique to solve PD-LMI conditions. Though the nonlinear parameter-dependent terms are pulled out from the LMI, their algebraic interdependence is implicitly injected into the LMI condition through an affine annihilator accompanied by a free matrix Lagrange multiplier (notion introduced by [160]). It is already shown in [150] that Finsler's lemma with affine annihilators have advantageous properties compared to the SOS approach for rational nonlinear inequality conditions.

In the last decade, some preliminary model construction and dimension reduction techniques were developed for the Finsler's lemma-based control optimization problems. With some restrictions on the structure of the storage function, a systematic construction of the differential-algebraic representation needed by Finsler's lemma can be found in [156; 158; 159]. In [156], a systematic model construction procedure is presented for the quadratic performance estimation with a fourth-order polynomial storage function candidate. In [158; 159], quadratic storage/Lyapunov functions are searched with affine parameter dependence to solve robust stability conditions in an automated manner for rational descriptor LPV systems using LFT. In order to reduce the dimension of the PD-LMI, [158; 159] proposed to solve the parameter independent part of the PD-LMI conditions separately.

1.5 Motivation and contributions

The grid-based approach, the LFT techniques, the multiplier results, the theory descriptor systems, the polynomial methods, and finally, the polytopic approaches with affine annihilators, are all relaxation techniques to solve robust and nonlinear control problems. However, the main methodological questions related to the Lyapunov-based solutions for rational nonlinear (or LPV) systems can still be improved in terms of conservatism, computational tractability, transparency, automation, and applicability to other problems in the passivity framework.

In this dissertation, I contribute to the former set of results, which are based on a polytopic approach with affine annihilators and Finsler's lemma. The major contributions of this thesis compared to the state-of-the-art solutions are the following:

(Automation) Compared to [16; 156], a *systematic* construction method is found to designate a parameter-dependent Lyapunov/storage function candidate. Furthermore, the required (constant, affine, or even multi-affine) annihilators are computed *automatically*, which makes the approach applicable to difficult nonlinear dynamical

models.

(Computational tractability) Compared to

- the computationally heavy iterative solutions of Zubov's equation [12],
- the recursive differential geometrical techniques to find a passivating output [41; 42],
- or the often bilinear Lyapunov-type SOS certificates [162],

a simple computational framework is developed, which preserves *convexity* (finite number of convex constraints), and at the same time provides *dimension reduction features* without compromising the solution's accuracy.

(Conservatism) A major focus is put on the *rich algebraic structure* of the candidate function and on *maximal annihilators*, which together provide an appropriate parameterization of the problem and *reduce conservatism* relatively to the available state-of-the-art optimization-based solutions.

(Transparency) Differently from

- the converse Lyapunov techniques, where a Lyapunov function is approximated numerically through solving a line integral,
- or the IQC and descriptor approaches, where the storage function is concealed in the soft IQC constraints,

the solution is given as a *direct Lyapunov method*, where the Lyapunov function is searched in a *closed* parameterized *form*.

(Passivating output selection) Differently, from the existing feedback passivating output selection attempts [41; 42; 48; 52; 60], the PD-LMI approach is capable to cope with the *nonlinear KYP equality/inequality* constraint for a *general LPV/LFT model*, such that the output function is searched in a *structure* form.

(Multiple attractors) Differently from the mainstream DOA computation research, where the point-like attractors are located in the origin, the proposed approach provides the possibility to generalize the computations for *multiple attractive equilibria* or *limit cycles*.

1.6 Hardware and software environment

The results presented in this dissertation were computed in the Matlab environment. For symbolic computations, I applied Matlab's built-in Symbolic Math Toolbox based on Mupad. To compute and manipulate the linear fractional representation (LFR) of a rational matrix function, I used the Enhanced LFR-toolbox for Matlab [95; 163] and the GSS Library [96] of the SMAC Toolbox [97]. To model and solve semidefinite programming (SDP) problems, I used YALMIP [164] with three different SDP solvers. Primarily, I used Mosek solver [165], then, SeDuMi [166–168], and SDPT3 [169] solvers are used to check the obtained solution if necessary. To solve systems of ordinary differential equations (ODEs), I used the Matlab's built-in 4th and 5th order adaptive explicit Runge-Kutta implementation [170] (`ode45`), unless it is stated otherwise. The computations were processed on a PC with Intel Core i7-4710MQ CPU at 2.50GHz and 16GB of RAM.

10.15774/PPKE.ITK.2021.004

Chapter 2

Motivational examples

Dynamical models with a rational parameter or state dependence cover a wide class of nonlinear and/or time-varying systems. To demonstrate the wide applicability of the proposed approaches, we consider the highly nonlinear inverted pendulum balancing system, which constitutes the primary benchmark physical example of this dissertation. After a detailed model description of the pendulum-cart system, a bioreactor model is presented in Section 2.2.

2.1 The pendulum-cart system

The Euler-Lagrange equations of the inverted pendulum balancing system of [34, Section 1.3] are:

$$\begin{cases} I\dot{\omega} = mg\ell\sin\theta - m\ell^2\dot{\omega} - m\ell\dot{v}\cos\theta, \\ M\dot{v} = F - m\Big(\dot{v} + \ell\dot{\omega}\cos\theta - \ell\omega^2\sin\theta\Big) - bv, \end{cases} \tag{2.1}$$

where M [kg] is the mass of the cart, m [kg] is the mass of the rod, the length of the rod is 2ℓ [n], and b [kg/s] is the friction coefficient. The moment of inertia of the rod rotating about the lower end (forced to the pivot) is $I = \frac{4}{3}m\ell^2$. The state variable v [m/s] is the velocity of the cart, θ [rad] is the angle of the rod with respect to the vertical axis, $\dot{\theta} = \omega$ [rad/s] is the angular velocity of the rod. Angle θ is measured clockwise and $\theta = 0$ when the pendulum is pointing upwards. Signal F [N] is an external force (input) applied to the cart acting parallelly to the cart's horizontal motion. The motion of the system is sketched in Figure 2.1.

The dynamic equations in (2.1), can be altered into the following state-space representation:

$$\dot{x} = f(x) + g(x)u, \text{ with } x = \begin{pmatrix} v & \theta & \omega \end{pmatrix}^\top, \ u = F, \tag{2.2a}$$

$$f(x) = \frac{1}{\sigma_2(\theta)}\begin{pmatrix} m\ell\sigma_1\omega^2\sin\theta - b\sigma_1 v - m^2 g\,\ell^2\sin\theta\cos\theta \\ \omega\sigma_2(\theta) \\ (m+M)mg\ell\sin\theta + mb\ell v\cos\theta - m^2\ell^2\omega^2\sin\theta\cos\theta \end{pmatrix}, \ g(x) = \frac{1}{\sigma_2(\theta)}\begin{pmatrix} \sigma_1, \\ 0 \\ -m\ell\cos\theta, \end{pmatrix},$$

where

$$\sigma_1 = I + m\ell^2, \ \sigma_2(\theta) = \sigma_1(m+M) - m^2\ell^2\cos^2\theta. \tag{2.2b}$$

This system has a stable equilibrium point when the rod is pointing downwards ($v = 0$, $\theta = (2k+1)\pi$, $\omega = 0$, $k \in \mathbb{Z}$), and an unstable equilibrium point when the rod is pointing upwards ($v = 0$, $\theta = 2k\pi$, $\omega = 0$, $k \in \mathbb{Z}$). Obviously, this system has multiple stable and unstable equilibria as its dynamical equations are periodic with respect to the pendulum's angle θ.

10.15774/PPKE.ITK.2021.004

Figure 2.1: A sketch of the inverted pendulum balancing system (left) and the illustration of its potential application in the Segway balancing (middle) and the aircraft landing problem (right). The sources of the middle and right figures are [179] and [180], respectively.

In the literature, different variants of model (2.2) were considered as benchmark examples for several control design techniques, see, e.g., [48; 171–177]. In [175], the authors also guaranteed a wide domain of attraction $(-\frac{\pi}{2}, \frac{\pi}{2})$ for θ if $v(0) = \omega(0) = 0$. On the other hand, the simple one degree-of-freedom pendulum-cart system (2.1) serves as a starting point for multiple control engineering problems [178], see, e.g., the Segway balancing of [179] or the rocket landing problem addressed in the master's thesis [180].

In this thesis, we do not address the synthesis of an advanced control feedback law for (2.2). Instead, we analyse the behaviour of the system (2.2), when a simple but possibly nonlinear feedback $u(\theta)$ is considered.

Note that the dynamical model (2.2) contains trigonometric terms in θ, however, the proposed computational techniques require rational models. In the following two subsections, we describe the pendulum-cart dynamics (2.2) by rational models. First, we give a dynamically equivalent nonlinear (but rational) time-invariant model. Secondly, we propose a conservative qLPV model by encapsulating the nonlinear terms of (2.2) in parameters.

2.1.1 Rational input-affine model

In order to embed the pendulum-cart dynamics into a rational model, we follow the techniques of [181; 182]. We introduce the following two auxiliary state variables:

$$z_3 = \sin\theta \text{ and } z_4 = 1 - \cos\theta. \tag{2.3}$$

Variables z_3 and z_4 are interdependent through the identity $z_3^2 + (1 - z_4)^2 = 1$. The dynamics of z_3 and z_4 are:

$$\begin{cases} \dot{z}_3 = \dot{\theta}\cos\theta = \omega(1 - z_4), \\ \dot{z}_4 = \dot{\theta}\sin\theta = \omega z_3. \end{cases} \tag{2.4}$$

We stress that a solution of (2.4) should satisfy the following identity

$$z_3^2(t) + \big(1 - z_4(t)\big)^2 = 1, \tag{2.4a}$$

for all $t \geq 0$. However, it can be shown that the quantity on the left hand side of (2.4a) is invariant along the solutions of (2.4). Therefore, it is enough to force (2.4a) only in

$t = 0$. Then, the augmented state-space model can be given as follows:

$$\begin{cases} \dot{v} = \frac{1}{\sigma_3(z)}\Big(m\ell\sigma_1\omega^2 z_3 - b\sigma_1 v - m^2 g\,\ell^2 z_3(1-z_4) + \sigma_1 F\Big), \\ \dot{\theta} = \omega, \\ \dot{\omega} = \frac{1}{\sigma_3(z)}\Big((m+M)mg\ell z_3 + mb\ell v(1-z_4) - m^2\ell^2\omega^2 z_3(1-z_4) - m\ell(1-z_4)F\Big), \\ \dot{z}_3 = \omega(1-z_4), \\ \dot{z}_4 = \omega z_3. \end{cases} \tag{2.5}$$

where

$$\sigma_1 = I + m\ell^2,\ \sigma_3(z) = \sigma_1(m+M) - m^2\ell^2 + m^2\ell^2 z_3^2. \tag{2.5a}$$

With the proposed change of variables in (2.3), the angle θ disappeared from the right hand side of the augmented model (2.5). Furthermore, the dynamics of the angle is encoded in the dynamical equations (2.4) of z_3 and z_4. Therefore, we are allowed to eliminate the second equation ($\dot{\theta} = \omega$) from (2.5). The remaining four equations can be written in the following qLPV form:

$$\dot{z} = A(z)z + B(z)u, \quad \text{with } z_3^2(0) + \big(1 - z_4(0)\big)^2 = 1, \tag{2.6}$$

where $z = (v\ \omega\ z_3\ z_4)^\top$, $u = F$, and

$$A(z) = \frac{1}{\sigma_3(z)}\begin{pmatrix} -b\sigma_1 & m\ell\sigma_1\omega z_3 & -m^2 g\,\ell^2(1-z_4) & 0 \\ mb\ell(1-z_4) & -m^2\ell^2\omega z_3(1-z_4) & (m+M)mg\ell & 0 \\ 0 & (1-z_4)\sigma_3(z) & 0 & 0 \\ 0 & 0 & \omega\sigma_3(z) & 0 \end{pmatrix},\ B(z) = \frac{1}{\sigma_3(z)}\begin{pmatrix} \sigma_1 \\ -m\ell(1-z_4) \\ 0 \\ 0 \end{pmatrix}.$$

Note that (2.6) is not a qLPV model, but a nonlinear (rational) time-invariant input-output model written in a qLPV form, where the output is the state.

It is important to mention that system (2.2) with output

$$y = h(v,\theta,\omega) = \begin{pmatrix} v & \omega & \sin\theta & 1-\cos\theta \end{pmatrix}^\top \tag{2.7}$$

is dynamically equivalent to system (2.6), in the sense that, for each $t \geq 0$, the output $y(t)$ of (2.2) for $(v(0), \theta(0), \omega(0))$ is equal to the output $z(t)$ of (2.6) with the same values for $(v(0), \theta(0), \omega(0))$, and $z_3(0) = \sin(\theta(0))$, $z_4(0) = 1 - \cos(\theta(0))$. Though, the state-space of (2.6) is embedded into a higher-dimensional Euclidean space ($\mathbb{R}^4$), the state trajectory z evolves in the following 3-dimensional cylindrical manifold:

$$z(t) \in M = \Big\{ z \in \mathbb{R}^4 \,|\, z_3^2 + (1 - z_4^2) = 1 \Big\} = \{ z = \Phi(v,\theta,\omega) \,|\, (v,\theta,\omega) \in U \}, \tag{2.8}$$

$$\text{where } \Phi(v,\theta,\omega) = (v, \omega, \sin\theta, 1-\cos\theta),\ \text{and } U = \mathbb{R} \times (-\pi, \pi] \times \mathbb{R}. \tag{2.8a}$$

Mapping $\Phi : U \to M$ is a diffeomorphism, and its Jacobian matrix is full-rank for all $(v,\theta,\omega) \in U$. Note that

$$A(z)z = \left(\frac{\partial\Phi}{\partial x} f \circ \Phi^{-1}\right)(z) \text{ and } B(z) = \left(\frac{\partial\Phi}{\partial x} g \circ \Phi^{-1}\right)(z), \tag{2.9}$$

where

$$\Phi^{-1} : (v, \omega, \sin\theta, 1-\cos\theta) \mapsto (v, \theta, \omega). \tag{2.10}$$

A possible explicit expression for Φ^{-1} (which is well-defined and differentiable for "almost" all $z \in M$) can be given as follows:

$$\Phi^{-1} : (v, \omega, z_3, z_4) \mapsto \Phi^{-1}(z) = (v, \operatorname{sgn}(\arcsin z_3)\arccos(1 - z_4), \omega), \tag{2.11}$$

where sgn denotes the sign function.

As the dynamics (2.6) are restricted to $M = \Phi(U) = \Phi(\mathbb{R}^3)$, system (2.6) has only two equilibria, which satisfy the initial identity (2.4a). The unstable equilibrium is $z^*_{\text{us}} = (0\ 0\ 0\ 0)^\top$, whereas, the stable equilibrium is $z^*_{\text{s}} = (0\ 0\ 0\ 2)^\top$.

Remark. We admit that the parametric definition for manifold M in (2.8) is not complete, as $\Phi(U)$ is not an *open* cover for M. Furthermore, Φ^{-1} (as it is given in (2.11)) is not differentiable in $z = (\cdot, \cdot, 0, 2)$. However, the loose definitions immediately make sense if the dynamics are controlled within the open set $U^\circ = \mathbb{R} \times (-\pi, \pi) \times \mathbb{R}$ or equivalently in the open manifold $M^\circ = \{z = \Phi(v, \theta, \omega) \,|\, (v, \theta, \omega) \in U^\circ\}$. ⋄

2.1.2 Rational qLPV model

In this section, we present a qLPV model for the nonlinear dynamics (2.2). First, we encapsulate the nonlinear terms of (2.2) in parameters, then, we compute the bounds for the parameters and their time-derivatives.

Following [171; 172], we introduce three state-dependent parameter signals

$$p_1 = \tfrac{\sin x_2}{x_2},\ p_2 = \cos x_2,\ p_3 = x_3 \sin x_2,\ p = \begin{pmatrix} p_1 \\ p_2 \\ p_3 \end{pmatrix}. \tag{2.12}$$

Then, the nonlinear system (2.2) can be embedded in the following LPV model:

$$\dot{x} = A(p)x + B(p)u, \tag{2.13}$$

where $x = (v\ \theta\ \omega)^\top$, $u = F$, and

$$A(p) = \frac{1}{\sigma_4(p)} \begin{pmatrix} -b\sigma_1 & -m^2 g \ell^2 p_1 p_2 & m\ell\sigma_1 p_3 \\ 0 & 0 & \sigma_4(p) \\ mb\ell p_2 & (m+M)mg\ell p_1 & -m^2\ell^2 p_2 p_3 \end{pmatrix},\ B(p) = \frac{1}{\sigma_4(p)} \begin{pmatrix} \sigma_1 \\ 0 \\ -m\ell p_2 \end{pmatrix} \tag{2.13a}$$

and $\sigma_1 = I + m\ell^2,\ \sigma_4(p) = \sigma_1(m + M) - m^2\ell^2 p_2^2$.

Note that model (2.13) is still not an approximation of the nonlinear dynamics (2.2). Differently from (2.6), the qLPV model in (2.13) is written in the initial state-space $\mathbb{R}^3$ of variables (v, θ, ω). Observe that, for a given input u and initial condition $x(0)$, there exists a parameter trajectory $p : t \mapsto p(x(t))$ such that the solution of (2.13) is identical to that of the nonlinear model (2.2). On the other hand, the proposed qLPV model can describe different dynamical behaviour by altering the parameter signals. We can say that (2.13) is a *conservative model* for the nonlinear dynamics.

2.1.2.1 Determining the parameter bounds. In order to obtain a complete LPV model description, which is aligned with the physical model (2.2), we need to compute the bounds of p and $\dot{p}$. For simplicity, let us assume that a state feedback $u = -Kx + v$ with $x(0) = 0$ can keep the state vector within the following rectangular set

$$\mathcal{X} = [-\overline{x}_1, \overline{x}_1] \times [-\overline{x}_2, \overline{x}_2] \times [-\overline{x}_3, \overline{x}_3] \subset U^\circ,\ \text{with } 0 < \overline{x}_2 < \tfrac{\pi}{2}. \tag{2.14}$$

Furthermore, let the disturbance signal v have an infinity norm less than or equal to $\bar{M}_\infty$. With these assumptions, we are able to define bounds for the parameter signal p as follows:

$$\begin{aligned} &p(t) \in \mathcal{P} = \mathcal{P}_1 \times \mathcal{P}_2 \times \mathcal{P}_3,\ \text{where} \\ &p_1(t) \in \mathcal{P}_1 = \left[\tfrac{\sin \overline{x}_2}{\overline{x}_2}, 1\right],\ p_2(t) \in \mathcal{P}_2 = [\cos(\overline{x}_2), 1], \\ &p_3(t) \in \mathcal{P}_3 = [-\overline{x}_3 \sin(\overline{x}_2), \overline{x}_3 \sin(\overline{x}_2)]. \end{aligned} \tag{2.15}$$

Due to the fact that $\frac{\partial p_1}{\partial x_2}$ is strictly decreasing on $x_2 \in [-\overline{x}_2, \overline{x}_2]$, the bounds of the time-derivative of p_1 can be given as follows:

$$\dot{p}_1 \in \mathcal{R}_1 = [-r_1, r_1],\ r_1 = \left(\tfrac{\cos(\overline{x}_2)}{\overline{x}_2} - \tfrac{\sin(\overline{x}_2)}{\overline{x}_2^2}\right) \overline{x}_3. \tag{2.16}$$

Note that $\dot{p}_2 = -p_3$, therefore, $\dot{p}_2 \in \mathcal{R}_2 = \mathcal{P}_3$. Finally, $\dot{p}_3 \in \mathcal{R}_3$ can be approximated numerically by evaluating $\dot{p}_3 = \frac{\partial p_3}{\partial x_2}\dot{x}_2 + \frac{\partial p_3}{\partial x_3}\dot{x}_3$ in a finite number of grid points in $\mathcal{X}$, for both $v = \pm\bar{M}_\infty$, and remembering that $u = -Kx + v$. ▲

***Remark* 2.1.** System (2.13) is unstable but stabilizable with a static state feedback. In

certain case studies (e.g., the crane system [183]), it is useful to consider the stable equilibrium as the operating point. Then, we have the possibility to translate the dynamic equation into $x^* = (0\ \pi\ 0)^\top$ by setting $x_1 = v$, $x_2 = \theta - \pi$, and $x_3 = \omega$. For simplicity the centered state variables are not distinguished in the notations. Considering the identities $\sin\theta = -\sin x_2$ and $\cos\theta = -\cos x_2$, the centered nonlinear state-space dynamics are

$$\dot{x} = f(x) + g(x)u, \text{ with } x = (v\ \ \theta - \pi\ \ \omega)^\top,\ u = F, \tag{2.17}$$
$$f(x) = \frac{-1}{\sigma_2(\theta)} \begin{pmatrix} m\ell\sigma_1\omega^2 \sin\theta + b\sigma_1 v + m^2 g\,\ell^2 \sin\theta\cos\theta \\ -\omega\sigma_2(\theta) \\ (m+M)mg\ell\sin\theta + mb\ell v\cos\theta + m^2\ell^2\omega^2\sin\theta\cos\theta \end{pmatrix},\ g(x) = \frac{1}{\sigma_2(\theta)} \begin{pmatrix} \sigma_1, \\ 0 \\ m\ell\cos\theta, \end{pmatrix},$$

which correspond to the following qLPV model

$$\Sigma : \dot{x} = A(p)x + B(p)u, \tag{2.18}$$

where $x = (v\ \ \theta - \pi\ \ \omega)^\top$, $u = F$, and

$$A(p) = \frac{-1}{\sigma_4(p)} \begin{pmatrix} b\sigma_1 & m^2 g\,\ell^2 p_1 p_2 & m\ell\sigma_1 p_3 \\ 0 & 0 & -\sigma_4(p) \\ mb\ell p_2 & (m+M)mg\ell p_1 & m^2\ell^2 p_2 p_3 \end{pmatrix},\ B(p) = \frac{1}{\sigma_4(p)} \begin{pmatrix} \sigma_1 \\ 0 \\ m\ell p_2 \end{pmatrix}. \tag{2.18a}$$

In (2.18), the parameters are functions of the *translated* state variables as given in (2.12) with $x_2 = \theta - \pi$. The expression for σ_1 and $\sigma_4(p)$ are the same as in (2.13a). For the translated model, the bounds for p and $\dot{p}$ can be similarly computed by considering $u = v$. ◇

In the following remark, we present a benchmark problem related to the hanging pendulum-cart system (i.e., that moves around the stable equilibrium point).

Problem 2.1 (The kidnapped scientist's problem)**.** Suppose that a scientist is kidnapped and locked down in a van, which is traveling on a highway at a variable speed. The scientist's ambition is to compute the distance took by the van from the point, where he was captured. In order to reconstruct the velocity function of the van, the scientist forces a pendulum on the ceiling of the cargo bay and measures the angle and the angular velocity of the pendulum. We are wondering whether the scientist can calculate the speed function of the van without the knowledge of the friction coefficient (b) and the mass of the van (M)? ◇

Problem 2.1 is revisited in Chapter 8, where a passivating output selection is proposed for system (2.18).

2.2 Continuous fermentation process

A *bioreactor* is a stirred tank, in which biological reactions occur simultaneously in a liquid medium [184, Chapter 1]. Through the *microbial growth reactions*, the nutrients or *substrates* are consumed by the microorganisms (bacteria, yeasts, etc.), which produce a resulting substance, called the *product*. The mass of living organisms is called the *biomass*.

In this section, we present an isothermal nonlinear continuous fermentation process model taken from [185] with constant volume V_0, constant physico-chemical properties and a (possibly) uncertain maximal growth rate $\mu_{\max}$. The principal reaction rate coefficient $\mu_{\max}$ is usually determined experimentally with relatively high uncertainty, causing a multiplicative uncertainty factor in the actual growth rate μ, which is a function of the substrate concentration S as follows:

$$\mu(S) = \frac{\mu_{\max} S}{K_2 S^2 + S + K_1}. \tag{2.19}$$

In (2.19), constants K_1 and K_2 are the saturation and inhibition parameters, respectively.

The dynamics of the biomass concentration (X) and substrate concentration (S) in the bioreactor tank is given by the following state-space model

$$\begin{cases} \dot{X} = \mu(S)X - \frac{XF}{V_0}, \\ \dot{S} = -\frac{\mu(S)X}{Y} + \frac{(S_F - S)F}{V_0}, \end{cases} \tag{2.20}$$

where constant Y is the yield coefficient. Signal $F = F_0 + u_C + u_F$ is the inlet feed flow rate, where constant F_0 is the optimal (nominal) flow rate, and u_C is a possible control input signal. The flow rate is perturbed by a disturbance signal u_F, which may be resulted, e.g., by the actuator's inaccuracy. Signal $S_F = S_{F,0} + u_S$ is the substrate concentration of the inflowing mixture to be processed, where constant $S_{F,0}$ is the assumed (operating point) concentration. In a real-life application the substrate concentration of the input flow may be rippling, this effect is encoded in the additive disturbance signal u_S.

The dynamics of the product concentration (P) in the bioreactor tank is given by the following equation [184, Eq. (1.9)]:

$$\dot{P} = \upsilon X - \frac{FP}{V_0} - Q \tag{2.21}$$

where Q is the rate of mass outflow of the product from the reactor in gaseous form, and υ is the specific production rate. The detached dynamical equation (2.21) of the product concentration is given for the sake of completeness, however, it does not influence the internal stability of the fermentation process (2.20). At the same time, a stable equilibrium solution of (2.20) with respect to F_0 entails a sustainable uniform input feed and product removal, i.e., a stable equilibrium solution for (2.21).

The dynamical modeling, analysis, and control of bioreactor systems are presented in details by Bastin and Dochain [184].

2.2.0.1 Optimal equilibrium solution. Let X_0 and S_0 denote the equilibrium concentrations of the biomass and the substrate, respectively, corresponding to the optimal inlet feed flow rate F_0. The equilibrium solution is computed so that the substrate feed concentration is assumed to be constant ($S_F(t) = S_{F,0}$ for all $t \geq 0$) and the biomass production X_0F_0 is maximized. First, the values of X_0 and F_0 are determined in the function of S_0 such that they satisfy

$$\mu(S_0)X_0 - \frac{X_0F_0}{V_0} = 0 \text{ and } -\frac{\mu(S_0)X_0}{Y} + \frac{(S_{F,0} - S_0)F_0}{V_0} = 0. \tag{2.22}$$

Namely,

$$X_0 = (S_{F,0} - S_0)Y \text{ and } F_0 = V_0\mu(S_0) = \frac{V_0S_0}{K_2S_0^2 + S_0 + K_1} \cdot \mu_{\max}. \tag{2.23}$$

Secondly, we find the optimal substrate concentration S_0, that maximizes X_0F_0:

$$S_0 = \underset{S_0>0}{\arg\max}\, (S_{F,0} - S_0)\mu(S_0) = \underset{S_0>0}{\arg\max}\, \underbrace{\frac{-S_0^2 + S_{F,0}S_0}{K_2S_0^2 + S_0 + K_1}}_{f(S_0)}. \tag{2.24}$$

If we differentiate function f with respect to S_0, we obtain:

$$f'(S_0) = \frac{(S_{F,0}K_2 + 1)\, S_0^2 + 2K_1S_0 - S_{F,0}K_1}{(K_2S_0^2 + S_0 + K_1)^2} = 0 \;\Rightarrow\; S_0 = \frac{-K_1 + \sqrt{K_1^2 + S_{F,0}^2K_1K_2 + S_{F,0}K_1}}{K_2S_{F,0} + 1}. \tag{2.25}$$

As the output signals, we consider the centered biomass concentration $x_1 = X - X_0$ and centered substrate concentration $x_2 = S - S_0$. ▲

It is worth mentioning that the optimal feed flow rate (F_0) depends linearly on the (possibly uncertain) maximal growth rate ($\mu_{\max}$), though, the equilibrium solution is independent of $\mu_{\max}$. Furthermore, the optimal (operating) equilibrium point (X_0, S_0)

10.15774/PPKE.ITK.2021.004

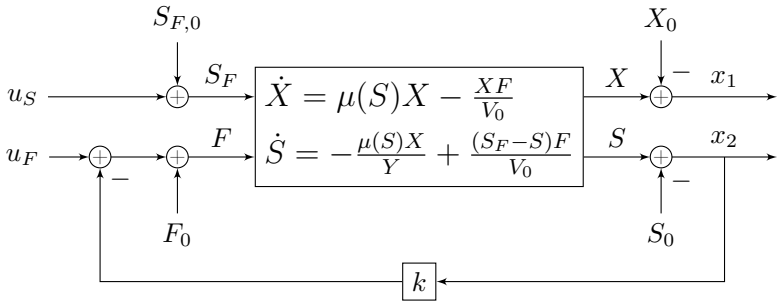

Figure 2.2: Block diagram of the closed-loop dynamics of the continuous fermenter.

is locally asymptotically stable, with a relatively small DOA. It is shown in [185] that a proportional substrate feedback $F = F_0 - k(S - S_0) + u_F$ can provide a significantly larger DOA for the operating point. In Figure 2.2, we present the block diagram of the closed-loop system with a proportional substrate feedback.

In this thesis, we address the following two system analysis problems.

Problem 2.2 (DOA estimation)**.** Assume an uncertain maximal growth rate $\mu_{\max}$, and that $u_F \equiv 0$, $u_S \equiv 0$. Estimate the robust domain of attraction of the closed-loop dynamics (Figure 2.2) when $F(t) = F_0 - k(S(t) - S_0)$ and $S_F(t) = S_{F,0}$ for all $t \geq 0$. In order to provide a robustness for the feedback controller, consider an additional integral feedback component, namely

$$F(t) = F_0 - k_P(S(t) - S_0) + k_I \int_0^t (S(\tau) - S_0) \text{ for all } t \geq 0. \tag{2.26}$$

Compute a stability region of the feedback system with input (2.26). Repeat the computations with different values of k, k_P, and k_I, then, draw the conclusions. ◇

Problem 2.3 (Disturbance attenuation analysis)**.** Assume that the maximal growth rate $\mu_{\max}$ is given. Upper estimate the disturbance attenuation level of the closed-loop system in Figure 2.2 from signals u_F, u_S to signals x_1, x_2. Analyse how the attenuation level is changing for different values of proportional feedback gain k. ◇

10.15774/PPKE.ITK.2021.004

Chapter 3

Background

In this chapter, the important notations, definitions, and known results are presented in brief, which will be used throughout the paper.

3.1 Signal spaces, operators, operator norms

Definition 3.1. *Let $\mathcal{L}_p^n[0,\infty)$ denote the signal space of the Lebesgue-integrable n-dimensional vector-valued signals having finite p-norm, namely*

$$\mathcal{L}_p^n[0,\infty) = \Big\{ x : [0,\infty) \to \mathbb{R}^n \,\Big|\, x \text{ is measurable and } \|x\|_p < \infty \Big\}, \tag{3.1}$$

$$\text{where } \|x\|_p = \left(\int_0^\infty \|x(t)\|^p \mathrm{d}t \right)^{\frac{1}{p}} \text{ for all } 1 \le p < \infty, \tag{3.1a}$$

$$\text{and } \|x\|_\infty = \operatorname*{ess\,sup}_{t\in[0,\infty)} \|x(t)\| \text{ if } p = \infty, \tag{3.1b}$$

are called the p-norm of signal $x \in \mathcal{L}_p^n[0,\infty)$. In (3.1a) *and* (3.1b)*, $\|x(t)\|$ denotes the Euclidean norm of vector $x(t) \in \mathbb{R}^n$.* ◇

Remark. Throughout the dissertation, we consider only causal signals mapping from $[0,\infty)$, therefore, we suppress the domain argument of $\mathcal{L}_p^n[0,\infty)$ for simplicity. Furthermore, superscript n denoting the dimensionality is suppressed when the signal's dimension is obvious or irrelevant. ◇

Definition 3.2. *A mapping $\Sigma : \mathcal{L}_p^{n_u} \to \mathcal{L}_q^{n_y}$ is called a system operator. The induced operator norm of system Σ is defined as follows:*

$$\|\Sigma\| = \sup_{0\not\equiv u\in\mathcal{L}_p^{n_u}} \frac{\|y\|_q}{\|u\|_p}, \text{ where } \Sigma : u \mapsto y = \Sigma[u]. \tag{3.2}$$

Signal $y \in \mathcal{L}_p^{n_y}$ is the output of system Σ obtained as a response for the given input signal $u \in \mathcal{L}_q^{n_u}$. ◇

***Remark* 3.1.** The dimensions of the signals are denoted correspondingly to their name, e.g., the dimension of signals x, y, z, p, u, v, w are denoted by n_x, n_y, n_z, n_p, n_u, n_v, n_w, respectively. For simplicity, the dimension of signal x is denoted by n when it is possible. Though, the values of signals at time instant t are denoted by $x(t)$, …, $w(t)$, the time argument (t) is often suppressed (as it is commonly done in the literature) and only used when it is necessary. Note that symbols $x \in \mathbb{R}^{n_x}$, $p \in \mathbb{R}^{n_p}$, … $w \in \mathbb{R}^{n_w}$ are often used as independent variables and not the value of a signal at time t. However, the context will clarify, whether we refer to the signal, its value at t, or an independent variable. ◇

10.15774/PPKE.ITK.2021.004

3.2 Local stability and domain of attraction

Definition 3.3 [40, Definition 10.1.1]**.** *A continuous function $\alpha : [0, a) \to [0, \infty)$ is said to belong to class $\mathcal{K}$ if it is strictly increasing and $\alpha(0) = 0$. If $a = \infty$ and $\lim_{r\to\infty} \alpha(r) = \infty$, the function is said to belong to class $\mathcal{K}_\infty$.* ◇

Definition 3.4. *A multivariate function f is called a C^1 function if it is continuously differentiable with respect to each variable.* ◇

We study nonlinear systems with time-varying parametric uncertainty in the form[1]:

$$\Sigma_a : \ \dot{x}(t) = f(x(t), p(t)), \ \text{with } x(0) = x_0 \in \mathcal{X} \subset \mathbb{R}^{n_x}, \tag{3.3}$$

where $x : [0, \infty) \to \mathbb{R}^{n_x}$ and $p : [0, \infty) \to \mathbb{R}^{n_p}$ are the state and parameter signals, respectively, $x(0) = x_0$ is the initial condition, $\mathcal{X}$ is a compact set, and $f : \mathbb{R}^{n_x+n_p} \to \mathbb{R}^{n_x}$ is a locally Lipschitz continuous function. For p, we consider the following restrictions.

Assumption 3.1. The parameter signal p is bounded and real-time available with a bounded time-derivative, namely, $p(t) \in \mathcal{P}$ for all $t \geq 0$ and $\dot{p}(t) \in \mathcal{R}$ for all $t > 0$, where $\mathcal{P}$ and $\mathcal{R}$ are (a-priori known) compact polytopes in the parameter space $\mathbb{R}^{n_p}$. ◇

Definition 3.5. *Signal p is called admissible if it satisfies Assumption 3.1.* ◇

We assume that $x^* \in \mathcal{X}$ is an equilibrium point of system (3.3), namely $f(x^*, p) = 0$ for all $p \in \mathcal{P}$.

Definition 3.6 [34, Definition 4.1]**.** *The equilibrium point $x^* \in \mathcal{X}$ of system Σ_a is stable if, for each $\varepsilon > 0$, there exists δ such that $\|x(0) - x^*\| < \delta$ implies $\|x(t) - x^*\| < \varepsilon$ for all $t > 0$. Furthermore, x^* is called asymptotically stable if it is stable and $\delta > 0$ can be chosen such that $\|x(0) - x^*\| < \delta$ implies $\lim_{t\to\infty} x(t) = x^*$.* ◇

Theorem 3.7 [40, Theorem 10.1.3]**.** *The equilibrium point $x^* = 0 \in \mathcal{X}$ of Σ_a is locally asymptotically stable for all admissible parameter trajectory p if there exists a possibly parameter-dependent C^1 function $V : \mathcal{X} \times \mathcal{P} \to \mathbb{R}$, called the Lyapunov function satisfying*

$$\underline{\alpha}(\|x\|) \leq V(x, p) \leq \overline{\alpha}(\|x\|) \qquad \text{for all } x \in \mathcal{X}, \ \text{all } p \in \mathcal{P}, \tag{3.4a}$$

and for some class $\mathcal{K}$ functions $\underline{\alpha}$, $\overline{\alpha}$, such that

$$\tfrac{\partial V}{\partial x}(x, p) f(x, p) + \tfrac{\partial V}{\partial p}(x, p)\varrho \leq -\alpha(\|x\|) \quad \text{for all } x \in \mathcal{X}, \ \text{all } (p, \varrho) \in \mathcal{P} \times \mathcal{R}, \tag{3.4b}$$

and for some class $\mathcal{K}$ function α.

The equilibrium point $x^* \in \mathcal{X}$ is globally asymptotically stable for all admissible parameter trajectory if (3.4a) *and* (3.4b) *are satisfied for all $x \in \mathbb{R}^{n_x}$, all $(p, \varrho) \in \mathcal{P} \times \mathcal{R}$, and for some class $\mathcal{K}_\infty$ functions $\underline{\alpha}$, $\overline{\alpha}$, and α.* ◇

3.2.1 Further results for autonomous models

As a special case of (3.3), consider an autonomous nonlinear system

$$\dot{x}(t) = f(x(t)), \ \text{with } x(0) = x_0 \in \mathcal{X}. \tag{3.5}$$

Observe that system (3.5) is the autonomous case of system (3.3) with $p \equiv 0$.

Definition 3.8 (Invariant set [34])**.** *A set M is said to be an invariant set with respect to* (3.5) *if $x(0) \in M$ implies $x(t) \in M$ for all $t \in \mathbb{R}$. A set M is said to be a positively invariant set if $x(0) \in M$ implies $x(t) \in M$ for all $t \geq 0$.* ◇

[1] Despite the hint of subscript "a", this system is *not autonomous* due to its time-varying dynamics.

Theorem 3.9 (LaSalle's theorem [34, Theorem 4.4])**.** *Let $\Omega \subset \mathcal{X}$ be a compact set that is positively invariant with respect to* (3.5)*. Let $V : \mathcal{X} \to \mathbb{R}$ be a continuously differentiable function such that $\frac{\partial V}{\partial x}(x)f(x) \leq 0$ in Ω. Let E be the set of all points $x \in \Omega$ where $\frac{\partial V}{\partial x}(x)f(x) = 0$. Let M be the largest invariant set in E. Then, every solution starting in Ω approaches M as $t \to \infty$.* ⋄

Theorem 3.9 formulates stability properties for autonomous dynamical systems with general (not necessarily point-like and possibly multiple) local attractors.

Lemma 3.10. *Consider an autonomous system* (3.5)*. Let $\Phi : \mathcal{X} \to M$ be a diffeomorphism satisfying $0 = \Phi(0)$, where $\mathcal{X} \subseteq \mathbb{R}^n$ and $M \subseteq \mathbb{R}^{n'}$. Assume that there exist positive finite scalars $\underline{\beta}_0$ and $\overline{\beta}_0$, such that*

$$\underline{\beta}_0\|x\| \leq \|\Phi(x)\| \leq \overline{\beta}_0\|x\|. \tag{3.6}$$

Consider the vector of state variables $z = \Phi(x)$ and its dynamics:

$$\dot{z} = \bar{f}(z), \text{ where } \bar{f} = \tfrac{\partial \Phi}{\partial x} f \circ \Phi^{-1}. \tag{3.7}$$

Assume that $W : \mathcal{Z} \to \mathbb{R}$ is a Lyapunov function for (3.7)*, where $M \subseteq \mathcal{Z}$. Then, $V = W \circ \Phi$ is a Lyapunov function for* (3.5) *in $\mathcal{X}$.* ⋄

Proof. Obviously, V is continuously differentiable and $V(x) = W(\Phi(x)) > 0$ for all $x \in \mathcal{X}$ as $W(z) > 0$ for all $z \in M = \Phi^{-1}(\mathcal{X})$. Furthermore, we show that

$$\left[\tfrac{\partial W}{\partial z}(z)\bar{f}(z)\right]_{z=\Phi(x)} = \tfrac{\partial V}{\partial x}(x)f(x) \text{ for all } x \in \mathcal{X}. \tag{3.8}$$

Considering (3.7), the Lie derivative of W in the terms of $x \in \mathcal{X}$ simplifies to

$$\begin{aligned} \tfrac{\partial W}{\partial z}\bar{f} \circ \Phi &= \left(\tfrac{\partial W}{\partial z} \circ \Phi\right)\left(\bar{f} \circ \Phi\right) \\ &= \left(\tfrac{\partial W}{\partial z} \circ \Phi\right)\left(\tfrac{\partial \Phi}{\partial x} f \circ \Phi^{-1} \circ \Phi\right) \\ &= \left(\left(\tfrac{\partial W}{\partial z} \circ \Phi\right)\tfrac{\partial \Phi}{\partial x}\right) f = \tfrac{\partial V}{\partial x} f. \end{aligned} \tag{3.9}$$

Finally, the existence of class $\mathcal{K}$ functions $\underline{\beta}$, $\overline{\beta}$, β satisfying

$$\underline{\beta}(\|z\|) \leq W(z) \leq \overline{\beta}(\|z\|) \text{ in } \mathcal{Z}, \tag{3.10a}$$

$$\tfrac{\partial W}{\partial z}(z)\bar{f}(z) \leq \beta(\|z\|) \text{ in } \mathcal{Z}, \tag{3.10b}$$

implies the existence of class $\mathcal{K}$ functions $\underline{\alpha}$, $\overline{\alpha}$, α, where

$$\underline{\alpha}(r) = \underline{\beta}(\underline{\beta}_0 r),\ \overline{\alpha}(r) = \overline{\beta}(\overline{\beta}_0 r),\ \alpha(r) = \beta(\overline{\beta}_0 r),$$

such that (3.4) are satisfied. □

A similar result to Lemma 3.10 is presented by Papachristodoulou and Prajna [182, Proposition 3] in the framework of the SOS approach.

3.2.2 Lyapunov transformation

Consider the following linear time-varying (LTV) state-space model:

$$\begin{cases} \dot{x}(t) = A(t)x(t) + B(t)u(t),\ x(0) = x_0. \\ y(t) = C(t)x(t) + D(t)u(t) \end{cases} \tag{3.11}$$

where $x : [0, \infty) \to \mathbb{R}^n$, $u : [0, \infty) \to \mathbb{R}^{n_u}$, $y : [0, \infty) \to \mathbb{R}^{n_y}$ are the state, input, and output signals, respectively, $x(0) = x_0$ is the initial condition, A, B, C, and D are Lipschitz continuous functions of the time having appropriate dimensions.

Definition 3.11 [186, Section 9.1]**.** *The time-varying state transformation $T : [0, \infty) \to$*

$\mathbb{R}^{n\times n}$ *is called a Lyapunov transformation if it satisfies the following properties:*

1. T *is continuously differentiable in* $(0,\infty)$, (3.12)
2. T *and* $\dot{T}$ *are bounded in* $[0,\infty)$,
3. *There exists a constant* $m>0$ *such that* $m \geq |\det T(t)|$ *for all* $t \geq 0$. ◇

According to [186], a Lyapunov transformation applied to the state space model (3.11) preserves the internal stability of the dynamics.

3.3 Dissipativity, induced $\mathcal{L}_2$ norm and passivity

We consider nonlinear input-output systems of the form

$$\Sigma : \begin{cases} \dot{x} = f(x,u,p), \\ y = h(x,u,p), \end{cases} \tag{3.13}$$

where x, u, y, and p are the state, input, output, and parameter signals, respectively, with p satisfying Assumption 3.1. Functions $f : \mathbb{R}^{n_x+n_u+n_p} \to \mathbb{R}^{n_x}$ and $h : \mathbb{R}^{n_x+n_u+n_p} \to \mathbb{R}^{n_y}$ are Lipschitz continuous on $\mathbb{R}^{n_x} \times \mathbb{R}^{n_u} \times \mathcal{P}$.

Let $s : \mathbb{R}^{n_u+n_y} \to \mathbb{R}$ be a mapping, called the *supply rate* or *supply function* and assume that, for all $t_0, t_1 \in \mathbb{R}$ and for all input-output pairs u, y satisfying (3.13), the composite function $s(t) = s(u(t), y(t))$ is locally integrable, namely, $\int_{t_0}^{t_1} |s(t)|\mathrm{d}t < \infty$. According to [62, Section 2.2.1], the supply function s should be interpreted as the "supply delivered to the system". A positive value for $\int_{t_0}^{t_1} s(t)\mathrm{d}t$ means that work is done *on* the system, otherwise, if $\int_{t_0}^{t_1} s(t)\mathrm{d}t < 0$, work is done *by* the system.

Definition 3.12 [40, Definition 10.7.1]**.** *System* Σ *is said to be strictly dissipative with respect to the supply rate* $s : \mathbb{R}^{n_u+n_y} \to \mathbb{R}$ *if there exists (a possibly parameter-dependent)* C^1 *function* $V : \mathbb{R}^{n_x} \times \mathcal{P} \to \mathbb{R}$*, called the storage function satisfying*

$$\underline{\alpha}(\|x\|) \leq V(x,p) \leq \overline{\alpha}(\|x\|) \text{ for all } x \in \mathbb{R}^{n_x}, \text{ all } p \in \mathcal{P}, \tag{3.14a}$$

and for some class $\mathcal{K}_\infty$ *functions* $\underline{\alpha}$, $\overline{\alpha}$*, such that*

$$\begin{aligned} \tfrac{\partial V}{\partial x}(x,p) f(x,u,p) + \tfrac{\partial V}{\partial p}(x,p)\varrho - s(u,y) \leq -\alpha(\|x\|) \text{ for all } (x,u) \in \mathbb{R}^{n_x+n_u}, \\ \text{all } (p,\varrho) \in \mathcal{P} \times \mathcal{R}, \end{aligned} \tag{3.14b}$$

and for $y = h(x,u,p)$*, where* α *is a* $\mathcal{K}_\infty$ *function. System* Σ *is said to be dissipative if* (3.14b) *holds for* $\alpha \equiv 0$. ◇

Note that the inequality in (3.14b) is stated for the independent variables x, u, p, and $\dot{p} = \varrho$. According to [39, Definition 3.1.2] an equivalent integral form of (3.14b) is as follows:

$$V\big(x(t_1),p(t_1)\big) - V\big(x(t_0),p(t_0)\big) \leq \int_{t_0}^{t_1} s(u(t),y(t))\mathrm{d}t. \tag{3.15}$$

for all $0 \leq t_1 \leq t_2$, and all admissible parameter and input signals.

Corollary 3.13 (based on [40, Definition 10.7.4, Example 10.7.1; 62, Corollary 2.18])**.** *System operator* $\Sigma : \mathcal{L}_2^{n_u} \to \mathcal{L}_2^{n_y}$ *has a finite induced* $\mathcal{L}_2$ *norm smaller than or equal to* γ *if it is dissipative with respect to the supply rate* $s(u,y) = \gamma^2\|u\|^2 - \|y\|^2$. ◇

As a special case of system Σ, consider now a nonlinear system of the form[2]:

$$\Sigma_p : \begin{cases} \dot{x} = f(x,u,p), \ x(0) = x_0, \\ y = h(x,p). \end{cases} \tag{3.16}$$

and having as many inputs as outputs ($n_u = n_y$). Note that the output y of Σ_p does not depend on the input u algebraically, but only dynamically through the state signal x.

Definition 3.14. *System Σ_p is called (strictly) passive if it is (strictly) dissipative with respect to the supply rate $s(u,y) = 2u^\top y$.* ◇

The dissipation inequality (3.14b) for strict passivity can be written as follows:

$$\begin{aligned} \tfrac{\partial V}{\partial x}(x,p) f(x,u,p) + \tfrac{\partial V}{\partial p}(x,p)\varrho \le y^\top u + u^\top y - \alpha(\|x\|) \text{ for all } (x,u) \in \mathbb{R}^{n_x+n_u}, \\ \text{all } (p,\varrho) \in \mathcal{P} \times \mathcal{R}, \end{aligned} \tag{3.17}$$

and for some $\mathcal{K}_\infty$ function α.

***Remark* 3.2.** A strictly passive system with storage function V (satisfying (3.14a)) is always asymptotically stable with Lyapunov function V if the input $u \equiv 0$. ◇

3.4 Parameter-dependent linear matrix inequalities

Definition 3.15 (Canonical form of LMIs)**.** *A linear matrix inequality (LMI) is a convex constraint of the following form*

$$M(x) = M_0 + \textstyle\sum_{i=1}^n x_i M_i \succeq 0 \tag{3.18}$$

where $M_i \in \mathbb{R}^{m\times m}$ are fixed constant symmetric matrices and x_i are free decision variables. LMI (3.18) *is said to be feasible if there exists $x \in \mathbb{R}^n$, such that $M(x) \succeq 0$. The feasible set (or solution set) of* (3.18) *is denoted by $\mathfrak{F} = \{x \,|\, M(x) \succeq 0\}$.* ◇

An LMI is a convex constraint in the sense that its feasible set is convex, formally, $\lambda x + (1-\lambda)y \in \mathfrak{F}$ for all $x, y \in \mathfrak{F}$ and all $\lambda \in [0,1]$.

Lemma 3.16 (Schur complement [62, Proposition 1.38])**.** *Let $M(x)$ be partitioned as follows: $M(x) = \left(\begin{smallmatrix} M_{11}(x) & M_{12}(x) \\ M_{21}(x) & M_{22}(x) \end{smallmatrix}\right)$, where $M_{11}(x)$ is a square matrix. Let*

$$\mathfrak{F}_1 = \{x \,|\, M(x) \succeq 0\}, \tag{3.19}$$

$$\mathfrak{F}_2 = \Big\{x \,|\, M_{11}(x) \succeq 0, \ M_{22}(x) - M_{12}(x)\big[M_{11}(x)\big]^{-1} M_{21}(x) \succeq 0\Big\}. \tag{3.20}$$

Then, $\mathfrak{F}_1 = \mathfrak{F}_2$. ◇

Schur's complement lemma makes possible to linearize nonlinear (typically quadratic) matrix inequalities.

Example 3.1. Consider the following simple scalar inequality $x_1^2 + x_2^2 \le 1$, which can be written in the following form $1 - \left(\begin{smallmatrix} x_1 \\ x_2 \end{smallmatrix}\right)^\top \left(\begin{smallmatrix} 1 & 0 \\ 0 & 1 \end{smallmatrix}\right)\left(\begin{smallmatrix} x_1 \\ x_2 \end{smallmatrix}\right) \ge 0$. According to Schur's complement lemma, the previous inequality is equivalent to the following LMI:

$$\begin{array}{r|c|l} 1 & & \\ & \mathfrak{F} & : \\ -1 & & \end{array} \qquad \begin{pmatrix} 1 & x_1 & x_2 \\ x_1 & 1 & 0 \\ x_2 & 0 & 1 \end{pmatrix} \succeq 0 \Leftrightarrow \begin{pmatrix} 1 & 0 & 0 \\ 0 & 1 & 0 \\ 0 & 0 & 1 \end{pmatrix} + x_1 \begin{pmatrix} 0 & 1 & 0 \\ 1 & 0 & 0 \\ 0 & 0 & 0 \end{pmatrix} + x_2 \begin{pmatrix} 0 & 0 & 1 \\ 0 & 0 & 0 \\ 1 & 0 & 0 \end{pmatrix} \succeq 0. \tag{3.21}$$

$\begin{smallmatrix} & & \\ -1 & & 1 \end{smallmatrix}$

Obviously, the solution set $\mathfrak{F}$ of (3.21) is the unit disc. ◇

Definition 3.17. *The canonical form of a semidefinite program (SDP) with a linear*

[2]System Σ_p is a sublclass of Σ, which is considered during the *passivity* analysis.

objective function can be formulated as follows:

$$\min c^\top x, \text{ subject to } M(x) \succeq 0, \tag{3.22}$$

where $c \in \mathbb{R}^n$ is a constant vector. ◇

Definition 3.18. *Let $M_i : \mathcal{W} \to \mathbb{R}^{m\times m}$, $i = 0, \dots, n$, where $\mathcal{W} \subset \mathbb{R}^{n_p}$. The matrix inequality condition*

$$M_0(w) + \sum_{i=1}^n x_i M_i(w) \succeq 0 \text{ for all } w \in \mathcal{W}, \tag{3.23}$$

is said to be a parameter-dependent LMI (PD-LMI) condition. The free variables $x \in \mathbb{R}^n$ are meant to be found such that (3.23) *is satisfied for all parameter values $w \in \mathcal{W}$.* ◇

Definition 3.19. *In the general case, when M_i are nonlinear functions of the parameter w, inequality* (3.23) *is said to be an infinite-dimensional problem, as the feasibility of* (3.23) *should be tested in infinitely many parameter points on $\mathcal{W}$.* ◇

Proposition 3.20 [62, Proposition 5.4]**.** *Assume that $\mathcal{W}$ is a compact polytope in $\mathbb{R}^{n_w}$ and M_i are affine functions, namely, $M_i(w) = M_{i0} + \sum_{j=1}^{n_w} M_{ij} w_j$. Then,* (3.23) *is satisfied for all $w \in \mathcal{W}$ if and only if* (3.23) *is satisfied in the (finite number of) corner points ($\mathbf{Ve}(\mathcal{W})$) of polytope $\mathcal{W}$.* ◇

3.5 Finsler's lemma

In this section, we present the parameter-dependent form [16] of Finsler's lemma [160].

Definition 3.21. *Let $\mathcal{W} \subseteq \mathbb{R}^{n_w}$ be a subset of the parameter space $\mathbb{R}^{n_w}$. A vector-valued function $\pi : \mathcal{W} \to \mathbb{R}^m$ is called well-defined on $\mathcal{W}$ if $\|\pi(w)\| < \infty$ for all $w \in \mathcal{W}$.* ◇

Lemma 3.22 [16, Lemma 2.1]**.** *Let $Q : \mathcal{W} \to \mathbb{R}^{m\times m}$ and $N : \mathcal{W} \to \mathbb{R}^{s\times m}$ be given well-defined functions on $\mathcal{W} \subseteq \mathbb{R}^{n_w}$, with $Q(w)$ symmetric. Then, the following are equivalent*

(i) $\pi^\top(w)Q(w)\pi(w) \geq 0$ *is satisfied for all $w \in \mathcal{W}$ and all well-defined $\pi : \mathcal{W} \to \mathbb{R}^m$, which fulfills $N(w)\pi(w) = 0$ for all $w \in \mathcal{W}$,* (3.24a)

(ii) $\exists L : \mathcal{W} \to \mathbb{R}^{m\times s}$ *such that $Q(w) + \mathrm{He}\{L(w)N(w)\} \succeq 0$ for all $w \in \mathcal{W}$,* (3.24b)

(iii) $(N^\perp)^\top(w)\ Q(w)\ N^\perp(w) \succeq 0$ *for all $w \in \mathcal{W}$,* (3.24c)

where $N^\perp$ is a basis for the kernel space of N (i.e., $N(w)N^\perp(w) = 0\ \forall w \in \mathcal{W}$). ◇

A proof for Lemma 3.22 is given in [160].

Definition 3.23 [16]**.** *Function $N : \mathcal{W} \to \mathbb{R}^{s\times m}$ is called an annihilator of $\pi : \mathcal{W} \to \mathbb{R}^m$ if $N\pi \equiv 0$ on $\mathcal{W}$ (i.e., $\pi(w)N(w) = 0$ for all $w \in \mathcal{W}$).* ◇

Definition 3.24 [160]**.** *Function $L : \mathcal{W} \to \mathbb{R}^{m\times s}$ in* (3.24b) *is called a matrix Lagrange multiplier.* ◇

***Remark* 3.3.** In this thesis, we consider parameter- (w) dependent matrix inequality conditions of the form (3.24a), in which Q is an unknown affine function and π is a priori given typically nonlinear function. Generally, it is not straightforward to solve the scalar inequality (3.24a). Instead, we have the opportunity to solve the affine PD-LMI $Q(w) \succeq 0$ over $\mathcal{W}$, but the obtained solution for Q is conservative due to the interdependence between the nonlinear coordinate functions of π. Observe that $Q(w) \succeq 0$ implies $z^\top Q(w)\, z \geq 0$ for all $z \in \mathbb{R}^m$, namely, the information about the structure of π is not taken into account at all. Fortunately, the annihilator N together with the free multiplier L makes possible to inject an amount of extra information into (3.24b), and,

in this way, N reduces the conservatism. Roughly speaking, annihilator N represents the algebraic coupling between the coordinate functions of π. ◇

***Remark* 3.4.** According to Proposition 3.20, PD-LMI (3.24b) can be solved in a convex computational framework if L is searched as a constant multiplier and $N : \mathcal{W} \to \mathbb{R}^{s\times m}$ is given as an affine function. ◇

3.6 Linear fractional transformation

The linear fractional transformation (LFT) plays an important role in modeling uncertain and/or nonlinear rational systems, and it is often used in the literature, e.g., as presented by El Ghaoui and Scorletti [90]. The LFT is discussed in detail in the book [187, Chapter 10] and in the users' manual [94].

Let us consider a rational function $A : \mathcal{W} \to \mathbb{R}^{m_1\times m_2}$ in the form:

$$A(w) = \sum_{j=1}^{J} \frac{q_{1j}(w)}{q_{2j}(w)} A_j, \tag{3.25}$$

where $w \in \mathcal{W}$ is a vector of some general parameters, $\mathcal{W}$ is a subset of the parameter space $\mathbb{R}^{n_w}$ and q_{ij} are multivariate polynomials with $q_{11} = q_{21} \equiv 1$. We assume that the fractions $q_{1j}(w)/q_{2j}(w)$ of polynomials q_{1j} and q_{2j} are irreducible for all $j > 1$.

Definition 3.25. *Two multivariate polynomials p_1 and p_2 are called relative prime, if they do not have common factors in their irreducible factorized form [188]. The fraction $p_1(w)/p_2(w)$ of two multivariate polynomials p_1 and p_2 is called irreducible if p_1 and p_2 are relative prime.* ◇

Definition 3.26. *We say that function A is well-defined (i.e., matrix $A(w)$ has a bounded norm) on $\mathcal{W}$ if A can be given by* (3.25)*, where $q_{2j}(w) \geq \varepsilon$ for all $j = 1, \ldots, J$, all $w \in \mathcal{W}$, and some $\varepsilon > 0$.* ◇

Lemma 3.27 [90, Lemma 2.1]**.** *For any rational function $A : \mathbb{R}^{n_w} \to \mathbb{R}^{m_1\times m_2}$ with no singularities at the origin, there exist non-negative integers $r_1, \ldots, r_{n_w}$ and matrices $F_{11} \in \mathbb{R}^{m_1\times m_2}$, $F_{12} \in \mathbb{R}^{m_1\times m}$, $F_{21} \in \mathbb{R}^{m\times m_2}$ and $F_{22} \in \mathbb{R}^{m\times m}$, with $m = r_1 + \ldots + r_{n_w}$, such that:*

$$\begin{aligned} A = \mathcal{F}_l\left\{\left(\begin{smallmatrix} F_{11} & F_{12} \\ F_{21} & F_{22} \end{smallmatrix}\right), \Delta\right\} &= F_{11} + F_{12}(I_m - \Delta F_{22})^{-1}\Delta F_{21} \\ &= F_{11} + F_{12}\Delta(I_m - F_{22}\Delta)^{-1}F_{21} \text{ on } \mathcal{W}, \end{aligned} \tag{3.26}$$

where $\Delta : \mathbb{R}^{n_w} \to \mathbb{R}^{m\times m}$, $\Delta(w) = \operatorname{diag}\{w_1 I_{r_1}, \ldots, w_{n_w} I_{r_{n_w}}\}$. ◇

***Remark* 3.5.** The so-called *uncertainty block* Δ is generally considered as an operator $\Delta : \eta_1 \mapsto \pi_1 = \Delta\eta_1$. In this case the arguments of Δ are suppressed. ◇

The form (3.26) is called the *linear fractional representation* (LFR) of function A. Operator Δ is said to have n_w blocks of dimensions $r = \{r_1, \ldots, r_{n_w}\}$. LFR (3.26) is said to be *well-posed* if $I_m - \Delta(w)F_{22}$ is invertible for all $w \in \mathcal{W}$. According to [94], function A is well-defined on $\mathcal{W}$ if and only if A admits a well-posed LFR on $\mathcal{W}$.

***Remark* 3.6.** Considering the LFR of function A, the nonlinear static operator $\mathcal{A} : u \mapsto y$, such that $y(t) = (\mathcal{A}u)(t) = A(w(t))u(t)$, is often represented in the literature by the following feedback interconnection:

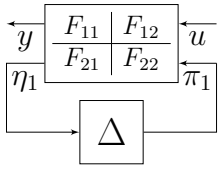

$$\begin{pmatrix} y \\ \eta_1 \end{pmatrix} = \left(\begin{array}{c|c} F_{11} & F_{12} \\ \hline F_{21} & F_{22} \end{array}\right) \cdot \begin{pmatrix} u \\ \pi_1 \end{pmatrix} \longleftrightarrow \begin{cases} y = F_{11}u + F_{12}\pi_1 \\ \eta_1 = F_{21}u + F_{22}\pi_1 \end{cases} \tag{3.27}$$

$$\text{with feedback } \pi_1 = \Delta\,\eta_1 \tag{3.27a}$$

Due to the lower position of block Δ relatively to block $F = \left(\begin{smallmatrix} F_{11} & F_{12} \\ F_{21} & F_{22} \end{smallmatrix}\right)$, the LFR realization (3.26) is called a *lower LFR* of A. For simplicity, we make no significant difference between the notations of operator $\mathcal{A} = \mathcal{F}_l\{F, \Delta\}$, the rational matrix-valued function $A = \mathcal{F}_l\{F, \Delta\}$, and the parameter-dependent matrix $A(w) = \mathcal{F}_l\{F, \Delta(w)\}$. ◇

Definition 3.28. *An $\{r_i, \ldots, r_{n_p}\}$-dimensional LFR $\mathcal{F}_l\left\{\left(\begin{smallmatrix} F_{11} & F_{12} \\ F_{13} & F_{14} \end{smallmatrix}\right), \Delta\right\}$ is equivalent to the $\left\{r'_i, \ldots, r'_{n_p}\right\}$-dimensional LFR $\mathcal{F}_l\left\{\left(\begin{smallmatrix} F'_{11} & F'_{12} \\ F'_{13} & F'_{14} \end{smallmatrix}\right), \Delta'\right\}$ if matrices $F_{11}, F'_{11} \in \mathbb{R}^{m_1 \times m_2}$ have compatible (i.e., the same) dimensions and*

$$F_{11} + F_{12}(I_m - \Delta(w)F_{22})^{-1}\Delta(w)F_{21} = F'_{11} + F'_{12}(I_{m'} - \Delta'(w)F'_{22})^{-1}\Delta'(w)F'_{21} \quad (3.28)$$

is satisfied for all $w \in \mathcal{W}$. ◇

***Remark* 3.7.** Consider a transfer function $G : \mathbb{C} \to \mathbb{R}^{m_1 \times m_2}$, such that $G(s) = D + C(sI - A)^{-1}B$. Then, G can be given by the following lower LFR:

$$G(s) = D + C\Big(I - \Big(\tfrac{1}{s}I\Big)A\Big)^{-1}\Big(\tfrac{1}{s}I\Big)B = \mathcal{F}_l\left\{\left(\begin{array}{c|c} D & C \\ \hline B & A \end{array}\right), \tfrac{1}{s}I\right\}, \quad (3.29)$$

where s denotes the Laplace operator. ◇

3.6.1 Basic operations with LFRs

Through the thesis, we will need to perform different operations on parameter-dependent matrices, namely, transposition, addition, multiplication, inversion, kernel computation, and block matrix composition, but also differentiation of rational matrix-valued functions. A few of these matrix operations (e.g., inversion) require intensive and computationally demanding computer algebra (i.e., symbolic manipulation) techniques, not to mention the hazardous tolerance-dependent rank decisions, which are involved by the interlaced symbolic and numeric manipulations [189].

The major advantage of the linear fraction transformation (LFT) is its ability to perform these algebraic operations on *rational functions* by using purely numerical tools. In the following, we revise the basic LFR operations as presented in the users' manual [94]. Consider two LFRs $\mathcal{F}_l\{F, \Delta_1\}$ and $\mathcal{F}_l\{G, \Delta_2\}$, where

$$F = \begin{pmatrix} F_{11} & F_{12} \\ F_{21} & F_{22} \end{pmatrix}, \; G = \begin{pmatrix} G_{11} & G_{12} \\ G_{21} & G_{22} \end{pmatrix}. \quad (3.30)$$

Henceforth, we assume that the two LFRs have compatible dimensions required for the corresponding matrix operations. The proofs for the following statements are given in [94, Section 7.1].

Lemma 3.29. *If Δ_1 is diagonal, the transposition of $\mathcal{F}_l\{F, \Delta_1\}$ is $\mathcal{F}_l\{F^\top, \Delta_1\}$.* ◇

Lemma 3.30. *The vertical matrix composition of $\mathcal{F}_l\{F, \Delta_1\}$, $\mathcal{F}_l\{G, \Delta_2\}$ is*

$$\begin{pmatrix} \mathcal{F}_l\{F, \Delta_1\} \\ \mathcal{F}_l\{G, \Delta_2\} \end{pmatrix} = \mathcal{F}_l\left\{\left(\begin{array}{c|cc} F_{11} & F_{12} & 0 \\ G_{11} & 0 & G_{12} \\ \hline F_{21} & F_{22} & 0 \\ G_{21} & 0 & G_{22} \end{array}\right), \begin{pmatrix} \Delta_1 & 0 \\ 0 & \Delta_2 \end{pmatrix}\right\}. \quad (3.31)$$

Whereas, the horizontal matrix composition is

$$\begin{pmatrix} \mathcal{F}_l\{F, \Delta_1\} & \mathcal{F}_l\{G, \Delta_2\} \end{pmatrix} = \mathcal{F}_l\left\{\left(\begin{array}{cc|cc} F_{11} & G_{12} & F_{12} & G_{12} \\ F_{21} & 0 & F_{22} & 0 \\ \hline 0 & G_{21} & 0 & G_{22} \end{array}\right), \begin{pmatrix} \Delta_1 & 0 \\ 0 & \Delta_2 \end{pmatrix}\right\}. \quad (3.32)$$

The block diagonal matrix composition of $\mathcal{F}_l\{F,\Delta_1\}$, $\mathcal{F}_l\{G,\Delta_2\}$ is

$$\begin{pmatrix}\mathcal{F}_l\{F,\Delta_1\} & 0\\ 0 & \mathcal{F}_l\{G,\Delta_2\}\end{pmatrix} = \mathcal{F}_l\left\{\left(\begin{array}{cc|cc} F_{11} & 0 & F_{12} & 0\\ 0 & G_{12} & 0 & G_{12}\\ \hline F_{21} & 0 & F_{22} & 0\\ 0 & G_{21} & 0 & G_{22}\end{array}\right), \begin{pmatrix}\Delta_1 & 0\\ 0 & \Delta_2\end{pmatrix}\right\}. \tag{3.33}$$

◇

Lemma 3.31. *The sum of $\mathcal{F}_l\{F,\Delta_1\}$ and $\mathcal{F}_l\{G,\Delta_2\}$ can be given as follows:*

$$\mathcal{F}_l\{F,\Delta_1\} + \mathcal{F}_l\{G,\Delta_2\} = \mathcal{F}_l\left\{\left(\begin{array}{c|cc} F_{11}+G_{11} & F_{12} & G_{12}\\ \hline F_{21} & F_{22} & 0\\ G_{21} & 0 & G_{22}\end{array}\right), \begin{pmatrix}\Delta_1 & 0\\ 0 & \Delta_2\end{pmatrix}\right\}. \tag{3.34}$$

◇

Lemma 3.32. *The product of $\mathcal{A} = \mathcal{F}_l\{F,\Delta_1\}$ and $\mathcal{B} = \mathcal{F}_l\{G,\Delta_2\}$ is:*

$$\mathcal{F}_l\{F,\Delta_1\}\,\mathcal{F}_l\{G,\Delta_2\} = \mathcal{F}_l\left\{\left(\begin{array}{c|cc} F_{11}G_{11} & F_{12} & F_{11}G_{12}\\ \hline F_{21}G_{11} & F_{22} & F_{21}G_{12}\\ G_{21} & 0 & G_{22}\end{array}\right), \begin{pmatrix}\Delta_1 & 0\\ 0 & \Delta_2\end{pmatrix}\right\}. \tag{3.35}$$

◇

Proof. Differently from the proof of [163], consider the input-output relation $z = \mathcal{A}\,y$ and $y = \mathcal{B}\,u$, then, $z = \mathcal{A}\,\mathcal{B}\,u$. If we eliminate variable y from

$$\mathcal{A}: \begin{cases} z = F_{11}y + F_{12}\pi_1\\ \eta_1 = F_{21}y + F_{22}\pi_1\\ \pi_1 = \Delta_1\eta_1\end{cases}, \qquad \mathcal{B}: \begin{cases} y = G_{11}u + G_{12}\pi_2\\ \eta_2 = G_{21}u + G_{22}\pi_2\\ \pi_2 = \Delta_2\eta_2\end{cases} \tag{3.36}$$

we obtain

$$\mathcal{A}\,\mathcal{B}: \begin{cases} z = F_{11}G_{11}u + F_{12}\pi_1 + F_{11}G_{12}\pi_2\\ \eta_1 = F_{21}G_{11}u + F_{22}\pi_1 + F_{21}G_{12}\pi_2\\ \eta_2 = G_{21}u + G_{22}\pi_2\\ \pi_1 = \Delta_1,\ \pi_2 = \Delta_2.\end{cases} \tag{3.37}$$

Considering $\eta = \left(\begin{smallmatrix}\eta_1\\ \eta_2\end{smallmatrix}\right)$ and $\pi = \left(\begin{smallmatrix}\pi_1\\ \pi_2\end{smallmatrix}\right)$, we obtain LFR (3.35). □

Lemma 3.33. *The matrix inverse of $\mathcal{F}_l\{F,\Delta_1\}$ is*

$$\mathcal{F}_l^{-1}\{F,\Delta\} = \mathcal{F}_l\left\{\left(\begin{array}{c|c} F_{11}^{-1} & -F_{11}^{-1}F_{12}\\ \hline F_{21}F_{11}^{-1} & F_{22} - F_{21}F_{11}^{-1}F_{12}\end{array}\right), \Delta\right\}. \tag{3.38}$$

◇

***Remark* 3.8.** Note that a separate LFR can be given for any uncertainty block Δ as follows:

$$\Delta = \mathcal{F}_l\left\{\left(\begin{array}{c|c} 0 & I\\ \hline I & 0\end{array}\right), \Delta\right\}. \tag{3.39}$$

Using the previous standard LFR operations, a few typical expressions of Δ can be written as follows:

$$\begin{aligned} I - \Delta M &= \mathcal{F}_l\left\{\left(\begin{smallmatrix} I & -I\\ M & 0\end{smallmatrix}\right), \Delta\right\},\\ I - M\Delta &= \mathcal{F}_l\left\{\left(\begin{smallmatrix} I & -M\\ I & 0\end{smallmatrix}\right), \Delta\right\},\end{aligned} \tag{3.40}$$

$$\begin{aligned} (I - \Delta M)^{-1} &= \mathcal{F}_l\{\left(\begin{smallmatrix} I & I\\ M & M\end{smallmatrix}\right), \Delta\} = I + (I - \Delta M)^{-1}\Delta M,\\ (I - M\Delta)^{-1} &= \mathcal{F}_l\{\left(\begin{smallmatrix} I & M\\ I & M\end{smallmatrix}\right), \Delta\} = I + M\Delta(I - M\Delta)^{-1}.\end{aligned} \tag{3.41}$$

Note that the identities in (3.41) are both a special case of the matrix inversion lemma [190, Section 2.1.4], which is not discussed in this dissertation. ◇

Lemma 3.34 (based on [163, Lemma 7.1.15])**.** *Assume that Δ is a diagonal block, namely, $\Delta(w) = \operatorname{diag}\{w_1 I_{r_1}, \dots, w_{n_w} I_{r_{n_w}}\}$. Then, the derivative of $\mathcal{F}_l\{F, \Delta\}$ with respect to variable w_i, $i \in \{1, \dots, n_w\}$ is*

$$\frac{\partial \mathcal{F}_l\{F,\Delta\}}{\partial w_i} = \mathcal{F}_l\left\{ \left(\begin{array}{c|cc} F_{12}H_iF_{21} & F_{12} & F_{12}H_iF_{22} \\ \hline F_{22}H_iF_{21} & F_{22} & F_{22}H_iF_{22} \\ F_{21} & 0 & F_{22} \end{array}\right), \begin{pmatrix} \Delta & 0 \\ 0 & \Delta \end{pmatrix} \right\}, \tag{3.42}$$

where $H_i \equiv \partial\Delta/\partial w_i$. ◇

Proof. The derivative of $\mathcal{F}_l(F, \Delta)$ with respect to w_i can be expressed as follows

$$\begin{aligned} \tfrac{\partial \mathcal{F}_l\{F,\Delta\}}{\partial w_i} &= F_{12}(I - \Delta F_{22})^{-1} H_i F_{22} (I - \Delta F_{22})^{-1} \Delta F_{21} + F_{12}(I - \Delta F_{22})^{-1} H_i F_{21} \\ &= F_{12}(I - \Delta F_{22})^{-1} H_i \Big(I + F_{22}(I - \Delta F_{22})^{-1}\Delta \Big) F_{21}. \end{aligned} \tag{3.43}$$

Considering the commutation property (3.26) of operator Δ, we can write:

$$\tfrac{\partial \mathcal{F}_l\{F,\Delta\}}{\partial w_i} = F_{12}(I - \Delta F_{22})^{-1} H_i \Big(I + F_{22}\Delta(I - F_{22}\Delta)^{-1} \Big) F_{21}. \tag{3.44}$$

Recalling the identities in (3.41), we obtain:

$$\tfrac{\partial \mathcal{F}_l\{F,\Delta\}}{\partial w_i} = F_{12}\mathcal{F}_l\Big\{ \left(\begin{smallmatrix} I & I \\ F_{22} & F_{22} \end{smallmatrix}\right), \Delta \Big\} H_i \mathcal{F}_l\Big\{ \left(\begin{smallmatrix} I & F_{22} \\ I & F_{22} \end{smallmatrix}\right), \Delta \Big\} F_{21}. \tag{3.45}$$

Then, the multiplication rule of Lemma 3.32 applied to (3.45) gives back the LFR (3.42), which completes the proof. □

Finally, the Kernel computation technique of [163, Section 7.1.8] makes possible for a given function $A : \mathcal{W} \to \mathbb{R}^{m_1 \times m_2}$ to find function $B : \mathcal{W} \to \mathbb{R}^{m_2 \times (m_2 - m_1)}$ such that $AB \equiv 0$ on $\mathcal{W}$.

Lemma 3.35. *Assume that matrix $F_{11} \in \mathbb{R}^{m_1 \times m_2}$ of $A = \mathcal{F}_l\{F, \Delta\}$ has maximal row rank. Let the columns of $Q \in \mathbb{R}^{m_2 \times (m_2 - m_1)}$ span the kernel space of matrix F_{11}. Then,*

$$B = \begin{pmatrix} \mathcal{F}_l\{F, \Delta\} \\ Q^\top \end{pmatrix}^{-1} \begin{pmatrix} 0_{m_1 \times (m_2 - m_1)} \\ I_{m_2 - m_1} \end{pmatrix} \tag{3.46}$$

satisfies $AB \equiv 0$ on $\mathcal{W}$. ◇

3.6.2 Recursive LFT realization

After we have introduced the standard LFR operations in the previous section, we are now allowed to compute a so-called *recursive (or direct) LFT realization* of any rational matrix-valued function having no singularities at the origin. In this section, we give a few examples, how a possible LFR is computed for some specific functions.

Example 3.2 (Elementary "building blocks" – the monomials)**.** Let p_1, p_2, …, p_{n_p} be independent variables. Then $p_i = \mathcal{F}_l\{\left(\begin{smallmatrix} 0 & 1 \\ 1 & 0 \end{smallmatrix}\right), p_i\}$. Using the multiplication rule of Lemma (3.32), the LFRs of some monomials are:

$$p_1 p_2 = \mathcal{F}_l\left\{ \left(\begin{array}{c|cc} 0 & 1 & 0 \\ \hline 0 & 0 & 1 \\ 1 & 0 & 0 \end{array}\right), \begin{pmatrix} p_1 & \\ & p_2 \end{pmatrix} \right\}, \; p_1^3 = \mathcal{F}_l\left\{ \left(\begin{array}{c|ccc} 0 & 1 & 0 & 0 \\ \hline 0 & 0 & 1 & 0 \\ 0 & 0 & 0 & 1 \\ 1 & 0 & 0 & 0 \end{array}\right), p_1 I_3 \right\}, \tag{3.47}$$

or in general

$$\prod_{i=1}^{n_p} p_i^{r_i} = \mathcal{F}_l\{M, \Delta\}, \text{ where } M = \left(\begin{smallmatrix} 0 & I_m \\ 1 & 0 \end{smallmatrix}\right), \Delta = \operatorname{diag}\Big\{ p_1 I_{r_1}, \dots, p_{n_p} I_{r_{n_p}} \Big\}, \tag{3.48}$$

and $m = r_1 + \cdots + r_{n_p}$. ◇

It is a well-known fact that a rational proper[3] transfer function G has infinitely many state-space realizations $G(s) = \mathcal{F}_l\left\{\left(\begin{smallmatrix} D & C \\ B & A \end{smallmatrix}\right), \frac{1}{s} I_n\right\}$, but there exist *minimal* realizations (with the smallest possible n). In a similar fashion, a rational multivariate function A has also infinitely many equivalent (Definition 3.28) LFR realizations $\mathcal{F}_l\{F, \Delta\}$. Assume that p_i and p_j are not commutative operators, namely $[p_i, p_j] = p_i p_j - p_j p_i \neq 0$, $1 \leq i < j \leq n_p$. Then, there exists a class of minimal LFR realizations $A = \mathcal{F}_l\{F, \Delta\}$, where the size of Δ is the smallest possible [92]. This minimal realization is called a *"relative-minimal"* LFR if p_i and p_j do commute [163]. In [92], the dimension ($m = r_1 + \cdots + r_{n_p}$) of the uncertainty block Δ of a static LFR $A(p) = \mathcal{F}_l\{F, \Delta(p)\}$ is called the *order* of the LFR.

It is worth mentioning, that the LFRs in Example 3.2 are all relative-minimal. In the following examples, however, we will experience that some operations will not result in a relative-minimal LFR. Not to mention the fact that a rational expression may result in completely different (but equivalent) LFRs, if the standard LFR operations are evaluated in a different sequence.

Example 3.3 (Polynomials)**.** Let us "compose" the LFR of a polynomial by applying the summation rule of Lemma 3.31 to some simple monomials of Example (3.2):

$$p_1 + p_1 p_2 = \mathcal{F}_l\left\{\left(\begin{array}{c|ccc} 0 & 1 & 1 & 0 \\ \hline 1 & 0 & 0 & 0 \\ 0 & 0 & 0 & 1 \\ 1 & 0 & 0 & 0 \end{array}\right), \begin{pmatrix} p_1 & & \\ & p_1 & \\ & & p_2 \end{pmatrix}\right\}. \tag{3.49}$$

Note that the order of LFR in (3.49) is 3 ($r = \{2, 1\}$). Consider again the same polynomial written in its Horner factorized form:

$$p_1(1 + p_2) = \mathcal{F}_l\left\{\left(\begin{array}{c|cc} 0 & 1 \\ \hline 1 & 0 \end{array}\right), p_1\right\} \mathcal{F}_l\left\{\left(\begin{array}{c|cc} 1 & 1 \\ \hline 1 & 0 \end{array}\right), p_2\right\} = \mathcal{F}_l\left\{\left(\begin{array}{c|cc} 0 & 1 & 0 \\ \hline 1 & 0 & 1 \\ 1 & 0 & 0 \end{array}\right), \begin{pmatrix} p_1 & \\ & p_2 \end{pmatrix}\right\} \tag{3.50}$$

Differently from (3.49), the resulting LFR (3.50) is a relative-minimal (second-order) LFR ($r = \{1, 1\}$). ◇

***Remark* 3.9.** A polynomial in its Horner factorized form not necessarily results in a relative-minimal LFR. ◇

Example 3.4 (Rational functions)**.** Using the inversion rule of Lemma 3.33, let us compute the LFR of the following inverse function:

$$\frac{1}{1 + p_3^2} = \mathcal{F}_l^{-1}\left\{\left(\begin{array}{c|cc} 1 & 1 & 0 \\ \hline 0 & 0 & 1 \\ 1 & 0 & 0 \end{array}\right), \begin{pmatrix} p_3 & \\ & p_3 \end{pmatrix}\right\} = \mathcal{F}_l\left\{\left(\begin{array}{c|cc} 1 & -1 & 0 \\ \hline 0 & 0 & 1 \\ 1 & -1 & 0 \end{array}\right), \begin{pmatrix} p_3 & \\ & p_3 \end{pmatrix}\right\}. \tag{3.51}$$

Applying the multiplication rule, we compute the LFR of the following rational function:

$$\frac{p_1(1 + p_2)}{1 + p_3^2} = \mathcal{F}_l\left\{\left(\begin{array}{c|cccc} 0 & 1 & 0 & -0 & -0 \\ \hline 1 & 0 & 1 & -1 & 0 \\ 1 & 0 & 0 & -1 & 0 \\ 0 & 0 & 0 & 0 & 1 \\ 1 & 0 & 0 & -1 & 0 \end{array}\right), \begin{pmatrix} p_1 & & & \\ & p_2 & & \\ & & p_3 & \\ & & & p_3 \end{pmatrix}\right\}. \tag{3.52}$$

Note that the LFR of the numerator ($p_1(1 + p_2)$) is given in (3.50). Finally, a matrix of rational functions can be computed by applying the matrix composition rules of Lemma 3.30. ◇

To conclude, the recursive (or direct) LFT realization of a rational expression is computed through in the in-order evaluation of a depth-first traversal of the corresponding

[3] the degree of the numerators in $G(s)$ are at most equal to the degree of denominators in $G(s)$.

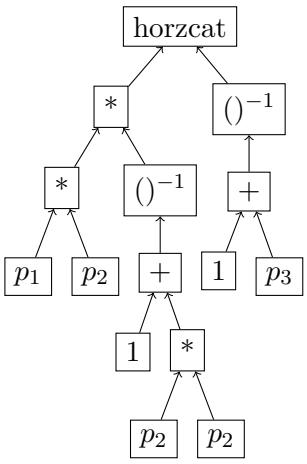

Figure 3.1: Expression tree of a rational matrix expression $\begin{pmatrix} \frac{p_1 p_2}{1+p_2^2} & \frac{1}{1+p_3} \end{pmatrix}$, where "horzcat" stands for the horizontal matrix composition operation.

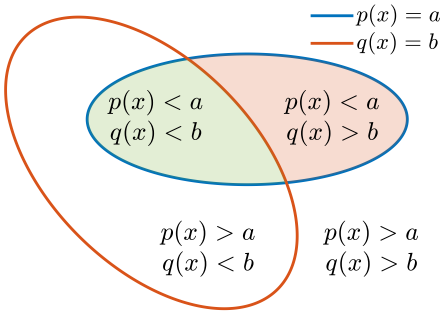

Figure 3.2: The geometrical interpretation of the conditional constraint (3.56).

expression tree (see, e.g., Figure 3.1). The leaves of the tree constitute the independent variables and constants appearing in the rational expression. The intermediate nodes represent to the standard arithmetic operations of the rational expression, such that the root of the tree corresponds to the outermost operation.

3.7 Positivstellensatz and the S-procedure

The Positivstellensatz (PS) constitutes an important result in the real algebraic geometry and it is also the major mathematical apparatus behind the sum-of-squares (SOS) approach. PS enables to formulate sufficient inequalities for set containment problems or conditional inequalities. In the robust control theory and LFT framework, multiple PS-like theorems were developed, such as the standard, or the full-block S-procedure. In this section, we focus on the generalized S-procedure, which is a special case of PS.

Lemma 3.36 (Generalized S-procedure [162, Lemma 2.3.1])**.** *Let $q, p_1, \dots, p_r : \mathbb{R}^n \to \mathbb{R}$ be scalar valued functions. Assume that there exist some non-negative functions $s_1, \dots, s_r$ such that*

$$-q(x) + \textstyle\sum_{i=1}^{r} s_i(x) p_i(x) \geq 0 \text{ for all } x \in \mathbb{R}, \tag{3.53}$$

then, the following set containment constraint

$$\{x \in \mathbb{R}^n \,|\, p_1(x) \leq 0\} \cap \dots \cap \{x \in \mathbb{R}^n \,|\, p_r(x) \leq 0\} \subseteq \{x \in \mathbb{R}^n \,|\, q(x) \leq 0\} \tag{3.54}$$

is satisfied. ◇

The set containment in (3.54) can be equivalently reformulated as the following conditional constraint:

$$\text{"}\textit{if } p_1(x) \leq 0\,,\ \dots\ ,\ p_r(x) \leq 0,\ \textit{then, } q(x) \leq 0.\text{"} \tag{3.55}$$

In Figure 3.2, we illustrate the set containment problem in the 2-dimensional space ($x \in \mathbb{R}^2$) with a single condition ($r = 1$). The equivalent conditional constraint is the following:

$$\text{"}\textit{if } p(x) \leq a,\ \textit{then, } q(x) \leq b,\text{"} \tag{3.56}$$

where $p, q : \mathbb{R}^n \to \mathbb{R}$ are multivariate functions. Geometrically, (3.56) prescribes the

a-level set of $p(x)$ to lay inside the b-level set of $q(x)$. Namely:

$$\Omega_a^p \subseteq \Omega_b^q, \text{ where } \Omega_c^f = \{x \in \mathbb{R}^n \,|\, f(x) \leq c\}. \tag{3.57}$$

According to Lemma 3.36, the conditional constraint in (3.56) is equivalent to any of the following two PS conditions:

$$\exists\, s : \mathbb{R}^n \to \mathbb{R}_+ \text{ such that } (p(x) - a) - s(x)(q(x) - b) \geq 0, \tag{3.58a}$$

$$\exists\, s : \mathbb{R}^n \to \mathbb{R}_+ \text{ such that } s(x)(p(x) - a) - (q(x) - b) \geq 0. \tag{3.58b}$$

Observe that the points belonging to the red region in Figure 3.2 do not satisfy the conditional constraint (3.56) nor its equivalent PS formulations (3.58a) and (3.58b).

In the following statement, we present a special case of Lemma 3.36, called the *standard S-procedure*, formulated for quadratic expressions.

Lemma 3.37 [191, Section III-A]**.** *Let $\Theta, M \in \mathbb{R}^{n\times n}$ be given symmetric matrices. We have the following equivalence:*

$$\begin{aligned} &x^\top \Theta x < 0 \text{ for all } x \in \mathbb{R}^n \text{ such that } x \neq 0,\, x^\top M x \leq 0 \\ &\quad \Leftrightarrow\ \Theta - \tau M < 0 \text{ for some } \tau \geq 0. \end{aligned} \tag{3.59}$$

On the other hand, if M is not positive semidefinite, we have that

$$\begin{aligned} &x^\top \Theta x \leq 0 \text{ for all } x \in \mathbb{R}^n \text{ such that } x^\top M x \leq 0 \\ &\quad \Leftrightarrow\ \Theta - \tau M \leq 0 \text{ for some } \tau \geq 0. \end{aligned} \tag{3.60}$$

$\diamond$

Note that Lemma 3.37 formulates equivalent conditions for the following two conditional constraints:

$$\begin{aligned} &\text{“}\textit{if } p(x) = x^\top M x \leq 0,\ \textit{then, } q(x) = x^\top \Theta x < 0\text{” and} \\ &\text{“}\textit{if } p(x) = x^\top M x \leq 0,\ \textit{then, } q(x) = x^\top \Theta x \leq 0\text{”, respectively.} \end{aligned} \tag{3.61}$$

Lemma 3.37 is used, e.g., in [90] and [156], to formulate sufficient LMI conditions to shape the storage function such that its certain level set be contained by a bounded polytope.

10.15774/PPKE.ITK.2021.004

Chapter 4

Related solutions in the literature

In this chapter, without any claim of completeness, I present a few reference solutions of literature. We can say that these approaches are a subset of the state-of-the-art solutions in the robust and nonlinear system theory.

The notations of the reference solutions are aligned with the notation system used in this dissertation. To keep the scope of this chapter between a reasonable limit, I present the reference solutions in a simplified, condensed form.

4.1 Performance analysis for nonlinear LPV systems: a grid based solution

Though it cannot be considered a "recent" solution, we feel reasonable to present the grid-based approach of Wu (1995). Due to its simplicity and transparency, this technique is frequently used to find approximate solutions of nonlinear problems.

As a subclass of (3.13), consider an LPV input-output system of the form

$$\Sigma : \begin{cases} \dot{x} = A(p)x + B(p)u, \\ y = C(p)x + D(p)u, \end{cases} \tag{4.1}$$

where p fulfills Assumption 3.1 with polytopes

$$\mathcal{P} = \bigtimes_{i=1}^{n_p} [\underline{p}_i, \overline{p}_i], \ \mathcal{R} = \bigtimes_{i=1}^{n_p} [-\overline{\varrho}_i, \overline{\varrho}_i]. \tag{4.2}$$

Functions A, B, C, D in (4.1) are Lipschitz continuous on $\mathcal{P}$.

In the following theorem, we summarize the results of Theorem 3.3.1 and Lemma 4.4.2 of the PhD dissertation of Wu [73].

Theorem 4.1. *Consider system Σ, and a finite number of C^1 functions $f_i : \mathbb{R}^{n_p} \to \mathbb{R}$, which form the parameterized structure of the quadratic parameter-dependent storage function candidate*

$$V(x,p) = x^\top P(p)\, x, \ \textit{with } P(p) = P_0 + \textstyle\sum_{i=1}^{m} P_i f_i(p). \tag{4.3}$$

Let T and δ be fixed positive scalars. Suppose that there exist symmetric matrices $M_i \in \mathbb{R}^{n_x \times n_x}$ and $P_i \in \mathbb{R}^{n_x \times n_x}$, $i = 0, \dots, m$, such that

$$P(p) - \delta I_{n_x} \succeq 0, \tag{4.4a}$$

$$\begin{pmatrix} I_{n_x} & P_i \\ P_i^\top & M_i \end{pmatrix} \succeq 0, \ \operatorname{Tr}(M_i) \le T, \tag{4.4b}$$

$$\begin{pmatrix} \operatorname{He}\{P(p)A(p)\} + \sum_{i=1}^{m} P_i \left(\frac{\partial f_i}{\partial p}(p) \varrho \right) & P(p)B(p) & \frac{1}{\gamma} C^\top(p) \\ B^\top(p)P(p) & -I_{n_u} & \frac{1}{\gamma} D^\top(p) \\ \frac{1}{\gamma} C(p) & \frac{1}{\gamma} D(p) & -I_{n_y} \end{pmatrix} + \delta I_{n_x+n_u+n_y} \preceq 0, \tag{4.4c}$$

are satisfied for all $p \in \mathbf{Gr}(\mathcal{P}, N_1 \times \cdots \times N_j \times \cdots \times N_{n_p})$*, and all* $\varrho \in \mathbf{Ve}(\mathcal{R})$*. Furthermore, assume that the number of grid points are selected such that*

$$N_j \geq 1+(\overline{p}_j-\underline{p}_j)\delta^{-1}n_pT\max\left\{\sum_{i=1}^{m}\left(2M_A^{ij}+M_B^{ij}\right)+\sum_{k=1}^{n_p}\nu_k\sum_{i=1}^{m}M_{ff}^{ijk},\sum_{i=1}^{m}M_f^{ij}\right\}, \tag{4.5}$$

where

$$\begin{aligned} M_A^{ij} &= \max_{p\in\mathcal{P}}\left\|\tfrac{\partial(f_iA)}{\partial p_j}(p)\right\|_{\mathrm{F}},\ M_f^{ij} = \max_{p\in\mathcal{P}}\left|\tfrac{\partial f_i}{\partial p_j}(p)\right|,\\ M_B^{ij} &= \max_{p\in\mathcal{P}}\left\|\tfrac{\partial(f_iB)}{\partial p_j}(p)\right\|_{\mathrm{F}},\ M_{ff}^{ijk} = \max_{p\in\mathcal{P}}\left|\tfrac{\partial^2 f_i}{\partial p_j\partial p_k}(p)\right|. \end{aligned} \tag{4.6}$$

Then, system Σ *has a finite induced-*$\mathcal{L}_2$*-gain smaller than or equal to* γ*.* ◇

Note that the pair of LMIs in (4.4b) assure that the Frobenius norm ($\|P_i\|_{\mathrm{F}}$) of matrices P_i are upper bounded by the positive scalar T. The upper-bounds for N_j in (4.5) were derived by following the clever arguments of [73, Proof of Lemma 4.4.2]. The values of M_A^{ij}, M_B^{ij}, M_f^{ij}, and M_{ff}^{ijk} can be well approximated by evaluating the corresponding derivative functions of (4.6) over a fine grid.

***Remark* 4.1.** The LMI constraints in (4.4) guarantee that γ is an upper bound on the induced $\mathcal{L}_2$-gain. However, the LMIs in (4.4) become more and more conservative as the value of T^{-1} and δ is increased. On the other hand, a small δ and large T generate a large number of grid points. ◇

***Remark* 4.2.** In the practical applications, the pair of LMIs in (4.4b) are not considered, and δ is often selected to be a small non-negative number (e.g., 10^{-5} or even zero). In this case, the necessary grid density is infinitesimal. To gain a first insight into the input-output behaviour of the system, the value of an upper bound γ is approximated ($\hat{\gamma}_1$) by considering a coarse grid with a much smaller number of grid points than necessary. The value of $\hat{\gamma}_1$ computed through a coarse grid is often smaller than the actual induced $\mathcal{L}_2$-gain. Therefore, the computations are performed again using a finer grid with a larger number of grid points (still less than necessary) to obtain a more precise approximation $\hat{\gamma}_2$ for γ. If the grid points of the initial coarse grid are included in the fine grid, the second approximation ($\hat{\gamma}_2$) is higher or equal to $\hat{\gamma}_1$ (see, e.g., the results in Figure 7.7). As the grid density is uniformly increased, the computed $\hat{\gamma}$ converges to an *upper bound* γ on the induced $\mathcal{L}_2$-gain. ◇

4.2 Stability and induced $\mathcal{L}_2$-gain of LFR systems

In this section, we present significant results from the computational nonlinear system theory. The studied reference solutions and theorems are not proved here, but they are commented with additional derivations for the sake of clarity.

Though the approach of El Ghaoui and Scorletti [89; 90] and that of Coutinho et al. [156] are fairly different, both techniques considered a nonlinear system model in the linear fractional representation of the form:

$$\mathcal{F}(\Sigma):\begin{cases} \dot{x} = F_{11}x + F_{12}u + F_{13}\pi, \quad x(0)=0\in\mathcal{X},\\ y = F_{21}x + F_{22}u + F_{23}\pi,\\ \eta = F_{31}x + F_{32}u + F_{33}\pi,\\ \pi = \Delta\eta,\ \Delta = \mathrm{diag}\Big(x_1I_{r_1},\ldots,x_{n_x}I_{r_{n_x}},p_1I_{r_{n_x+1}},\ldots,p_{n_p}I_{r_{n_x+r_{n_p}}}\Big), \end{cases} \tag{4.7}$$

where x, u, y are the state, input, and output signals respectively, $p \in \mathcal{P} \subset \mathbb{R}^{n_p}$ is a constant uncertain parameter, finally, $\mathcal{X}$ and $\mathcal{P}$ are again compact polytopes. Signals

$\pi, \eta : [0, \infty) \to \mathbb{R}^m$ are the auxiliary feedback signals of the LFR.

4.2.1 Induced $\mathcal{L}_2$-gain approach of El Ghaoui and Scorletti (1996)

In this section, we present another elder solution, which is probably one of the fathers of the computational *nonlinear* approaches. In the 80's, the linear fractional transformation (LFT) was deployed to model uncertainty in LTI models [66; 67; 86]. This general LFT framework is applied by El Ghaoui and Scorletti [89; 90] to model nonlinearity, and perform system analysis on time-invariant nonlinear autonomous and input-output models.

Consider system (4.7) with $F_{22} = F_{23} = 0$ and assume that Δ does not depend on the parameter, namely, $\Delta(x) = \operatorname{diag}(x_1 I_{r_1}, \ldots, x_{n_x} I_{r_{n_x}})$.

***Remark* 4.3.** According to [112], block Δ can be considered as a static LTV operator $\Delta : \mathcal{L}_2^m \to \mathcal{L}_2^m$ such that

$$\pi(t) = (\Delta\eta)(t) = \Delta(x(t))\,\eta(t).$$

At the same time, the (time-varying) matrix $(\Delta(x(t)))$ of operator Δ is defined through a function of the state, namely, $\Delta : x \mapsto \operatorname{diag}(x_1 I_{r_1}, \ldots, x_{n_x} I_{r_{n_x}})$. With an abuse of notation, symbol Δ represents an operator and a diagonal matrix-valued function of x at the same time. Whereas, $\Delta(x)$ constitute the value of function Δ in state x. Similarly, symbols η and π denote signals and independent variables at the same time. The context will then clarify which interpretation of these symbols we are considering. $\diamond$

Assume that the induced 2-norm of matrix $\Delta(x)$ is less than or equal to σ^{-1} for all $x \in \mathcal{X}$, namely

$$\|\Delta(x)\| = \sup_{0 \neq \eta \in \mathbb{R}^m} \frac{\|\Delta(x)\,\eta\|}{\|\eta\|} \leq \sigma^{-1} \text{ for all } x \in \mathcal{X}. \tag{4.8}$$

Assuming that $x(t) \in \mathcal{X}$ for all $t \geq 0$, the norm of operator Δ is less than or equal to σ^{-1}. This fact can be shown as follows:

$$\|\Delta\|^2 = \sup_{0 \neq \eta \in \mathcal{L}_2^m} \frac{\|\pi\|_2^2}{\|\eta\|_2^2} = \sup_{0 \neq \eta \in \mathcal{L}_2^m} \|\eta\|_2^{-2} \cdot \int_0^\infty \|\Delta(x(t))\,\eta(t)\|^2 \mathrm{d}t \tag{4.9}$$

$$\leq \sup_{0 \neq \eta \in \mathcal{L}_2^m} \|\eta\|_2^{-2} \cdot \int_0^\infty \|\Delta(x(t))\|^2\,\|\eta(t)\|^2 \mathrm{d}t \tag{4.9a}$$

$$\leq \sigma^{-2} \cdot \sup_{0 \neq \eta \in \mathcal{L}_2^m} \|\eta\|_2^{-2} \cdot \int_0^\infty \|\eta(t)\|^2 \mathrm{d}t \;=\; \sigma^{-2}. \tag{4.9b}$$

To rephrase, the norm of the uncertainty block Δ can be kept below σ^{-1} if we can define a set of admissible input signals, which maintain the state function inside $\mathcal{X}$. In [89], a number of sufficient LMI constraints are introduced, which provide a type of input-to-state stability for system (4.7).

Let e_k denote the kth column of the identity matrix I_{n_x} and let

$$\begin{aligned} \mathcal{S}(r) &= \Big\{ S = \operatorname{diag}(S_1, \ldots, S_{n_x}) \,\Big|\, 0 \prec S_i = S_i^\top \in \mathbb{R}^{r_i \times r_i},\ i = 1, \ldots, n_x \Big\}, \\ \mathcal{G}(r) &= \Big\{ G = \operatorname{diag}(G_1, \ldots, G_{n_x}) \,\Big|\, G_i = -G_i^\top \in \mathbb{R}^{r_i \times r_i},\ i = 1, \ldots, n_x \Big\}. \end{aligned} \tag{4.10}$$

Using these notations, we summarize the results of [89, Theorem 4.1] for induced $\mathcal{L}_2$-gain estimation.

Theorem 4.2. *Consider system $\mathcal{F}(\Sigma)$ in (4.7) with $\|\Delta\| \leq \sigma^{-1}$. Suppose that there exist $P, S \in \mathcal{S}(r)$, $G \in \mathcal{G}(r)$, and a scalar $\gamma > 0$, such that the LMIs*

$$\begin{pmatrix} \gamma^{-2}\sigma^{-2} & e_k^\top \\ e_k & P \end{pmatrix} \succ 0,\ k = 1, \ldots, n_x, \tag{4.11}$$

$$\Lambda = \begin{pmatrix} \mathrm{He}\{PF_{11}\}+F_{21}^\top F_{21}+F_{31}^\top S F_{31} & PF_{12}+F_{31}^\top S F_{32} & PF_{13}+F_{31}^\top S F_{33}-F_{31}^\top G \\ F_{12}^\top P+F_{32}^\top S F_{31} & F_{32}^\top S F_{32}-\gamma^2 I_{n_u} & F_{32}^\top S F_{33}-F_{32}^\top G \\ F_{13}^\top P+F_{33}^\top S F_{31}+G F_{31} & F_{33}^\top S F_{32}+G F_{32} & F_{33}^\top S F_{33}+G F_{33}-F_{33}^\top G-\sigma^2 S \end{pmatrix} \prec 0, \tag{4.12}$$

are satisfied. Then, we have:

1. *System* (4.7) *is well-posed over*
$$\mathcal{X} = \left\{ x \in \mathbb{R}^{n_x} \,\middle|\, |x_i| \le \tfrac{1}{\sigma},\ i = 1, \dots, n_x \right\} = \left[-\tfrac{1}{\sigma}, \tfrac{1}{\sigma} \right]^{n_x}. \tag{4.13}$$
2. *Every trajectory of system* (4.7) *with* $x(0) = 0$ *and input* $u \in \mathcal{L}_2^{n_u}$ *such that* $\|u\|_2 \le 1$ *is entirely contained in*
$$\Omega_{\gamma^2} = \left\{ x \in \mathbb{R}^{n_x} \,\middle|\, x^\top P\, x \le \gamma^2 \right\} \subset \mathcal{X}^\circ. \tag{4.14}$$
3. *System* $\mathcal{F}(\Sigma)$ *has a finite induced* $\mathcal{L}_2$ *norm less than or equal to* γ. ◇

It is worth mentioning that LMI (4.12) is equivalent to the following scalar inequality stated for all $x \in \mathbb{R}^{n_x}$, $u \in \mathbb{R}^{n_u}$, and all $\pi \in \mathbb{R}^m$:

$$\begin{aligned} \begin{pmatrix} x \\ u \\ \pi \end{pmatrix}^\top \Lambda \begin{pmatrix} x \\ u \\ \pi \end{pmatrix} &= x^\top P \left(F_{11} x + F_{12} u + F_{13} \pi \right) + \left(x^\top F_{11}^\top + u^\top F_{12}^\top + \pi^\top F_{13}^\top \right) P x \\ &+ x^\top F_{21}^\top F_{21} x - \gamma^2 u^\top u - \sigma^2 \pi^\top S \pi + x^\top F_{31}^\top S \left(F_{31} x + F_{32} u + F_{33} \pi \right) \\ &+ u^\top F_{32}^\top S \left(F_{31} x + F_{32} u + F_{33} \pi \right) + \pi^\top F_{33}^\top S \left(F_{31} x + F_{32} u + F_{33} \pi \right) \\ &+ \pi^\top G \left(F_{31} x + F_{32} u + F_{33} \pi \right) - \left(x^\top F_{31}^\top + u^\top F_{32}^\top + \pi^\top F_{33}^\top \right) G \pi \\ &= \mathrm{He}\left\{ x^\top P \dot{x} \right\} + y^\top y - \gamma^2 u^\top u \underbrace{- \sigma^2 \pi^\top S \pi + \eta^\top S \eta}_{\ge 0} + \underbrace{\pi^\top G \eta - \eta^\top G \pi}_{=0} \le 0, \end{aligned} \tag{4.15}$$

Matrices S and G are block diagonal corresponding to the $r = \{r_1, \dots, r_{n_x}\}$ dimensional blocks of Δ. Therefore, Δ commutes with both S and G. Inequality (4.15) contains two zeros terms $\pi^\top G \eta = -\eta^\top G \pi = 0$. This is due to the fact that

$$\pi^\top G \eta = \eta^\top \Delta G \eta = \eta^\top G \Delta \eta = \eta^\top G \pi = -\pi^\top G \eta = 0. \tag{4.16}$$

On the other hand, $\|\Delta\| \le \sigma^{-1}$ implies that

$$\sigma^2 \pi^\top \pi - \eta^\top \eta = \left(\begin{smallmatrix} \pi \\ \eta \end{smallmatrix} \right)^\top \begin{pmatrix} \sigma^2 I & 0 \\ 0 & -I \end{pmatrix} \left(\begin{smallmatrix} \pi \\ \eta \end{smallmatrix} \right) = \eta^\top \left(\begin{smallmatrix} \Delta \\ I \end{smallmatrix} \right) \begin{pmatrix} \sigma^2 I & 0 \\ 0 & -I \end{pmatrix} \left(\begin{smallmatrix} \Delta \\ I \end{smallmatrix} \right) \eta \le 0 \text{ for all } \eta \in \mathbb{R}^m. \tag{4.17}$$

Therefore,

$$\begin{aligned} \left(\begin{smallmatrix} \Delta \\ I \end{smallmatrix} \right) \begin{pmatrix} \sigma^2 I & 0 \\ 0 & -I \end{pmatrix} \left(\begin{smallmatrix} \Delta \\ I \end{smallmatrix} \right) \prec 0 &\Leftrightarrow \left(\begin{smallmatrix} \Delta \\ I \end{smallmatrix} \right) \begin{pmatrix} \sigma^2 I & 0 \\ 0 & -I \end{pmatrix} \left(\begin{smallmatrix} \Delta \\ I \end{smallmatrix} \right) S = \left(\begin{smallmatrix} \Delta \\ I \end{smallmatrix} \right) \begin{pmatrix} \sigma^2 S & 0 \\ 0 & -S \end{pmatrix} \left(\begin{smallmatrix} \Delta \\ I \end{smallmatrix} \right) \prec 0 \\ &\Leftrightarrow \sigma^2 \pi^\top S \pi - \eta^\top S \eta \le 0 \text{ for all } \eta, \pi \in \mathbb{R}^m : \pi = \Delta \eta. \end{aligned} \tag{4.18}$$

Finally, (4.15) can be lower estimated as follows:

$$\mathrm{He}\left\{ x^\top P\, \dot{x} \right\} + y^\top y - \gamma^2 u^\top u \le \begin{pmatrix} x \\ u \\ \pi \end{pmatrix}^\top \Lambda \begin{pmatrix} x \\ u \\ \pi \end{pmatrix} \le 0, \tag{4.19}$$

which, implies that system (4.7) has an induced $\mathcal{L}_2$-gain less than or equal to γ with a quadratic storage function $V : \mathbb{R}^{n_x} \to \mathbb{R}_+$, $V(x) = x^\top P x$. Matrices G and S are practically a sort of Lagrange multipliers and S is related to the S-procedure method applied to the conditional dissipation inequality:

$$\text{“}\textit{if } \sigma^2 \pi^\top \pi \le \eta^\top \eta, \textit{ then, } \mathrm{He}\left\{ x^\top P\, \dot{x} \right\} + y^\top y - \gamma^2 u^\top u \le 0\text{” for all } x, u, \pi, \eta. \tag{4.20}$$

In the literature (see, e.g.,[62]), another common equivalent form of LMI (4.12) is the following:

$$\begin{pmatrix} I & 0 & 0 \\ F_{11} & F_{12} & F_{13} \\ \hline 0 & I & 0 \\ F_{21} & F_{22} & F_{23} \\ \hline 0 & 0 & I \\ F_{31} & F_{32} & F_{33} \end{pmatrix}^\top \left(\begin{array}{cc|c} 0 & P & 0 \\ P & 0 & \\ \hline & & 0 \\ 0 & & \begin{matrix} -\gamma^2 I & 0 \\ 0 & I \end{matrix} \\ \hline 0 & & \begin{matrix} -\sigma^2 S & G \\ -G & S \end{matrix} \end{array} \right) \begin{pmatrix} I & 0 & 0 \\ F_{11} & F_{12} & F_{13} \\ \hline 0 & I & 0 \\ F_{21} & F_{22} & F_{23} \\ \hline 0 & 0 & I \\ F_{31} & F_{32} & F_{33} \end{pmatrix} \prec 0. \tag{4.21}$$

Note that both F_{22} and F_{23} are presented in (4.21), though they are assumed to be zero matrices. In this sense, (4.21) is a generalization of (4.12).

The matrix inequalities in (4.11) are additional geometrical constraints for the storage function. Namely, they force the γ^2-level set Ω_{γ^2} of the storage function to fit into polytope $\mathcal{X}$. Considering Schur's complement lemma (Lemma 3.16), the LMI in (4.11) is equivalent to

$$P - e_k \gamma^2 \sigma^2 e_k^\top \succ 0,\ k = 1, \dots, n_x. \tag{4.22}$$

Then, by pre- and post-multiplying with $x^\top$ and x, respectively, we obtain:

$$\begin{aligned} x^\top \Big(P - e_k \gamma^2 \sigma^2 e_k^\top \Big)\, x &= (x^\top P x - \gamma^2) - (x^\top e_k \gamma^2 \sigma^2 e_k^\top x - \gamma^2) \\ &= (x^\top P x - \gamma^2) - \gamma^2 \sigma^2 \Big(\|e_k^\top x\| - \sigma^{-2} \Big) > 0,\ k = 1, \dots, n_x. \end{aligned} \tag{4.23}$$

Inequality (4.23) implies the following set of conditional constraints

$$\text{“}\textit{if } x^\top P x < \gamma^2\textit{, then, } |e_k^\top x| \le \tfrac{1}{\sigma},\text{”}\ \ k = 1, \dots, n_x, \tag{4.24}$$

which are the equivalent formulation of the set containment relationship in (4.14).

4.2.2 Induced $\mathcal{L}_2$-gain approach of Coutinho et al. (2008)

Following the ideas of El Ghaoui and Scorletti [89; 90], an efficient nonlinear performance analysis approach is introduced by Coutinho et al. [156], who proposed to exploit the advantages of affine annihilators and Finsler's lemma (Section 3.5).

Consider system (4.7) in the following differential-algebraic representation

$$\begin{cases} \dot{x} = F_{11} x + F_{12} u + F_{13}\, \pi(x, u, p), \\ y = F_{21} x + F_{22} u + F_{23}\, \pi(x, u, p), \\ 0 = \Pi_1(x, p) x + \Pi_2(x, p) u + \Pi_3(x, p)\, \pi(x, u, p), \end{cases} \tag{4.25}$$

where $p \in \mathbb{R}^{n_p}$ is constant, and Π_1, Π_2, Π_3 are affine functions of the state and the parameter, such that

$$\Pi_1 = \Delta F_{31},\ \Pi_2 = \Delta F_{32},\ \Pi_3 = \Delta F_{33} - I_m. \tag{4.26}$$

Observer that nonlinear feedback $\pi = \Delta\eta$ of (4.7), is eliminated from (4.25), therefore, π cannot be considered as a signal any more, but a nonlinear function of the state and the parameter.

Furthermore, consider the following storage function candidate

$$V(x, p) = x^\top \mathbf{P}(x, p)\, x,\ \mathbf{P}(x, p) = \Theta^\top(x, p)\, P\, \Theta(x, p), \tag{4.27}$$

where Θ is a well-defined (possibly rational) function of x and p. Let $\zeta(x, p)$ denote $\Theta(x, p)\, x$. Then, the storage function can be written in the terms of ζ as follows:

$$V(x, p) = \zeta^\top(x, p)\, P\, \zeta(x, p). \tag{4.28}$$

To promote a systematic model construction, Coutinho et al. [156] proposed to use an affine function of (x, p) defined as follows:

$$\Theta : \mathcal{X} \times \mathcal{P} \to \mathbb{R}^{\bar{m} \times n_x},\ \text{ such that } \Theta = \begin{pmatrix} I_{n_x} \\ \Theta_1 \\ \Theta_2 \end{pmatrix},\ \Theta_1 = x \otimes I_{n_x},\ \Theta_2 = p \otimes I_{n_x}, \tag{4.29}$$

where $\bar{m} = n_x + \bar{m}_1 + \bar{m}_2$, $\bar{m}_1 = n_x^2$, $\bar{m}_2 = n_x n_p$.

Theorem 4.3 [156, Theorem 1]**.** *Consider system* (4.7) *in representation* (4.25) *with affine functions* (4.29) *and*

$$\begin{aligned} &\Psi_0 : \mathcal{X} \to \mathbb{R}^{s_0 \times n_x}, && \Psi_2 : \mathcal{X} \times \mathcal{P} \to \mathbb{R}^{\bar{m} \times (\bar{m}+1)}, \\ &\Psi_1 : \mathcal{X} \times \mathcal{P} \to \mathbb{R}^{(\bar{m}_1 + \bar{m}_2) \times \bar{m}}, && \Psi_3 : \mathcal{X} \times \mathcal{P} \to \mathbb{R}^{(m+s_0) \times (\bar{m}+m+n_u)}, \end{aligned} \tag{4.30}$$

such that $\Psi_0\, x \equiv 0$ *and*

$$\Psi_1 = \begin{pmatrix} \Theta_1 & -I_{\bar{m}_1} & 0 \\ \Theta_2 & 0 & -I_{\bar{m}_2} \end{pmatrix},\ \Psi_2 = \begin{pmatrix} x & -E_a \\ 0 & \Psi_1 \end{pmatrix},\ \Psi_3 = \begin{pmatrix} \Pi_1 E_a & \Pi_3 & \Pi_2 \\ \Psi_0 E_a & 0 & 0 \end{pmatrix}, \tag{4.31}$$

$$\text{where } E_a = (I_{n_x}\ 0_{n_x\times\bar{m}_1}\ 0_{n_x\times\bar{m}_2}). \tag{4.31a}$$

Let $\mathcal{X}\subset\mathbb{R}^{n_x}$ and $\mathcal{P}\subset\mathbb{R}^{n_p}$ be given polytopes, with $\mathcal{X}$ be represented by a collection of hyperplanes as follows:

$$\mathcal{X} = \Big\{x\in\mathbb{R}^n \,\Big|\, a_k^\top x \le 1,\ k=1,\dots,m_{\mathcal{X}}\Big\}, \tag{4.32}$$

where $a_k\in\mathbb{R}^{n_x}$ are perpendicular vectors to the associated faces of $\mathcal{X}$. Suppose that positive scalars μ,γ, and matrices $P=P^\top$, L, W, M_k, $k=1,\dots,m_{\mathcal{X}}$ are solutions of the following LMIs:

$$P + \mathrm{He}\{L\Psi_1(x,p)\} \succ 0 \qquad \text{for all } (x,p)\in \mathbf{Ve}(\mathcal{X}\times\mathcal{P}), \tag{4.33}$$

$$\begin{pmatrix} 2\mu-1 & -\mu a_k^\top E_a \\ -\mu E_a^\top a_k & P\end{pmatrix} + \mathrm{He}\{M_k\Psi_2(x,p)\} \succ 0 \qquad \text{for all } (x,p)\in \mathbf{Ve}(\mathcal{X}\times\mathcal{P}), \tag{4.34}$$

$$\Lambda(x,p) + \begin{pmatrix} \mathrm{He}\{W\Psi_3(x,p)\} & 0 \\ 0 & 0_{n_y\times n_y}\end{pmatrix} \prec 0 \qquad \text{for all } (x,p)\in \mathbf{Ve}(\mathcal{X}\times\mathcal{P}), \tag{4.35}$$

where $k=1,\dots,m_{\mathcal{X}}$ and

$$\Lambda = \begin{pmatrix} \mathrm{He}\big\{P\tilde{\Theta}F_{11}E_a\big\} & P\tilde{\Theta}F_{13} & P\tilde{\Theta}F_{12} & E_a^\top F_{21}^\top \\ F_{13}^\top\tilde{\Theta}^\top P & 0 & 0 & F_{23}^\top \\ F_{12}^\top\tilde{\Theta}^\top P & 0 & -\gamma I_{n_u} & F_{22}^\top \\ F_{21}E_a & F_{23} & F_{22} & -\gamma I_{n_y}\end{pmatrix},\ \tilde{\Theta} = \begin{pmatrix} I_{n_x} \\ \Theta_1 + I_{n_x}\otimes x \\ \Theta_2\end{pmatrix}. \tag{4.35a}$$

Then, the trajectory x starting from $x(0)=0$ and driven by an admissible disturbance signal $u\in\mathcal{L}_2^{n_u}$, $\|u\|_2\le\gamma^{-1}$ lies in the set

$$\Omega_1 = \{x\in\mathcal{X} \mid \exists\, p\in\mathcal{P},\ \text{such that } V(x,p)\le 1\}, \tag{4.36}$$

for all constant uncertain parameter $p\in\mathcal{P}$. Moreover, $\|y\|_2\le\gamma\|u\|_2$. ◇

Observe that Ψ_1, Ψ_2, and Ψ_3 are affine annihilators of vector-valued functions ζ, $\begin{pmatrix}1\\ \zeta\end{pmatrix}$, and $\begin{pmatrix}\zeta\\ \pi\\ u\end{pmatrix}$, respectively. Furthermore, a possible affine annihilator for x is, e.g., $\Psi_0 = (I_{n_x}\otimes x) - (x\otimes I_{n_x})$.

Pre- and post-multiplying (4.33) by $\zeta^\top$ and ζ, we obtain that $V(x,p)>0$ for all $(x,p)\in\mathcal{X}\times\mathcal{P}$, $x\neq 0$.

According to Schur's complement lemma (Lemma 3.16) and Proposition 3.20, LMI (4.35) is equivalent to

$$\Lambda_1(x,p) + \begin{pmatrix} E_a^\top F_{21}^\top \\ F_{23}^\top \\ F_{22}^\top\end{pmatrix}\frac{1}{\gamma}\begin{pmatrix} E_a^\top F_{21}^\top \\ F_{23}^\top \\ F_{22}^\top\end{pmatrix}^\top + \mathrm{He}\{W\Psi_3(x,p)\} \prec 0 \quad \text{in } \mathcal{X}\times\mathcal{P}, \tag{4.37}$$

$$\text{where } \Lambda_1 = \begin{pmatrix} \mathrm{He}\big\{P\tilde{\Theta}F_{11}E_a\big\} & P\tilde{\Theta}F_{13} & P\tilde{\Theta}F_{12} \\ F_{13}^\top\tilde{\Theta}^\top P & 0 & 0 \\ F_{12}^\top\tilde{\Theta}^\top P & 0 & -\gamma I_{n_u}\end{pmatrix}. \tag{4.37a}$$

If we pre-multiply (4.37) by $(\zeta^\top\ \pi^\top\ u^\top)$ and post-multiply by the transpose, the terms with Ψ_3 vanish, then, we obtain

$$\mathrm{He}\Big\{\zeta^\top(x,p)\,P\,\dot{\zeta}(x,p)\Big\} - \gamma u^\top u + \tfrac{1}{\gamma}y^\top y < 0. \tag{4.38}$$

In the previous step, we took into consideration that the full derivative of ζ can be expressed as follows:

$$\dot{\zeta}(x,p) = \frac{\mathrm{d}}{\mathrm{d}t}\begin{pmatrix} x \\ \Theta_1(x)\,x \\ \Theta_2(p)\,x\end{pmatrix} = \begin{pmatrix} \dot{x} \\ \Theta_1(\dot{x})\,x + \Theta_1(x)\,\dot{x} \\ \Theta_2(p)\,\dot{x}\end{pmatrix},\ \text{where } \Theta_1(\dot{x})\,x = (\dot{x}\otimes I_{n_x})\,x = (I_{n_x}\otimes x)\,\dot{x}.$$

Similarly to (4.11), the LMIs in (4.34) correspond to the geometrical conditions captured through the S-procedure to enforce the 1-level set of V to belong to $\mathcal{X}$. Pre- and post-multiplying (4.34) by $\begin{pmatrix}1\\ \zeta\end{pmatrix}^\top$ and $\begin{pmatrix}1\\ \zeta\end{pmatrix}$, we obtain the PS condition:

$$-2\mu(a_k^\top x - 1) + (x^\top\mathbf{P}(x,p)\,x - 1) > 0 \text{ for all } (x,p)\in\mathcal{X}\times\mathcal{P}. \tag{4.39}$$

Inequality (4.39) implies the following conditional constraint:

$$\text{“}\textit{if } V(x,p)<1,\ \textit{then, } a_k^\top x \le 1\text{”} \text{ for all } k=1,\dots,m_{\mathcal{X}}, \tag{4.40}$$

or equivalently $\Omega_1 \subset \mathcal{X}^\circ$.

4.2.3 DOA computation approach of Trofino and Dezuo (2013)

In this section, we present the stability analysis and DOA computation approach of Trofino and Dezuo [16], which is closely related to the nonlinear $\mathcal{L}_2$-gain approach of Coutinho et al. [156]. Similarly to [156], affine annihilators and Finsler's lemma is applied efficiently in [16] to formulate sufficient polytopic LMIs for stability.

Consider a non-autonomous rational nonlinear system (3.3) in the following differential-algebraic representation

$$\begin{cases} \dot{x} = F_{11}x + F_{12}\,\pi_1(x,p), \text{ with } x(0)=x_0\in\mathcal{X}, \\ 0 = N(x,p)\,\pi(x,p) \text{ for all } (x,p)\in\mathcal{X}\times\mathcal{P}, \text{ where } \pi = \left(\begin{smallmatrix} x \\ \pi_1 \end{smallmatrix}\right), \end{cases} \tag{4.41}$$

and with a time-varying parameter signal p satisfying Assumptions 3.1. Furthermore, consider a Lyapunov function candidate $V:\mathcal{X}\times\mathcal{P}\to\mathbb{R}$ in the following form

$$V(x,p) = x^\top \mathbf{Q}(x,p)\,x = \pi^\top(x,p)\,Q(x,p)\,\pi(x,p), \tag{4.42}$$

$$\text{with } Q(x,p) = Q_0 + \textstyle\sum_{i=1}^{n_x} Q_{1i}x_i + \sum_{j=1}^{n_p} Q_{2j}p_j \in \mathbb{R}^{m\times m}, \tag{4.42a}$$

where function $\pi:\mathcal{X}\times\mathcal{P}\to\mathbb{R}^m$, $m=n_x+m_1$ is the same that appear in (4.41). Function $\pi_1:\mathcal{X}\times\mathcal{P}\to\mathbb{R}^{m_1}$ can be given manually, e.g., a set of monomials up to a given degree:

$$\pi_1^\top(x,p) = \left(\begin{smallmatrix} x_1 & x_2 & x_1^2 & x_1x_2 & x_2^2 & x_1^3 & x_1^2x_2 & x_1x_2^2 & x_2^2 & p_1x_1 & p_1x_2 & p_1x_1^2 & p_1x_1x_2 & p_1x_2^2 \end{smallmatrix}\right), \tag{4.43}$$

or it may originate from a possible linear fractional representation ($\dot{x} = F_{11}x + F_{12}\,\pi_1$, $\eta_1 = F_{21}x + F_{22}\pi_1$, $\pi_1 = \Delta\eta_1$) of (4.41) as follows: $\pi_1 = (I_{m_1} - \Delta F_{22})^{-1}\Delta F_{21}x$.

***Remark* 4.4.** In [16], the Lyapunov function candidate (4.42) is considered with a constant matrix Q instead of an affine function (4.42a) of x and p. In this sense, the approach in this presentation is a slight generalization of that proposed in [16]. ◇

To formulate sufficient convex conditions for the Lyapunov inequality (3.4b), Trofino and Dezuo [16] proposed to factorize the total derivative of the Lyapunov function as presented in the following proposition.

Proposition 4.4 (based on [16, Section 4])**.** *Consider function $V=\pi^\top Q\,\pi$ (4.42) and constant matrices*[1]

$$E_r = \begin{pmatrix} I_m & 0_{m\times(m_1+n_xm)} \end{pmatrix},\ A_r = \begin{pmatrix} F_{11} & F_{12} & 0 & 0_{m_1\times(n_xm)} \\ 0 & 0 & I_{m_1} & 0_{m_1\times(n_xm)} \end{pmatrix},\ W_r = \begin{pmatrix} 0_{mn_x\times(n_x+2m_1)} & I_{mn_x} \end{pmatrix}.$$

Then, the derivative function $\dot{V}$ with $\dot{x}=f(x,p)$ and $\dot{p}=\varrho$ can be expressed as follows

$$\dot{V}(x,p) = \pi_r^\top(x,p,\varrho)\,Q_r(x,p,\varrho)\,\pi_r(x,p,\varrho), \tag{4.44}$$

$$\textit{where } Q_r(x,p,\varrho) = \mathrm{He}\Big\{E_r^\top Q(x,p)A_r + \tfrac{1}{2}E_r^\top \bar{Q}_1 W_r\Big\} + E_r^\top Q_2(\varrho)E_r, \tag{4.44a}$$

$$\textit{and } Q_2(\varrho) = \textstyle\sum_{j=1}^{n_p} Q_{2j}\,\varrho_j,\ \bar{Q}_1 = \begin{pmatrix} Q_{11} & \dots & Q_{1n_x} \end{pmatrix}. \qquad \diamond$$

Furthermore, function π_r is given as follows

$$\pi_r = \left(\begin{smallmatrix} \pi_d \\ \mu \end{smallmatrix}\right),\ \textit{with } \pi_d = \left(\begin{smallmatrix} \pi \\ \pi_1 \end{smallmatrix}\right) \textit{ and } \mu = \left(\begin{smallmatrix} \mu_1 \\ \dots \\ \mu_{n_x} \end{smallmatrix}\right) = (f\otimes I_m)\,\pi,\ \textit{(i.e., } \mu_i = \dot{x}_i\pi\textit{)}, \tag{4.45}$$

[1] Subscript r in $\pi_r, Q_r(x,p,\varrho), E_r, A_r$, etc. does not have a specific meaning. Other subscript letters are already assigned.

where $\dot{\pi}_1 = \frac{\partial \pi_1}{\partial x} f + \frac{\partial \pi_1}{\partial p} \varrho.$ (4.46)

Proof. Observe the following identities:

$$\pi = E_r \pi_r,\ \dot{\pi} = \begin{pmatrix} f \\ \dot{\pi}_1 \end{pmatrix} = A_r \pi_r,\ \mu = W_r \pi_r. \tag{4.47}$$

Then, the full derivative of function Q can be given as follows:

$$\dot{Q}(x,p) = \sum_{i=1}^{n_x} Q_{1i} \dot{x}_i + \sum_{j=1}^{n_p} Q_{2j} \varrho = \bar{Q}_1 (f(x,p) \otimes I_m) + Q_2(\varrho).$$

Accordingly, the derivative function $\dot{V}$ can be expressed in the terms of π_r:

$$\begin{aligned} \dot{V} &= \mathrm{He}\{\pi^\top Q \dot{\pi}\} + \pi^\top \dot{Q} \pi && (4.48)\\ &= \mathrm{He}\{\pi_r^\top E_r^\top Q A_r \pi_r\} + \pi^\top \bar{Q}_1 (f \otimes I_m) \pi + \pi^\top \dot{Q}_2 \pi && (4.49)\\ &= \pi_r^\top \mathrm{He}\{E_r^\top Q A_r\} \pi_r + \tfrac{1}{2} \mathrm{He}\Big\{\pi^\top \bar{Q}_1 \mu\Big\} + \pi_r^\top E_r^\top \dot{Q}_2 E_r \pi_r && (4.50)\\ &= \pi_r^\top \Big(\mathrm{He}\{E_r^\top Q A_r + \tfrac{1}{2} E_r^\top \bar{Q}_1 W_r\} + E_r^\top \dot{Q}_2 E_r\Big) \pi_r. && (4.51) \end{aligned}$$

Finally, the derivative function can be written as follows:

$$\dot{V}(x,p) = \pi_r^\top(x,p,\varrho) \Big(\mathrm{He}\{E_r^\top Q(x,p) A_r + \tfrac{1}{2} E_r^\top \bar{Q}_1 W_r\} + E_r^\top Q_2(\varrho) E_r\Big) \pi_r(x,p,\varrho),$$

which completes the proof. □

The quadratic reformulation (4.44) of the derivative function $\dot{V}$ brings us closer to the point, where Finsler's lemma is applicable to formulate convex LMIs for stability. However, we still need to determine an affine annihilator for function π_r.

Proposition 4.5 (based on [16, Section 4])**.** *Assume that N and N_d are affine annihilators of π and $\pi_d = \left(\begin{smallmatrix} \pi \\ \dot{\pi}_1 \end{smallmatrix}\right)$, respectively, with*

$$N(x,p) = N_0 + N_1(x) + N_2(p) = N_0 + \textstyle\sum_{i=1}^{n_x} N_{1i} x_i + \sum_{j=1}^{n_p} N_{2j} p_j.$$

Consider function N_r defined as follows:

$$N_r(x,p,\varrho) = \begin{pmatrix} N_d(x,p,\varrho) & 0 \\ 0 & I_{n_x} \otimes N(x,p) \\ N_2(\varrho) E_d + N(x,p) A_d & \bar{N}_1 \\ (I_{n_x} \otimes x) H_d & -I_{n_x} \otimes \begin{pmatrix} I_{n_x} & 0_{n_x \times m_1} \end{pmatrix} \end{pmatrix}, \tag{4.52}$$

where $E_d = \begin{pmatrix} I_m & 0_{m \times (4m_1)} \end{pmatrix}$, $A_d = \left(\begin{smallmatrix} F_{11} & F_{12} & 0 \\ 0 & 0 & I_{m_1} \end{smallmatrix}\right)$, $H_d = \begin{pmatrix} F_{11} & F_{12} & 0 \end{pmatrix}$,

and $N_2(\varrho) = \sum_{j=1}^{n_p} N_{2j}\, \varrho_j$, $\bar{N}_1 = \begin{pmatrix} N_{11} & \dots & N_{1n_x} \end{pmatrix}$.

Then, $N_r \pi_r \equiv 0$, i.e., N_r is an affine annihilator of π_r. ◇

Proof. Affine function N is an annihilator of π, and hence of $\mu_i = \dot{x}_i \pi$. On the other hand, if we express the derivative of $N\pi$ and consider that $\dot{\pi} = A_d \pi_d$, we obtain the following identity:

$$\begin{aligned} \tfrac{\mathrm{d}}{\mathrm{d}t}(N\pi) = \dot{N}\pi + N\dot{\pi} &= \textstyle\sum_{i=1}^{n_x} N_{1i} (\pi \dot{x}_i) + \Big(\sum_{j=1}^{n_p} N_{2j} \varrho_j\Big) \pi + N\dot{\pi} && (4.53)\\ &= \textstyle\sum_{i=1}^{n_x} N_{1i} \mu_i + N_2(\varrho) E_d \pi_d + N A_d \pi_d = \bar{N}_1 \mu + (N_2(\varrho) E_d + N A_d) \pi_d = 0. \end{aligned}$$

Identity (4.54) gives back the third row of $N_r(x,p,\varrho)$. Finally, we can observe that

$$(I_{n_x}\ 0_{n_x \times m_1})\, \mu_i = x \dot{x}_i, \tag{4.54}$$

therefore, if we collect vectors $x\, \dot{x}_i$ into a composed vector, we obtain an affine relationship between μ and π_d:

$$\left[I_{n_x} \otimes (I_{n_x}\ 0_{n_x \times m_1})\right] \mu = \begin{pmatrix} x\, \dot{x}_1 \\ \dots \\ x\, \dot{x}_n \end{pmatrix} = (I_{n_x} \otimes x)\, \dot{x} = (I_{n_x} \otimes x)\, H_d\, \pi_d. \tag{4.55}$$

Identity (4.55) gives the last row of annihilator N_r. □

In the following theorem, we present sufficient LMI conditions for stability as proposed by [16].

Theorem 4.6 (based on [16, Theorem 4.1])**.** *Consider system* (3.3) *in representation* (4.41)*, and a Lyapunov function candidate in the form* (4.42)*. Assume that there exist full matrices L and L_r of the appropriate dimensions such that*

$$Q(x,p) + \mathrm{He}\{L\, N(x,p)\} - \underline{\alpha}_0 \left(\begin{smallmatrix} I_{n_x} & 0 \\ 0 & 0 \end{smallmatrix}\right) \succeq 0 \qquad \text{for all } (x,p) \in \mathbf{Ve}(\mathcal{X}\times\mathcal{P}), \tag{4.56a}$$

$$Q_r(x,p,\varrho) + \mathrm{He}\{L_r\, N_r(x,p,\varrho)\} + \alpha_0 \left(\begin{smallmatrix} I_{n_x} & 0 \\ 0 & 0 \end{smallmatrix}\right) \preceq 0 \quad \text{for all } (x,p,\varrho) \in \mathbf{Ve}(\mathcal{X}\times\mathcal{P}\times\mathcal{R}), \tag{4.56b}$$

where Q_r and N_r were defined in (4.44) *and* (4.52)*, respectively. Then, the equilibrium point $x^* = 0$ of system* (3.3) *is locally asymptotically stable.* ◇

4.2.4 Boundary conditions of Trofino and Dezuo (2013)

Note that El Ghaoui and Scorletti [89; 90] and Coutinho et al. [156] used the S-procedure to solve the level-set containment problem $\Omega_1 \subset \mathcal{X}^\circ$. A possible alternative solution to guarantee $\Omega_1 \subset \mathcal{X}^\circ$ is presented by Trofino and Dezuo [16], who considered the following boundary conditions:

$$V(x,p) > 1 \text{ for all } x \in \partial X \text{ and all } p \in \mathcal{P}. \tag{4.57}$$

To formulate convex constraints, inequality (4.57) is enforced over all (convex polytopic) facets $\mathcal{F}_k$ of polytope $\mathcal{X}$, $k = 1, \ldots, m_{\mathcal{X}}$. This result of [16, Section 5.1], which is a consequence of Lemma 3.22, is summarized in the following corollary.

Corollary 4.7 [16]**.** *Consider function $V = \pi^\top Q\, \pi$* (4.42) *over $\mathcal{X}\times\mathcal{P}$ with polytope $\mathcal{X}$ given by its bounding hyperplanes as presented in* (4.32)*. Assume that affine function $N : \mathcal{X}\times\mathcal{P} \to \mathbb{R}^{s\times(n_x+1)}$ satisfies $N(\left(\begin{smallmatrix} 1 \\ \pi \end{smallmatrix}\right)) \equiv 0$ on $\mathcal{X}\times\mathcal{P}$, and consider constant matrices*

$$E_a = \begin{pmatrix} I_{n_x} & 0_{n_x\times m_1} \end{pmatrix},\ N_k = \begin{pmatrix} -1 & a_k^\top E_a \end{pmatrix},\ \text{and } N_k^\perp = \left(\begin{smallmatrix} a_k^\top E_a \\ I_m \end{smallmatrix}\right). \tag{4.58}$$

Suppose that for all $k = 1, \ldots, m_{\mathcal{X}}$ there exists full matrix $L_k \in \mathbb{R}^{(n_x+1)\times s}$, which satisfies

$$\left(N_k^\perp\right)^\top \left(\left(\begin{smallmatrix} -1 & 0 \\ 0 & Q(x,p) \end{smallmatrix}\right) + \mathrm{He}\{L_k N(x,p)\} \right) N_k^\perp \succ 0 \text{ for all } (x,p) \in \mathbf{Ve}(\mathcal{F}_k\times\mathcal{P}). \tag{4.59}$$

Then, $V(x,p) > 1$ for all $x \in \partial\mathcal{X}$ and all $p \in \mathcal{P}$, thus, $\Omega_1 \subset \mathcal{X}^\circ$. ◇

Note that constant matrix N_k satisfies $N_k(\left(\begin{smallmatrix} 1 \\ \pi \end{smallmatrix}\right)) \equiv 0$ on $\mathcal{F}_k \times \mathcal{P}$. According to the implication (3.24c) $\Rightarrow$ (3.24a) of Finsler's lemma, we can conclude that (4.59) implies

$$\left(\begin{smallmatrix} 1 \\ \pi(x,p) \end{smallmatrix}\right)^\top \left(\left(\begin{smallmatrix} -1 & 0 \\ 0 & Q(x,p) \end{smallmatrix}\right) + \mathrm{He}\{L_k N(x,p)\} \right) \left(\begin{smallmatrix} 1 \\ \pi(x,p) \end{smallmatrix}\right) \succ 0 \text{ for all } (x,p) \in \mathcal{F}_k\times\mathcal{P}. \tag{4.60}$$

Evaluating the products in (4.60), we get back the boundary condition in (4.57).

In order to fill $\mathcal{X}$ by Ω_1 us much as possible, Trofino and Dezuo [16] prescribed further boundary inequalities, namely

$$V(x,p) < \tau_k \text{ for all } (x,p) \in \mathcal{F}_k \times \mathcal{P}, \text{ and all } k = 1, \ldots, m_{\mathcal{X}}, \tag{4.61}$$

where the slack variables τ_k are meant to be minimized through the optimization. Similarly to (4.57), these inequalities in (4.61) can be enforced by sufficient LMIs.

4.3 Dissipativity analysis of affine descriptor systems

In this section, we present the powerful theoretical and computational results of [123–127; 192] written for LTI, and a class of multi-affine parameter dependent LPV descriptor systems.

Consider a linear parameter varying LFR system (4.7), where the uncertainty block

is only parameter-dependent, namely, $\Delta(p) = \operatorname{diag}\left(p_1 I_{r_1}, \dots, p_{n_p} I_{r_{n_p}}\right)$ and the possibly time-varying parameter signal p satisfies Assumption 3.1. Similarly to (4.25), let us rewrite (4.7) into the following descriptor model form:

$$\begin{cases} E\dot{\xi} = A(p)\xi + B(p)u \\ y = C\xi + Du \end{cases} \quad \text{with } \xi = \left(\begin{smallmatrix} x \\ \pi \end{smallmatrix}\right) \in \mathbb{R}^{n_x+m}, \tag{4.62}$$

where

$$A = \begin{pmatrix} F_{11} & F_{13} \\ \Delta F_{31} & \Delta F_{33} - I \end{pmatrix}, \; B = \begin{pmatrix} B_u \\ \Delta F_{32} \end{pmatrix}, \tag{4.63}$$

$$E = \left(\begin{smallmatrix} I & 0 \\ 0 & 0 \end{smallmatrix}\right), \; C = \begin{pmatrix} F_{21} & F_{23} \end{pmatrix}, \; D = F_{22}. \tag{4.64}$$

Suppose that the LFR (4.7) is well-posed (i.e., $I - \Delta(p)F_{33}$ is invertible for all $p \in \mathcal{P}$). Then, according to [124, Definition 1], the descriptor system (4.62) is regular and impulse-free if the following assumptions are fulfilled.

Assumption 4.1. Matrix $sE - A(p)$ is regular (with respect to $s \in \mathbb{C}$), i.e., does not exist $p \in \mathcal{P}$, such that the determinant of $sE - A(p) = \left(\begin{smallmatrix} sI_{n_x} - F_{11} & -F_{13} \\ -\Delta(p)F_{31} & I - \Delta(p)F_{33} \end{smallmatrix}\right)$ is identically zero. Furthermore, the pair (E, A) does not have impulsive modes, i.e., does not exist real vectors $v_1, v_2, \dots$, such that $Ev_1 = 0$ and $Ev_k = A(p)v_{k-1}$, $k = 2, 3, 4, \dots$. $\diamond$

Although, the following notions and statements are all applicable for a more general class of descriptor systems (with A, B, C, D being multi-affine functions of p), they all assume that the descriptor system is regular and impulse-free.

The descriptor system (4.62) with the initial condition $\xi(0) = 0$ is said to be dissipative with respect to the supply rate

$$\begin{aligned} s(u, y) &= -\left(\begin{smallmatrix} u \\ y \end{smallmatrix}\right)^\top S \left(\begin{smallmatrix} u \\ y \end{smallmatrix}\right), \\ \text{with } S = S^\top &= \begin{pmatrix} S_{11} & S_{12} \\ S_{12}^\top & S_{22} \end{pmatrix} \in \mathbb{R}^{n_u+n_y \times n_u+n_y}, \; S_{22} = \Gamma_{22}\Gamma_{22}^\top \succ 0, \end{aligned} \tag{4.65}$$

if the following integral quadratic constraint (IQC)

$$\int_0^T s(u(t), y(t)) \mathrm{d}t \geq 0 \tag{4.66}$$

holds for any $T \geq 0$. Note that (4.66) is a special case of the more general integral dissipation inequality (3.15) formulated with a trivial initial condition. According to [123–125], the IQC (4.66) holds if there exist

$$\begin{aligned} &P(p) = \begin{pmatrix} P_1(p) & 0 \\ P_2(p) & P_3(p) \end{pmatrix} \in \mathbb{R}^{(n_x+m)\times(n_x+m)}, \text{ with } P_1(p) = P_1^\top(p) \in \mathbb{R}^{n_x \times n_x}, \\ &W_1(p) = \begin{pmatrix} 0_{n_x \times n_u} \\ W_{12}(p) \end{pmatrix} \in \mathbb{R}^{(n_x+m)\times n_u}, \; W_2(p) = \begin{pmatrix} 0_{n_x \times n_y} \\ W_{22}(p) \end{pmatrix} \in \mathbb{R}^{(n_x+m)\times n_y}, \end{aligned} \tag{4.67}$$

such that

$$P^\top(p)E \succ 0, \tag{4.68a}$$

$$\left(\begin{array}{cc} I & 0 \\ A(p) & B(p) \\ \hline 0 & I \\ C(p) & D(p) \end{array}\right)^\top \left(\begin{array}{cc|cc} \check{P}^\top(p, \varrho)E & P(p) & 0 & 0 \\ P(p) & W_2(p)W_2^\top(p) & W_1(p) & W_2(p)\Gamma_{22}^\top \\ \hline 0 & W_1^\top(p) & S_{11} & S_{12} \\ 0 & \Gamma_{22}W_2^\top(p) & S_{12}^\top & \Gamma_{22}\Gamma_{22}^\top \end{array}\right) \left(\begin{array}{cc} I & 0 \\ A(p) & B(p) \\ \hline 0 & I \\ C(p) & D(p) \end{array}\right) \prec 0, \tag{4.68b}$$

are satisfied for all $(p, \varrho) \in \mathcal{P} \times \mathcal{R}$, where $\check{P}(p, \varrho) = \sum_{i=1}^{n_p} \frac{\partial P}{\partial p_i}(p)\varrho_i$. Applying Schur's complement lemma to (4.68b), we obtain

$$\left(\begin{array}{cc|c} I & 0 & 0 \\ A(p) & B(p) & 0 \\ \hline 0 & I & 0 \\ C(p) & D(p) & 0 \\ \hline 0 & 0 & I \end{array}\right)^\top \left(\begin{array}{cc|cc|c} \check{P}^\top(p, \varrho)E & P(p) & 0 & 0 & 0 \\ P(p) & 0 & W_1(p) & 0 & W_2(p) \\ \hline 0 & W_1^\top(p) & S_{11} & S_{12} & 0 \\ 0 & 0 & S_{12}^\top & 0 & \Gamma_{22} \\ \hline 0 & W_2^\top(p) & 0 & \Gamma_{22}^\top & -I \end{array}\right) \left(\begin{array}{cc|c} I & 0 & 0 \\ A(p) & B(p) & 0 \\ \hline 0 & I & 0 \\ C(p) & D(p) & 0 \\ \hline 0 & 0 & I \end{array}\right) \prec 0. \tag{4.69}$$

Two equivalent (expanded and bilinear) form of (4.69) is

$$\begin{pmatrix} \mathrm{He}\{P^\top(p)A(p)\} + \check{P}^\top(p,\varrho)E & P^\top(p)B(p) + C^\top(p)S_{12}^\top + A^\top(p)W_1(p) & C^\top(p)\Gamma_{22} + A^\top(p)W_2(p) \\ B^\top(p)P(p) + S_{12}C(p) + W_1^\top(p)A(p) & S_{11} + \mathrm{He}\{S_{12}D(p) + W_1^\top(p)B(p)\} & D^\top(p)\Gamma_{22} + C^\top(p)W_2(p) \\ \Gamma_{22}^\top C(p) + W_2^\top(p)A(p) & \Gamma_{22}^\top D(p) + W_2^\top(p)B(p) & -I \end{pmatrix} \tag{4.70}$$

$$= \mathrm{He}\left\{ \begin{pmatrix} P^\top(p) & 0 & 0 \\ W_1^\top(p) & I_{n_u} & 0 \\ W_2^\top(p) & 0 & I_{n_y} \end{pmatrix} \begin{pmatrix} I_{n_x} & 0 \\ 0 & S_{12} \\ 0 & \Gamma_{22}^\top \end{pmatrix} \begin{pmatrix} A(p) & B(p) & 0 \\ C(p) & D(p) & 0 \end{pmatrix} \right\} + \begin{pmatrix} \check{P}^\top(p,\varrho)E & 0 & 0 \\ 0 & S_{11} & 0 \\ 0 & 0 & -I_{n_y} \end{pmatrix} \prec 0. \tag{4.71}$$

According to [125], $P(p)$ is non-singular as it satisfies (4.68) with $S_{22} \succeq 0$. Let us introduce the following (non-singular) transformation matrix

$$T(p) = \begin{pmatrix} Q(p) & 0 & 0 \\ Z_1(p) & I_{n_u} & 0 \\ Z_2(p) & 0 & I_{n_y} \end{pmatrix}, \text{ where } Z_1(p) = -W_1^\top(p)P(p),\ Z_2(p) = -W_2^\top(p)P(p) \tag{4.72}$$

$$\text{and } Q(p) \in \mathbb{R}^{(n_x+m)\times(n_x+m)}, \text{ such that } P(p)\,Q^\top(p) = Q(p)\,P^\top(p) = I. \tag{4.73}$$

If we pre- and post-multiply (4.71) by $T(p)$ and $T^\top(p)$, respectively, we finally obtain the PD-LMI condition [125, Eq. (5) and (6)] sufficient for the dissipation inequality. These results of [125] are summarized in the following theorem.

Theorem 4.8 [123–125]**.** *Consider a linear parameter varying descriptor system*

$$\Sigma_d : \begin{cases} E\dot{\xi} = A(p)\xi + B(p)u, \\ y = C(p)\xi + D(p)u, \end{cases} \tag{4.74}$$

$$\text{with } E = \begin{pmatrix} I_{n_x} & 0 \\ 0 & 0_{m\times m} \end{pmatrix},\ A(p) = \begin{pmatrix} A_{11}(p) & A_{12}(p) \\ A_{21}(p) & A_{22}(p) \end{pmatrix},\ \xi = \begin{pmatrix} x \\ \pi \end{pmatrix} \in \mathbb{R}^{n_x+m},$$

where $A_{22}(p)$ is non-singular for all $p \in \mathcal{P}$. The following statements are equivalent:

1. *There exist functions P, W_1, W_2 of p as defined in* (4.67)*, such that $P^\top(p)E \succeq 0$ and* (4.71) *are satisfied for all $p \in \mathcal{P}$.*

2. *There exist functions Q, Z_1, Z_2 of p:*

$$Q(p) = \begin{pmatrix} Q_1(p) & Q_2(p) \\ 0 & Q_3(p) \end{pmatrix} \in \mathbb{R}^{(n_x+m)\times(n_x+m)},\ \text{with } Q_1(p) = Q_1^\top(p) \in \mathbb{R}^{n_x\times n_x}, \tag{4.75}$$

$$Z_1(p) = (0_{n_u\times n_x}\ Z_{12}(p)) \in \mathbb{R}^{n_u\times(n_x+m)},\ Z_2(p) = \big(0_{n_y\times n_x}\ Z_{22}(p)\big) \in \mathbb{R}^{n_y\times(n_x+m)},$$

such that they satisfy $Q(p)E \succeq 0$ and the "pseudo-dual" matrix inequality

$$\mathrm{He}\left\{ \begin{pmatrix} I_{n_x} & 0 \\ 0 & S_{12} \\ 0 & \Gamma_{22}^\top \end{pmatrix} \begin{pmatrix} A(p) & B(p) & 0 \\ C(p) & D(p) & 0 \end{pmatrix} \begin{pmatrix} Q^\top(p) & Z_1^\top(p) & Z_2^\top(p) \\ 0 & I_{n_u} & 0 \\ 0 & 0 & I_{n_y} \end{pmatrix} \right\} + \begin{pmatrix} -E\check{Q}^\top(p,\varrho) & 0 & 0 \\ 0 & S_{11} & 0 \\ 0 & 0 & -I_{n_y} \end{pmatrix} \prec 0. \tag{4.76}$$

for all $(p,\varrho) \in \mathcal{P}\times\mathcal{R}$, where $\check{Q}(p,\varrho) = \sum_{i=1}^{n_p} \frac{\partial Q}{\partial p_i}(p)\varrho_i$.

3. *System Σ_d is dissipative with respect to the supply rate* (4.65)*.* ◇

Until to this point, we did not discuss about a storage function of system Σ_d. We will demonstrate that the PD-LMI (4.70) corresponds to a dissipation inequality with a (practically quadratic) storage function

$$V(x) = \xi^\top P^\top(p)E\xi = x^\top P_1(p)\,x, \tag{4.77}$$

Let $\varphi = \Gamma_{22}y$ denote the artificial signal introduced through the Schur's complement lemma. Furthermore, we pre- and post-multiply LMI (4.70) by $(x^\top\ u^\top\ \varphi^\top)$ and by its transpose. Then, we obtain:

$$\mathrm{He}\big\{x^\top P^\top(p)E\dot{x}\big\} + x^\top\dot{P}^\top(p)Ex + \mathrm{He}\big\{\varphi^\top W_1^\top(p)Eu\big\} + \mathrm{He}\big\{\varphi^\top W_2^\top(p)E\dot{x}\big\} - s(u,y) < 0 \tag{4.78}$$

Observe that $W_1^\top(p)E = 0$, $W_2^\top(p)E = 0$, and $P^\top(p)E = E^\top P(p)$, each for all $p \in \mathcal{P}$, therefore, inequality (4.78) simplifies to $\dot{V} < s(u,y)$.

4.3.1 Cross-corner evaluation technique of Masubuchi (1999)

It is worth mentioning that both the primal and the dual matrix inequalities in (4.71) and (4.76), respectively, are often infinite-dimensional problems in the sense, that the inequalities should be tested in infinitely many points over $\mathcal{P}$. However, if we assume that $A, B, C, D, P, Q, W_1, W_2, Z_1, Z_2$ are all multi-affine functions of p, the relaxation technique of Masubuchi [126; 127] makes possible to formulate a system of ordinary LMIs, which together imply the nonlinear PD-LMI ((4.71) or (4.76)). This relaxation method can be considered a (non-trivial) extension of the corner evaluation technique for affine PD-LMIs defined over polytopes (Proposition 3.20).

In this section, the dimension of vector p is denoted by $n = n_p$ for simplicity.

Definition 4.9 [126, Section 2.2]**.** *Function $F : \mathcal{P} \to \mathbb{R}^{m_1 \times m_2}$ is called a multi-affine function of $(p_1, \dots, p_n) \in \mathcal{P}$ (or simply $p \in \mathcal{P}$) if F is affine with respect to any single independent variable p_i while the other variables are fixed. Formally,*

$$F(p) = \sum_{\tau \in \mathcal{I}_n} F_\tau \prod_{i=1}^{n} p_i^{\tau_i}, \text{ where } \mathcal{I}_n = \{\tau = (\tau_1, \tau_2, \dots, \tau_n) \,|\, \tau_i \in \{0, 1\},\ i = 1, \dots, n\}.$$

and $F_\tau = F_{\tau_1 \tau_2 \dots \tau_n} \in \mathbb{R}^{m_1 \times m_2}$ are constant matrices. Furthermore, $\mathcal{P}$ is a hyper-rectangle in $\mathbb{R}^n$, namely

$$\mathcal{P} = \bigtimes_{i=1}^{n} \left[\underline{p}_i, \overline{p}_i\right]. \tag{4.79}$$

Each "tuple of indices" τ in $\mathcal{I}_n$ corresponds to a vertex p_τ of $\mathcal{P}$, e.g.,

$$(0, \dots, 0) \mapsto (\underline{p}_1, \dots, \underline{p}_n),\ (1, \dots, 1) \mapsto (\overline{p}_1, \dots, \overline{p}_n),$$
$$(\dots, 0^{(ith)}, \dots) \mapsto (\dots, \underline{p}_i, \dots),\ (\dots, 1^{(ith)}, \dots) \mapsto (\dots, \overline{p}_i, \dots). \qquad \diamond$$

Differently, from [126; 127], we introduce an equivalence relation on $\mathcal{I}_n \times \mathcal{I}_n$ to simplify the further notations. Consider two pair of tuples (τ, μ) and $(\tau', \mu') \in \mathcal{I}_n \times \mathcal{I}_n$. Let say that (τ, μ) and (τ', μ') are equivalent if (τ', μ') can be obtained from (τ, μ) by interchanging one or more corresponding coordinates in tuples τ and μ, e.g.,

$$\big((\tau_1,\dots,\tau_i,\dots,\tau_n),(\mu_1,\dots,\mu_i,\dots,\mu_n)\big) \equiv \big((\tau_1,\dots,\mu_i,\dots,\tau_n),(\mu_1,\dots,\tau_i,\dots,\mu_n)\big). \tag{4.80}$$

If $n = 2$, the following pairs of tuples from $\mathcal{I}_2 \times \mathcal{I}_2$ are equivalent

$$(\mathscr{P}_{2,9}:) \quad \big((0,0),(1,1)\big) \equiv \big((0,1),(1,0)\big) \equiv \big((1,1),(0,0)\big) \equiv \big((1,0),(0,1)\big). \tag{4.81}$$

Each pair in (4.81), was obtained by swapping the corresponding coordinates of the previous pair. This equivalence relation generates a partitioning of $\mathcal{I}_n \times \mathcal{I}_n$, namely,

$$\bigcup_{k=1}^{3^n} \mathscr{P}_{n,k} = \mathcal{I}_n \times \mathcal{I}_n, \tag{4.82}$$

where partitions $\mathscr{P}_{n,k}$ are pairwise disjoint, namely, $\mathscr{P}_{n,k} \cap \mathscr{P}_{n,l} = \varnothing$ if $k \neq l$.

It can be shown that a partition $\mathscr{P}_{n,k}$ may have 1, 2, ..., or 2^n number of distinct elements from $\mathcal{I}_n \times \mathcal{I}_n$. Furthermore, $C_n^i \cdot 2^{n-i}$ number of distinct partitions exist, which have 2^i elements, $i = 0, \dots, n$. Then, we can show that the number of partitions in total is 3^n, whereas, the number of elements in $\mathcal{I}_n \times \mathcal{I}_n$ is 2^{2n}. In Appendix A, we provided the partitioning of $\mathcal{I}_n \times \mathcal{I}_n$ for $n = 1, 2, 3$.

In the following lemma we present an important result of Masubuchi [126], namely a special case of [126, Lemma 4].

Lemma 4.10. *Consider two multi-affine functions $F : \mathbb{R}^n \to \mathbb{R}^{m_1 \times m_2}$ and $G : \mathbb{R}^n \to \mathbb{R}^{m_2 \times m_3}$. Let "$<$" denote a partial ordering on $\mathbb{R}^{m_1 \times m_3}$. Let p_τ denote the vertex of*

hyper-rectangle $\mathcal{P}$ *corresponding to the tuple of indices* $\tau \in \mathcal{I}_n$. *Suppose that*

$$\sum_{(\tau,\mu)\in\mathscr{P}_{n,k}} F(p_\tau)G(p_\mu) < 0, \text{ for all } k = 1,\dots,3^n. \tag{4.83}$$

Then, $F(p)G(p) < 0$ *for all* $p \in \mathcal{P}$. ◇

Lemma 4.10 is a special case of [126, Lemma 4] in the sense that [126] considered a more general class of functions, namely, piecewise multi-affine functions. Therefore, [126] proposed to split up $\mathcal{P}$ into sub-domains.

Lemma 4.10 has an important consequence.

Corollary 4.11. *Consider two multi-affine functions* $F : \mathbb{R}^{n_p+n_\varrho} \to \mathbb{R}^{m_1\times m_2}$ *and* $G : \mathbb{R}^{n_p} \to \mathbb{R}^{m_2\times m_3}$. *Let "*$<$*" denote a partial ordering on* $\mathbb{R}^{m_1\times m_3}$. *Let* p_{τ_1} *and* ϱ_{τ_2} *denote the appropriate vertex of hyper-rectangles* $\mathcal{P} \subset \mathbb{R}^{n_p}$ *and* $\mathcal{R} \in \mathbb{R}^{n_\varrho}$, *respectively, where* $\tau_1 \in \mathcal{I}_{n_p}$ *and* $\tau_2 \in \mathcal{I}_{n_\varrho}$, *respectively. Suppose that*

$$\sum_{(\tau_1,\mu_1)\in\mathscr{P}_{n_p,k}} F(p_{\tau_1},\varrho_{\tau_2})G(p_{\mu_1}) < 0 \text{ for all } k = 1,\dots,n^3 \text{ and all } \tau_2 \in \mathcal{I}_{n_\varrho}. \tag{4.84}$$

Then, $F(p,\varrho)G(p) < 0$ *for all* $(p,\varrho) \in \mathcal{P}\times\mathcal{R}$. ◇

In Corollary 4.11, we provided sufficient conditions to test an inequality, which is multi-affine in ϱ but contains products of multi-affine functions in p. In this case, it is enough the test the inequality only in the corner points of $\mathcal{R}$ with respect to ϱ. However, with respect to p, the inequality should be evaluated as presented in Lemma 4.10.

A further consequence of Corollary 4.11 is that a multi-affine parameter-dependent inequality can be enforced on a hyperrectangle $\mathcal{P}$ by testing its feasibility in the corner points of $\mathcal{P}$.

Finally, observe that the bilinear form of the dissipation inequality (4.71) (but also its dual formulation (4.76)) can be written in the form

$$\mathrm{He}\{F(p)G(p)\} + H(p,\varrho), \tag{4.85}$$

where F and G are multi-affine functions of p, and H is a multi-affine function of (p,ϱ). Therefore, both PD-LMIs (4.71) and (4.76) can be ensured by testing their feasibility as presented in Corollary 4.11.

4.4 Performance analysis for LPV systems using integral quadratic constraints

In this section, we study one of the most powerful state-of-the-art approaches for robust analysis and controller synthesis. Without going into the technicalities, we provide a slight insight into the IQC-framework with a special interest in the stability and performance analysis of nominal LPV plants with rate-bounded parameters and dynamic multipliers.

The major idea behind the IQC-theory is to encapsulate the input-output relations of an uncertain nonlinear (static or dynamic) operator Δ into a so-called *integral quadratic constraint* of the form

$$\int_{-\infty}^{\infty} \begin{pmatrix} \hat\eta(i\omega) \\ \hat\pi(i\omega) \end{pmatrix}^\top \Pi(i\omega) \begin{pmatrix} \hat\eta(i\omega) \\ \hat\pi(i\omega) \end{pmatrix} \mathrm{d}\omega \geq 0, \text{ and } \Delta : \eta \mapsto \pi = \Delta\eta, \tag{4.86}$$

where $\hat\eta$, $\hat\pi$ denote the Fourier transforms of signals η, π, respectively, $i = \sqrt{-1}$ denotes the imaginary unit, ω denotes the angular frequency. The (possibly static) transfer function Π is called a multiplier.

As it already appeared in (4.66), a dissipativity relation can be written in the form of an IQC (4.86). For instance, the fact that block Δ is passive can be captured by $\Pi = \left(\begin{smallmatrix} 0 & I \\ I & 0 \end{smallmatrix}\right)$, or $\Pi = \left(\begin{smallmatrix} \kappa^2 I & 0 \\ 0 & I \end{smallmatrix}\right)$ describes that operator Δ has an induced $\mathcal{L}_2$-gain smaller than or equal to κ.

Consider again the LPV system Σ in (4.1) in the LFR (4.7). Let s denote the Laplace operator, and observe that the input-output relationship of Σ can be given by the following feedback interconnection system

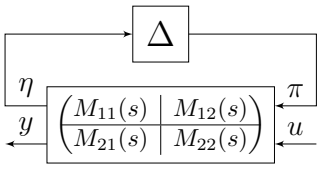

$$\Sigma : \begin{cases} \eta = M_{11}(s)\pi + M_{12}(s)u, \\ y = M_{21}(s)\pi + M_{22}(s)u, \\ \pi = \Delta\eta, \qquad \text{where } M(s) = \left(\begin{smallmatrix} M_{11}(s) & M_{12}(s) \\ M_{21}(s) & M_{22}(s) \end{smallmatrix}\right). \end{cases} \tag{4.87}$$

Let a possible state-space realization of $M(s)$ be written in the following lower LFR:

$$M(s) = \mathcal{F}_l\left\{ \left(\begin{array}{cc|c} F_{33} & F_{32} & F_{31} \\ F_{23} & F_{22} & F_{21} \\ \hline F_{13} & F_{12} & F_{11} \end{array}\right), \tfrac{1}{s} I_{n_x} \right\}. \tag{4.88}$$

Setting $u \equiv 0$, the autonomous part of system (4.87) is given by the feedback interconnection system below:

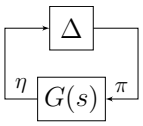

$$\begin{cases} \eta = G(s)\pi, \\ \pi = \Delta\eta, \end{cases} \quad \text{where } G(s) = M_{11}(s) = \mathcal{F}_l\left\{ \left(\begin{array}{c|c} F_{33} & F_{31} \\ \hline F_{13} & F_{11} \end{array}\right), \tfrac{1}{s} I_{n_x} \right\}. \tag{4.89}$$

Now, we present the celebrated IQC stability criterion of Megretski and Rantzer [99] for the interconnected system (4.89).

Theorem 4.12 [99, Theorem 1]**.** *Assume that the set of admissible uncertainty* ($\boldsymbol{\Delta}$) *is star shaped namely* $\tau\Delta \in \boldsymbol{\Delta}$ *if* $\Delta \in \boldsymbol{\Delta}$ *and* $\tau \in [0,1]$*. Consider a stable LTI system* $G(s)$ *and let* $\Delta \in \boldsymbol{\Delta}$*. Assume that*

1. *the feedback interconnection system* (4.89) *is well-posed for* $\tau\Delta$*,* $\tau \in [0,1]$*, namely,* $I_m - \tau F_{33}\Delta$ *is nonsingular,*
2. *for all* $\tau \in [0,1]$*, the IQC* (4.86) *defined by* $\Pi = \Pi^*$ *is satisfied by* $\tau\Delta$*,*
3. *there exists* $\epsilon > 0$ *such that*
$$\left(\begin{smallmatrix} G(i\omega) \\ I \end{smallmatrix}\right)^* \Pi(i\omega) \left(\begin{smallmatrix} G(i\omega) \\ I \end{smallmatrix}\right) + \epsilon I \preceq 0, \text{ for all } \omega \in \mathbb{R}. \tag{4.90}$$

Then, the feedback interconnection of operators $G(s)$ *and* Δ *is stable.*

If assumptions 1. and 2. hold for every $\Delta \in \boldsymbol{\Delta}$*, the interconnection is* ***robustly*** *stable (i.e., for all admissible* $\Delta \in \boldsymbol{\Delta}$*).* ◇

According to [110], the results of Theorem 4.12 can be extended for dissipativity analysis by "injecting a performance channel" into the frequency-domain inequality (4.90).

Corollary 4.13 [110, Corollary 3]**.** *Assume that*

1. *the feedback interconnection system* (4.87) *is well-posed for all* $\Delta \in \boldsymbol{\Delta}$*,*
2. *the IQC* (4.86) *defined by* $\Pi = \Pi^*$ *is satisfied by all* $\Delta \in \boldsymbol{\Delta}$*,*
3. *there exists* $\epsilon > 0$ *such that*
$$\left(\begin{smallmatrix} M_{11}(i\omega) & M_{12}(i\omega) \\ I & 0 \\ M_{21}(i\omega) & M_{22}(i\omega) \\ 0 & I \end{smallmatrix}\right)^* \left(\begin{smallmatrix} \Pi(i\omega) & 0 \\ 0 & S \end{smallmatrix}\right) \left(\begin{smallmatrix} M_{11}(i\omega) & M_{12}(i\omega) \\ I & 0 \\ M_{21}(i\omega) & M_{22}(i\omega) \\ 0 & I \end{smallmatrix}\right) + \epsilon I \preceq 0, \text{ for all } \omega \in \mathbb{R}. \tag{4.91}$$

Then, the feedback interconnection of LTI system $M(s)$ and the uncertain operator Δ is robustly stable and robust performance with respect to the supply rate $s(u,y) = \left(\begin{smallmatrix} y \\ u \end{smallmatrix}\right)^\top S \left(\begin{smallmatrix} y \\ u \end{smallmatrix}\right)$ is guaranteed. ◇

***Remark* 4.5.** The Laplace operator and the supply function are denoted by the same latter s, however, they can be identified obviously as their roles are different. ◇

Note that, the choice of the IQC multiplier Π constitutes an important degree of freedom in the analysis problem, which makes possible to represent a wide variety of uncertain perturbations. In this section, we focus on parametric uncertainty

$$\boldsymbol{\Delta} = \Big\{ \Delta \circ p \,\big|\, \Delta(p) = \operatorname{diag}\{p_i I_{r_i}\}_{i=1,\dots,n_p},\ p : [0,\infty) \to \mathcal{P},\ \dot{p} : (0,\infty) \to \mathcal{R} \Big\}, \tag{4.92}$$

with rate-bounded parameters p satisfying Assumptions 3.1, where $\mathcal{P}$ and $\mathcal{R}$ are a bounded polytopes and $0 \in \mathcal{P}$. Observe that $\Delta : p \mapsto \Delta(p)$ is a linear function of $p \in \mathcal{P}$, therefore, $\dot{\Delta}(p(t)) = \Delta(\dot{p}(t))$.

Observe that in Corollary 4.13, the (physical) limitations on $\dot{p}$ are not taken into consideration. Therefore, the inequality (4.90) formulated with a given multiplier Π would give a conservative solution, as it is satisfied for all (essentially) bounded parameter signal $p : [0,\infty) \to \mathcal{P}$.

In order to inject the parameter rates into the stability analysis, Helmersson [103] proposed to use the *swapping lemma* of Jönsson [102]. Before we formulate the swapping lemma, we need to introduce some auxiliary notations. First, consider the transfer function T as follows

$$T(s) = \operatorname{diag}\{T_i(s)\}_{i=1,\dots,n_p} = \mathcal{F}_l\left\{ \left(\begin{array}{c|c} \hat{D} & \hat{C} \\ \hline \hat{B} & \hat{A} \end{array}\right), \tfrac{1}{s} I_{n'} \right\}, \tag{4.93}$$

$$\text{where } T_i(s) = \mathcal{F}_l\left\{ \left(\begin{array}{c|c} \hat{D}_i & \hat{C}_i \\ \hline \hat{B}_i & \hat{A}_i \end{array}\right), \tfrac{1}{s} I_{n'_i} \right\} \in \mathbb{C}^{m'_i \times r_i}. \tag{4.94}$$

Integers n'_i and m'_i denote the number of states and outputs, respective, of operator $T_i(s)$. Throughout the dissertation, integer r_i denotes the dimension of the ith parameter block $(p_i I_{r_i})$ in operator Δ. Obviously, matrices $\hat{D}$, $\hat{C}$, $\hat{B}$, $\hat{A}$ are all block diagonal matrices of blocks

$$\hat{D}_i \in \mathbb{R}^{m'_i \times r_i},\ \hat{C}_i \in \mathbb{R}^{m'_i \times n'_i},\ \hat{B}_i \in \mathbb{R}^{n'_i \times r_i},\ \hat{A}_i \in \mathbb{R}^{n'_i \times n'_i}, \tag{4.95}$$

respectively.

Due to its specific block diagonal structure, $T(s)$ fulfills an important algebraic relation, which is summarized in a special case of the swapping lemma.

Lemma 4.14 [104, Lemma 1]**.** *Consider operator $T(s)$ in (4.93) and let*

$$U(s) = \mathcal{F}_l\left\{ \left(\begin{array}{c|c} 0 & \hat{C} \\ \hline I & \hat{A} \end{array}\right), \tfrac{1}{s} I_{n'} \right\},\ V(s) = \mathcal{F}_l\left\{ \left(\begin{array}{c|c} 0 & I \\ \hline \hat{B} & \hat{A} \end{array}\right), \tfrac{1}{s} I_{n'} \right\}, \tag{4.96}$$

$$\hat{\Delta} : p \mapsto \operatorname{diag}\Big\{ p_i I_{n'_i} \Big\}_{i=1,\dots,n_p},\ \bar{\Delta} : p \mapsto \operatorname{diag}\Big\{ p_i I_{m'_i} \Big\}_{i=1,\dots,n_p}. \tag{4.97}$$

Assume that the real part of the eigenvalues of $\hat{A}$ are strictly negative. Then,

$$\begin{pmatrix} T(s) & U(s) \\ 0 & I \end{pmatrix} \begin{pmatrix} \Delta \\ \dot{\Delta} V(s) \end{pmatrix} = \begin{pmatrix} \bar{\Delta} & 0 \\ 0 & \dot{\bar{\Delta}} \end{pmatrix} \begin{pmatrix} T(s) \\ V(s) \end{pmatrix}. \qquad \diamond$$

***Remark* 4.6.** Due to their block diagonal structure, matrices in (4.93) and (4.97) satisfy the following identity:

$$\begin{pmatrix} \hat{A} & \hat{B} \\ \hat{C} & \hat{D} \end{pmatrix} \begin{pmatrix} \hat{\Delta} & 0 \\ 0 & \Delta \end{pmatrix} = \begin{pmatrix} \hat{\Delta} & 0 \\ 0 & \bar{\Delta} \end{pmatrix} \begin{pmatrix} \hat{A} & \hat{B} \\ \hat{C} & \hat{D} \end{pmatrix}. \tag{4.98}$$

Lemma 4.14 can be considered as a special case of [103, Lemma 1]. ◇

Provided by Lemma 4.14, a specific IQC-type certificate can be formulated for the robust stability of interconnection (4.89).

Theorem 4.15 [103, Theorem 2]**.** *Assume that* $\Delta \circ p \in \mathbf{\Delta}$ (4.92) *is a bounded parameter uncertainty and there exists a symmetric matrix* P *satisfying*

$$\begin{pmatrix} I & 0 \\ 0 & I \\ \bar{\Delta}(p) & 0 \\ 0 & \hat{\Delta}(\varrho) \end{pmatrix}^{\top} P \begin{pmatrix} I & 0 \\ 0 & I \\ \bar{\Delta}(p) & 0 \\ 0 & \hat{\Delta}(\varrho) \end{pmatrix} \succeq 0 \text{ for all } (p, \varrho) \in \mathcal{P} \times \mathcal{R}. \tag{4.99a}$$

Then, the interconnection (4.89) *of* $G(s)$ *and* Δ *is robustly stable for any admissible parameter trajectory* p *satisfying Assumptions 3.1 if*

$$\begin{pmatrix} G(i\omega) & 0 \\ I & 0 \\ 0 & I \end{pmatrix}^{*} \Pi(i\omega) \begin{pmatrix} G(i\omega) & 0 \\ I & 0 \\ 0 & I \end{pmatrix} + \epsilon I \preceq 0 \tag{4.99b}$$

is satisfied for all $\omega \in \mathbb{R} \cup \{\infty\}$ *and some* $\epsilon > 0$*, where*

$$\Pi(s) = \Psi^{*}(s)\, P\, \Psi(s), \quad \text{and } \Psi(s) = \begin{pmatrix} T(s) & 0 & 0 \\ V(s) & 0 & 0 \\ 0 & T(s) & U(s) \\ 0 & 0 & I \end{pmatrix} \tag{4.100}$$

constitutes the IQC multiplier of the IQC program. ◇

The IQC certificates in (4.99) correspond to the original IQC stability criterion of Theorem 4.12, but written in a different form and applied to the following augmented interconnection system:

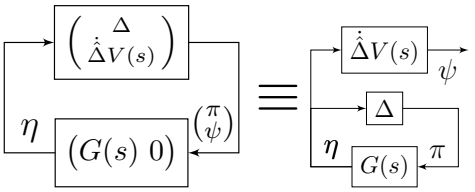

$$\begin{cases} \eta = G(s)\pi, \\ \pi = \Delta\eta, \\ \psi = \dot{\hat{\Delta}}V(s)\eta. \end{cases} \equiv \begin{cases} \eta = (G(s)\ 0)\binom{\pi}{\psi}, \\ \binom{\pi}{\psi} = \begin{pmatrix} \Delta \\ \dot{\hat{\Delta}}V(s) \end{pmatrix}\eta. \end{cases} \tag{4.101}$$

It is worth mentioning that the internal dynamics of (4.89) is not altered, but an auxiliary (practically output) signal ψ is introduced, which depends on the parameter's time-derivative. In this way, the IQC-type constraint (4.99a) corresponding to (4.101) involves $\dot{p} = \varrho$. As the rate bounds in (4.99) are taken into consideration, these conditions are less conservative than the IQC certificates of Theorem 4.12.

As the reader may have observed, (4.99a) is a time-domain matrix inequality, whereas, in Theorem 4.12, the corresponding constraint (4.86) is given as a frequency-domain IQC. In [103], it is shown that (4.99a) has the following frequency-domain IQC equivalent:

$$\int_{-\infty}^{\infty} \begin{pmatrix} \hat{\eta}(i\omega) \\ \hat{\pi}(i\omega) \\ \hat{\psi}(i\omega) \end{pmatrix}^{*} \Pi(i\omega) \begin{pmatrix} \hat{\eta}(i\omega) \\ \hat{\pi}(i\omega) \\ \hat{\psi}(i\omega) \end{pmatrix} \mathrm{d}\omega \geq 0. \tag{4.102}$$

As the final step, we seek for an IQC-type certificate for the robust stability and performance of an input-output feedback interconnection with rate-bounded parameters. Following the technique of Theorem 4.15, we introduce again the output signal ψ as it was done in (4.101):

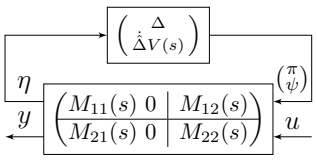

$$\begin{cases} \eta = M_{11}(s)\pi + M_{12}(s)u, \\ y = M_{21}(s)\pi + M_{22}(s)u, \\ \pi = \Delta\eta, \\ \psi = \dot{\hat{\Delta}}V(s)\eta, \end{cases} \equiv \begin{cases} \eta = (M_{11}(s)\ 0)\binom{\pi}{\psi} + M_{12}(s)u, \\ y = (M_{21}(s)\ 0)\binom{\pi}{\psi} + M_{22}(s)u, \\ \binom{\pi}{\psi} = \begin{pmatrix} \Delta \\ \dot{\hat{\Delta}}V(s) \end{pmatrix}\eta. \end{cases} \tag{4.103}$$

Finally, an IQC specification for system (4.101) can be formulated obviously, by following Corollary 4.13 and Theorem 4.15.

Corollary 4.16. *Assume that* $\Delta \circ p \in \mathbf{\Delta}$ (4.92) *is a bounded parameter uncertainty and*

there exists a symmetric matrix P *satisfying* (4.99a). *Consider multiplier* Π *in* (4.100). *Then, the feedback interconnection* (4.87) *of operators* $M(s)$ *and* Δ *is robustly stable and robust performance with respect to the supply rate* $s(u,y) = \left(\begin{smallmatrix} y \\ u \end{smallmatrix}\right)^\top S \left(\begin{smallmatrix} y \\ u \end{smallmatrix}\right)$ *is guaranteed if*

$$\begin{pmatrix} M_{11}(i\omega) & 0 & M_{12}(i\omega) \\ I & 0 & 0 \\ 0 & I & 0 \\ M_{21}(i\omega) & 0 & M_{22}(i\omega) \\ 0 & 0 & I \end{pmatrix}^* \begin{pmatrix} \Pi(i\omega) & 0 \\ 0 & S \end{pmatrix} \begin{pmatrix} M_{11}(i\omega) & 0 & M_{12}(i\omega) \\ I & 0 & 0 \\ 0 & I & 0 \\ M_{21}(i\omega) & 0 & M_{22}(i\omega) \\ 0 & 0 & I \end{pmatrix} + \epsilon I \preceq 0, \tag{4.104}$$

is satisfied for all $\omega \in \mathbb{R} \cup \{\infty\}$ *and some* $\epsilon > 0$. ◇

***Remark* 4.7.** Applying the celebrated Kalman-Yakubovich-Popov (KYP) lemma [193] the frequency-domain inequalities in (4.90), (4.91), (4.99b), (4.104) can be enforced by equivalent LMIs. ◇

4.4.0.1 IQC software tools. In this paragraph, we present two IQC analysis implementations, namely, *LPVMAD – The IQC analysis tool* (LPVMAD) [112], and the `lpvwcgain` method of `plftss` class in LPVTools [113]. Both implementations are based on Corollary 4.104, however, the selection for $T(s)$ in the two implementation are different. In LPVMAD, the structure of the dynamic multiplier of the IQC problem is defined by $T(s) = \text{blkdiag}(T_i(s))$, $T_i(s) = \begin{pmatrix} I_{r_i} \\ a(s) \otimes I_{r_i} \end{pmatrix}$, $i = 1,2,3$, where $a(s)$ is a column vector of some basis transfer functions. LPVMAD's default value for $a(s)$ is $a(s) = \left(\frac{1}{s+1}\right)$. Whereas, in `lpvwcgain` $T_i(s) = \begin{pmatrix} (1 \dots 1) \otimes a(s) \\ I_{r_i} \end{pmatrix}$, $i = 1,2,3$, where the poles in $a(s)$ are selected algorithmically by LPVTools. On the other hand, LPVMAD solves the KYP (time-domain) LMIs, whereas, `lpvwcgain` enforces the corresponding frequency-domain inequalities on a frequency grid using the iterative cutting plane algorithm of [194]. ▲

10.15774/PPKE.ITK.2021.004

Chapter 5

Computational framework for the analysis of dynamical systems

In this chapter, I provide an efficient computational framework for stability, dissipativity and nominal performance analysis of nonlinear systems with time-varying and rate-bounded parametric uncertainty.

5.1 Motivation – domain of attraction computation

As an introductory motivation example, let us consider the van der Pol oscillator introduced by the Dutch electrical engineer and physicist Balthasar van der Pol. The dynamical motion of the oscillator is described by the following scalar ordinary differential equation [195, Eq. (6)]:

$$\ddot{y} - p\,(1 - y^2)\dot{y} + y = 0. \tag{5.1}$$

If p is a positive constant the dynamics of (5.1) has a globally stable limit cycle.

In this chapter, we consider the time-reversed dynamics of (5.1) in the following state space model

$$\Sigma_a : \ \dot{x} = f(x,p) = A(x,p)x, \ \text{with } x(0) \in \mathcal{X}, \tag{5.2}$$

where

$$A(x,p) = \begin{pmatrix} 0 & -1 \\ 1 & x_1^2 p - p \end{pmatrix} x, \ \text{and } x(t) = \begin{pmatrix} x_1(t) \\ x_2(t) \end{pmatrix} = \begin{pmatrix} y(-t) \\ \dot{y}(-t) \end{pmatrix}. \tag{5.3}$$

Let p be an uncertain (possibly time-varying) parameter satisfying Assumption 3.1 with $\mathcal{P} \subset (0,\infty)$ and $\mathcal{R} = [-\overline{\varrho}, \overline{\varrho}]$.

The origin of the time-reversed model (5.3) is locally asymptotically stable. To prove local stability and compute a positively invariant domain, we seek for a local Lyapunov function V in a specific parameterized form, which will be described later.

5.1.1 Dynamical model representation

In general, we assume that function A in (5.2) is a well-defined rational function of $(x,p) \in \mathcal{X} \times \mathcal{P}$, consequently, A admits a well-posed LFR:

$$A(x,p) = \mathcal{F}_l\left\{ \begin{pmatrix} F_{11} & F_{12} \\ F_{21} & F_{22} \end{pmatrix}, \Delta(x,p) \right\} \in \mathbb{R}^{n_x \times n_x}, \ \text{with } \Delta(x,p) \in \mathbb{R}^{m_1 \times m_1}. \tag{5.4}$$

Then, the dynamics can be given by the following feedback interconnection:

$$\mathcal{F}(\Sigma_a) : \begin{pmatrix} \dot{x} \\ \eta_1 \end{pmatrix} = \begin{pmatrix} F_{11} & F_{12} \\ F_{21} & F_{22} \end{pmatrix} \begin{pmatrix} x \\ \pi_1 \end{pmatrix}, \ \text{with } \pi_1 = \Delta\,\eta_1, \tag{5.5}$$

where $\pi_1, \eta_1 : [0,\infty) \to \mathbb{R}^{m_1}$ are the feedback signals through the uncertainty block Δ.

Definition 5.1. *The alternative algebraic form*

$$\mathcal{G}(\Sigma_a): \ \dot{x} = f(x,p) = F_{11}x + F_{12}\pi_1(x,p) = (F_{11}\ F_{12})\pi(x,p) \tag{5.6}$$

of the system equation is said to be the generator form realization of Σ, and the rational function $\pi = \left(\begin{smallmatrix} x \\ \pi_1 \end{smallmatrix}\right)$ is called a generator corresponding to LFR (5.4). Generator π is determined from the LFR of the system equations as follows:

$$\pi(x,p) = \Pi(x,p)x \in \mathbb{R}^m \text{ and } \pi_1(x,p) = \Pi_1(x,p)x \in \mathbb{R}^{m_1}, \tag{5.7}$$

$$\text{where } \Pi = \begin{pmatrix} I_{n_x} \\ \Pi_1 \end{pmatrix} : \mathcal{X}\times\mathcal{P} \to \mathbb{R}^{m\times n_x},\ m = n_x + m_1, \tag{5.7a}$$

$$\text{and } \Pi_1 = \mathcal{F}_l\left\{\begin{pmatrix} 0 & I_{m_1} \\ F_{21} & F_{22} \end{pmatrix}, \Delta\right\} = (I_{m_1} - \Delta F_{22})^{-1}\Delta F_{21} : \mathcal{X}\times\mathcal{P} \to \mathbb{R}^{m_1\times n_x}. \tag{5.7b}$$

The matrix compositions in (5.7a), (5.7b), or in $\pi = \left(\begin{smallmatrix} x \\ \pi_1 \end{smallmatrix}\right)$ are interpreted for functions, as presented in (4), instead of their values in (x,p). ◇

Example 5.1. Considering the recursive LFT realization of Section 3.6.2, the LFR of the van der Pol equation (5.3) is the following:

$$A(x,p) = \mathcal{F}_l\left\{\left(\begin{array}{cc|ccc} 0 & -1 & 0 & 0 & 0 \\ 1 & 0 & -1 & 1 & 0 \\ \hline 0 & 1 & 0 & 0 & 0 \\ 0 & 0 & 0 & 0 & 1 \\ 0 & 0 & 1 & 0 & 0 \end{array}\right), \begin{pmatrix} p & \\ & x_1 I_2 \end{pmatrix}\right\}, \text{ then, } \pi_1(x,p) = \begin{pmatrix} p\,x_2 \\ p\,x_1^2 x_2 \\ p\,x_1 x_2 \end{pmatrix}, \tag{5.8}$$

and $\pi = \left(\begin{smallmatrix} x \\ \pi_1 \end{smallmatrix}\right)$ is the generator of (5.6) corresponding to the LFR in (5.8). ◇

Naturally, the different LFR realizations of A define different generator form realizations for mapping f. However, a given LFR uniquely determines a certain set of rational functions through the generator π. The main reason for using the term "generator" is that function π *generates* a certain algebraic structure for the Lyapunov function.

Local asymptotic stability of nonlinear uncertain systems. In order to prove local asymptotic stability for system Σ_a, we are looking for a Lyapunov function in the following form:

$$V(x,p) = x^\top \mathbf{Q}(x,p)\, x = \pi^\top(x,p)\, Q(p)\, \pi(x,p), \tag{5.9}$$

$$\text{with } \mathbf{Q}(x,p) = \Pi^\top(x,p)\, Q(p)\, \Pi(x,p), \tag{5.9a}$$

$$\text{where } Q(p) = Q_0 + \textstyle\sum_{i=1}^{n_p} Q_i\, p_i \in \mathbb{R}^{m\times m}. \tag{5.9b}$$

Matrix $Q(p)$ should not be necessarily positive definite. Matrices Q_i, $i = 0,\dots,n_p$ are free symmetric matrix variables, and function π is defined in (5.7). With reference to Theorem 3.7, system Σ_a is locally asymptotically stable, if there exist positive constants $\underline{\alpha}_0$ and α_0 such that the following inequalities are satisfied:

$$x^\top \mathbf{Q}(x,p)x - \underline{\alpha}_0\|x\|^2 \geq 0 \qquad \text{for all } (x,p) \in \mathcal{X}\times\mathcal{P}, \tag{5.10}$$

$$x^\top\Big(\mathrm{He}\{\mathbf{Q}(x,p)A(p)\} + \check{\mathbf{Q}}(x,p,\varrho)\Big)x + \alpha_0\|x\|^2 \leq 0 \qquad \text{for all } (x,p,\varrho) \in \mathcal{X}\times\mathcal{P}\times\mathcal{R},$$

where $\check{\mathbf{Q}}(x,p,\varrho) = \sum_{i=1}^{n_p} \frac{\partial \mathbf{Q}}{\partial p_i}(x,p)\varrho_i$.

Global asymptotic stability of LPV systems. Now, assume that A is a function of p only. Then, the system equation simplifies to an LPV system of the form

$$\Sigma_a : \dot{x} = f(x,p) = A(p)\, x \text{ with } p \text{ satisfying Assumptions 3.1.} \tag{5.11}$$

In this case, generator Π in (5.7a) and hence $\mathbf{Q}$ in (5.9a) are independent of x. Therefore, according to Theorem 3.7, the system is globally asymptotically stable if there exist positive constants $\underline{\alpha}_0$ and α_0 such that the following PD-LMIs are satisfied

$$\mathbf{Q}(p) - \underline{\alpha}_0 I_{n_x} \succeq 0, \qquad \text{for all } p \in \mathcal{P}, \tag{5.12}$$

$$\mathrm{He}\{\mathbf{Q}(p)A(p)\} + \check{\mathbf{Q}}(p,\varrho) + \alpha_0 I_{n_x} \preceq 0, \qquad \text{for all } (p,\varrho) \in \mathcal{P}\times\mathcal{R}.$$

with some $\underline{\alpha}_0, \alpha_0 > 0$

In the general case, $\mathbf{Q}$ is a nonlinear symmetric matrix-valued function, therefore, the scalar inequalities in (5.10) and the PD-LMIs in (5.12) for the asymptotic stability, are infinite-dimensional problems (Definition 3.19). Fortunately, the left hand side of both inequalities in (5.10) and (5.12) can be formulated as a quadratic expression of some rational terms similarly to the quadratic structure of the Lyapunov function in (5.9).

Definition 5.2. *The quadratic algebraic form* (5.9a) *of function V is called a quadratic generator form or quadratic factorized form of function V.* ◇

In this chapter, we present convex LMI relaxation techniques for rational parameter-dependent inequality conditions written in a quadratic expression of rational terms. The proposed techniques are based on the LFR, Finsler's lemma, and the duality of the minimal generators and the maximal annihilators.

5.2 Notions and problem formulation

Henceforth, in this chapter, we consider a general parameter- (p), state- (x), and parameter rate- (ϱ) dependent rational PD-LMI condition in the following general quadratic form:

$$\mathbf{Q}(w) = \Pi^\top(w) Q(w) \Pi(w) \succeq 0 \text{ for all } w \in \mathcal{W}, \tag{5.13}$$

$$\text{with } Q \in \mathcal{S}^m_\varphi(\mathcal{W}), \tag{5.13a}$$

where $\mathcal{S}^m_\varphi(\mathcal{W})$ denotes the following set of symmetric matrix-valued functions:

$$\mathcal{S}^m_\varphi(\mathcal{W}) = \{Q = \textstyle\sum_{i=1}^{m_\varphi} Q_i\varphi_i : \mathcal{W}\to\mathbb{R}^{m\times m} \,|\, Q_i = Q_i^\top \in \mathbb{R}^{m\times m},\ \varphi : \mathcal{W}\to\mathbb{R}^{m_\varphi}\}, \tag{5.13b}$$

and φ_i denote the *distinct monomial* coordinate functions of $\varphi : \mathcal{W}\to\mathbb{R}^{m_\varphi}$.

In (5.13), $\mathbf{Q} : \mathcal{W}\to\mathbb{R}^{n\times n}$ is a rational function of some general parameters collected in vector $w \in \mathbb{R}^{n_w}$ belonging to a bounded polytope $\mathcal{W} \subset \mathbb{R}^{n_w}$. Generator $\Pi : \mathcal{W}\to\mathbb{R}^{m\times n}$ is a rational function of w with $n \geq 1$.

Matrices Q_i, $i = 1,\dots,m_\varphi$ are free symmetric matrix variables, which are meant to be found such that (5.13) is satisfied for all parameter values $w \in \mathcal{W}$, and that a certain linear objective function is minimized. Generator Π and functions φ_i are fixed before the optimization. The distinct monomials φ_i determine a structure for function Q, therefore, φ is called again a generator.

In order to find a solution for the (infinite-dimensional) rational PD-LMI (5.13), we formulate a *sufficient* PD-LMI condition for (5.13), which can be computed in a convex computational framework.

***Remark* 5.1.** As an algebraic structure, $\mathcal{S}^m_\varphi(\mathcal{W})$ forms an *R-module* [196, Chapter 3] over the ring of symmetric $m\times m$ matrices $R = (\mathcal{S}^m, +, \cdot)$. E.g., when $\varphi(w) = \left(\begin{smallmatrix}1\\ w\end{smallmatrix}\right)$, $\mathcal{S}^m_\varphi(\mathcal{W})$ denotes the module of symmetric matrix-valued *affine* functions. The abstract structure for $Q \in \mathcal{S}^m_\varphi(\mathcal{W})$ allows us to describe the further results in a more general framework.

1. In the computational examples, we generally use *affine* parameter dependence in Q with $\varphi(w) = \left(\begin{smallmatrix}1\\ w\end{smallmatrix}\right)$, which makes possible to formulate for (5.13) the following *sufficient* but *polytopic* PD-LMI condition:

$$Q(w) \succeq 0 \text{ for all } w \in \mathcal{W}. \tag{5.14}$$

According to Proposition 3.20, a solution $Q \in \mathcal{S}_{\varphi}^{m}(\mathcal{W})$ with $\varphi(w) = \left(\begin{smallmatrix} 1 \\ w \end{smallmatrix}\right)$ for the *affine* PD-LMI (5.14) can be found by checking the feasibility of (5.14) in the corner points of polytope $\mathcal{W}$.

2. Moreover, a rectangular polytope

$$\mathcal{W} = \bigtimes_{i=1}^{n_w} [\underline{w}_i, \overline{w}_i]. \tag{5.15}$$

makes possible to solve (5.14) with a multi-affine structure for Q with,

$$\varphi : \mathcal{W} \to \mathbb{R}^{n^{n_w}},\ \varphi(w) = \left(\varphi_1(w)\ \ldots\ \varphi_i(w)\ \ldots\ \varphi_{2^{n_w}}(w)\right)^{\top},\ \varphi_i(w) = \prod_{j=1}^{n_w} w_i^{\tau_{ij}}, \tag{5.16}$$

$$\text{where } \tau_{ij} \in \{0,1\} \text{ satisfy } i = 1 + \sum_{j=1}^{n_w} 2^{j-1}\tau_{ij} \text{ for all } i = 1, \ldots, 2^{n_w}. \tag{5.16a}$$

As a direct consequence of Lemma 4.10, a solution $Q \in \mathcal{S}_{\varphi}^{m}(\mathcal{W})$ with (5.16) for the *multi-affine* PD-LMI (5.14) can be found by checking the feasibility of (5.14) only the corner points of the rectangular polytope $\mathcal{W}$ in (5.15). ⋄

***Remark* 5.2.** Observe that constraining $Q(w)$ to be positive semidefinite for all $w \in \mathcal{W}$ is a restrictive condition for (5.13) as it provides the non-negativity of $z^{\top}Q(w)\,z$ for all $z \in \mathbb{R}^m$ and all $w \in \mathcal{W}$, without taking into account the nonlinear structure of Π. ⋄

According to a special case of Finsler's lemma (Lemma 3.22), a less conservative, but still sufficient (multi-)affine PD-LMI condition for (5.13) can be given as follows:

$$Q(w) + \mathrm{He}\{LN(w)\} \succeq 0 \text{ for all } w \in \mathcal{W}, \tag{5.17}$$

where $N : \mathcal{W} \to \mathbb{R}^{s \times m}$ is a *(multi-)affine annihilator* for Π and $L \in \mathbb{R}^{m \times s}$ is a free matrix Lagrange multiplier. Naturally, PD-LMI (5.17) is less conservative than (5.14).

Alongside the conservatism, a second important attribute of the LMI problem (5.17) is its dimension. To find a solution for (5.13), it is often enough to solve a dimensionally reduced sufficient PD-LMI condition as follows

$$S^{\top}\big(Q(w) + \mathrm{He}\{LN(w)\}\big)\,S \succeq 0 \text{ for all } w \in \mathcal{W}, \tag{5.18}$$

where $S \in \mathbb{R}^{m \times m'}$ is a full column-rank matrix ($m' < m$). See that (5.18) is a, so to say, "projection" of (5.17), therefore, it is not trivial to foresee, how conservative is the reduced-dimensional PD-LMI condition (5.18) compared to (5.17).

To cope with the conservatism and the dimensionality of the resulting sufficient PD-LMI condition (5.17), we introduce the notion of the *maximal annihilator* (to enlarge the set of feasible solutions) and the *minimal generator* (to reduce the dimensionality without compromising the solution set).

5.2.1 Finsler's lemma and Lagrange multipliers

It is worth mentioning that annihilator N and its multiplier L in PD-LMI (5.17), have the same role as the Lagrange multipliers have in [133; 145]. The authors of [133; 145] used SOS techniques to check the positivity of a polynomial function. They used polynomial Lagrange multipliers to enforce some coupling constraints between the monomials of the state variables (x). In [197], *rational* multipliers are used and factorized using LFT.

In our framework, the matrix Lagrange multiplier L comprise the coefficient matrices of some structured rational Lagrange multipliers. If we pre- and post-multiply (5.17) by $\Pi^{\top}(w)$ and $\Pi(w)$, respectively, we obtain an identical Lagrange inequality condition

$$\mathbf{Q}(w) + \textstyle\sum_{i=1}^{s} \lambda_i^{\top}(w)\Phi_i(w) > 0, \text{ for all } w \in \mathcal{W} \tag{5.19}$$

that is solved in [145, Section 2.2], where $\lambda_i(w) \in \mathbb{R}^{1\times n}$ and $\Phi_i(w) = 0_{1\times n}$ are the ith row of $L^\top\Pi(w)$ and $N(w)\Pi(w) = 0_{s\times n}$, respectively. Similarly to [197], λ_i are rational multiplier functions. Due to the fact that the nonlinear terms of $\Pi(w)$ are factorized out from $\mathbf{Q}(w)$ in our case, the rational parameter dependence in $\lambda_i(w)$ does not need to be handled separately.

The maximal (multi-)affine annihilator has the advantage of involving as much coupling constraints $\Phi_i(w)$ as possible while keeping the parameter-dependent matrix inequality of the form (5.17) convex.

5.3 Maximal annihilator for handling conservatism

The choice of the annihilator represents an important source of freedom in the LMI (5.17) problem formulation. The annihilator in (5.17) directly affects the *solution set* of the PD-LMI with respect to Q.

Definition 5.3 [P3]**.** *Let*

$$\mathfrak{F}^*_\varphi = \{Q \in \mathcal{S}^m_\varphi(\mathcal{W}) \mid \mathbf{Q}(w) = \Pi^\top(w)Q(w)\Pi(w) \succeq 0 \text{ for all } w \in \mathcal{W}\} \text{ and} \tag{5.20}$$

$$\mathfrak{F}_\varphi(N) = \{Q \in \mathcal{S}^m_\varphi(\mathcal{W}) \mid \exists L \in \mathbb{R}^{m\times s} : Q(w) + \mathrm{He}\{LN(w)\} \succeq 0 \ \forall w \in \mathcal{W}\} \tag{5.21}$$

denote the solution set or feasible set of PD-LMIs (5.13) *and* (5.17)*, respectively.* ◇

In the formalism of Definition 5.3, let $\mathfrak{F}_\varphi(0)$ denote the feasible set of (5.14). Then, $Q \in \mathfrak{F}_\varphi(0)$ is obviously a solution of (5.17) with $L = 0_{m\times s}$. Furthermore, let $Q \in \mathfrak{F}_\varphi(N)$, namely, Q satisfies (5.17) for some L. Then, if we pre-multiply (5.17) by $\Pi^\top(w)$ and post-multiply by $\Pi(w)$, we have that $\Pi^\top(w)Q(w)\Pi(w) \succeq 0$ (i.e., $Q \in \mathfrak{F}^*_\varphi$). Finally, we can state that $\mathfrak{F}_\varphi(0) \subseteq \mathfrak{F}_\varphi(N) \subseteq \mathfrak{F}^*_\varphi$.

In this section, we consider two *fixed* generators Π and φ. Then, we will show the existence of a so-called *maximal annihilator* of the form

$$N \in \mathcal{N}^{s\times m}_\varphi(\mathcal{W}) = \left\{\textstyle\sum_{i=1}^{m_\varphi} \bar{N}_i\varphi_i : \mathcal{W} \to \mathbb{R}^{s\times m} \mid \bar{N}_i \in \mathbb{R}^{s\times m},\ \varphi : \mathcal{W} \to \mathbb{R}^{m_\varphi}\right\}, \tag{5.22}$$

that generates the largest possible feasible set $\mathfrak{F}_\varphi(\mathcal{W})$ for PD-LMI condition (5.17). Note that constant s in (5.22) denotes the number of rows in $N(w)$.

Definition 5.4 [P3]**.** *Function $N \in \mathcal{N}^{s\times m}_\varphi(\mathcal{W})$ is said to be a maximal annihilator of Π over $\mathcal{W}$ with respect to φ if $N\Pi \equiv 0$ on $\mathcal{W}$ and $\mathfrak{F}_\varphi(N_1) \subseteq \mathfrak{F}_\varphi(N)$ for any other $N_1 \in \mathcal{N}^{s_1\times m}_\varphi(\mathcal{W})$ such that $N_1\Pi \equiv 0$ on $\mathcal{W}$.* ◇

The existence of (infinitely many) maximal annihilators is proved in Section 5.3.2.

5.3.1 Row reduced equivalent of an annihilator

In this section, we show that an annihilator $N \in \mathcal{N}^{s\times m}_\varphi(\mathcal{W})$ with linearly dependent rows is *redundant*. In other words, there exists another annihilator $N_0 \in \mathcal{N}^{s_0\times m}_\varphi(\mathcal{W})$ with less rows ($s_0 < s$) but generating the same solution set for Q.

Definition 5.5 [P3]**.** *The two annihilators $N \in \mathcal{N}^{s\times m}_\varphi(\mathcal{W})$ and $N_0 \in \mathcal{N}^{s_0\times m}_\varphi(\mathcal{W})$ of generator Π are called f-equivalent if $\mathfrak{F}_\varphi(N) = \mathfrak{F}_\varphi(N_0)$, i.e., the solution set of PD-LMI* (5.17) *with respect to Q is the same for both annihilators.* ◇

Definition 5.6. *Vector-valued functions $v_1, \dots, v_m : \mathcal{W} \to \mathbb{R}^{1\times m}$ are said to be linearly independent if $\sum_{j=1}^m \alpha_j v_j \equiv 0$ on $\mathcal{W}$ implies that $\alpha_1, \dots, \alpha_m = 0$.* ◇

To ease further notations and derivations, let us introduce the following algebraic

representation of an annihilator $N \in \mathcal{N}_{\varphi}^{s\times m}(\mathcal{W})$.

Definition 5.7 (based on [P3])**.** *The factorized algebraic form $N(w) = \Theta\Xi(w)$ of function N, $N(w) = \sum_{i=1}^{m_\varphi} \bar{N}_i w_i \in \mathbb{R}^{s\times m}$ is said to be the generator form of N, where*

$$\Xi(w) = \varphi(w) \otimes I_m \text{ and } \Theta = \begin{pmatrix} \bar{N}_1 & \cdots & \bar{N}_{m_\varphi} \end{pmatrix}. \tag{5.23}$$

Constant matrix Θ and function Ξ are called the coefficient matrix and the generator, respectively, of function N. ◇

Example 5.2. The generator form of an affine function N, $N(w) = \bar{N}_0 + \sum_{i=1}^{n_w} \bar{N}_i w_i$ can be given by the following generator and coefficient matrix:

$$\Xi(w) = \begin{pmatrix} 1 \\ w \end{pmatrix} \otimes I_m = \begin{pmatrix} I_m \\ w_1 I_m \\ \cdots \\ w_{n_w} I_m \end{pmatrix} = \mathcal{F}_l \left\{ \left(\begin{array}{c|ccc} I_m & 0 & \cdots & 0 \\ 0 & I_m & \cdots & 0 \\ \cdots & \cdots & \cdots & \cdots \\ 0 & 0 & \cdots & I_m \\ \hline I_m & \multicolumn{3}{c}{\multirow{2}{*}{0}} \\ \cdots & & & \\ I_m & & & \end{array} \right), \Delta_N(w) \right\}, \tag{5.24}$$

$$\Theta = \begin{pmatrix} \bar{N}_0 & \bar{N}_1 & \cdots & \bar{N}_{n_w} \end{pmatrix}, \text{ and } \Delta_N(w) = \operatorname{diag}\{w_1 I_m, \cdots, w_{n_w} I_m\}. \qquad \diamond$$

Note that for the fixed generator φ, the coefficient matrix Θ is a unique alternative numerical representation of function $N \in \mathcal{N}_{\varphi}^{s\times m}(\mathcal{W})$. Moreover, it can be shown that Θ is row-rank deficient if and only if the rows of N are linearly dependent. In the following, we prove that an annihilator N and its row-reduced alternative N_0 are f-equivalent, namely, they generate the same solution set $\mathfrak{F}_\varphi(N) = \mathfrak{F}_\varphi(N_0)$ for (5.17).

Proposition 5.8 [P3]**.** *Suppose that $N = \Theta\Xi \in \mathcal{N}_{\varphi}^{s\times m}(\mathcal{W})$ is an annihilator of Π and $\operatorname{rank}(\Theta) = s_0 < s$. Then, there exists $\Theta_0 \in \mathbb{R}^{s_0\times(m\cdot m_\varphi)}$, such that $N_0 = \Theta_0\Xi \in \mathcal{N}_{\varphi}^{s_0\times m}(\mathcal{W})$ is an annihilator of Π, $\operatorname{rank}(\Theta_0) = s_0$, and N_0 is f-equivalent to N.* ◇

Proof. First, we give a candidate function N_0, then, we prove its correctness.

(Candidate row-reduced annihilator) Without the loss of generality, we can assume that the first s_0 rows (Θ_0) of $\Theta = \begin{pmatrix} \Theta_0 \\ \Theta_1 \end{pmatrix}$ are linearly independent. Consequently, there exist $\Gamma = \Theta_1\Theta_0(\Theta_0\Theta_0^\top)^{-1} \in \mathbb{R}^{(s-s_0)\times s_0}$ and $S = \begin{pmatrix} I \\ \Gamma \end{pmatrix}$, such that the following identities hold $\Theta_1 = \Gamma\Theta_0$, $\Theta = S\Theta_0$, $N(w) = SN_0(w)$, and $N_0(w) = \Theta_0\Xi(w)$ for all $w \in \mathcal{W}$.

(Correctness of the row-reduced annihilator – "if") Let $L \in \mathbb{R}^{m\times s}$ be given. Then,

$$LN = L\begin{pmatrix} \Theta_0 \\ \Theta_1 \end{pmatrix}\Xi = LS\Theta_0\Xi = L_0\Theta_0\Xi = L_0N_0 \text{ on } \mathcal{W}, \text{ where } L_0 = LS. \tag{5.25}$$

Now, assume that $Q \in \mathfrak{F}_\varphi(N)$ for some L, then, $Q \in \mathfrak{F}_\varphi(N_0)$ as

$$Q(w) + \operatorname{He}\{LN(w)\} = Q(w) + \operatorname{He}\{L_0N_0(w)\} \succeq 0 \text{ for all } w \in \mathcal{W}. \tag{5.26}$$

Equation (5.26) proves that $\mathfrak{F}_\varphi(N) \subseteq \mathfrak{F}_\varphi(N_0)$.

("only if") Conversely, assume that $Q \in \mathfrak{F}_\varphi(N_0)$ for some L_0, then, there exists matrix $L = (L_0\ 0)$, for which $Q \in \mathfrak{F}_\varphi(N)$, namely,

$$Q(w) + \operatorname{He}\{L_0N_0(w)\} = Q(w) + \operatorname{He}\{(L_0\ 0)N(w)\} \succeq 0 \text{ for all } w \in \mathcal{W}, \tag{5.27}$$

as $L_0N_0(w) = L_0\Theta_0\Xi(w) = (L_0\ 0)\begin{pmatrix} \Theta_0 \\ \Theta_1 \end{pmatrix}\Xi(w)$. □

It is worth mentioning that the number of free decision variables collected in L_0 are less (ms_0) than the number of variables in L (ms). In other words, using annihilator N_0 instead of N will result in an optimization problem with less free variables, but no real degrees of freedom are lost in the optimization.

***Remark* 5.3.** Let $\Theta_0^\top$ be a basis for the image space of $\Theta^\top$. Then annihilator $N_0 = \Theta_0\Xi$ is a row reduced f-equivalent of $N = \Theta\Xi$. ◇

5.3.2 Existence of maximal annihilators

It is obvious from the problem formulation that an infinite number of row vector-valued functions $r \in \mathcal{N}_\varphi^{1\times m}(\mathcal{W})$ exist, such that $r\Pi \equiv 0$ on $\mathcal{W}$. However, in order to reduce the conservatism of (5.17), it is not reasonable to collect as many rows into N as possible. Due to Proposition 5.8, there exists a guaranteed maximal number of (well selected) annihilator rows ($\leq m \cdot m_\varphi$), to which if we append any further rows, the feasible set will not change anymore.

For $N \in \mathcal{N}_\varphi^{s\times m}(\mathcal{W})$ to be a maximal annihilator, we may expect that the solution set generated by every other annihilator be contained by the solution set $\mathfrak{F}_\varphi(N)$ generated by the maximal annihilator N. The following lemma together with the row-reduction result (Proposition 5.8) gives evidence to the existence of such a maximal annihilator.

Lemma 5.9 [P3]**.** *For any two annihilators $N_1 \in \mathcal{N}_\varphi^{s_1\times m}(\mathcal{W})$ and $N_2 \in \mathcal{N}_\varphi^{s_2\times m}(\mathcal{W})$ of Π, we can construct an annihilator $N_{12} = \binom{N_1}{N_2} \in \mathcal{N}_\varphi^{(s_1+s_2)\times m}(\mathcal{W})$ for Π, such that $\mathfrak{F}_\varphi(N_1) \cup \mathfrak{F}_\varphi(N_2) \subseteq \mathfrak{F}_\varphi(N_{12})$.* ◇

Proof. If $Q \in \mathfrak{F}_\varphi(N_1)$ for some L_1, then $Q \in \mathfrak{F}_\varphi(N_{12})$ for $L_{12} = (L_1\, 0)$, namely, $\mathfrak{F}_\varphi(N_1) \subseteq \mathfrak{F}_\varphi(N_{12})$. Similarly, we can prove that $\mathfrak{F}_\varphi(N_2) \subseteq \mathfrak{F}_\varphi(N_{12})$. □

As an obvious consequence of Proposition 5.8, we are able to give a sufficient condition for $N \in \mathcal{N}_\varphi^{s\times m}(\mathcal{W})$ to be a maximal annihilator for Π.

Corollary 5.10 [P3]**.** *Let the rows of $\Theta \in \mathbb{R}^{s\times(m\cdot m_\varphi)}$ span the co-vector space*

$$\left\{\vartheta \in \mathbb{R}^{1\times(m\cdot m_\varphi)} \,\middle|\, \vartheta\,(\varphi \otimes I_m)\,\Pi \equiv 0 \text{ on } \mathcal{W}\right\}. \tag{5.28}$$

Then, $N = \Theta\,(\varphi \otimes I_m) \in \mathcal{N}_\varphi^{s\times m}(\mathcal{W})$ is a maximal annihilator of Π. ◇

Let us say that the co-vector space (5.28) is the *constant left kernel space* of function $(\varphi \otimes I_m)\,\Pi$. We say that Θ is a maximal *constant annihilator* of $(\varphi \otimes I_m)\,\Pi$ if the rows of Θ span (5.28). In the formalism of Corollary 5.10, we are able to formulate a second definition of a maximal annihilator as follows.

Definition 5.11. *Let $\Pi : \mathcal{W} \to \mathbb{R}^{m\times n}$ and $\varphi : \mathcal{W} \to \mathbb{R}^{m_\varphi}$ be well-defined functions, where φ_i are distinct monomials in w. Then, $N = \Theta\,(\varphi\otimes I_m) \in \mathcal{N}_\varphi^{s\times m}(\mathcal{W})$ is a maximal annihilator of Π with respect to φ if the rows of $\Theta \in \mathbb{R}^{s\times q}$ span (5.28).* ◇

Provided by Proposition 5.8, Definition 5.4 and Definition 5.11 are equivalent.

5.3.2.1 Maximal annihilator computation. Corollary 5.10 highlights that a general maximal annihilator computation can be traced back to a maximal constant annihilator computation for function $(\varphi \otimes I_m)\,\Pi$. A few special classes of the maximal annihilator of a *fixed* generator Π are as follows:

1. A maximal *constant* annihilator of Π (with respect to $\varphi(w) = 1$) is a basis of the constant left kernel space of function Π.

2. Let $\mathcal{W} = \mathcal{X} \times \mathcal{P}$ and $w = \binom{x}{p}$. Then, a maximal *p-dependent* affine annihilator $N : \mathcal{P} \to \mathbb{R}^{s\times m}$ of generator $\Pi : \mathcal{X} \times \mathcal{P} \to \mathbb{R}^{m\times n}$ can be computed by considering $\varphi(x,p) = \binom{1}{p}$.

3. A maximal *multi-affine* annihilator $N : \mathcal{W} \to \mathbb{R}^{s\times m}$ of generator $\Pi : \mathcal{W} \to \mathbb{R}^{m\times n}$ can be computed by considering function φ in (5.16).

Henceforth, the word "maximal" is often suppressed but used when it is significant. ▲

5.3.3 Constant annihilator computation

As the reader possibly observed, the notion of a constant annihilator is very close to the standard notion of the kernel space. Consider a matrix-valued function $\Pi : \mathcal{W} \to \mathbb{R}^{m\times n}$. We assume that $\Pi(w)$ has a full column-rank ($n < m$) for all $w \in \mathcal{W} \setminus \{0\}$. Then, the kernel space of $\Pi^\top(w)$ is a vector space, which depends on $w \in \mathcal{W}$, formally,

$$\mathrm{Ker}(\Pi^\top) = \Big\{ \textstyle\sum_{i=1}^{m-n} \alpha_i g_i \,\big|\, \alpha_i \in \mathbb{R},\, g_i : \mathcal{W} \to \mathbb{R}^m,\, g_i\Pi \equiv 0,\, i = 1, \dots, m-n \Big\}. \tag{5.29}$$

From g_i in (5.29), we also require that $\mathrm{rank}\,(g_1(w) \;\dots\; g_{m-n}(w)) = m-n$ for all $w \in \mathcal{W}\setminus\{0\}$. In [27, Section 1.3], $\mathrm{Ker}(\Pi^\top)$ constitutes a so-called *distribution* as it constitutes a family of vector spaces spanned by functions g_i. Suppose that $\mathrm{Ker}(\Pi^\top)$ has a, so to say, *subdistribution*, which is independent of w.

Example 5.3. Let $\Pi^\top(w) = \left(\begin{smallmatrix} 1 & w & w^2 & w+w^2 \\ 0 & 1 & w & 1+w \end{smallmatrix}\right)$. Then, the *kernel distribution* of $\Pi^\top$ is

$$\mathrm{Ker}(\Pi^\top) = \Big\{ \alpha_1\, g_1 + \alpha_2\, g_2 \,\big|\, (\alpha_1, \alpha_2) \in \mathbb{R}^2 \Big\},\ \text{where } g_1(w) = \begin{pmatrix} 0 \\ w \\ -1 \\ 0 \end{pmatrix},\ g_2 = \begin{pmatrix} 0 \\ 1 \\ 1 \\ -1 \end{pmatrix}.$$

Observe that g_2 is constant, therefore, it spans the parameter independent subdistribution of $\mathrm{Ker}(\Pi^\top)$. In other words, $g_2^\top$ is a constant annihilator of Π and it spans the constant left kernel space of Π. ◇

In Lemma 3.35, we presented a possible numerical method to find a kernel distribution for a matrix-valued rational function given in a well-posed LFR. But now, we seek for constant matrix $N_0 \in \mathbb{R}^{s_0\times m}$ such that $N_0\Pi(w) = 0$ for all $w \in \mathcal{W}$. Here, we present two different computational methods to find N_0.

Procedure 5.12 [P2] (symbolical construction)**.** To compute the basis N_0 of the constant left kernel space of Π, we proceed with the following algebraic manipulation steps:

1. Let $u \in \mathbb{R}^n$ be an auxiliary vector of parameters, that are independent of w, and let $\vartheta \in \mathbb{R}^{1\times m}$ be a vector of free coefficients, that are meant to be found, such that $\vartheta\Pi(w)u = 0$ for all $w \in \mathbb{R}^{n_w}$ and all $u \in \mathbb{R}^n$.

2. Let $\frac{q_1(w,u;\vartheta)}{q_2(w)} = \vartheta\Pi(w)u$ denote the (unique) irreducible fractional form of $\vartheta\Pi(w)u$, where $q_1(w, u; \vartheta)$ and $q_2(w)$ are multivariate polynomials.

3. Collect the terms of $q_1(w, u; \vartheta)$ having a common degree in w and u, namely: $q_1(w, u; \vartheta) = \sum_{j=1}^{J} c_j(\vartheta) q_{1j}(w, u) = 0$ for all $(w, u) \in \mathbb{R}^{2n_w}$.

4. Coefficients $c_j(\vartheta)$ are linear in ϑ. Therefore, the identity conditions $c_j(\vartheta) = 0$ for all $j = 1, \dots, J$ can be equivalently formulated as a system of linear equations: $\mathbf{A}\vartheta^\top = 0$, where $\mathbf{A} \in \mathbb{R}^{J\times m}$ is a constant matrix.

5. Let $N_0^\top$ be a basis for the kernel space of matrix $\mathbf{A}$.

The resulting matrix N_0 is a constant annihilator of Π, namely, $N_0\Pi \equiv 0$. ◇

An alternative numerical method to compute a basis N_0 for the constant left kernel space of Π is given in the following procedure.

Procedure 5.13 [P1] (numerical construction)**.** The following steps generate a basis N_0 for the constant left kernel space of Π.

1. Following the guidelines of Remark 5.4, select a few points $w^{(1)}, \dots, w^{(M)}$ from $\mathcal{W}$.

2. Evaluate $\Pi(w)$ in the selected points, and collect its values in a block matrix as follows: $\Pi_M = \Big(\Pi(w^{(1)}) \quad \cdots \quad \Pi(w^{(M)})\Big) \in \mathbb{R}^{m\times Mn}$.

3. Compute a basis $N_0^\top$ for the kernel space of $\Pi_M^\top$, that constitutes the transpose of a constant annihilator N_0.

Finally, check that the norm of matrix $O(w) = N_0\Pi(w)$ is below a given tolerance value $0 < \varepsilon \ll 1$. ◇

***Remark* 5.4** [P1]**.** When selecting some distinctive points $w^{(1)}, \dots, w^{(M)}$ to evaluate matrix $\Pi(w) \in \mathbb{R}^{m\times n}$ we consider the following guidelines.

- From the author's experience, it is a good strategy to choose $M = \max\{\dim(\mathcal{W}) + 1, \lceil \frac{m}{n} \rceil\}$ nr. of characteristic (possibly random) points in $\mathcal{W}$, where $\dim(\mathcal{W})$ denotes the local dimension of manifold $\mathcal{W} \subset \mathbb{R}^{n_w}$ at an arbitrary point $w \in \mathcal{W}$. Furthermore, $\lceil \frac{m}{n} \rceil$ denotes the smallest integer value M, such that $\frac{m}{n} \leq M$.
- The selected points should span $\mathcal{W}$, i.e for all $w \in \mathcal{W}$ there exist $\alpha_1, \dots, \alpha_M \in \mathbb{R}$ such that $w = w^{(1)}\alpha_1 + \dots + w^{(M)}\alpha_M$.
- It is a good policy if the selected points include the corner points of $\mathcal{W}$.

As a possible random sampling implementation for LFRs, we refer to the (`dbsample`) subroutine of the GSS Library [96] of the SMAC Toolbox [97]. ◇

***Remark* 5.5.** Also note that the precision of the kernel computation may depend on the domain, from which the random points are selected. For instance, if $\Pi(w)$ contains higher order monomials in w_1, but lower order monomials in w_2 (e.g., $w_1^6 w_2^2$), then, the "normalized" polytope $\mathcal{W} = [-2, 2] \times [-8, 8]$ is a better choice to compute N_0 than, e.g., $\mathcal{W} = [-2, 2] \times [-2, 2]$. ◇

***Remark* 5.6.** Procedure 5.12 considers that polytope $\mathcal{W}$ spans the whole parameter space $\mathbb{R}^{n_w}$. In comparison, Procedure 5.13 allows $\mathcal{W}$ to be a polytope in an affine submanifold of $\mathbb{R}^{n_w}$. ◇

5.4 Minimal generators for dimension reduction

In this section, we cope with the dimensionality of the generated sufficient convex PD-LMI conditions for dynamic system analysis. Consider again the infinite-dimensional PD-LMI condition $\mathbf{Q}(w) = \Pi^\top(w)Q(w)\Pi(w) \succeq 0$ (5.13), that is feasible for all $w \in \mathcal{W}$ if the convex PD-LMI $Q(w) + \mathrm{He}\{LN(w)\} \succeq 0$ (5.17) is satisfied for all $w \in \mathcal{W}$. Similarly to (5.17), we aim to formulate a reduced-dimensional sufficient PD-LMI (5.18) to solve (5.13).

Assume that the rows of $\Pi : \mathcal{W} \to \mathbb{R}^{m\times n}$ are linearly dependent (i.e., Π admits a constant annihilator). Then, there exist a full column-rank matrix $S \in \mathbb{R}^{m\times m'}$ $(m' < m)$ and generator $\widehat{\Pi} : \mathcal{W} \to \mathbb{R}^{m'\times n}$ satisfying $\Pi = S\widehat{\Pi}$ on $\mathcal{W}$. Consequently, the quadratic factorization (5.13) of $\mathbf{Q}$ is redundant, in the sense that $\mathbf{Q}$ can be decomposed differently:

$$\mathbf{Q}(w) = \widehat{\Pi}^\top(w)\widehat{Q}(w)\widehat{\Pi}(w) \succeq 0 \text{ for all } w \in \mathcal{W}, \tag{5.30}$$

with a smaller dimensional matrix $\widehat{Q}(w) = S^\top Q(w)S \in \mathbb{R}^{m'\times m'}$. Having (5.30), a reduced-dimensional sufficient PD-LMI for (5.13) can be formulated as follows:

$$\widehat{Q}(w) + \mathrm{He}\{\widehat{L}\widehat{N}(w)\} \succeq 0 \text{ for all } w \in \mathcal{W}, \tag{5.31}$$

where $\widehat{N} \in \mathcal{N}_\varphi^{s'\times m'}(\mathcal{W})$ is an annihilator for $\widehat{\Pi}$.

Definition 5.14 [P1]**.** *We say that* $\Pi : \mathcal{W} \to \mathbb{R}^{m\times n}$ *is a* minimal generator *if the rows of* Π *are linearly independent in the sense of Definition 5.6.* ◇

***Remark* 5.7.** According to Definition 5.6, generator Π is minimal if and only if it does not have a constant annihilator. $\diamond$

Based on the constant annihilator computation approach of Section 5.3.3, we present an efficient method for minimal generator selection in Section 5.4.1. Then, in Section 5.4.2, we show that the initial (5.17) and the reduced-dimensional affine PD-LMIs (5.31) are equivalent if the annihilator $\widehat{N}(w) = N(w)S$ is transformed appropriately.

5.4.1 Minimal generator selection

Let $\sigma = (\sigma_1, \ldots, \sigma_m)$ be a permutation. Let $I_\sigma \in \mathbb{R}^{m\times m}$ denote a *permutation matrix*, in which the ith row corresponds to the σ_ith row of the identity matrix I_m.

Procedure 5.15 [P1]**.** Assume that Π is not a minimal generator. In order to find a full column-rank matrix S and a minimal generator $\widehat{\Pi}$ satisfying $\Pi = S\widehat{\Pi}$ on $\mathcal{W}$, proceed the following steps:

Step 1. Compute a constant annihilator $N_0 \in \mathbb{R}^{(m-m')\times m}$ for generator Π as presented in Section 5.3.3.

Step 2. Compute a basis $\Lambda \in \mathbb{R}^{m\times m'}$ for the kernel space of matrix N_0 ($N_0\Lambda = 0$).

Step 3. Let the first m' nr. of values of permutation σ be the indices of the linearly independent rows of matrix Λ.

Step 4. Let $\binom{V}{W} = I_\sigma^\top \Lambda$, where $V \in \mathbb{R}^{m'\times m'}$ is invertible.

Step 5. Let $S_\sigma = \begin{pmatrix} I_{m'} \\ \Gamma \end{pmatrix}$ and $\widehat{\Pi}$ be the first m' rows of $I_\sigma\Pi$, where $\Gamma = WV^{-1}$.

Finally, we obtain matrices I_σ, S_σ and generator $\widehat{\Pi}$ such that $I_\sigma\Pi = S_\sigma\widehat{\Pi}$. Introducing $S = I_\sigma^\top S_\sigma$, we also have that $\Pi = S\widehat{\Pi}$. $\diamond$

Theorem 5.16 [P1]**.** *Function $\widehat{\Pi}$ obtained through Procedure 5.15 is a minimal generator satisfying $I_\sigma\Pi = S_\sigma\widehat{\Pi}$.* $\diamond$

Proof. Step 2 of Procedure 5.15 implies the existence of a generator $\Pi_0 : \mathcal{W} \to \mathbb{R}^{m'\times n}$ such that $\Pi = \Lambda\Pi_0$. As Λ has a maximal column-rank, we have that $\Lambda^\dagger\Pi = \Pi_0$.

(Generator Π_0 is minimal) Assume that Π_0 admits a constant annihilator $r_0 \neq 0$ such that $r_0\Pi_0 \equiv 0$. Then, $r_0\Lambda^\dagger\Pi = r_0\Pi_0 \equiv 0$, namely, $r_0\Lambda^\dagger$ is a constant annihilator for Π. Since N_0 is a basis for the constant left kernel space of Π, it must exist an $\alpha \in \mathbb{R}^m$ such that $r_0\Lambda^\dagger = \alpha^\top N_0$. Post-multiplying by Λ we have that $r_0 = 0$. By contradiction, Π_0 does not admit a constant annihilator, i.e., Π_0 is a minimal generator.

(Generator $\widehat{\Pi}$ is minimal) Step 4 of Procedure 5.15 implies that

$$I_\sigma\Pi = \begin{pmatrix} \widehat{\Pi} \\ \widetilde{\Pi} \end{pmatrix} = \begin{pmatrix} V \\ W \end{pmatrix} \Pi_0 \;\Rightarrow\; \begin{cases} \Pi_0 = V^{-1}\widehat{\Pi}, \\ \widetilde{\Pi} = WV^{-1}\widehat{\Pi}. \end{cases} \tag{5.32}$$

Therefore, $\Pi = V\Pi_0$ is minimal and satisfies $I_\sigma\Pi = S_\sigma\widehat{\Pi}$. $\square$

***Remark* 5.8** [P1]**.** Without the loss of generality, we may assume that $\mathcal{G}(\Sigma_a)$ in (5.6) is a *minimal* generator form realization for system Σ (i.e., vector π is minimal). Otherwise, let $f(x,p) = (G_{11}\, G_{12})\,\widehat{\pi}$, where $\pi = S\widehat{\pi}$ and $(G_{11}\, G_{12}) = (F_{11}\, F_{12})S$. $\diamond$

5.4.2 Equivalent reduced-dimensional PD-LMI

Due to the fact that the values of the annihilators N and $\widehat{N}$ are different for PD-LMIs (5.17) and (5.31), it is not trivial to foresee whether the two PD-LMIs define the same solution set for Q or not. Another interesting question arises: how the annihilator should

be transformed to obtain an equivalent reduced-dimensional PD-LMI. The main result related to the dimension reduction transformation is concluded in the next theorem.

Theorem 5.17 [P1; P2]**.** *Assume that generator* Π *in* (5.13) *admits a factorization* $\Pi = S\widehat{\Pi}$ *with* $S = I_\sigma^\top \left(\begin{smallmatrix} I \\ \Gamma \end{smallmatrix}\right)$ *and with a minimal generator* $\widehat{\Pi}$*. Let functions* $N \in \mathcal{N}_\varphi^{s\times m}(\mathcal{W})$ *and* $\widehat{N} \in \mathcal{N}_\varphi^{s'\times m'}(\mathcal{W})$ *denote the maximal annihilators of* Π *and* $\widehat{\Pi}$*, respectively. Then, the PD-LMIs* (5.17) *and* (5.31) *are equivalent in the sense that* $\mathfrak{F}_\varphi(N) = \mathfrak{F}_\varphi(\widehat{N}, S)$*, where*

$$\mathfrak{F}_\varphi(\widehat{N}, S) = \{Q \in \mathcal{S}_\varphi^m(\mathcal{W}) \mid \exists \widehat{L} \in \mathbb{R}^{m'\times s'} : S^\top Q(w) S + \mathrm{He}\{\widehat{L}\widehat{N}(w)\} \succeq 0 \ \forall w \in \mathcal{W}\} \tag{5.33}$$

denotes the solution set of the reduced PD-LMI (5.31)*.* ◇

The implication scheme is the following:

$$\begin{array}{ccc} \mathbf{Q}(w) = \Pi^\top(w) Q(w) \Pi(w) & = & \widehat{\Pi}^\top(w) \widehat{Q}(w) \widehat{\Pi}(w) \succeq 0 \quad \text{for all } w \in \mathcal{W} \\ \Uparrow & & \Uparrow \\ \text{PD-LMI (5.17)} & \Leftrightarrow & \underline{\text{PD-LMI (5.31)}}. \end{array}$$

Proof. (only if) Assume that the pair (Q, L) is a solution for the initial PD-LMI (5.17) with annihilator N. Then, multiplying PD-LMI (5.17) by $S^\top$ from the left and by S from the right, we obtain that pair $(S^\top Q S, S^\top L)$ is a solution for (5.31) with the transformed annihilator $\widehat{N} = NS \in \mathcal{N}_\varphi^{s'\times m'}(\mathcal{W})$, $s = s'$. Now, we showed that $\mathfrak{F}_\varphi(N) \subseteq \mathfrak{F}_\varphi(\widehat{N}, S)$. *(if)* Conversely, for each solution $(\widehat{Q}, \widehat{L})$ of (5.31) with annihilator $\widehat{N}$, there exists a sufficiently small value $\varepsilon > 0$, such that the pair (Q, L) with

$$Q = I_\sigma^\top \begin{pmatrix} \widehat{Q} - \varepsilon \Gamma^\top \Gamma & 0 \\ 0 & \varepsilon I_{m-m'} \end{pmatrix} I_\sigma, \ L = I_\sigma^\top \begin{pmatrix} \widehat{L} \\ 0 \end{pmatrix},$$

satisfy both $\widehat{Q} = S^\top Q S$ and (5.17) with annihilator N. Therefore, $\mathfrak{F}_\varphi(N) \supseteq \mathfrak{F}_\varphi(\widehat{N}, S)$. *(with maximal annihilators)* Finally, the following lemma provides that the projection $\widehat{N} = NS$ preserves the maximality of N and $\widehat{N}$ with respect to generators Π and $\widehat{\Pi}$ respectively. □

Lemma 5.18 [P1]**.** *Suppose that* $N = \Theta(\varphi \otimes I_m) \in \mathcal{N}_\varphi^{s\times m}(\mathcal{W})$ *is a maximal annihilator of* $\Pi = S\widehat{\Pi}$*. Then,* $\widehat{N} = NS \in \mathcal{N}_\varphi^{s\times m'}(\mathcal{W})$ *is also a maximal annihilator of* $\widehat{\Pi}$*.* ◇

Proof. It is enough to show that for any annihilator row $\widehat{r} = \widehat{\vartheta}\,(\varphi \otimes I_{m'})$ of $\widehat{\Pi}$ there exists a constant row vector α such that $\widehat{r} = \alpha\, NS$ on $\mathcal{W}$.

First, observe that constant matrix $I_{m_\varphi} \otimes S$ has maximal column-rank, therefore, there exists $(I_{m_\varphi} \otimes S)^\dagger$ such that $(I_{m_\varphi} \otimes S)^\dagger (I_{m_\varphi} \otimes S) = I_{m_\varphi m'}$. Then, $\widehat{r}\,\widehat{\Pi}$ can be expressed as follows:

$$0 \equiv \widehat{r}\,\widehat{\Pi} = \widehat{\vartheta}\,(\varphi \otimes I_{m'})\,\widehat{\Pi} = \widehat{\vartheta}\,(I_{m_\varphi} \otimes S)^\dagger \underbrace{(I_{m_\varphi} \otimes S)\,(\varphi \otimes I_{m'})\,\widehat{\Pi}}_{(\varphi \otimes I_m)\,\Pi}. \tag{5.34}$$

Applying twice the mixed multiplication property (2) of the Kronecker tensor product (1), the braced term can be developed further as follows:

$$\begin{aligned} (I_{m_\varphi} \otimes S)\,(\varphi \otimes I_{m'})\,\widehat{\Pi} &= ((I_{m_\varphi}\varphi) \otimes (S I_{m'}))\,\widehat{\Pi} = (\varphi \otimes S)\,\widehat{\Pi} \\ &= ((\varphi \cdot 1) \otimes (I_m S))\,\widehat{\Pi} = (\varphi \otimes I_m)(1 \otimes S)\,\widehat{\Pi} = (\varphi \otimes I_m)\,S\,\widehat{\Pi} = (\varphi \otimes I_m)\,\Pi. \end{aligned} \tag{5.35}$$

Identity (5.34) implies that $r = \vartheta(\varphi \otimes I_m)$ is an annihilator of Π with $\vartheta = \widehat{\vartheta}\,(I_{m_\varphi} \otimes S)^\dagger$.

As N is a maximal annihilator of Π, the rows of Θ span the constant left kernel space of $(\varphi \otimes I_m)\Pi$. Therefore, there exists a constant row vector α such that $\widehat{\vartheta}\,(I_{m_\varphi} \otimes S)^\dagger = \alpha\,\Theta$. Then, following the reasoning of (5.34) and (5.35), we can conclude that

$$\widehat{r} = \widehat{\vartheta}\,(\varphi \otimes I_{m'}) = \alpha\,\Theta\,(I_{m_\varphi} \otimes S)(\varphi \otimes I_{m'}) = \alpha\,\Theta\,(\varphi \otimes I_m)\,S = \alpha\,\widehat{N}, \tag{5.36}$$

10.15774/PPKE.ITK.2021.004

which completes the proof. □

5.5 A tuning knob against conservatism

In this section, we propose a systematic method to formulate less conservative sufficient convex conditions for rational PD-LMIs. This technique introduces new degrees of freedom into the convex conditions, at the same time, it results in higher dimensional LMI problems.

Up to this point, Π was a called a generator, and $f = F\Pi$ was called a generator form realization of function f. According to Definition 5.2, let $\mathbf{Q} = \Pi^\top Q\,\Pi$ be called a *quadratic generator form* realization of the symmetric matrix-valued function $\mathbf{Q}$. Consider the following matrix inequality in two possible quadratic generator form realizations:

$$\mathbf{Q}(w) = \Pi^\top(w)Q(w)\Pi(w) = \Pi_g^\top(w)Q_g(w)\Pi_g(w) \succeq 0 \text{ for all } w \in \mathcal{W}, \tag{5.37}$$

where both generators $\Pi : \mathcal{W} \to \mathbb{R}^{m\times n}$ and $\Pi_g : \mathcal{W} \to \mathbb{R}^{m_g\times n}$ are minimal, but there exists a full row-rank matrix H_g such that $\Pi = H_g\Pi_g$. Observe that Π carries less information than Π_g ($m < m_g$), as Π can be expressed by Π_g.

Let $N \in \mathcal{N}_\varphi^{s\times m}(\mathcal{W})$ and $N_g \in \mathcal{N}_\varphi^{s_g\times m_g}(\mathcal{W})$ be two maximal annihilators for Π and Π_g, respectively. Then, two sufficient PD-LMIs for (5.37) can be formulated as follows:

$$Q(w) + \mathrm{He}\{LN(w)\} \succeq 0 \text{ for all } w \in \mathcal{W}, \tag{5.38}$$

$$Q_g(w) + \mathrm{He}\{L_gN_g(w)\} \succeq 0 \text{ for all } w \in \mathcal{W}. \tag{5.39}$$

It can be demonstrated (through examples) that PD-LMI (5.39) is typically less conservative than (5.38).

The need to inflate generator Π with new nonlinear terms may arise when Π does not originate from an LFR. This typical case occurs when we seek for a solution to the Lyapunov inequality (3.4b) or the dissipativity relation (3.14b). In Proposition 4.4, it was already presented that the Lyapunov inequality (3.4b) can be altered into a quadratic generator form, where the corresponding generator (4.45) is given manually in a special structured form, and it does not originate from an LFR. In this case, it may happen that the algebraic coupling between the rows (or coordinates) of Π cannot be given by a (multi-)affine annihilator. Or, the maximal annihilator for Π is not descriptive enough to reduced the conservatism as much as we expect.

Example 5.4. Let $\Pi(x) = \begin{pmatrix} x & x^3 & x^4 & x^6 & x^8 \end{pmatrix}^\top$, then, $N(x) = \begin{pmatrix} 0 & -x & 1 & 0 & 0 \end{pmatrix}$ is its maximal (multi-)affine annihilator. Obviously, the algebraic interdependences between the terms x, x^3, x^6, and x^8 are not represented. Therefore, the solution of (5.17) will handle these terms as independent variables. If $Q \in \mathbb{R}^{5\times5}$ is a solution for (5.17), then, $\Pi^\top(z)\,Q\,\Pi(z) \geq 0$ for all $z \in \mathbb{R}^4$, where $\Pi(z) = \begin{pmatrix} z_1 & z_2 & z_2^2 & z_3 & z_4 \end{pmatrix}^\top$ and $M(z) = \begin{pmatrix} 0 & -z_2 & 1 & 0 & 0 \end{pmatrix}$ is its maximal annihilator. Note that if we introduce the intermediate terms x^2, x^5, x^7 into Π, we will obtain an optimization problem, where the algebraic interdependences in the augmented vector $\begin{pmatrix} x & x^3 & x^4 & x^6 & x^8 & x^2 & x^5 & x^7 \end{pmatrix}^\top$ are well represented. ◇

5.5.0.1 LFR-based tuning of quadratic generator forms [P2]**.** In order to introduce the "missing" terms into Π, we consider an LFR realization of Π as follows:

$$\Pi = \mathcal{F}_l\Big\{\begin{pmatrix} H_{11} & H_{12} \\ H_{21} & H_{22} \end{pmatrix}, \Delta_g\Big\}, \tag{5.40}$$

where the corresponding generator

$$\Pi_g^{(\text{initial})} = \begin{pmatrix} I \\ (I-\Delta_gH_{22})^{-1}\Delta_gH_{21} \end{pmatrix} \tag{5.41}$$

is typically not minimal. Therefore, we compute a full column-rank matrix S_g and minimal generator Π_g such that $\Pi_g^{(\text{initial})} = S_g \Pi_g$. Then, function Π can be given in the following minimal generator form realization:

$$\Pi = H_g \Pi_g, \text{ where } H_g = (H_{11}\ H_{12}) S_g. \tag{5.42}$$

Practically, $\Pi_g : \mathcal{W} \to \mathbb{R}^{m_g \times n}$ is a minimal generator for the minimal generator form realization of minimal generator Π (☺). Then, a solution for (5.37) can be given by solving the "tuned-up" PD-LMI

$$H_g^\top Q(w)\, H_g + \text{He}\{L_g N_g(w)\} \succeq 0 \text{ for all } w \in \mathcal{W}, \tag{5.43}$$

where N_g is a maximal annihilator for the new generator Π_g. ▲

Proposition 5.19. *The solution set of* $Q + \text{He}\{LN\} \succeq 0$ (5.38) *is subset of that of* (5.43) *namely,* $\mathfrak{F}_\varphi(N) \subseteq \mathfrak{F}_\varphi(N_g, H_g)$. *The notation for* $\mathfrak{F}_\varphi(N_g, H_g)$ *should be interpreted mutatis mutandis as presented in* (5.33). ◇

Proof. Note that NH_g is an annihilator for Π_g, and it is typically conservative (not maximal). Let N_g denote a maximal annihilator for Π_g. According to Corollary 5.10, there exists Γ_g such that $NH_g = \Gamma_g N_g$. Let (Q, L) denote a solution for (5.43), then, (Q, L_g) with $L_g = H_g^\top L\, \Gamma_g$ is a solution for (5.43). This completes the proof of $\mathfrak{F}_\varphi(N) \subseteq \mathfrak{F}_\varphi(N_g, H_g)$. □

***Remark* 5.9.** The tuning knob of Paragraph 5.5.0.1 results in a higher dimensional PD-LMI (5.43), therefore, it is useful when the solution set for Q is considerably expanded in this way, namely, $\mathfrak{F}_\varphi(N) \subsetneq \mathfrak{F}_\varphi(N_g, H_g)$. Assume that (Q, L_g) is a solution for (5.43). In order to find matrix $L \in \mathbb{R}^{m \times s}$ such that the pair (Q, L) satisfies (5.43), we need to solve the following equation:

$$L_g = H_g^\top L\, \Gamma_g, \text{ where } L_g \in \mathbb{R}^{m_g \times s_g},\ H_g^\top \in \mathbb{R}^{m_g \times m},\ \Gamma_g \in \mathbb{R}^{s \times s_g} \text{ are given.} \tag{5.44}$$

Equation (5.44) has a solution in L if $\text{Im}\{L_g\} \subseteq \text{Im}\{H_g^\top\}$ and $\text{Im}\{L_g^\top\} \subseteq \text{Im}\{\Gamma_g^\top\}$. It is easy to see that equation (5.44) is overdetermined ($m < m_g$ and $s < s_g$), which is due to the $m_g - m$ and $s_g - s$ number of new rows in Π_g and N_g relatively to Π and N, respectively. To conclude, the new (linearly independent rows) in N_g carry important additional information about the nonlinear structure of function $\mathbf{Q}$. ◇

Example 5.5. Here, we give an example, for which $\mathfrak{F}_\varphi(N) = \mathfrak{F}_\varphi(0) \subsetneq \mathfrak{F}_\varphi(N_g, H_g)$. Let us define the following variables:

$$\Pi(x) = \begin{pmatrix} x \\ x^3 \end{pmatrix},\ H_g = \begin{pmatrix} 1 & 0 & 0 \\ 0 & 0 & 1 \end{pmatrix},\ \Pi_g(x) = \begin{pmatrix} x \\ x^2 \\ x^3 \end{pmatrix},\ N_g(x) = \begin{pmatrix} x & -1 & 0 \\ 0 & x & -1 \end{pmatrix}. \tag{5.45}$$

Generator Π does not admit a (multi-)affine annihilator. Observe that there exists an indefinite matrix $Q = \begin{pmatrix} 1 & 0 \\ 0 & -1 \end{pmatrix} \notin \mathfrak{F}_\varphi(0)$, such that $Q \in \mathfrak{F}_\varphi(N_g, H_g)$, namely:

$$H_g^\top Q H_g + \text{He}\{L_g N_g(x)\} = \begin{pmatrix} 1 & -x & 0 \\ -x & 2 & -x \\ 0 & -x & 1 \end{pmatrix} \succeq 0 \text{ for all } x \in [-a, a],\ L_g = \begin{pmatrix} 0 & 0 \\ -1 & 0 \\ 0 & -1 \end{pmatrix},$$

where $0 < a < 1$. ◇

***Remark* 5.10.** The results of Theorem 5.17 and that of Proposition 5.19 are very similar. The former states that the solution set of (5.38) does not change after a projection if the rows of Π are linearly dependent. Whereas, Proposition 5.19 and Remark 5.9 demonstrated that the solution set can be expanded if the already minimal generator Π is augmented by further linearly independent rows. ◇

***Remark* 5.11** [P2]**.** It can be shown that the LFR-based tuning of Paragraph 5.5.0.1 finds the "missing intermediate" terms from Π. Namely, the algebraic coupling between

each pair of rows (coordinates) in generator Π_g can be represented by an *affine* annihilator $N_g \in \mathcal{N}_\varphi^{s_g \times m_g}(\mathcal{W})$ with $\varphi = \left(\begin{smallmatrix}1\\ w\end{smallmatrix}\right)$. ◇

Example 5.6. In this example, we demonstrate how the "missing intermediate" terms will appear in Π_g in case when Π is matrix. In the following set of equations (5.46), one can see the initially given generator Π, its maximal affine annihilator N, then, the computed generator Π_g, matrix H_g, and the corresponding maximal affine annihilator N_g:

$$N(x) = \begin{pmatrix} -x_2 & -x_1 & -x_2 & 1 \end{pmatrix},\ \Pi = \begin{pmatrix} 1 & 0 \\ 0 & 1 \\ x_1^2 & x_2 \\ x_2(x_1^2+1) & x_2^2+x_1 \end{pmatrix},\ H_g = \left(\begin{smallmatrix} 1&0&0&0&0&0&0&0&0&0 \\ 0&1&0&0&0&0&0&0&0&0 \\ 0&0&1&0&0&0&0&1&0&0 \\ 0&0&0&0&1&0&1&0&0&1 \end{smallmatrix}\right) \tag{5.46}$$

$$N_g(x) = \begin{pmatrix} 0 & 0 & 1 & -x_1 & 0 & 0 & 0 & 0 & 0 & 0 \\ -x_1 & 0 & 0 & 1 & 0 & 0 & 0 & 0 & 0 & 0 \\ 0 & 0 & -x_2 & 0 & 1 & 0 & 0 & 0 & 0 & 0 \\ 0 & 0 & 0 & -x_2 & 0 & 1 & 0 & 0 & 0 & 0 \\ 0 & -x_1 & 0 & 0 & 0 & 0 & 1 & 0 & 0 & 0 \\ 0 & -x_2 & 0 & 0 & 0 & 0 & 0 & 1 & 0 & 0 \\ -x_2 & 0 & 0 & 0 & 0 & 0 & 0 & 0 & 1 & 0 \\ 0 & 0 & 0 & 0 & 0 & 0 & 0 & -x_2 & 0 & 1 \\ 0 & 0 & -x_2 & 0 & 0 & x_1 & 0 & 0 & 0 & 0 \\ 0 & 0 & 0 & 0 & 0 & 0 & -x_2 & x_1 & 0 & 0 \\ 0 & 0 & 0 & -x_2 & 0 & 0 & 0 & 0 & x_1 & 0 \end{pmatrix},\ \Pi_g = \begin{pmatrix} 1 & 0 \\ 0 & 1 \\ x_1^2 & 0 \\ x_1 & 0 \\ x_1^2 x_2 & 0 \\ x_1 x_2 & 0 \\ 0 & x_1 \\ 0 & x_2 \\ x_2 & 0 \\ 0 & x_2^2 \end{pmatrix}.$$

Compared to the pair (Π, N), the algebraic coupling constraints in the inflated generator Π_g are better represented by its maximal affine annihilator N_g. ◇

5.6 Concluding remarks and summary

***Remark* 5.12** (A slight difference between the nonlinear and the LPV case)**.** If the state transition matrix $A(x,p)$ of system (5.2) does not depend on the state variables, system (5.2) becomes an LPV system (5.11). In the case of LPV systems, generator $\Pi(p)$ can be considered separately from x, since $\Pi(p)$ does not depend on the state. However, in the case of a nonlinear system (5.2), considering $\Pi(x,p)$ separately from x can be disadvantageous. For example, let $x = \left(\begin{smallmatrix}x_1\\ x_2\end{smallmatrix}\right)$ and

$$\Pi(x) = \begin{pmatrix} x_1x_2 & x_1^2 \\ 0 & x_1^2 \\ x_2^2 & 0 \end{pmatrix} \Rightarrow \pi(x) = \begin{pmatrix} 2x_1^2x_2 \\ x_1^2x_2 \\ x_1x_2^2 \end{pmatrix} \text{ with } N_\Pi(x) = \begin{pmatrix} x_2 & -x_2 & -x_1 \end{pmatrix},\ N_\pi(x) = \begin{pmatrix} 1 & -2 & 0 \\ x_1 & -2x_1 & 0 \\ x_2 & 0 & -2x_1 \\ 0 & x_2 & -x_1 \end{pmatrix}$$

It is visible that the generator Π is minimal, whereas, $\pi = \Pi x$ is not minimal. Furthermore, a maximal affine annihilator for Π is N_Π, however, the maximal affine annihilator N_π for π represents more algebraic coupling between the coordinates of π. Consequently, applying the LMI relaxation techniques (minimal generator and maximal annihilator selection) of Chapter 5 for the quadratic form $\pi^\top Q(p)\pi$ (instead of $\Pi^\top Q(p)\Pi$) may result in a reduced-dimensional and less conservative affine PD-LMI condition. ◇

In this chapter, I introduced a complete framework to model and solve rational PD-LMI conditions by convex optimization. We introduced the notion of a maximal annihilator, which injects the maximal parameter scheduled degree of freedom into the convex constraints. The notion of a minimal generator was introduced in order to allow LMI dimension reduction. We gave efficient numerical methods to find a minimal generator and to compute a maximal annihilator. A maximal annihilator computation technique (Section 5.3), and then, a minimal generator selection method was presented in Section (5.4.1).

The proposed algorithm in Theorem 5.10 with the numerical decomposition of Π in Procedure 5.15 allow us to apply this relaxation technique to arbitrary rational PD-LMI constraints in a (possibly numerically given) quadratic generator form (5.13).

10.15774/PPKE.ITK.2021.004

Chapter 6

Domain of attraction estimation for uncertain nonlinear systems

In this chapter, I propose a systematic method to estimate the domain of attraction of the origin for nonlinear uncertain systems using the computational techniques of Chapter 5. Through the analysis, I consider closed-loop autonomous ($\dot{x}(t) = f(x(t))$), uncertain autonomous ($\dot{x}(t) = f(x(t), p)$), and non-autonomous ($\dot{x}(t) = f(x(t), p(t))$) systems.

Chapter specific notations

In this chapter, we consider both continuous-time (CT) and discrete-time (DT) systems, therefore, a specific notation system is used in this chapter in order to cover both CT and DT model description. Let $x(t)$ denote the value of the vector-valued signal x at time instant t, where $t \geq 0$ in the CT case and $t = 0, 1, 2, \dots$ in the DT case. Let $x^+(t) = \dot{x}(t)$ and $x^+(t) = x(t+1)$, for CD and DT cases, respectively. For simplicity and transparency, we suppress the time arguments in both CT and DT cases, except when it is necessary.

6.1 System class, Lyapunov function, model representation

We consider a nonlinear uncertain (CT or DT) model imported from (5.2), as follows:

$$\Sigma_a : \; x^+ = f(x, p) = A(x, p)x \text{ with } x(0) = x_0 \in \mathcal{X}, \tag{6.1}$$

We assume that Σ_a is given in the following LFR:

$$\mathcal{F}(\Sigma_a) : \begin{cases} x^+ = F_{11}x + F_{12}\pi_1, & A = \mathcal{F}_l\Big\{\left(\begin{smallmatrix} F_{11} & F_{12} \\ F_{21} & F_{22} \end{smallmatrix}\right), \Delta\Big\}, \; \Delta : \mathcal{X} \times \mathcal{P} \to \mathbb{R}^{m_1 \times m_1} \\ \eta_1 = F_{21}x + F_{22}\pi_1, & f = (F_{11} \; F_{12})\pi, \; \pi = \left(\begin{smallmatrix} x \\ \pi_1 \end{smallmatrix}\right), \\ \pi_1 = \Delta_1\eta_1, & \pi_1 = \Pi_1 x, \; \Pi_1 = (I_{m_1} - \Delta F_{22})^{-1}\Delta F_{21}. \end{cases} \tag{6.2}$$

A detailed description of the system class Σ_a and its model representation is presented in details in Section 5.1

Assumption 6.1. Signal p is bounded with a bounded rate, namely, there exist (*a-priori given*) compact polytopes $\mathcal{P}, \mathcal{R} \subset \mathbb{R}^{n_p}$ such that $p(t) \in \mathcal{P}$ for all $t \geq 0$ and

CT case: $\varrho(t) = \dot{p}(t) \in \mathcal{R}$ for all $t > 0$.

DT case: $\varrho(t) = p(t+1) - p(t) \in \mathcal{R}$ for all $t = 0, 1, 2, \cdots$.

With an abuse of notation, we can write: (CT-case) $p^+ = \varrho$, (DT-case) $p^+ = p + \varrho$. $\diamond$

Note that ϱ conceals the different notations in the continuous- and discrete-time cases. With this notation, we are allowed to consider both CT and DT models in a unified RSD

computation framework. Symbol ϱ is often used as an independent variable.

***Remark* 6.1.** Observe that the origin $x^* = 0$ is inherently a (stable or possibly unstable) equilibrium point of Σ_a independently of the parameter's actual value. If Σ_a is a continuous-time model, then, $\dot{x} = A(x,p)x$, $x(0) = 0$ implies that $\dot{x} \equiv 0$, and hence $x(t)$ does not move out from the origin. If Σ_a is a discrete-time model, the recursion $x(t+1) = A(x(t),p(t))x(t)$, with $x(0) = 0$ has again the trivial solution $x(t) = 0$ for all $t = 0, 1, 2, \ldots$. ◇

Definition 6.1 [198]**.** *Assume that x^* is at least locally asymptotically stable. The robust domain of attraction (rDOA) of x^* comprise all initial conditions, from which the solutions of* (6.1) *converge to x^* for all admissible parameter trajectories satisfying Assumption 6.1.* ◇

Definition 6.2. *Set $\Omega \subset \mathbb{R}^{n_x}$ is called a robust stability domain (RSD) of equilibrium point x^*, if the system trajectory converges to x^* from any initial condition $x_0 \in \Omega$ and for any admissible parameter trajectory.* ◇

Note that an RSD of x^* is always a subset of the rDOA, moreover, the computed RSD can be considered as an estimate of the rDOA. Clearly, an RSD of system (6.1) can be given by an appropriate level set of a local Lyapunov function V.

***Remark* 6.2.** Even though the rDOA of x^* might be unbounded, we consider only a compact polytopic set of initial conditions $\mathcal{X}$, including $x^* = 0 \in \mathcal{X}$. Therefore, the computed RSD, which should be located entirely in the interior of $\mathcal{X}$, is inherently bounded. ◇

A suitable parameter-dependent Lyapunov function $V : \mathcal{X} \times \mathcal{P} \to \mathbb{R}$ for Σ_a is searched in the form $V(x,p) = x^\top \mathbf{Q}(x,p)x = \pi^\top(x,p)Q(p)\pi(x,p)$ (5.9), where $\pi : \mathcal{X} \times \mathcal{P} \to \mathbb{R}^m$ is a fixed minimal generator. Affine function $Q : \mathcal{P} \to \mathbb{R}^{m\times m}$ is unknown and meant to be found, such that the equivalent conditions (3.4) for local stability are satisfied.

According to Theorem 3.7, function V should satisfy the following conditions for local stability of Σ_a[1]:

$$\underline{\alpha}(\|x\|) \le V(x,p) = \pi^\top(x,p)Q(p)\pi(x,p) \le \overline{\alpha}(\|x\|) \qquad \forall (x,p) \in \mathcal{X} \times \mathcal{P}, \tag{6.3a}$$

$$\delta V(x,p,\varrho) = \pi_d^\top(x,p,\varrho)Q_d(p,\varrho)\pi_d(x,p,\varrho) \le -\alpha(\|x\|) \quad \forall (x,p,\varrho) \in \mathcal{X} \times \mathcal{P} \times \mathcal{R}, \tag{6.3b}$$

for some class $\mathcal{K}_\infty$ functions $\underline{\alpha}$, $\overline{\alpha}$, and α. In (6.3b), notation δV stands for the rate of the Lyapunov function along the system trajectory. In the CT case $\delta V(x,p,\varrho) = \frac{\partial V}{\partial x}(x,p)f(x,p) + \frac{\partial V}{\partial p}(x,p)\varrho$, whereas, in DT case $\delta V(x,p,\varrho) = V(A(x,p)x, \varrho + p) - V(x,p)$.

As it will be shown in Section 6.2, the rate of the Lyapunov function V in time can be written again in a quadratic factorized form as follows:

$$\delta V = x^\top \mathbf{Q}_d\, x = \pi_d^\top Q_d \pi_d \text{ with } \mathbf{Q}_d = \Pi_d^\top Q_d \Pi_d \text{ and } \pi_d = \Pi_d x, \tag{6.4}$$

where $\mathbf{Q}_d : \mathcal{X} \times \mathcal{P} \times \mathcal{R} \to \mathbb{R}^{n_x \times n_x}$, $\Pi_d : \mathcal{X} \times \mathcal{P} \times \mathcal{R} \to \mathbb{R}^{m \times n_x}$, $\pi_d : \mathcal{X} \times \mathcal{P} \times \mathcal{R} \to \mathbb{R}^m$ are rational functions, and $Q_d \in \mathcal{P} \times \mathcal{R} \to \mathbb{R}^{m\times m}$ is an affine function. Obviously, the quadratic factorization (6.4) of δV with generator π_d is not unique.

[1]Functions $\mathbf{Q}_d$, Q_d, and π_d are related to the rate of the Lyapunov function δV, therefore, subscript d in these notations stands for *derivative* or *difference*.

6.2 Sources of freedom in the model description

In the LMI problem formulation for RSD computation, we have important sources of freedom. The bounds of the parameter value and those of its rate are naturally coming from some physical or technological constraints. However, we also need to define a bounded polytopic domain $\mathcal{X}$ for the state vector. Polytope $\mathcal{X}$ constitutes a subset of the state-space, where the local stability of system Σ_a is tested. The first important degree of freedom therefore is the choice of $\mathcal{X}$, which is not trivial and it is often determined iteratively [16; P8] by gradually enlarging an initial polytope $\mathcal{X}_0$.

Furthermore, we have three important sources of freedom in the model representation. First, we have to a-priori fix the rational structure of the Lyapunov function (selection of π). Secondly, we need to find an appropriate quadratic generator form realization for the rate of the Lyapunov function (selection of π_d). Finally, two annihilators have to be appropriately computed for generator π and π_d.

The shape of the Lyapunov function and hence the area/volume of the computed RSD depends not only on the shape of polytope $\mathcal{X}$ but also on the choice of the generators π and π_d and on their annihilators.

The problem of selecting the "best" annihilators for generator π and π_d is already addressed in Section 5.3, and an efficient numerical procedure is proposed in Section 5.3 to find a *maximal* affine annihilator for a given generator.

However, the choice of generators π and π_d is a trade-off between the computational tractability and the accuracy of the estimated rDOA. Based on the LFT and the proposed minimal generator selection technique in Procedure 5.15, we already defined a possible minimal generator π for Σ_a in Remark 5.8.

In Sections 6.2.1 and 6.2.2, we give alternative quadratic techniques for the rate of the Lyapunov function. But also an LFR-based tuning of a quadratic factorization was presented in Section 5.5.

As we consider parameter-dependent Lyapunov functions, the notion of a robust stability domain is described in Section 6.3 as an abstracted notion of a positively invariant set (Definition 3.8). To expand the robust stability domain as much as possible, a set of convex boundary constraint are presented in Section 6.3.2 with a non-conventional PD-LMI dimension reduction technique. Finally, in Section 6.3.3, convex conditions are formulated for the local asymptotic stability of system Σ_a.

6.2.1 Total derivative of the Lyapunov function

In the continuous-time case, the time-derivate of $V = x^\top \mathbf{Q} x$ (5.9) along the trajectory of system $\Sigma_a : \dot{x} = f(x,p)$ can be computed as follows

$$\delta V(x,p,\varrho) = \dot{V}(x,p) = \tfrac{\partial V}{\partial x}(x,p) f(x,p) + \tfrac{\partial V}{\partial p}(x,p)\varrho = x^\top \mathbf{Q}_d(x,p,\varrho) x \tag{6.5}$$

$$\text{with } \mathbf{Q}_d(x,p,\varrho) = \mathrm{He}\{\mathbf{Q}(x,p)A(x,p)\} + \check{\mathbf{Q}}(x,p,\varrho), \tag{6.5a}$$

$$\text{and } \check{\mathbf{Q}}(x,p,\varrho) = \left\langle \tfrac{\partial \mathbf{Q}}{\partial x}(x,p), f(x,p) \right\rangle + \left\langle \tfrac{\partial \mathbf{Q}}{\partial p}(x,p), \varrho \right\rangle. \tag{6.5b}$$

where $\dot{p} = \varrho$ and the bracketed notation $\langle \cdot, \cdot \rangle$ denotes a tensor contraction operation [199, Section 4.5] as follows:

$$\left\langle \tfrac{\partial \mathbf{Q}}{\partial x}, f \right\rangle = (\nabla_x \otimes \mathbf{Q})(f \otimes I_{n_x}) \text{ and } \left\langle \tfrac{\partial \mathbf{Q}}{\partial p}, \varrho \right\rangle = (\nabla_p \otimes \mathbf{Q})(\varrho \otimes I_{n_x}) = \textstyle\sum_{i=1}^{n_p} \tfrac{\partial \mathbf{Q}}{\partial p_i} \varrho_i, \tag{6.6}$$

$$\text{where } \nabla_x = \begin{pmatrix} \frac{\partial}{\partial x_1} \cdots \frac{\partial}{\partial x_{n_x}} \end{pmatrix} \text{ and } \nabla_p = \begin{pmatrix} \frac{\partial}{\partial p_1} \cdots \frac{\partial}{\partial p_{n_p}} \end{pmatrix} \text{ are the gradient operators.} \tag{6.6a}$$

In the following two propositions, we provide two possible quadratic factorizations for

(6.5) with dynamics $\Sigma_a : \dot{x} = (F_{11}\ F_{12})\pi(x,p)$ and Lyapunov function V in the form $V(x,p) = \pi^\top(x,p)Q(p)\pi(x,p)$ (5.9).

Proposition 6.3. *Function $\dot{V}$ with $\dot{x} = f(x,p)$ and $\dot{p} = \varrho$ can be written as follows:*

$$\dot{V}(x,p) = \pi_d^\top(x,p,\varrho)\, Q_d(p,\varrho)\, \pi_d(x,p,\varrho), \tag{6.7}$$

$$\text{with } Q_d(p,\varrho) = \mathrm{He}\{E_d^\top Q(p) A_d\} + E_d^\top \check{Q}(\varrho) E_d,\ \pi_d = \left(\begin{smallmatrix}\pi\\ \dot{\pi}_1\end{smallmatrix}\right), \tag{6.7a}$$

$$\text{where } E_d = \begin{pmatrix} I_m & 0_{m\times(4m_1)}\end{pmatrix},\ A_d = \left(\begin{smallmatrix} F_{11} & F_{12} & 0\\ 0 & 0 & I_{m_1}\end{smallmatrix}\right), \tag{6.7b}$$

$$\text{and } \dot{\pi}_1(x,p) = \check{\pi}_1(x,p,\varrho) = \tfrac{\partial \pi_1}{\partial x}(x,p) f(x,p) + \tfrac{\partial \pi_1}{\partial p}(x,p)\varrho, \tag{6.7c}$$

$$\text{finally, } \dot{Q}(p) = \check{Q}(\varrho) = \textstyle\sum_{i=1}^{n_p} Q_i \varrho_i. \tag{6.7d}$$

Matrices F_{11} and F_{12} are given in (6.1). ◇

Proof. The time-derivative of the Lyapunov function is $\dot{V} = \mathrm{He}\{\pi^\top Q \dot{\pi}\} + \pi^\top \dot{Q} \pi$, where $\dot{\pi} = A_d \pi_d$ and $\pi = E_d \pi_d$. □

***Remark* 6.3.** The quadratic realization (6.7) for the time-derivative of the Lyapunov function may be conservative. Note that the derivative function $\dot{\pi}_1$ in (6.7c) contains sums of multiple typically high degree terms multiplied by the independent variables ϱ. Therefore, the algebraic coupling between π and $\dot{\pi}_1$ in generator π_d in (6.7b) is often not possible to be represented by affine annihilators. For instance, consider $\dot{x} = xp + x^2 p$, $\dot{p} = \varrho$, and $\pi_1 = \left(\begin{smallmatrix} xp\\ x^2p\end{smallmatrix}\right)$, then, the time-derivative of π_1 is $\dot{\pi}_1 = \left(\begin{smallmatrix} xp^2+x^2p^2+x\varrho\\ 2x^2p^2+2x^3p^2+x^2\varrho\end{smallmatrix}\right)$. A maximal affine annihilator for π_d is as follows:

$$N_d = \left(\begin{smallmatrix} p & -1 & 0 & 0 & 0\\ \dot{p} & p & p & -1 & 0\\ 0 & x & -1 & 0 & 0\end{smallmatrix}\right),\ \pi_d = \begin{pmatrix} x\\ xp\\ x^2p\\ xp^2+x^2p^2+x\varrho\\ 2x^2p^2+2x^3p^2+x^2\varrho\end{pmatrix}. \tag{6.8}$$

Observe that the last coordinate of function π_d does not appear in $N_d\pi_d \equiv 0$. For more details and examples, we refer back to Section 5.5 and to [P2, Section 4] ◇

Proposition 6.4. *Another factorization for $\dot{V}$ can be given in the form* (6.7) *with the modified matrices:*

$$E_d = \begin{pmatrix} I_m & 0_{m\times(4m_1)}\end{pmatrix},\quad A_d = \left(\begin{smallmatrix} F_{11} & F_{12} & 0 & 0 & 0 & 0\\ 0 & 0 & I_{m_1} & I_{m_1} & I_{m_1} & I_{m_1}\end{smallmatrix}\right),\quad \text{and } \pi_d = \underbrace{\begin{pmatrix} \Pi\\ \Pi_1 F_{11}\\ \Pi_1 F_{12}\Pi_1\\ \langle \partial\Pi_1/\partial x\,, f\rangle\\ \langle \partial\Pi_1/\partial p\,, \varrho\rangle\end{pmatrix}}_{\Pi_d}\cdot x, \tag{6.9}$$

where $\Pi_1 = \mathcal{F}_l\left\{\left(\begin{smallmatrix} 0 & I_{m_1}\\ F_{21} & F_{22}\end{smallmatrix}\right), \Delta\right\}$ (5.7b), *and* $\Pi = \left(\begin{smallmatrix} I_{n_x}\\ \Pi_1\end{smallmatrix}\right)$. ◇

Proof. It is enough to show that $\dot{\pi} = A_d\pi_d$ and $\pi = E_d\pi_d$. From representation (6.2), we have that $\dot{x} = F_{11}x + F_{12}\Pi_1 x$. Therefore, $\dot{\pi}_1 = \dot{\Pi}_1 x + \Pi_1 \dot{x}$, where

$$\dot{\Pi}_1 = \left\langle \tfrac{\partial \Pi_1}{\partial x},\, f\right\rangle + \left\langle \tfrac{\partial \Pi_1}{\partial p},\, \varrho\right\rangle \tag{6.10}$$

and $\Pi_1\dot{x} = \Pi_1 F_{11} x + \Pi_1 F_{12}\Pi_1 x$. The inner products $\langle\cdot,\cdot\rangle$ should be interpreted as presented in (6.6). □

***Remark* 6.4.** Note that in (6.9), the higher order nonlinearities of π_d in (6.9) are introduced gradually by the terms Π_1F_{11}, $\Pi_1F_{12}\Pi_1$, $\left\langle \frac{\partial\Pi_1}{\partial x},\, f\right\rangle$, $\left\langle \frac{\partial\Pi_1}{\partial p},\, \varrho\right\rangle$. This makes possible to introduce some "intermediate" terms into function π_d. From the author's experience, the algebraic coupling between the coordinates of π_d is more likely to be characterized by an affine annihilator in this way. If we continue the example in Remark 6.3, we obtain that

$$F_{11} = 0,\ F_{12} = (1\ 1),\ \Pi_1 = \left(\begin{smallmatrix} p\\ xp\end{smallmatrix}\right),\ \tfrac{\partial\Pi_1}{\partial x} f = \begin{pmatrix} 0\\ xp^2+x^2p^2\end{pmatrix},\ \tfrac{\partial\Pi_1}{\partial p}\varrho = \left(\begin{smallmatrix} \varrho\\ x\varrho\end{smallmatrix}\right). \tag{6.11}$$

Function π_d is not a minimal generator, hence, we compute S and $\widehat{\pi}_d$ such that $\pi_d = S\widehat{\pi}_d$. Matrix S, function $\widehat{\pi}_d$, and its maximal affine annihilator is given as below:

$$\Pi_d = \begin{pmatrix} 1 \\ p \\ xp \\ 0 \\ 0 \\ p^2x+p^2 \\ p^2x^2+p^2x \\ 0 \\ p^2x^2+p^2x \\ \varrho \\ x\varrho \end{pmatrix}, \; S = \begin{pmatrix} 1&0&0&0&0&0&0&0 \\ 0&1&0&0&0&0&0&0 \\ 0&0&1&0&0&0&0&0 \\ 0&0&0&0&0&0&0&0 \\ 0&0&0&0&0&0&0&0 \\ 0&0&0&1&0&0&0&0 \\ 0&0&0&0&1&0&0&0 \\ 0&0&0&0&0&0&0&0 \\ 0&0&0&0&1&0&0&0 \\ 0&0&0&0&0&1&0&0 \\ 0&0&0&0&0&0&1&0 \\ 0&0&0&0&0&0&0&1 \end{pmatrix}, \; \widehat{N}_d = \begin{pmatrix} p&-1&0&0&0&0&0 \\ \varrho&0&0&0&0&-1&0 \\ 0&x&-1&0&0&0&0 \\ 0&p&p&-1&0&0&0 \\ 0&\varrho&0&0&0&-p&0 \\ 0&0&\varrho&0&0&0&-p \\ 0&0&0&x&-1&0&0 \\ 0&0&0&0&0&x&-1 \end{pmatrix}, \; \widehat{\pi}_d = \begin{pmatrix} x \\ px \\ px^2 \\ p^2x^2+p^2x \\ p^2x^3+p^2x^2 \\ \varrho x \\ \varrho x^2 \end{pmatrix}. \tag{6.12}$$

Observe that each coordinate function of $\widehat{\pi}_d$ appears at least in a single algebraic expressions $\widehat{N}_d\widehat{\pi}_d \equiv 0$. ◇

When $Q : \mathcal{X} \times \mathcal{P} \to \mathbb{R}^{m\times m}$ is a function of both x and p, and

$$Q(x,p) = Q_0 + \textstyle\sum_{i=1}^{n_x} Q_{1i}x_i + \sum_{j=1}^{n_p} Q_{2j}p_j, \tag{6.13}$$

the quadratic generator form realization for the Lyapunov function's time-derivative is more technical and is given in Proposition 4.4. Though, the factorization in Proposition 4.4 is essentially based on the derivations of [16], our slight improvement consists in the affine state and parameter dependence in function Q. By comparison, Trofino and Dezuo [16] considered a constant matrix Q.

6.2.2 Rate of the Lyapunov function

Similarly to the technique presented in Proposition 6.3, the Lyapunov inequality (6.3a) can be written in a quadratic form (6.4) in the discrete-time case as well.

Proposition 6.5. *The rate of function $V = x^\top \mathbf{Q}\, x = \pi^\top Q\, \pi$ (5.9) along the trajectories of $x^+ = f(x,p) = A(x,p)\, x$ with $p^+ = \varrho + p$ is*

$$\delta V(x,p,\varrho) = V(f(x,p), p+\varrho) - V(x,p) = x^\top \mathbf{Q}_d(x,p,\varrho)x \tag{6.14}$$

$$\text{where } \mathbf{Q}_d(x,p,\varrho) = A^\top(x,p)\mathbf{Q}(f(x,p),p+\varrho)A(x,p) - \mathbf{Q}(x,p). \tag{6.14a}$$

Then, a possible quadratic factorization of (6.14) *is*

$$\delta V(x,p,\varrho) = \pi_d^\top(x,p,\varrho)\, Q_d(p,\varrho)\, \pi_d(x,p,\varrho) \tag{6.15}$$

$$\text{with } Q_d(p,\varrho) = A_d^\top Q(p+\varrho)A_d - E_d^\top Q(p)E_d \text{ and } \pi_d = \begin{pmatrix} \pi \\ \pi_1^+ \end{pmatrix} = \Pi_d x, \tag{6.15a}$$

$$\text{where } \Pi_d(x,p,\varrho) = \begin{pmatrix} \Pi(x,p) \\ \Pi_1(f(x,p),p+\varrho)(F_{11}+F_{12}\,\Pi_1(x,p)) \end{pmatrix}. \tag{6.15b}$$

Matrices A_d and E_d in (6.15a) *are the same as in* (6.7b). ◇

Proof. Substitute π_d and $Q_d(p,\varrho)$ into (6.15) to obtain (6.14). □

Note that generator $\pi_d = \begin{pmatrix} \pi \\ \pi_1^+ \end{pmatrix}$ in Proposition 6.5 is very similar to $\pi_d = \begin{pmatrix} \pi \\ \dot{\pi}_1 \end{pmatrix}$ in Proposition 6.3, but applied to the discrete-time dynamics, namely,

$$\pi_1^+(x,p) = \pi_1(f(x,p), p+\varrho). \tag{6.16}$$

We stress that the explicit value of π_1^+ depends on the parameter rate $\varrho = p^+ - p$, which is considered as an independent variable in (6.3b).

In Section 4.2.3, we have presented an alternative approach (for the CT case) to factorize the total derivative of the Lyapunov function. Furthermore, a (possibly not maximal) annihilator is given explicitly for the corresponding generator (π_r) in Proposition 4.5. Based on these results, we present a similar factorization in the DT case.

The proposed decomposition is motivated by the uniformly zero "annihilation" ex-

pression of $N(x,p)\pi(x,p)=0$ but evaluated in the subsequent time step as follows:

$$N(f(x,p),p+\varrho)\,\pi(f(x,p),p+\varrho)=0. \tag{6.17}$$

In expression (6.17), important nonlinear terms may appear, which, collected in a generator π_r may result in an more representative annihilator and hence in a less conservative convex condition.

Proposition 6.6 [P2]. *Considering the rational terms of expression* (6.17)*, an alternative factorization for $\delta V(x,p,\varrho)$ can be given as follows*

$$\delta V(x,p,\varrho)=\pi_r^\top(x,p,\varrho)\,H_r^\top\,Q_d(p,\varrho)\,H_r\,\pi_r(x,p,\varrho), \tag{6.18}$$
$$\text{with } H_r=\begin{pmatrix} I_{n_x+2m_1} & 0_{(n_x+2m_1)\times(n_x^2+2n_xm_1)}\end{pmatrix},$$

Generator $\pi_r(x,p,\varrho)$ is defined as follows:

$$\pi_r=\begin{pmatrix}\pi_d\\ \mu\end{pmatrix},\ \text{with } \mu=\begin{pmatrix}\mu_1\\ \cdots\\ \mu_{n_x}\end{pmatrix}=(f\otimes I_m)\,\pi_d,\ \mu_i=x_i^+\pi_d, \tag{6.19}$$

where vector π_d and matrix $Q_d(p,\varrho)$ are given in (6.15) *and $x^+=f(x,p)$.* ⋄

Proof. Considering the fact that $H_r\pi_r=\pi_d$ it is easy to see that factorization (6.18) gives back function $\delta V=\pi_d^\top Q_d\pi_d$ (6.4). □

Factorization (6.18) also makes possible to define a (not necessarily maximal) affine annihilator for vector $\pi_r(x,p,\varrho)$.

Proposition 6.7 [P2]. *A possible annihilator for $\pi_r(x,p,\varrho)$ in* (6.19) *is*

$$N_r(x,p,\varrho)=\begin{pmatrix} N_d(x,p,\varrho) & 0\\ 0 & I_{n_x}\otimes N_d(x,p,\varrho)\\ N_0(p+\varrho)A_d & \begin{pmatrix}N_1A_d & N_2A_d & \cdots & N_{n_x}A_d\end{pmatrix}\\ (I_{n_x}\otimes x)\cdot\begin{pmatrix}F_{11} & F_{12} & 0_{n_x\times p}\end{pmatrix} & -I_{n_x}\otimes\begin{pmatrix}I_{n_x} & 0_{n_x\times 2p}\end{pmatrix}\end{pmatrix}, \tag{6.20}$$

where N_i are constant matrices and N_0 is an affine matrix function of p such that:

$$N(x,p)=N_0(p)+\textstyle\sum_{i=1}^{n_x}N_ix_i \tag{6.21}$$

and matrix $N(x,p)$ is an annihilator for vector $\pi=\Pi x$. ⋄

Proof. Affine matrix $N_d(x,p,\varrho)$ is an annihilator of π_d and hence of $\mu_i=x_i^+\pi_d$ for all $i=1,\dots,n_x$. On the other hand, if we evaluate expression (6.17) and considering that $\pi^+=A_d\pi_d$, we obtain the following identity:

$$\begin{aligned}0&=N(f(x,p),p+\varrho)\,\pi^+\\ &=N_0(p+\varrho)A_d\pi_d+\textstyle\sum_{i=1}^{n_x}N_iA_d\mu_i\end{aligned} \tag{6.22}$$

Finally, we can observe that

$$\begin{pmatrix}I_{n_x} & 0_{n_x\times 2p}\end{pmatrix}\mu_i=xx_i^+, \tag{6.23}$$

therefore, if we collect vectors xx_i^+ into a composed vector, we obtain an affine relationship between μ and π_d:

$$\left[I_{n_x}\otimes\begin{pmatrix}I_{n_x} & 0_{n_x\times 2p}\end{pmatrix}\right]\cdot\mu=\begin{pmatrix}x\,x_1^+\\ \cdots\\ x\,x_n^+\end{pmatrix}=(I_{n_x}\otimes x)\,x^+=(I_{n_x}\otimes x)\cdot H_d\pi_d. \tag{6.24}$$

Identity (6.24) gives the last row of annihilator $N_r(x,p,\varrho)$. □

6.3 Robust stability domain computation

It is well-known that a (parameter independent) Lyapunov function $V:\mathcal{X}\to\mathbb{R}$ satisfying (6.3), determines a positively invariant level set $\Omega_\alpha=\{x\in\mathcal{X}\,|\,V(x)\le\alpha\}$ with measure greater than zero. Then, Ω_α is a robust stability domain (RSD) for the (possibly non-autonomous) system $\Sigma_a:\dot{x}=f(x,p)$ in the sense of Definition 6.2.

In general, we consider a parameter-dependent Lyapunov function $V : \mathcal{X} \times \mathcal{P} \to \mathbb{R}$ with a time-varying parameter $p : [0, \infty) \to \mathcal{P}$. Then, it is less straightforward how an RSD can be determined for the non-autonomous system $\Sigma_a : \dot{x} = f(x, p)$.

6.3.1 Level set of a parameter-dependent Lyapunov function

In this section, we present a step-by-step construction of a possible RSD.

1. First of all, let us consider the "hyper" level set of V in the unified state and parameter space $\mathbb{R}^{n_x+n_p}$ as follows:

$$\Psi_\alpha = \{(x, p) \in \mathbb{R}^{n_x} \times \mathcal{P} \mid V(x, p) \leq \alpha\}. \tag{6.25}$$

   Note that each point (x, p), for which $p \notin \mathcal{P}$, is irrelevant in the stability analysis, therefore, they are not an element of Ψ_α. The truncated level set Ψ_α is illustrated by the filled orange region in Figure 6.1. Due to the geometry (6.3a) of the Lyapunov function, there exists some $\alpha > 0$, such that the truncated level set Ψ_α is contained (entirely) in $\mathcal{X} \times \mathcal{P}$. In this case, Ψ_α is positively invariant with respect to the system dynamics. In other words, $(x(0), p(0)) \in \Psi_\alpha$ implies that $(x(t), p(t)) \in \Psi_\alpha$ for all $t \geq 0$.

   Suppose that the Lyapunov function $V = x^\top \mathbf{Q}\, x$ (5.9) is quadratic with a positive definite $\mathbf{Q}(x, p)$ for all $(x, p) \in \mathcal{X} \times \mathcal{P}$. Then, according to [16, Corollary 4.1], the Lyapunov inequalities (6.3) imply that the solution x of Σ_a will converge to the equilibrium point $x^* = 0$, for all $(x(0), p(0)) \in \Psi_\alpha$ and all admissible parameter signal p satisfying Assumption 6.1.

2. Secondly, we introduce an auxiliary set, which can be considered as a "projection" of Ψ_α onto the subspace of the state variables ($\mathbb{R}^{n_x}$) defined in the following way (Figure 6.1, blue interval):

$$\begin{aligned} \Omega_\alpha &= \{x \in \mathbb{R}^{n_x} \mid \exists p \in \mathcal{P} \text{ such that } V(x, p) \leq \alpha\} \\ &= \textstyle\bigcup_{p \in \mathcal{P}} \{x \in \mathbb{R}^{n_x} \mid V(x, p) \leq \alpha\}. \end{aligned} \tag{6.26}$$

   Note that $\Omega_\alpha \subset \mathcal{X}$ if $\Psi_\alpha \subset \mathcal{X} \times \mathcal{P}$.

3. Finally, we give a robust stability domain for the equilibrium point:

$$\begin{aligned} \Omega_\alpha^{x_0} &= \{x \in \mathbb{R}^{n_x} \mid V(x, p) \leq \alpha \text{ for all } p \in \mathcal{P}\} \\ &= \textstyle\bigcap_{p \in \mathcal{P}} \{x \in \mathbb{R}^{n_x} \mid V(x, p) \leq \alpha\} \subseteq \Omega_\alpha. \end{aligned} \tag{6.27}$$

   Superscript x_0 in the notation of set (6.27) emphasizes that $\Omega_\alpha^{x_0}$ is a set of initial conditions $x(0) = x_0$, from which the state vector will remain inside Ω_α and will converge to the equilibrium point independently of the time evolution of the uncertain parameters.

Though a positively invariant domain cannot be given for a parameter-dependent Lyapunov function, we are able to determine two subsets $\Omega_\alpha^{x_0} \subset \Omega_\alpha$, which provide a more specific stability property. Namely, $x(t) \in \Omega_\alpha$ for all $t \geq 0$ if $x(0) \in \Omega_\alpha^{x_0}$. If the Lyapunov function is parameter-independent $\Omega_\alpha = \Omega_\alpha^{x_0}$ is positively invariant.

In [16, Eqs. (89) and (90)], the authors introduced two further LMI conditions, which ensure that the truncated unitary level set

$$\Psi_1 = \Psi_{\alpha=1} = \{(x, p) \in \mathbb{R}^{n_x} \times \mathcal{P} \mid V(x, p) \leq 1\}. \tag{6.28}$$

is entirely inside of $\mathcal{X} \times \mathcal{P}$. Furthermore, an objective function is proposed to be minimized in order to $\mathcal{X} \times \mathcal{P}$ by Ψ_1 as much as possible.

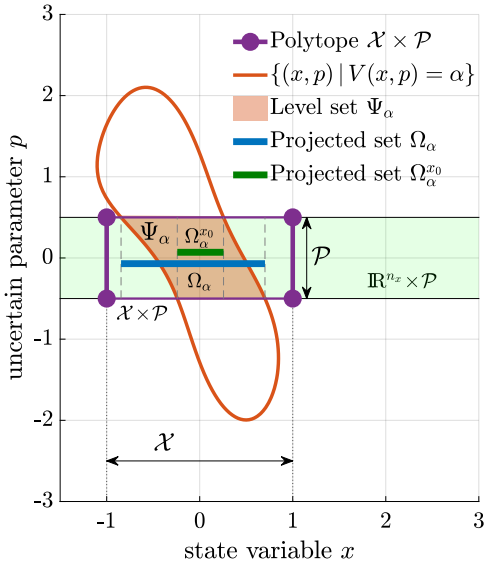

Figure 6.1: In this figure, we illustrate how the robust stability domain is computed by using a specific level set of the obtained parameter-dependent Lyapunov function. For simplicity, the RSD of a first order system is illustrated in this figure with a single uncertain parameter. The orange contour line illustrates the α level set of the Lyapunov function V. The light green band ($\mathbb{R}^{n_x} \times \mathcal{P}$) highlights the region, where $p \in \mathcal{P}$. The filled orange region illustrates the truncated level set Ψ_α. This truncated set is positively invariant with respect to the system dynamics. The blue and green intervals illustrate the projected sets Ω_α and $\Omega_\alpha^{x_0}$, respectively. If the initial value of the state variable $x(0)$ belongs to the computed robust stability domain $\Omega_\alpha^{x_0}$, the state $x(t)$ will remain inside Ω_α for all $t \geq 0$ and will converge to the origin, independently of $p(t)$, i.e., $x(t) \in \Omega_\alpha$ and $x(t) \to x^*$ for all $x(0) \in \Omega_\alpha^{x_0}$ and for any admissible parameter trajectory $p(t)$ satisfying Assumption 6.1.

6.3.2 Boundary conditions

Instead of the S-procedure approach of El Ghaoui and Scorletti (Section 4.2.1) or Coutinho et al. (Section 4.2.2) we present a generalized version of the approach proposed by Trofino and Dezuo (Section 4.2.4).

Trofino and Dezuo [16] prescribed the Lyapunov function to be greater than 1 along the bounds $\partial\mathcal{X}$ of polytope $\mathcal{X}$. Furthermore, an auxiliary slack variable are introduced, by which the Lyapunov function is upper-bounded and minimized to spread the unitary level set Ω_1 in $\mathcal{X}$ as much as possible. Then, the boundary conditions are

$$1 \leq V(x,p) \leq \tau \text{ for all } x \in \partial\mathcal{X} \text{ and all } p \in \mathcal{P}. \tag{6.29}$$

The previous constraint is obviously not convex, as $\partial\mathcal{X}$ is not convex. However, as $\mathcal{X}$ is a polytope, we have the possibility to cover $\partial\mathcal{X}$ by a number of convex sets, namely, $\partial\mathcal{X} = \bigcup_{k=1}^{m_\mathcal{X}} \mathcal{F}_k$, where

$$\mathcal{F}_k \subset \left\{ x \in \mathbb{R}^{n_x} \;\middle|\; a_k^\top x = 1 \right\} \tag{6.30}$$

denotes the kth facet of polytope $\mathcal{X}$. Vector $a_k \in \mathbb{R}^{n_x}$ is a vector perpendicular to $\mathcal{F}_k$ and its norm is inversely proportional to the distance of the origin (d_k) to facet $\mathcal{F}_k$, namely, $\|a_k\| = d_k^{-1}$. See also Figure 6.2.

Finally, the set of boundary conditions are presented as follows:

$$1 \leq V(x,p) \leq \tau_k \text{ for all } (x,p) \in \mathcal{F}_k \times \mathcal{P} \text{ and for some } \tau_k \geq 1. \tag{6.31}$$

Note that in (6.31), multiple slack variables appear (τ_k) corresponding to each facet $\mathcal{F}_k$, $k = 1, \ldots, m_\mathcal{X}$. The sum of variables τ_k is meant to be minimized through the optimization procedure.

Inequalities (6.31) can be rewritten as follows[2]:

$$\pi_f^\top Q_f(p,1)\pi_f \geq 0 \text{ and } \pi_f^\top Q_f(p,\tau_k)\pi_f \leq 0 \text{ for all } (x,p) \in \mathcal{F}_k \times \mathcal{P}, \tag{6.32}$$
$$\text{where } Q_f(p,\alpha) = \begin{pmatrix} -\alpha & 0 \\ 0 & Q(p) \end{pmatrix} \text{ and } \pi_f = \begin{pmatrix} 1 \\ \pi \end{pmatrix} = \begin{pmatrix} 1 \\ x \\ \pi_1 \end{pmatrix}, \pi_1 = \Pi_1 x.$$

By construction (Procedure 5.15), rational vector π is a minimal generator for $V(x,p)$,

[2]Subscript f in π_f and Q_f suggests that these variables are related to the boundary conditions on the *facets* of polytope $\mathcal{X}$.

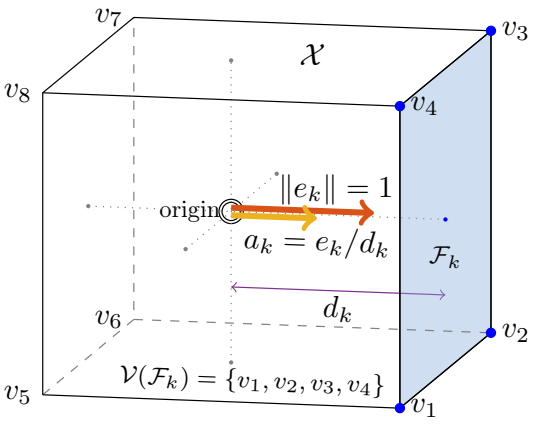

Figure 6.2: This figure illustrates how to calculate vector a_k for a given facet $\mathcal{F}_k$. Vector e_k (red arrow) is a unit length vector orthogonal to $\mathcal{F}_k$, d_k is the distance of the origin from $\mathcal{F}_k$, then $a_k = \frac{e_k}{d_k}$ (yellow arrow) is an orthogonal vector with a length inversely proportional to d_k. If a point $x \in \mathbb{R}^n$ is an element of polytope $\mathcal{X}$, then $e_k^\top x \leq d_k$, or alternatively, $a_k^\top x \leq 1$ for every facet $\mathcal{F}_k$. Additionally, this figure illustrates the case of a rectangular polytope in a three-dimensional state-space, with $n_{\mathcal{X}} = 2^3 = 8$ number of corner points. This polytope has $M_{\mathcal{X}} = 2 \cdot 3 = 6$ facets, and each facet has $n_{\mathcal{F}_k} = 2^{3-1} = 4$ vertices.

in other words, the coordinate function of π are linearly independent (Definition 5.6). Therefore, vector π_f is again a minimal generator. However, each inequality in (6.32) is meant to be solved over an $(n_x - 1)$-dimensional submanifold $\mathcal{F}_k$ of polytope $\mathcal{X} \subset \mathbb{R}^{n_x}$. This fact involves additional algebraic interdependence ($a_k^\top x = 1$) between the state variables, and hence in the (possibly minimal) generator π_f, e.g., $\begin{pmatrix} 1 & a_k^\top & 0 \end{pmatrix} \pi_f = 0$. In the following example, we demonstrate that even a simple vector π_f may admit multiple linearly independent constant annihilator rows when $x \in \mathcal{F}_k$.

Example 6.1. Let $x = \left(\begin{smallmatrix} x_1 \\ x_2 \end{smallmatrix}\right) \in \mathbb{R}^2$, and let $\pi_1 = \begin{pmatrix} x_1^2 & x_1 x_2 & x_2^2 \end{pmatrix}^\top$, then constraining x to satisfy $x_1 + x_2 + 1 = 0$, a possible constant annihilator for $\pi_f = \begin{pmatrix} 1 & x_1 & x_2 & \pi_1^\top \end{pmatrix}^\top$ is $N_0 = \left(\begin{smallmatrix} 1 & 1 & 1 & 0 & 0 & 0 \\ 0 & 1 & 0 & 1 & 1 & 0 \\ 0 & 0 & 1 & 0 & 1 & 1 \end{smallmatrix}\right)$. ◇

In the following corollary, we summarize the sufficient boundary LMIs for function V.

Corollary 6.8 (Boundary LMIs)**.** *Consider function $V : \mathcal{X} \times \mathcal{P} \to \mathbb{R}$ in the form (5.9), namely, $V(x,p) = \pi^\top(x,p) Q(p) \pi(x,p)$, where $\pi : \mathcal{X} \times \mathcal{P} \to \mathbb{R}^m$ is a minimal generator, and $Q(p) = Q_0 + \sum_{i=1}^{n_p} Q_i p_i$. For each facet $\mathcal{F}_k$ ($k = 1, \ldots, m_{\mathcal{X}}$) of polytope $\mathcal{X}$, compute*

1. *full column-rank matrix $S_{f,k} \in \mathbb{R}^{(m+1) \times m_{f,k}}$ ($m_{f,k} \leq m$), and minimal generator $\pi_{f,k} : \mathcal{F}_k \times \mathcal{P} \to \mathbb{R}^{m_{f,k}}$, such that $\pi_f(x,p) = S_{f,k} \pi_{f,k}(x,p)$ for all $(x,p) \in \mathcal{F}_k \times \mathcal{P}$, where $\pi_f = \left(\begin{smallmatrix} 1 \\ \pi \end{smallmatrix}\right) : \mathcal{F}_k \times \mathcal{P} \to \mathbb{R}^{m+1}$,*

2. *affine annihilator $N_{f,k} : \mathcal{F}_k \times \mathcal{P} \to \mathbb{R}^{s_{f,k} \times m_{f,k}}$, such that $N_{f,k} \pi_{f,k} \equiv 0$ on $\mathcal{F}_k \times \mathcal{P}$.*

Assume that for each facet $\mathcal{F}_k$, there exist matrices $L_{f,k}^{(1)}, L_{f,k}^{(2)} \in \mathbb{R}^{m_{f,k} \times s_{f,k}}$ such that the following PD-LMIs are satisfied

$$Q_{f,k}(p,1) + \mathrm{He}\{L_{f,k}^{(1)} N_{f,k}(x,p)\} \succeq 0, \qquad \text{for all } (x,p) \in \mathbf{Ve}(\mathcal{F}_k \times \mathcal{P}), \tag{6.33a}$$

$$Q_{f,k}(p,\tau_k) + \mathrm{He}\{L_{f,k}^{(2)} N_{f,k}(x,p)\} \preceq 0, \qquad \text{for all } (x,p) \in \mathbf{Ve}(\mathcal{F}_k \times \mathcal{P}), \tag{6.33b}$$

where $Q_{f,k}(p,\alpha) = S_{f,k}^\top Q_f(p,\alpha) S_{f,k}$. Then, inequality (6.31) is satisfied.

Symmetric matrices $Q_0, \ldots, Q_{n_p}$ and full matrices $L_{f,k}^{(1)}$, $L_{f,k}^{(2)}$, $k = 1, \ldots, m_{\mathcal{X}}$ are free decision variables of the semidefinite program, and are meant to be found such that $\sum_{k=1}^{m_{\mathcal{X}}} \tau_k$ is minimized. ◇

Proof. To obtain (6.32), multiply both PD-LMIs from the left and right hand side by $\widehat{\pi}_{f,k}^\top$ and by $\widehat{\pi}_{f,k}$, respectively. □

Note that Corollary 6.8 extends the results of [16, Section 5.1] in the terms of automation and dimensional reduction.

***Remark* 6.5.** In order to determine the decomposition $\pi_f = S_{f,k}\widehat{\pi}_{f,k}$, we find a constant matrix $N_{0,k}$ satisfying $N_{0,k}\pi_f = 0$ for all $(x,p) \in \mathcal{F}_k \times \mathcal{P}$ (Procedure 5.13 with Remark 5.4). Then, apply Procedure 5.15 to obtain $S_{f,k}$ and $\widehat{\pi}_{f,k}$. $\diamond$

6.3.3 Final optimization solution for DOA computation

Up to this point, we collected the necessary ingredients to formulate the final optimization task for DOA estimation. First, we presented the LFR system representation (6.2) to select generator π. In Section 6.2.1, multiple factorization techniques were presented for the Lyapunov inequality $\delta V = \pi_d^\top Q_d \pi_d$ (6.4). Finally, boundary LMIs were introduced to shape the Lyapunov function conveniently.

In the following corollary, we present the overall optimization problem for RSD computation. Corollary 6.9 should be interpreted in the foreground of the computational framework of Chapter 5, and in companion with the boundary LMIs in Corollary 6.8.

Corollary 6.9 (SDP for DOA estimation)**.** *Consider system $\Sigma_a : x^+ = A(x,p)x$ (6.1), function $V = \pi^\top Q\,\pi$ (5.9), and a possible factorization of $\delta V = \pi_d^\top Q_d \pi_d$ (6.4) where $\pi : \mathcal{X}\times\mathcal{P} \to \mathbb{R}^m$ is a minimal generator, $\pi_d : \mathcal{X}\times\mathcal{P}\times\mathcal{R} \to \mathbb{R}^{m_d}$ is not necessarily a minimal generator, and $\mathcal{X} \subset \mathbb{R}^{n_x}$, $\mathcal{P}, \mathcal{R} \subset \mathbb{R}^{n_p}$ are compact polytopes. Compute*

1. *full column-rank matrix $S_d \in \mathbb{R}^{m_d \times m'_d}$ and minimal generator $\widehat{\pi}_d : \mathcal{X}\times\mathcal{P}\times\mathcal{R} \to \mathbb{R}^{m'_d}$ such that $\pi_d = S_d\widehat{\Pi}_d$,*
2. *affine functions $N : \mathcal{X}\times\mathcal{P} \to \mathbb{R}^{s\times m}$ and $N_d : \mathcal{X}\times\mathcal{P}\times\mathcal{R} \to \mathbb{R}^{s_d\times m'_d}$, such that $N\pi \equiv 0$ and $N_d\pi_d \equiv 0$.*
3. *matrices $S_{f,k}$, generators $\pi_{f,k}$, and annihilators $N_{f,k}$ as requested by Corollary 6.8.*

Consider some positive constants $0 < \underline{\alpha}_0, \alpha_0 \ll 1$. Then, system Σ_a is locally asymptotically stable with the Lyapunov function V if there exist matrices $L \in \mathbb{R}^{m\times s}$, $L_d \in \mathbb{R}^{m'_d\times s_d}$, and $L_{f,k}^{(1)}, L_{f,k}^{(2)} \in \mathbb{R}^{m_{f,k}\times s_{f,k}}$, $k = 1,\dots,m_{\mathcal{X}}$, such that the LMIs (6.33) in Corollary 6.8 and the LMIs above are satisfied:

$$Q(p) + \mathrm{He}\{LN(x,p)\} - \begin{pmatrix} \underline{\alpha}_0 I_{n_x} & \\ & 0 \end{pmatrix} \succeq 0 \qquad \forall\,(x,p) \in \mathbf{Ve}(\mathcal{X}\times\mathcal{P}), \tag{6.34a}$$

$$S_d^\top\Big(Q_d(p,\varrho) + \begin{pmatrix} \alpha_0 I_{n_x} & \\ & 0 \end{pmatrix}\Big)S_d + \mathrm{He}\{L_d N_d(x,p,\varrho)\} \preceq 0 \;\; \forall\,(x,p,\varrho) \in \mathbf{Ve}(\mathcal{X}\times\mathcal{P}\times\mathcal{R}). \tag{6.34b}$$

Symmetric matrices $Q_0,\dots,Q_{n_p}$, full matrices L, L_d, $L_{f,k}^{(1)}$, and $L_{f,k}^{(2)}$ are free decision variables of the semidefinite program and are meant to be found such that they minimize the cost function $\sum_{k=1}^{m_{\mathcal{X}}} \tau_k$ of Corollary 6.8. $\diamond$

Note that the PD-LMIs in (6.33) and (6.34) are affine in (x,p,ϱ), therefore, they can be solved with a semidefinite solver if we evaluate them in the corner points of the corresponding polytopic domains. In this way, we obtain a system of a finite number of LMIs. For convenience, we collected the number of LMIs and their dimensions in Table 6.1, where $n_{\mathcal{X}}$, $n_{\mathcal{P}}$, and $n_{\mathcal{R}}$ denote the number of corner points of polytopes $\mathcal{X}$, $\mathcal{P}$ and $\mathcal{R}$, respectively, and $m_{\mathcal{X}}$ denotes number of facets of $\mathcal{X}$. The dimension of PD-LMIs (6.34b) and (6.33) depends on the dimensions (m'_d and $m'_{f,k} \le m$) $\widehat{\pi}_d$ and $\widehat{\pi}_{f,k}$, respectively.

In the case of rectangular polytopes $\mathcal{X} \subset \mathbb{R}^{n_x}$ and $\mathcal{P}, \mathcal{R} \subset \mathbb{R}^{n_p}$, the number of vertices are $n_{\mathcal{X}} = 2^{n_x}$, $n_{\mathcal{P}} = n_{\mathcal{R}} = 2^{n_p}$, $n_{\mathcal{F}_k} = 2^{n_x-1}$ $\forall k = \overline{1, m_{\mathcal{X}}}$, furthermore, the number of facets of $\mathcal{X}$ is $m_{\mathcal{X}} = 2n_x$ (Figure 6.2). Therefore, the feasibility of PD-LMIs (6.34a) and (6.34b) should be checked in $2^{n_x+n_p}$ and $2^{n_x+2n_p}$ number of vertices, respectively. On the other hand, the two parameter-dependent LMIs (6.33) for every facet of $\mathcal{X}$ should be

eq. nr.	description	dim.	nr. of LMIs (rect. $\mathcal{X}, \mathcal{P}$ and $\mathcal{R}$)	
(6.34a)	positivity of $V(x,p)$	m	$n_{\mathcal{X}} \cdot n_{\mathcal{P}}$	$(= 2^{n_x+n_p})$
(6.34b)	negativity of $\dot{V}(x,p)$	m'_d	$n_{\mathcal{X}} \cdot n_{\mathcal{P}} \cdot n_{\mathcal{R}}$	$(= 2^{n_x+2n_p})$
(6.33)	$1 \leq V(x,p) \leq \tau_k$	$m'_{f,k} \leq m$	$2n_{\mathcal{P}} \sum_{k=1}^{m_{\mathcal{X}}} n_{\mathcal{F}_k}$	$(= n_x \cdot 2^{n_x+n_p+1})$

Table 6.1: Computational complexity of the optimization problem for RSD computation. The third column presents the dimensions of LMIs, the fourth column comprise the number of corner points, in which the PD-LMI are evaluated.

checked in each vertex of $\mathcal{F}_k \times \mathcal{P}$, which means $2 \cdot 2^{n_x-1+n_p} = 2^{n_x+n_p}$ number of simple LMIs for each facet, in all, $2n_x \cdot 2^{n_x+n_p} = n_x \cdot 2^{n_x+n_p+1}$ simple LMIs.

In general, truncating vector π (decreasing its dimension m) reduces significantly the number of decision variables and the sizes of the LMIs, especially the LMIs corresponding to the rate of the Lyapunov function. On the other hand, more independent rational terms in π may result in a better estimate for the DOA.

6.4 Numerical examples

In this section, we illustrate the applicability of the approach presented above through different numerical examples.

6.4.1 Uncertain Van der Pol dynamics

In this subsection, we revisit the time-reversed Van der Pol system (5.3) with an uncertain possibly time-varying parameter p. Here, we consider three different classes of uncertainty, namely,

1. constant unknown parametric uncertainty $p \in \mathcal{P}$,
2. rate-bounded manipulating input p satisfying Assumptions 6.1 encapsulated in a parameter,
3. a nonlinear term $p : \mathcal{X} \to \mathcal{P}$ encapsulated in a parameter such that $p \circ x$ satisfies Assumptions 6.1.

The boundary of the system's largest achievable DOA can be approximated (or at least estimated) by simulating the Van der Pol oscillator model (5.1) with the given parameter signal.

The Lyapunov function is searched in the form (5.9), where π and its annihilator is given below:

$$N(x,p) = \begin{pmatrix} 0 & 0 & 0 & 1 & -x_1 \\ 0 & 0 & x_1 & 0 & -1 \\ 0 & p & -1 & 0 & 0 \\ x_2 & -x_1 & 0 & 0 & 0 \end{pmatrix}, \; \pi(x,p) = \begin{pmatrix} x_1 \\ x_2 \\ px_2 \\ px_1^2 x_2 \\ px_1 x_2 \end{pmatrix}. \tag{6.35}$$

Due to their different nature, the three types of parametric uncertainty have to be treated differently. In the following paragraphs, we study the three cases separately. For simplicity, the Lyapunov function is searched in a quadratic form (5.9) with a constant "Lyapunov matrix" Q. In each case study, polytope $\mathcal{X}$ is evaluated gradually in an automated manner as described in [P18, Section 3.6]. The initial polytope was chosen to be $\mathcal{X}^{(0)} = [-0.3, 0.3]^2$. In Figures 6.3-6.5, the bounds of the approximated (robust) DOA are illustrated by the black trajectories.

Unknown constant. First, we consider $p \in [1,3]$ to be an unknown constant model parameter. For Q, the following value was computed:

$$Q = \begin{pmatrix} 0.681 & -0.213 & -0.019 & 0.03 & 0 \\ -0.213 & 0.462 & 0.002 & 0.017 & 0.002 \\ -0.019 & 0.002 & 0.001 & 0 & 0 \\ 0.03 & 0.017 & 0 & 0.001 & 0 \\ 0 & 0.002 & 0 & 0 & -0.011 \end{pmatrix}. \tag{6.36}$$

In Figure 6.3, the maximal achievable DOAs are shown for three different values of $p = 1, 2, 3$. The area of the computed RSD $\Omega_1^{x_1}$ (highlighted by the filled green region) is $5.677u^2$.

Rate-bounded input. Secondly, we considered a time-varying (known) parameter function $p : [0, \infty) \to \mathcal{P} = [p_0 - a, p_0 + a]$ with a bounded derivative $\dot{p} : (0, \infty) \to \mathcal{R} = [-a\omega, a\omega]$. Let $p(t) = p_0 + a\sin(\omega t)$, with $p_0 = 1$, $a = 0.8$, $\omega = 10.5$. The obtained value for the Lyapunov matrix is

$$Q = \begin{pmatrix} 0.879 & -0.08 & -0.002 & 0.003 & 0 \\ -0.08 & 0.861 & -0.001 & 0.002 & 0 \\ -0.002 & -0.001 & 0 & 0 & 0 \\ 0.003 & 0.002 & 0 & 0 & 0 \\ 0 & 0 & 0 & 0 & -0.001 \end{pmatrix}. \tag{6.37}$$

Figure 6.6 illustrates the shape of the Lyapunov function V and its derivative function if the parameter $p(t) = p_0$ is fixed for all $t \geq 0$. The area of the computed RSD is $3.6226u^2$, which is illustrated by the green region in Figure 6.5. Furthermore, we simulated the nonlinear time-dependent system from different initial conditions $(x_0^{(i)})$ close to the bounds of the RSD. Then, we computed the values $v^{(i)}(t) = V(x^{(i)}(t), p(t))$ of the Lyapunov function along the trajectories $x^{(i)}$. As Figure 6.5 illustrates, functions $v^{(i)}$ are non-increasing. To estimate the robust DOA of the system we simulated (5.1) with the time-varying parameter function.

Trigonometric term in the system equation. Finally, assume that p is a nonlinear function of the state. Let $p(x) = p_0 + a\sin(\omega x_1)$, where $p_0 = 2$, $a = 1.5$, $\omega = 10$. In the same way as we presented in Paragraph 2.1.2.1 for the inverted pendulum model, we can compute the bounds of $p(x)$ and its total derivative $\frac{\partial p}{\partial x}(x)f(x, p(x))$ in the knowledge of the a priori given polytope $\mathcal{X}$. In this particular case, the derivative function of p simplifies to $\frac{\partial p}{\partial x}(x)f(x, p(x)) = -a\omega x_2 \cos(\omega x_1)$, thus, the rate of p may vary between $[-a\omega x_2^{(\max)}, a\omega x_2^{(\max)}]$, where $x_2^{(\max)} = \max_{x \in \mathcal{X}} |x_2|$. The generated Lyapunov function is characterized by

$$Q = \begin{pmatrix} 0.942 & -0.158 & -0.001 & 0.001 & 0 \\ -0.158 & 0.844 & -0.001 & 0.003 & 0 \\ -0.001 & -0.001 & 0 & 0 & 0 \\ 0.001 & 0.003 & 0 & -0.001 & 0 \\ 0 & 0 & 0 & 0 & 0 \end{pmatrix}. \tag{6.38}$$

Compared to the previous two cases a positively invariant region can be given by the 1-level set Ω_1 of the Lyapunov function $W = V \circ p$, namely, $W(x) = V(x, p(x))$. In Figure 6.7, one can see the shape of the Lyapunov function W, and its derivative $L_f W = \frac{\partial W}{\partial x}(f \circ p)$, where $L_f W(x) = \frac{\partial W}{\partial x}(x)f(x, p(x))$. The area of the estimated DOA is $3.5895u^2$ (Figure 6.4). In this case, the DOA can be precisely computed through simulating (5.1) with $p(x)$.

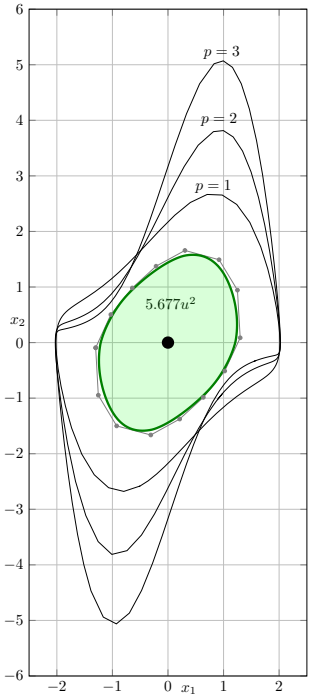

Figure 6.3: Computed stability region (green) for the Van der Pol system with an unknown time-invariant model parameter $p \in [1, 3]$. The black contour lines illustrate the limit cycle of the original Van der Pol oscillator for different values of $p \in \{1, 2, 3\}$.

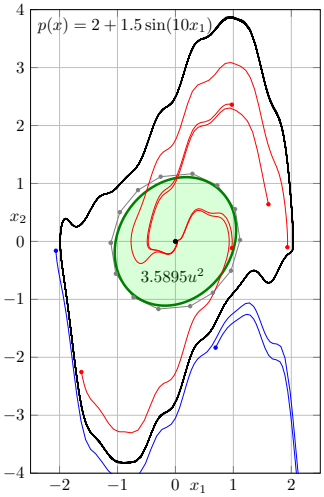

Figure 6.4: Stability region for the Van der Pol system with a non-rational nonlinear term in its system equation, and handled as an uncertain parameter.

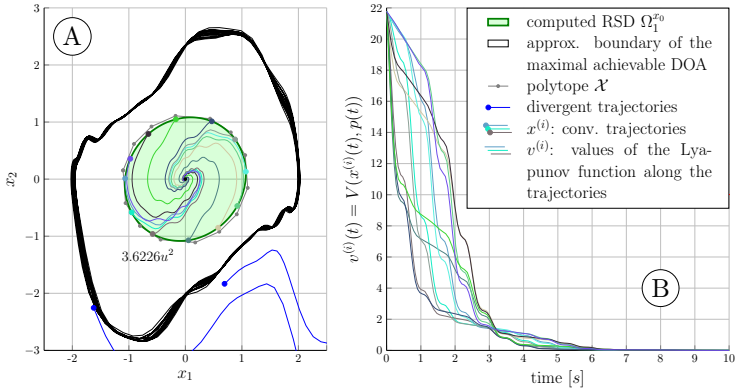

Figure 6.5: Van der Pol system with a time-dependent parameter. In the simulations we used a sinusoid function $p(t) = 1 + 0.8\sin(10.5t)$. The approximated limit cycle of the original Van der Pol oscillator with $p(t) \in \mathcal{P}$ and $\dot{p}(t) \in \mathcal{R}$ is illustrated by the black line in panel A, and some trajectories $x^{(i)}(t)$ can be seen in different colors with initial conditions $x_0^{(i)}$ close to the boundary of the obtained stability region $\Omega_{\overline{\alpha}}$ (green). The values of the Lyapunov function $v^{(i)}(t)$ along the trajectories are presented in panel B, respectively.

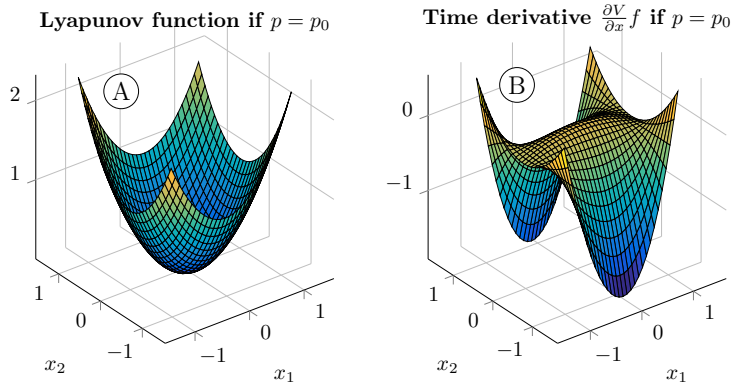

Figure 6.6: Lyapunov function $V(x, p_0)$ for Van der Pol system with time-varying uncertainty, and its time-derivative considering the system dynamics. Both functions were evaluated at the nominal values of $p(t)$ and $\dot{p}(t)$.

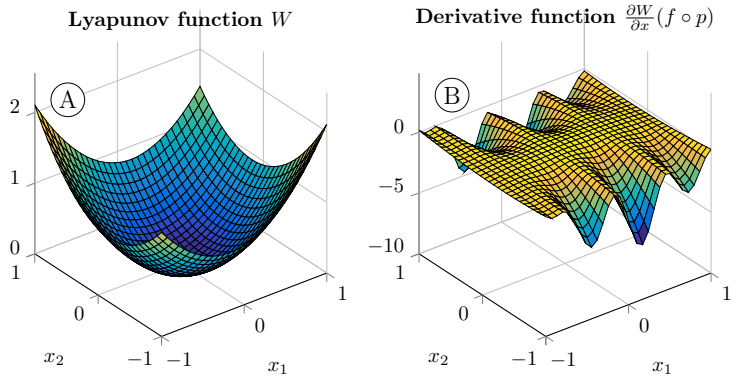

Figure 6.7: Lyapunov function W, for Van der Pol system with a trigonometric nonlinearity, and its derivative function $\frac{\partial W}{\partial x}(f \circ p)$.

6.4.2 A third-order rational system – continuous-time model

Here, we consider a third-order rational system taken from [16; P2; P3]:

$$\begin{cases} \dot{x}_1 = x_2 + \varepsilon_3 x_3 + \varepsilon_1 \zeta(x) \\ \dot{x}_2 = -x_1 - x_2 + \varepsilon_2 x_1^2 \\ \dot{x}_3 = \varepsilon_3(-2x_1 - 2x_3 - x_1^2), \end{cases}, \quad \text{where } \zeta(x) = \frac{x_1}{x_2^2+1},\ \varepsilon_1 = \varepsilon_2 = \varepsilon_3 = \frac{1}{2} \tag{6.39}$$

A possible qLPV representation $\dot{x} = A(x)x$ for system (6.39) can be given by matrix

$$A(x) = \begin{pmatrix} \frac{\varepsilon_1}{x_2^2+1} & 1 & \varepsilon_3 \\ \varepsilon_2 x_1 - 1 & -1 & 0 \\ -\varepsilon_3 x_1 - 2\varepsilon_3 & 0 & -2\varepsilon_3 \end{pmatrix}. \tag{6.40}$$

It is easy to see that (6.39) has an equilibrium point at $x^* = 0$. This equilibrium is locally asymptotically stable, that can be justified by the negative real eigenvalues of the Jacobian matrix of $f(x) = A(x)x$ at x^*. The problem to be solved is to compute a three-dimensional positively invariant domain as an estimate of the DOA around x^*.

Using the recursive LFT implementation of Section 3.6.2, we obtain the following LFR for $A(x)$ generating the following set of rational functions:

$$A(x) = \mathcal{F}_l\left\{ \left(\begin{array}{ccc|cccc} 0.5 & 1 & 0.5 & 0 & 0 & -0.5 & 0 \\ -1 & -1 & 0 & 0.5 & 0 & 0 & 0 \\ -1 & 0 & -1 & 0 & -0.5 & 0 & 0 \\ \hline 1 & 0 & 0 & 0 & 0 & 0 & 0 \\ 1 & 0 & 0 & 0 & 0 & 0 & 0 \\ 0 & 0 & 0 & 0 & 0 & 0 & 1 \\ 1 & 0 & 0 & 0 & 0 & -1 & 0 \end{array}\right), \begin{pmatrix} x_1 & 0 & 0 & 0 \\ 0 & x_1 & 0 & 0 \\ 0 & 0 & x_2 & 0 \\ 0 & 0 & 0 & x_2 \end{pmatrix} \right\} \Rightarrow \pi_1 = \begin{pmatrix} x_1^2 \\ x_1^2 \\ x_2^2\zeta(x) \\ x_2\zeta(x) \end{pmatrix} \tag{6.41}$$

We can see that monomial x_1^2 appears twice in π_1, therefore, $\binom{x}{\pi_1}$ is not minimal. After the proposed minimal generator selection technique of Procedure 5.15, we obtain the following minimal generator form realization for the dynamic equation (6.39):

$$A(x)x = \left(\begin{array}{ccc|cc} 0.5 & 1 & 0.5 & 0 & -0.5\ 0 \\ -1 & -1 & 0 & 0.5 & 0\ 0 \\ -1 & 0 & -1 & -0.5 & 0\ 0 \end{array}\right) \pi, \text{ where } \pi = \binom{x}{\pi_2} \text{ and } \pi_2 = \begin{pmatrix} x_1^2 \\ x_2^2\zeta(x) \\ x_2\zeta(x) \end{pmatrix}. \tag{6.42}$$

The obtained vector π is now a minimal generator. A maximal affine annihilator for π can be obtained by using the technique in Theorem 5.10:

$$N(x) = \begin{pmatrix} x_1 & 0 & 0 & -1 & 0 & 0 \\ x_2 & 0 & 0 & 0 & -x_2 & -1 \\ x_3 & 0 & -x_1 & 0 & 0 & 0 \\ 0 & x_1 & 0 & 0 & -x_2 & -1 \\ 0 & x_3 & -x_2 & 0 & 0 & 0 \\ 0 & 0 & 0 & 0 & 1 & -x_2 \end{pmatrix}.$$

The Lyapunov function is searched in the form $V(x) = x^\top Q\, x$ (5.9), with a constant matrix $Q \in \mathbb{R}^{m\times m}$. For the quadratic factorization of $\dot{V}(x)$, we followed two different approaches:

1. that proposed by Trofino and Dezuo [16] (Proposition 4.4) with an annihilator of Proposition 4.5,
2. and our new LFR-based approach presented in Paragraph 5.5.0.1 with a maximal annihilator.

In both cases, we used maximal annihilators for vector π_d. Polytope $\mathcal{X}$ is selected manually:

$$\mathcal{X} = [-3.771, 3.5195] \times [-4.6077, 5.1943] \times [-8.4274, 6.7204]. \tag{6.43}$$

In order to find a Lyapunov function and a positively invariant level set (i.e., RSD), we solved the SDP described in Corollary 6.9, namely, we evaluated the PD-LMIs (6.33) and (6.34) in each corner point of $\mathcal{X}$. The obtained ordinary LMI constraints can be solved by an SDP solver like SeDuMi [166–168] or Mosek [165]. In the computations, we considered two different quadratic realizations for $\dot{V}(x,p)$, that is illustrated in Figure 6.8 and Figure 6.9.

In order to evaluate the obtained RSD estimate, we approximated numerically the true DOA of the continuous-time model (6.39). We simulated the system from different initial conditions located on a dense grid $x_0 \in \mathbf{Gr}(12 \cdot \mathcal{X}, 201 \times 201 \times 201)$, where $12 \cdot \mathcal{X}$ denotes the set $\{12x \,|\, x \in \mathcal{X}\}$. This grid density allows us to illustrate the true DOA on a 3D plot in Figure 6.10. During the ODE simulation, we have considered two terminal conditions. First, we assumed that x_0 is not an element of the DOA if the trajectory leaves the ball $\mathcal{B}_M = \{x \in \mathbb{R}^{n_x} \,|\, \|x\| \leq M\}$, where $M = 254$. Secondly, x_0 is an element of the DOA if the trajectory approaches the unit ball $\mathcal{B}_1$. Note that $\mathcal{B}_1$ is a subset of the RSD Ω_1 computed for system (6.39). The numerical approximation results suggest, that the system has an unbounded DOA with an infinite volume.

6.4.3 A third-order rational system – discrete-time model

In this section, we consider the discrete-time version of model (6.39) first presented in Section 6.4.2. Using Euler's method, we can give a discrete-time model for this system:

$$\begin{aligned} x^+ &= x + hA(x)x = A_{DT}(x)x, \\ &\text{with } A_{DT}(x) = I + hA(x), \end{aligned} \tag{6.44}$$

where h denotes the constant sampling period. In the computations, we used $h = 0.1$. The final transformed LFR realization for matrix $A_{DT}(x)$ generated the same set of rational terms π_1 and hence the same structure for the candidate Lyapunov function as before obtained for the CT model (6.39).

We used again two different approaches to construct vector π_d for the PD-LMI (6.34b).

1. First, we generated $\pi_d^{(1)}$ as presented in Proposition 6.6, and used an annihilator as presented by 6.7. This approach is the discrete-time reformulation of the technique of [16] presented in Section 4.2.3
2. Then, we used the LFR-based approach in Paragraph 5.5.0.1 with a maximal annihilator.

In order to be able to evaluate the results and compare to those obtained for the CT model, we used the same polytope as given previously in (6.43). The results of the RSD computation (including the volume of the computed estimate) are presented in Table 6.2, and the corresponding stability domains are illustrated in Figures 6.8-6.12.

3D rational model	m	m_d	#vars	volume	solver time
CT + Proposition 4.4 (Fig. 6.8)	6	27	1926	314.479	4.758 sec
CT + Paragraph 5.5.0.1 (Fig. 6.9)	6	21	1575	304.804	3.349 sec
DT + Proposition 6.6 (Fig. 6.11)	6	36	2223	279.382	8.401 sec
DT + Paragraph 5.5.0.1 (Fig. 6.12)	6	54	6705	318.521	247.143 sec

Table 6.2: Results of the RSD computation for the continuous-time (Section 6.4.2) and discrete-time models (Section 6.4.3) using two different quadratic generator form realizations for the rate of the Lyapunov function. Column m_d contains the number of coordinates of the selected generator π_d. The value of m_d constitutes the size of PD-LMI (6.34b). In the 4th column we present the number of free decision variables of the optimization problem. The last column presents the processing time of the semidefinite optimization solver (Mosek).

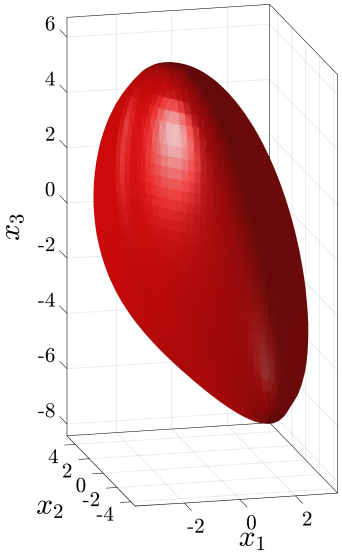

Figure 6.8: Computed RSD for the CT model (with Proposition 4.4). Vol.: 314.479.

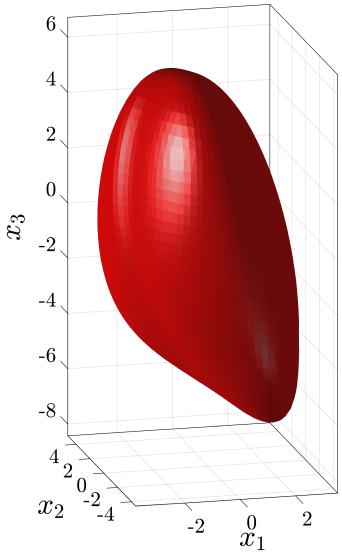

Figure 6.9: Computed RSD for the CT model (with Paragraph 5.5.0.1). Vol.: 304.804. asd asd

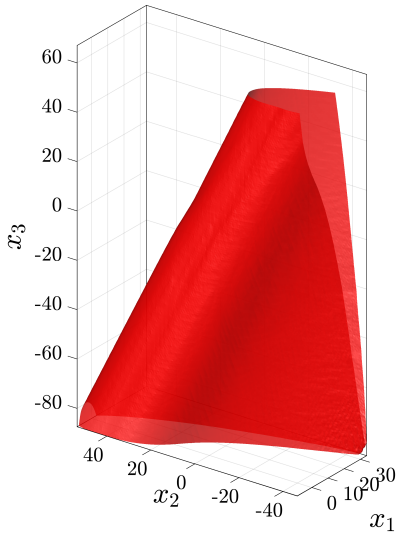

Figure 6.10: Approximated true DOA for the CT model (6.39). asdasdasdas as dasd asd as

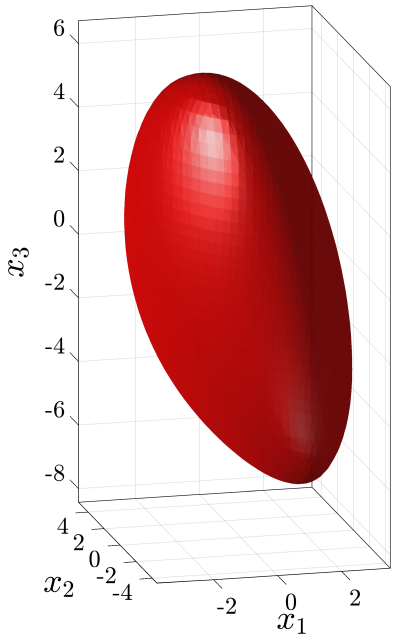

Figure 6.11: Computed RSD for the DT model (with Proposition 6.6). Vol.: 279.382.

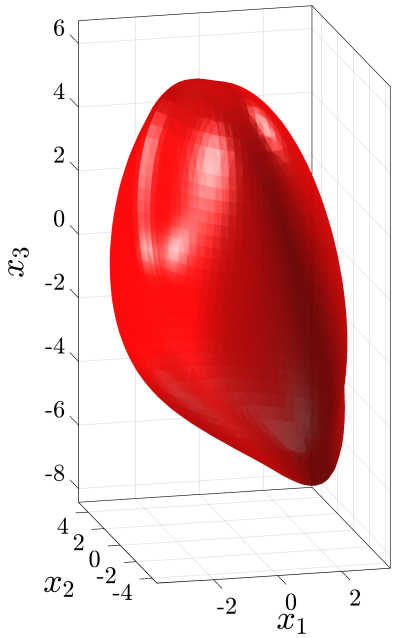

Figure 6.12: Computed RSD for the DT model (with Paragraph 5.5.0.1). Vol.: 318.521.

6.4.4 Stability and DOA analysis of the gradient descent method

In the literature, there exist many approaches to prove stability and convergence of the diverse alternatives of the steepest descent and other fixed-point algorithms. Two of the most popular techniques are based on Banach's contraction mapping theorem (see e.g. [22]) and on the well-known Lyapunov theorem. In [200] a Lyapunov function is considered to prove stability for a continuous-time version of the steepest descent dynamics. In [201] a multi-variable robust adaptive gradient-descent training algorithm is developed to train a recurrent neural network. The convergence of the weight vector was proven using a diagonal quadratic Lyapunov function.

In this section, we consider the dynamics of the classical gradient descent algorithm in order to demonstrate the operations of the proposed method. The objective function to be minimized is chosen to be the energy (i.e., Hamiltonian) function of the "Moon beam" dynamics [202], which is a special variant of the Duffing oscillator having negative linear stiffness [203, Section 2.6], [204]. For the sake of completeness, we give the dimensionless differential equation, which describes the free motion of the undamped Duffing dynamics

$$\ddot{y} - \beta y + \alpha y^3 = 0, \text{ where } \beta = b^2, \ \alpha = a^2. \tag{6.45}$$

If we introduce the state variables $\bar{x}_1 = y$ and $\bar{x}_2 = \dot{y}$, the Hamiltonian function of the oscillator is the following

$$H(\bar{x}) = \tfrac{1}{4}\Big(2\bar{x}_2^2 - 2b^2\bar{x}_1^2 + a^2\bar{x}_1^4\Big). \tag{6.46}$$

This function has two local minima in $(b/a, 0)$ and $(-b/a, 0)$ for every nonzero a, b parameter values. The gradient descent dynamics for this specific objective function $H(\bar{x})$ can be given as follows:

$$\bar{x}^+ = f(\bar{x}, p) = \bar{x} - p \cdot \nabla H(\bar{x}), \ p \in \mathcal{P} = [0.01, 0.1], \tag{6.47}$$

where $\nabla H(\bar{x})$ denotes the gradient of function $H(\bar{x})$, and $p > 0$ is the value of the variable step-size belonging to the given bounded interval. Furthermore, we make no restrictions on the rate of the parameter's change, the only constraint is that the value of parameter p in any future step should belong to the same bounded interval, namely, $p^+ = p + \varrho \in \mathcal{P}$. In the computations, we used $a = 0.5$, $b = 1$.

The dynamics of the centered state vector $x = (\bar{x}_1 + b/a, \bar{x}_2)^\top$ can be written in a qLPV form $x^+ = A(x,p)x$, where

$$A(x,p) = \begin{pmatrix} -a^2\, p\, x_1^2 + 3\, a\, b\, p\, x_1 - 2\, p\, b^2 + 1 & 0 \\ 0 & 1 - p \end{pmatrix}. \tag{6.48}$$

Using the direct LFT realization, we computed a minimal generator form realization of $A(x,p)x = \left(\begin{smallmatrix} 1 & 0 \\ 0 & 1 \end{smallmatrix} \middle| \begin{smallmatrix} -4 & 0 & 3 & 1 \\ 0 & 1 & 0 & 0 \end{smallmatrix}\right)\pi$, where the minimal generator π and its maximal affine annihilator are given as follows:

$$N(x,p) = \begin{pmatrix} x_2 & -x_1 & 0 & 0 & 0 & 0 \\ p & 0 & -2 & 0 & 0 & 0 \\ 0 & p & 0 & 1 & 0 & 0 \\ 0 & 0 & x_1 & 0 & -1 & 0 \\ 0 & 0 & x_2 & 0.5x_1 & 0 & 0 \\ 0 & 0 & 0 & 0 & x_1 & 2 \end{pmatrix}, \ \pi = \begin{pmatrix} x_1 \\ x_2 \\ 0.5\, p x_1 \\ -p x_2 \\ 0.5\, p x_1^2 \\ -0.25\, p x_1^3 \end{pmatrix}. \tag{6.49}$$

To give a PD-LMI (6.34b) for the negativity of $\delta V(x,p,\varrho)$, we have considered three different quadratic generator form realizations for $\delta V(x,p,\varrho)$:

$\pi_d^{(1)}$: Firstly, we used the simple factorization given in Proposition 6.5, which resulted in a small dimensional but conservative PD-LMI.

$\pi_d^{(2)}$: Secondly, we used the technique proposed in Proposition 6.6 with annihilator computed in Proposition 6.7, which resulted in a less conservative PD-LMI, but the

processing time increased significantly.

$\pi_d^{(3)}$: Finally, as presented in Paragraph 5.5.0.1, we used LFT and minimal generator selection (Procedure 5.15) to generate vector $\pi_d = \pi_d^{(3)}$. This LMI results in the largest RSD, but the processing time increased by more than one order of magnitude compared to the second setup (with $\pi_d^{(2)}$).

For vectors $\pi_d^{(1)}$ and $\pi_d^{(3)}$, we used maximal annihilators, whereas for $\pi_d^{(2)}$ we considered annihilator $N_r(x, p, \varrho)$ computed as presented in Proposition 6.7. In order to compare the operations of the three models, we used three different polytopes:

$$\begin{aligned}\mathcal{X}_0 &= [-3.65, -0.9] \times [-2.2, 2.2],\\ \mathcal{X}_1 &= [-4.55, -0.3] \times [-3.4, 3.4],\\ \mathcal{X}_2 &= [-5, 0] \times [-4, 4],\end{aligned} \tag{6.50}$$

for which the PD-LMIs (6.34) and (6.33) are solved. Table 6.3 summarizes the results of the RSD computation for each factorization strategy for $\delta V(x, p, \varrho)$ and for each polytope $\mathcal{X}_i$. In Figure 6.13 and Figure 6.14, the obtained RSD Ω_1 with $\Omega_1^{x_0}$ are illustrated. Additionally, the truncated level set Ψ_1 is shown in Figure 6.13 alongside with a possible trajectory $(x(t), p(t))$.

6.4.5 Continuous fermentation process

In this section, we revisit Problem 2.2, where the continuous fermentation process model is considered with an uncertain maximal growth rate $\mu_{\max} = p$. In the numerical calculations, we used the following model constants: $V_0 = 4\,\mathrm{l}$, $K_1 = 0.03\,\mathrm{g/l}$, $K_2 = 0.5\,\mathrm{l/g}$, $Y = 0.5$, and $S_{F,0} = 10\,\mathrm{g/l}$. Furthermore, we assumed that p belongs to the interval $\mathcal{P} = [0.8, 1.2]\,1/\mathrm{h}$.

Let $x = (x_1 \;\; x_2)^\top = (X - X_0 \quad S - S_0)^\top$ denote the centered biomass and substrate concentrations. We assume that the uncertain maximal growth rate (p) can be measured or estimated on-line, and the optimal operating point inlet flow rate $F_0(p) = p \cdot 3.2089\,\mathrm{l}$ is scheduled accordingly. Then, the optimal equilibrium biomass ($X_0 = 4.8907\,\mathrm{g/l}$) and substrate ($S_0 = 0.2187\,\mathrm{g/l}$) concentrations are independent of p. The values for X_0, S_0, and $F_0(p)$ were computed as presented in Paragraph 2.2.0.1.

Model (2.20) can be written in the standard input-affine form with the centered state vector x and the centered input flow rate $u = F - F_0(p)$. The centered model is: $\dot{x} = f(x, p) + g(x)u$, where

$$f(x,p) = \begin{pmatrix} (x_1+X_0)\cdot\mu(x_2+S_0) - \frac{(x_1+X_0)F_0(p)}{V_0} \\ -\frac{(x_1+X_0)\cdot\mu(x_2+S_0)}{Y} + \frac{(S_{F,0}-(x_2+S_0))F_0(p)}{V_0} \end{pmatrix},\; g(x) = -\frac{1}{V_0}\begin{pmatrix} x_1+X_0 \\ x_2+S_0-S_{F,0} \end{pmatrix} \tag{6.51}$$

Function $f(x, p)$ can also be written in the factorized form $f(x, p) = A_1(x, p)x$, where

$$A_1(x,p) = \begin{pmatrix} -\frac{F_0(p)(c_2x_2^2+c_1x_2)}{q(x_2)V_0} & \frac{pV_0(x_1+X_0)-X_0F_0(p)(c_2x_2+c_1)}{q(x_2)V_0} \\ -\frac{pS_0}{q(x_2)Y} & -\frac{F_0(p)}{V_0} - \frac{p(x_1+X_0)}{q(x_2)Y} - \frac{F_0(p)(S_0-S_{F,0})(c_2x_2+c_1)}{q(x_2)V_0} \end{pmatrix} \tag{6.52}$$

with $q(x_2) = c_2x_2^2 + c_1x_2 + c_0$, where $c_0 = K_2S_0^2 + S_0 + K_1$, $c_1 = 2K_2S_0 + 1$, $c_2 = K_2$

Though the centered open-loop system (6.51) with $u \equiv 0$ is locally asymptotically stable, it has a relatively small domain of attraction [P6]. Therefore, we consider two different substrate feedback control laws, which ensure a much larger stability domain. First, we estimate the domain of attraction generated through a static proportional feedback $u = -k_P x_2$. Then, a PI (proportional-integral) controller is considered, namely, $u = -(k_P + \frac{k_I}{s})S$, where, s denotes the complex Laplace variable. Note that capital

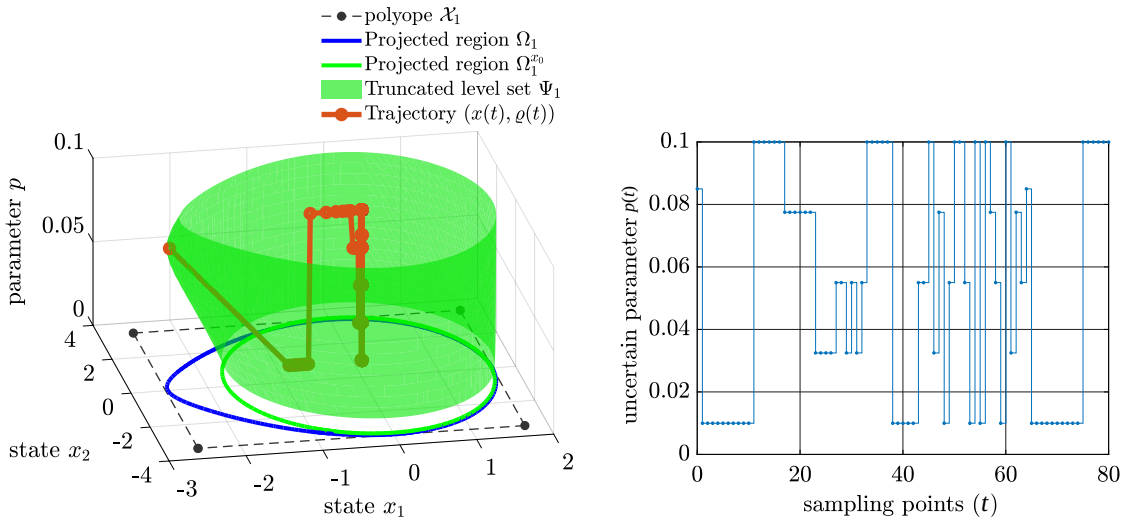

Figure 6.13: Trajectory $(x(t), p(t))$ for the gradient-descent dynamics (left) in the case of a time-varying step size $p(t)$ (right). The computed truncated level set Ψ_1 (green surface) was obtained when using vector $\pi_d^{(2)}$ with polytope $\mathcal{X}_1$ (*5th* row of Table 6.3, see also Figure 6.14d),

selected π_d, polytope	area of Ω_1	$\Omega_1^{x_0}$	$\mathcal{X}_i$ in cubic units	proc. time
vector $\pi_d^{(1)}$ (Prop. 6.5), $\mathcal{X}_0$	7.5909	8.7803	12.1 (Fig. 6.14a)	0.1472 sec
vector $\pi_d^{(2)}$ (Prop. 6.6), $\mathcal{X}_0$	7.7690	8.7122	12.1 (Fig. 6.14b)	4.2773 sec
vector $\pi_d^{(3)}$ (Par. 5.5.0.1), $\mathcal{X}_0$	9.2163	9.2168	12.1 (Fig. 6.14c)	86.014 sec
vector $\pi_d^{(1)}$ (Prop. 6.5), $\mathcal{X}_1$	*no solution found*			
vector $\pi_d^{(2)}$ (Prop. 6.6), $\mathcal{X}_1$	18.2780	20.4107	28.9 (Fig. 6.14d)	4.4903 sec
vector $\pi_d^{(3)}$ (Par. 5.5.0.1), $\mathcal{X}_1$	22.1316	22.1516	28.9 (Fig. 6.14e)	112.968 sec
vector $\pi_d^{(1)}$ (Prop. 6.5), $\mathcal{X}_2$	*no solution found*			
vector $\pi_d^{(2)}$ (Prop. 6.6), $\mathcal{X}_2$	*no solution found*			
vector $\pi_d^{(3)}$ (Par. 5.5.0.1), $\mathcal{X}_2$	28.1455	28.2825	40 (Fig. 6.14f)	172.517 sec

Table 6.3: Results of the optimization problem for the three different sets of rational functions $\pi_d^{(1)}$, $\pi_d^{(2)}$, $\pi_d^{(3)}$, and for the three different polytopes $\mathcal{X}_0 \subset \mathcal{X}_1 \subset \mathcal{X}_2$.

selected π_d	dim. of π_d	dim. of its annihilator	average proc. time
$\pi_d^{(1)}$ (Prop. 6.5)	10	8×10	0.1472 sec
$\pi_d^{(2)}$ (Prop. 6.6)	30	34×30	4.3838 sec
$\pi_d^{(3)}$ (Par. 5.5.0.1)	52	102×52	123.833 sec

Table 6.4: Dimension of the selected vector π_d and its corresponding annihilator with the estimated overall solver time in the three different cases.

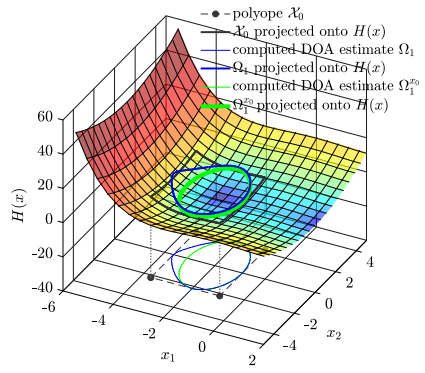

(a) Computed RSD for $\pi_d^{(1)}$ and $\mathcal{X}_0$.

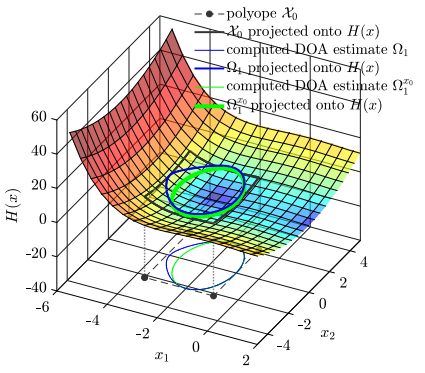

(b) Computed RSD for $\pi_d^{(2)}$ and $\mathcal{X}_0$.

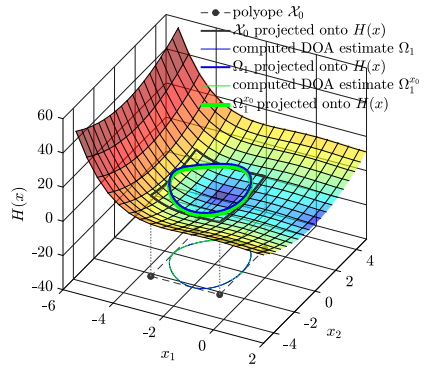

(c) Computed RSD for $\pi_d^{(3)}$ and $\mathcal{X}_0$.

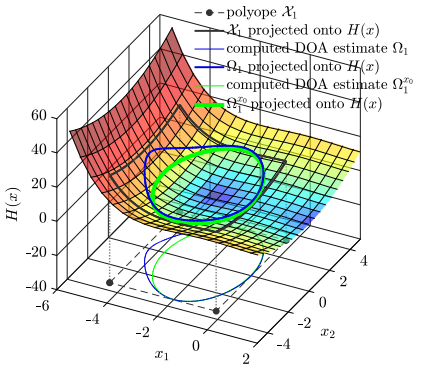

(d) Computed RSD for $\pi_d^{(2)}$ and $\mathcal{X}_1$.

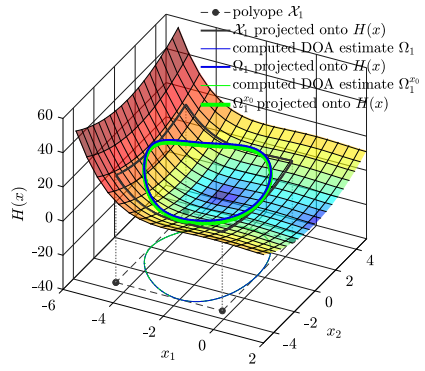

(e) Computed RSD for $\pi_d^{(3)}$ and $\mathcal{X}_1$.

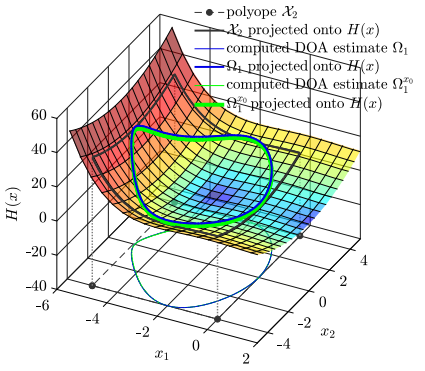

(f) Computed RSD for $\pi_d^{(3)}$ and $\mathcal{X}_2$.

Figure 6.14: Computed RSD for the classical gradient descent dynamics applied to the Hamiltonian function $H(x)$ of the Duffing oscillator (colored surface). The dashed black rectangular region illustrates polytope $\mathcal{X}$, in which the PD-LMIs were tested. The blue and green contour lines bound the computed regions Ω_1 and $\Omega_1^{x_0}$, respectively. In order to make the computed DOA estimate more visible, we projected $\mathcal{X}$, Ω_1 and $\Omega_1^{x_0}$ onto the surface of the objective function $H(x)$. These are illustrated by the solid black, blue and green lines, respectively.

letter "P" in the notation k_P stands for "proportional", furthermore, the value of k_P is independent of the uncertain parameter p.

Linear proportional substrate feedback

Let us define the centered input flow rate as $u = -k_P x_2$, where $k_P > 0$ is the feedback gain. The equation of the closed-loop system can be transformed into the following form:

$$\dot{x} = A_2(x,p)x \text{ where } A_2(x,p) = (A_1(x,p) - g(x)K_P) \ , \qquad K_P = (0 \ k_P) \tag{6.53}$$

To obtain a generator form realization for mapping $f(x,p)$ in (6.51), we applied the recursive LFT realization to (6.53), then, we used the minimal generator selection technique of Procedure (5.15). We computed the RSD of system (6.53) for different feedback gain values $k_P \in [0.125, 5.125]$ with a rectangular polytope selection. In Figure 6.18, we illustrate the RSD's area in the function of k_P. Observe that the area suddenly increases between the values $k_P^{(i)} = 0.916$ ($\text{area}^{(i)} = 0.6634$) and $k_P^{(i+1)} = 0.917$ ($\text{area}^{(i+1)} = 6.5188$). In Figure 6.15, we illustrate the obtained RSD region and the corresponding rectangular polytope $\mathcal{X}$ for different feedback gain values.

The largest area is obtained when $k_P = 0.917$. In this case, matrices F_{11}, F_{12} of representation (5.5) and the obtained generator π_1 corresponding to the system equation (6.52) are the following:

$$F_{11} = \left(\begin{smallmatrix} 0 & 1.121 \\ 0 & -2.242 \end{smallmatrix}\right), \ F_{12} = \left(\begin{smallmatrix} 0 & 0.219 & 0 & 0.0447 & 0.229 & -0.802 & 0\,0\,0\,0 & -3.92 & 0 \\ -0.875 & -0.437 & -0.802 & -4 & 0 & 0 & 0\,0\,0\,0 & 7.85 & 0.229 \end{smallmatrix}\right) \tag{6.54}$$

$$\pi_1^\top = \left(\tfrac{px_1}{\zeta(x_2)} \ \tfrac{px_2}{\zeta(x_2)} \ px_2 \ \tfrac{px_1x_2}{\zeta(x_2)} \ x_1x_2 \ \tfrac{px_1x_2^2}{\zeta(x_2)} \ \tfrac{x_1x_2^2}{\zeta(x_2)} \ \tfrac{x_1x_2}{\zeta(x_2)} \ \tfrac{x_2^3}{\zeta(x_2)} \ \tfrac{x_2^2}{\zeta(x_2)} \ \tfrac{px_2^2}{\zeta(x_2)} \ x_2^2 \right), \ \zeta(x_2) = \tfrac{q(x_2)}{c_2} = \tfrac{q(x_2)}{K_2}$$

Figure 6.17 illustrates the obtained Lyapunov function V in two different view points when $p = p_0$. Figure 6.16 illustrates a possible RSD computed with an irregular polytope when $k_P = 0.917$. Note that the irregular polytope resulted in a larger RSD than a rectangular polytope.

In each case, polytope $\mathcal{X}$ was selected manually through multiple trials. Though there are systematic techniques in the literature (see, e.g., [16] or [P8]), the automatic polytope evaluation is not addressed in this thesis.

Linear proportional and integral substrate feedback

Let the centered input flow rate be $u = -k_P x_2 - k_I \int_{t_0}^{\top} x_2(\tau)\mathrm{d}\tau$. In this case the equation of the closed-loop system is $\dot{\xi} = A_3(x,p)\xi$, where $\xi = [x_1 \ x_2 \ u]^\top$ is the state vector of the obtained three dimensional system. Using the variables from (6.51) and (6.52), the state-transition matrix function $A_3(x,p)$ can be composed as follows:

$$A_3(x,p) = \left(\begin{smallmatrix} A_1(x,p) & g(x) \\ -K_P A_1(x,p) - K_I & -K_P g(x) \end{smallmatrix}\right), \text{ with } K_P = \begin{pmatrix} 0 & k_P \end{pmatrix} \text{ and } K_I = \begin{pmatrix} 0 & k_I \end{pmatrix}. \tag{6.55}$$

After the proposed model transformation of Remark 5.8, the augmented dynamic equation is written in a generator form realization $A_3(x,p)\xi = F_{11}\xi + F_{12}\pi_1$, where

$$F_{11} = \begin{pmatrix} 0 & 0 & -1.22 \\ 0 & 0 & 2.45 \\ 0 & -2.0 & -4.89 \end{pmatrix}, \ F_{12} = \left(\begin{smallmatrix} 0 & 0.219 & 0 & 0.0447 & -0.25 & -0.802 & 0\,0\,0\,0 & -3.92 & 0 \\ -0.875 & -0.437 & -0.802 & -4.0 & 0 & 0 & 0\,0\,0\,0 & 7.85 & -0.25 \\ 1.75 & 0.875 & 1.6 & 8.0 & 0 & 0 & 0\,0\,0\,0 & -15.7 & 0.5 \end{smallmatrix}\right),$$

$$\pi_1^\top = \left(\tfrac{px_1}{\zeta(x_2)} \ \tfrac{px_2}{\zeta(x_2)} \ px_2 \ \tfrac{px_1x_2}{\zeta(x_2)} \ x_1x_3 \ \tfrac{px_1x_2^2}{\zeta(x_2)} \ \tfrac{x_1x_2^2}{\zeta(x_2)} \ \tfrac{x_1x_2}{\zeta(x_2)} \ \tfrac{x_2^3}{\zeta(x_2)} \ \tfrac{x_2^2}{\zeta(x_2)} \ \tfrac{px_2^2}{\zeta(x_2)} \ x_2x_3 \right). \tag{6.56}$$

In Figure 6.19, we presented the computed (3-dimensional) RSD for two different feedback configurations. First, we fixed $k_P = 0.917$ and $k_I = 1$, then, we selected $k_P = 2$ and $k_I = 2$. For the two different cases, we used polytopes:

$$\begin{aligned} &(x_1, x_2, u) \in [-2.172, 3.087] \times [-0.2, 2.311] \times [-1, 1], \\ &(x_1, x_2, u) \in [-2.873, 3.813] \times [-0.2, 2.154] \times [-2, 2], \text{ respectively.} \end{aligned} \tag{6.57}$$

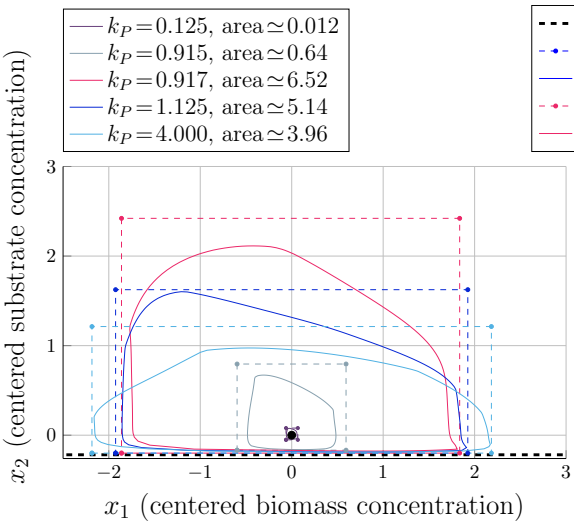

Figure 6.15: Computed RSD (solid lines) and the corresponding polytope $\mathcal{X}$ (dashed lines) for different feedback gain values, with a rectangular polytope selection.

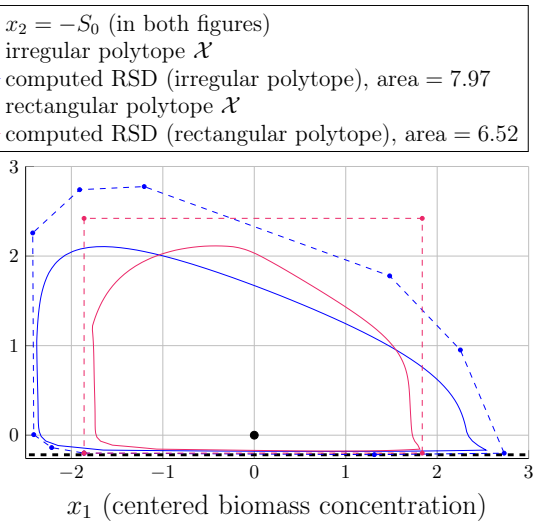

Figure 6.16: Computed RSD, when an irregular polytope is selected (blue line) compared to that when a rectangular polytope is considered (red line). In both cases, the feedback gain is $k_P = 0.917$.

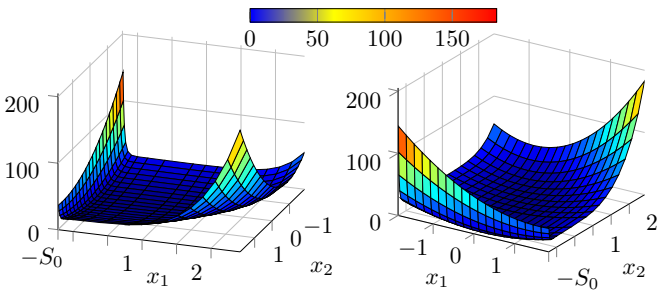

Figure 6.17: Plot of the Lyapunov function V from two different angles, when $k_P = 0.917$ and $p = 1$.

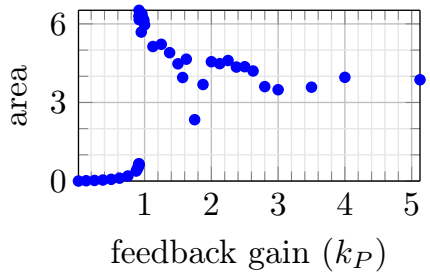

Figure 6.18: The area of the computed robust DOA for different k_P feedback gain values.

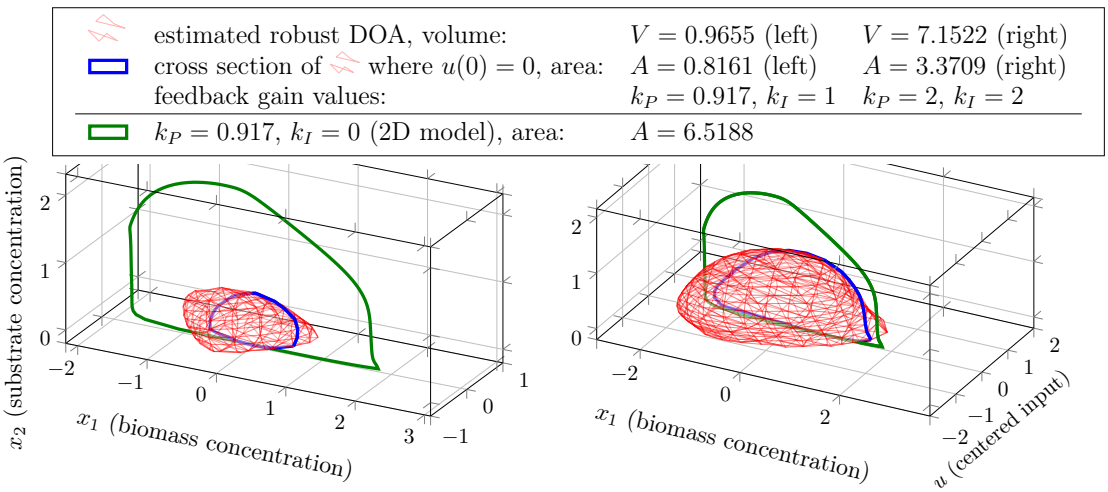

Figure 6.19: The computed RSD in the case of two different feedback gain configurations, when an additional integral substrate feedback is applied. In both cases, the figure illustrates the used polytope $\mathcal{X}$ (bounding box), the maximal robust stability domain (red mesh) and its cross section when $u(0) = 0$ (blue line).

Note that in a higher dimensional Euclidean space (e.g., 3D), a rectangular polytope is a more conservative polytope selection than in 2D. Therefore, the obtained estimates in both integral feedback configurations are smaller than that obtained when no integral feedback is applied.

6.4.6 A simple disease model

In this example, we consider a susceptible-infectious-recovered-deceased (SIRD) model taken from [205]. The system equations are the following:

$$\begin{aligned}
\dot{\bar{x}}_1 &= \pi - (\beta_1 \bar{x}_2 + \beta_2 \bar{x}_4 + \lambda \bar{x}_5)\bar{x}_1 - \mu \bar{x}_1 \\
\dot{\bar{x}}_2 &= (\beta_1 \bar{x}_2 + \beta_2 \bar{x}_4 + \lambda \bar{x}_5)\bar{x}_1 - (\mu + \delta + \gamma)\bar{x}_2 \\
\dot{\bar{x}}_3 &= \gamma \bar{x}_2 - \mu \bar{x}_3 \\
\dot{\bar{x}}_4 &= (\mu + \delta)\bar{x}_2 - b\bar{x}_4 \\
\dot{\bar{x}}_5 &= \sigma + \xi \bar{x}_2 + \alpha \bar{x}_4 - \eta \bar{x}_5
\end{aligned} \tag{6.58}$$

where $\bar{x}_1$, $\bar{x}_2$, $\bar{x}_3$, $\bar{x}_4$ denote the scaled numbers of susceptible, infectious, recovered and deceased human individuals, respectively, while $\bar{x}_5$ denotes the scaled concentration of virus pathogens in the environment. The values of model parameters are chosen to be as follows: $\pi = 10$, $\eta = 0.03$, $\xi = 0.04$, $\alpha = 0.04$, $\delta = 0.05$, $\beta_1 = 0.006$, $\beta_2 = 0.012$, $\lambda = 0.01$, $\gamma = 0.06$, $\mu = 0.5$, $b = 0.8$, $\sigma = 0$. For this parameter configuration, system (6.58) has a unique positive (endemic) equilibrium point $\bar{x}^* = \begin{pmatrix} 16.5986 & 2.788 & 0.3346 & 1.9168 & 6.273 \end{pmatrix}^\top$, which is locally asymptotically stable [205, Theorem 5.1]. The value of $\bar{x}^*$ can be derived analytically, as it was shown in [205]. If we introduce the centered state variable $x = \bar{x} - \bar{x}^*$, the numerical form of the centered system's equation will be the following:

$$\dot{x}_1 = -0.006x_1x_2 - 0.012x_1x_4 - 0.01x_1x_5 - 0.6025x_1 - 0.0996x_2 - 0.1992x_4 - 0.166x_5 \tag{6.59a}$$

$$\dot{x}_2 = 0.006x_1x_2 + 0.012x_1x_4 + 0.01x_1x_5 + 0.1025x_1 - 0.5104x_2 + 0.1992x_4 + 0.166x_5 \tag{6.59b}$$

$$\dot{x}_3 = 0.06x_2 - 0.5x_3 \tag{6.59c}$$

$$\dot{x}_4 = 0.55x_2 - 0.8x_4 \tag{6.59d}$$

$$\dot{x}_5 = 0.04x_2 + 0.04x_4 - 0.03x_5 \tag{6.59e}$$

Considering every second-order monomial of the state variables x_1, x_2, x_4 and x_5 to appear in π, we will have $\dim(\pi) = 10$. If we skip every second-order monomial in which a certain state variable is on the power of 2 (i.e., monomials of the form x_i^2), we obtain $\dim(\pi) = 6$ monomials. Using the LFT and then the minimal generator selection technique of Section 5.4.1, we obtained the following minimal generator form realization (Definition 5.1) for system (6.59):

$$F_{11} = \begin{pmatrix} -0.6025 & -0.0996 & 0 & -0.1992 & -0.166 \\ 0.1025 & -0.5104 & 0 & 0.1992 & 0.166 \\ 0 & 0.06 & -0.5 & 0 & 0 \\ 0 & 0.55 & 0 & -0.8 & 0 \\ 0 & 0.04 & 0 & 0.04 & -0.03 \end{pmatrix}, \; F_{12} = \begin{pmatrix} -0.006 & -0.012 & -0.01 \\ 0.006 & 0.012 & 0.01 \\ 0 & 0 & 0 \\ 0 & 0 & 0 \\ 0 & 0 & 0 \end{pmatrix}, \quad \pi_1 = \begin{pmatrix} x_1x_2 \\ x_1x_4 \\ x_1x_5 \end{pmatrix}$$

The annihilators for both π_d and π were computed using the proposed technique in Paragraph 5.3.2.1. Before the optimization, we selected a rectangular polytope:

$$\mathcal{X} = [-4.42, 4.96] \times [-2.79, 3.55] \times [-0.33, 0.43] \times [-1.92, 2.18] \times [-3.83, 3.96]. \tag{6.60}$$

The volume of the obtained positively invariant region is approximately $107.22u^5$. In comparison, the volume of $\mathcal{X}$ is $1444.34u^5$. Figure 6.20 illustrates the cross sections of the estimated DOA along the different axes.

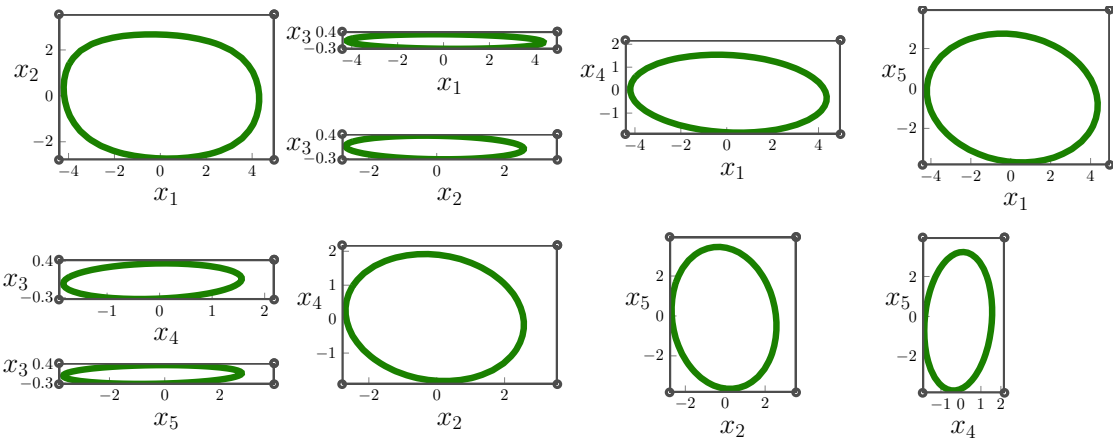

Figure 6.20: DOA for the 5-dimensional disease model. The area bounded by the closed green line illustrates the cross sections of the obtained positively invariant domain. The gray rectangle is the cross section of polytope $\mathcal{X}$ along the respective axes.

6.4.7 Inverted pendulum balancing system with state feedback

We consider the rational embedded model (2.6) of the inverted pendulum balancing system given in the form:

$$\dot{z} = A(z)z + B(z)u,\ z^\top = (v\ \ \omega\ \ z_3\ \ z_4),\ z_3 = \sin\theta,\ z_4 = 1 - \cos\theta, \tag{6.61}$$

where matrices $A(z)$ and $B(z)$ are given in Section 2.1.1 alongside a detailed model description. The origin is an unstable equilibrium point of the open-loop system (6.61) with $u \equiv 0$, therefore, a locally stabilizing static state feedback is considered:

$$u = -Kz. \tag{6.62}$$

The closed-loop dynamics in the embedding state-space are

$$\dot{z} = \bar{f}_{\mathrm{cl}}(z) = (A(z) - B(z)K)z. \tag{6.63}$$

For DOA computation, we consider initial conditions $z(0)$ in a compact rectangular subset of the state-space $\mathcal{Z} \subseteq \mathbb{R}^4$, which corresponds to

$$x(0) = \Phi^{-1}(z(0)) \in \Phi^{-1}(\mathcal{Z} \cap M) = \mathcal{X} \subset \mathbb{R}^3, \tag{6.64a}$$

in the state-space of system (2.2). The converse statement is also true, namely:

$$z(0) = \Phi(x(0)) \in \mathcal{Z} \cap M = \Phi(\mathcal{X}) \subset \mathbb{R}^4. \tag{6.64b}$$

Mapping Φ and manifold M were defined in Section 2.1.1 as follows:

$$M = \left\{ z \in \mathbb{R}^4 \,|\, z_3^2 + (1 - z_4^2) = 1 \right\} = \{ z = \Phi(x) \,|\, x \in U = \mathbb{R} \times (-\pi, \pi] \times \mathbb{R} \}, \tag{6.65}$$

$$z = \Phi(x) = (v, \omega, \sin\theta, 1 - \cos\theta),\ \text{where } x = (v\ \theta\ \omega)^\top. \tag{6.65a}$$

Let the state (x) of (2.2) be restricted to $\mathcal{X} \subset U^\circ = \mathbb{R} \times (-\pi, \pi) \times \mathbb{R}$, then, $\Phi : \mathcal{X} \to \mathcal{R} \cap M$ is a diffeomorphism and $\mathcal{R} \cap M \subset \{ z = \Phi(x) \,|\, z \in U^\circ \}$. Also note that the initial condition $z(0) \in \mathcal{Z} \setminus M$ does not correspond to a physically interpretable state for system (2.2). It can be shown further that the diffeomorphism in (6.65a) satisfies $0 = \Phi(0)$ and

$$\tfrac{1}{2}\|x\| \le \|\Phi(x)\| \le \|x\| \text{ for all } x \in U. \tag{6.66}$$

Observe that $\frac{1}{4}\theta^2 \le 2(1 - \cos\theta) \le \theta^2$ in $[-\pi, \pi]$, therefore, the inequality

$$\tfrac{1}{4}(v^2 + \omega^2) + \tfrac{1}{4}\theta^2 \le v^2 + \omega^2 + 2(1 - \cos\theta) \le v^2 + \omega^2 + \theta^2 \text{ in } U, \tag{6.67}$$

gives back (6.66).

Suppose that $W : \mathcal{Z} \to \mathbb{R}$ is a C^1 (continuously differentiable) Lyapunov function for

the dynamics (6.61). Then, according to Lemma 3.10, function $V = W \circ \Phi : \mathcal{X} \to \mathbb{R}$ is a C^1 Lyapunov function for the closed-loop dynamics

$$\dot{x} = f_{\mathrm{cl}}(x) = f(x) + g(x)u(x) \tag{6.68}$$

of system (2.2), with the nonlinear feedback $u(x) = -K\Phi(x)$.

In the numerical computations, we considered the following model constants $m = 1$, $M = 0.5$, $\ell = 1$, $g = 10$, $b = 0$, and $I = \frac{4}{3}m\ell^2$. Furthermore, the locally stabilizing feedback gain $K = (-1 \;\; -16.45 \;\; -38.56 \; 0)$ in (6.62) was computed by considering the (v, ω, z_3) subsystem of the linearized model of (6.61) around $z^* = 0$. Note that the pair $(\bar{A}, \bar{B})$ of the linearized state-space model

$$\dot{z} = \bar{A}z + \bar{B}u, \text{ where } \bar{A} = \frac{\partial \bar{f}}{\partial z}(z^*), \text{ and } \bar{B} = B(z^*), \tag{6.69}$$

is not controllable. However, the controllable subsystem (v, ω, z_3) can be detached from the LTI model (6.69). Therefore, K was computed through a linear quadratic regulator design [49, Section 3.5.4] with $Q = I_3$ and $R = 1$ for the pair $(\bar{A}_{1:3,1:3}, \bar{B}_{1:3,:})$, where $\bar{A}_{1:3,1:3}$ denotes the upper-left 3×3 block of matrix $\bar{A}$, and $\bar{B}_{1:3,:}$ denotes the upper 3×1 block of matrix $\bar{B}$.

During the analysis we considered initial conditions satisfying

$$(v(0), \theta(0), \omega(0)) \in \mathcal{X} = [-18, 18]\,\tfrac{\mathrm{m}}{\mathrm{s}} \times \left[-\tfrac{\pi}{4}, \tfrac{\pi}{4}\right] \mathrm{rad} \times [-3, 3]\,\tfrac{\mathrm{rad}}{\mathrm{s}}. \tag{6.70}$$

Correspondingly, let

$$\mathcal{Z} = [-18, 18] \times [-3, 3] \times [-0.751, 0.751] \times [-0.1, 0.34], \tag{6.71}$$

which satisfies (6.64).

Considering the LFR realization of rational function $\bar{f}_{\mathrm{cl}}$, we obtain generator π, having $m = 28$ coordinate functions. Using the proposed approach of Section 5.4, we computed a reduced-dimensional minimal generator $\widehat{\pi}$ satisfying

$$\bar{f}_{\mathrm{cl}}(z) = \begin{pmatrix} F_{11} & F_{12} \end{pmatrix} \widehat{\pi}(z), \;\; \widehat{\pi}(z) = \begin{pmatrix} z \\ \widehat{\pi}_1(z) \end{pmatrix} \in \mathbb{R}^{19}, \text{ where} \tag{6.72}$$

$$\widehat{\pi}_1^{\top}(z) = \tfrac{1}{2z_3^2+5}\big(\, vz_3 \;\; vz_4 \;\; \omega z_3 \;\; \omega z_4 \;\; z_3z_4 \;\; z_3^2 \;\; vz_3^2 \;\; \omega z_3 z_4 \;\; \omega z_3^2 \;\; \omega^2 z_3 \;\; z_3^2 x_4 \;\; z_3^3 \;\; \omega z_3^3 \;\; \omega z_3^2 x_4 \;\; \omega^2 z_3 z_4 \, \big),$$

$$F_{11} = \begin{pmatrix} 0.933 & 15.4 & 32 & 0 \\ -0.4 & -6.58 & -9.42 & 0 \\ 0 & 1 & 0 & 0 \\ 0 & 0 & 0 & 0 \end{pmatrix}, \; F_{12} = \begin{pmatrix} -16 & 0 & -0.467 & 0.467 & 0 & 5 & 0 & -7.68 & 1.17 & 0 & 0 & 0 & 0 & 0 & 0 \\ -3.51 & 8.22 & 0.2 & -0.2 & 0.5 & 19.3 & -0.5 & 3.29 & 0 & 0 & 0 & 0 & 0 & 0.5 & 0 \\ 1.25 & -1.25 & 0 & 0 & 0 & 0 & 0 & -0.5 & 0 & 0 & 0 & 0 & 0.5 & 0 & 0 \\ 0 & 0 & 1.25 & 0 & 0 & 0 & 0 & 0 & 0 & 0 & 0.5 & 0 & 0 & 0 & 0 \end{pmatrix}.$$

Therefore, a Lyapunov function W is computed in a form $W(z) = \pi^{\top}(z)P\pi(z)$, with a free symmetric matrix P. To formulate a PD-LMI for the Lyapunov inequality ("$\dot{W} < 0$"), we computed $\pi_d(z) = \begin{pmatrix} \widehat{\pi}(z) \\ \frac{\partial \widehat{\pi}_1}{\partial z}(z)\bar{f}_{\mathrm{cl}}(z) \end{pmatrix} \in \mathbb{R}^{34}$, which admits an affine annihilator N_d with $s_d = 58$ rows. To reduce the conservatism of the solution, we used the factorization technique of Paragraph 5.5.0.1. Then, we obtained a minimal generator $\pi_g(z) \in \mathbb{R}^{50}$, which satisfies $\pi_d(z) = H_g\pi_g(z)$, and admits an affine annihilator N_g with $s_g = 113$ rows.

Solving the SDP of Corollary (6.9) for DOA computation, we obtained the following value for the free matrix P in the Lyapunov function W:

$$\begin{pmatrix}
0.005 & 0.0228 & 0.0468 & 0.0002 & 0 & -0.0107 & -1.95 & 1.03 & -0.869 & 0.31 & -0.0402 & -0.782 & 1.04 & -0.0071 & 0.713 & -0.253 & 0.209 & -0.557 & 0.132 \\
0.0228 & 0.314 & 0.504 & 0.0002 & 1.95 & -1.05 & 0.0212 & 0.798 & -1.6 & -2.31 & -0.158 & -4.62 & 1.47 & -0.007 & -3.21 & -0.766 & -0.617 & -4.54 & -5.39 \\
0.0468 & 0.504 & 2.45 & 0 & -0.316 & 11.7 & 2.36 & 36.3 & -86.2 & -0.0674 & 0.113 & 16.4 & 2.45 & -3.58 & -38.6 & 17.1 & -0.382 & -1.64 & 7.62 \\
0.0002 & 0.0002 & 0 & 100 & -11.1 & -0.0027 & -39.4 & -0.0036 & 0.0062 & -162 & -0.811 & -18.8 & 6.54 & -1.09 & -346 & 23.8 & -4.27 & 8.92 & -0.728 \\
0 & 1.95 & -0.316 & -11.1 & 0.432 & 0.0011 & -4.46 & -13.9 & 36.3 & -1.48 & 0.0039 & 21.3 & -0.302 & 0.0043 & 16.3 & -0.467 & -3.54 & -4.69 & -0.028 \\
-0.0107 & -1.05 & 11.7 & -0.0027 & 0.0011 & -0.876 & 17.8 & -5.33 & -5.33 & -35.5 & 0.586 & -0.0063 & -3.76 & -0.671 & -0.497 & -3.09 & 6.61 & 4.33 & -0.116 \\
-1.95 & 0.0212 & 2.36 & -39.4 & -4.46 & 17.8 & 30.1 & 28.3 & -25.1 & -25.8 & -0.764 & -30 & 2.72 & 0.0895 & 83.3 & -2.56 & 1.25 & 27.6 & -1.81 \\
1.03 & 0.798 & 36.3 & -0.0036 & -13.9 & -5.33 & 28.3 & -110 & 58 & -71.7 & -7.37 & 4.18 & 10 & 24.3 & -55.2 & 6.59 & -7.84 & 8.16 & 4.64 \\
-0.869 & -1.6 & -86.2 & 0.0062 & 36.3 & -5.33 & -25.1 & 58 & -691 & 75.1 & 1.3 & 7.87 & 0.645 & 77.3 & -9.41 & 10.1 & 9.7 & 0.467 & -1.95 \\
0.31 & -2.31 & -0.0674 & -162 & -1.48 & -35.5 & -25.8 & -71.7 & 75.1 & 319 & 0.485 & 94.3 & 1.09 & -0.313 & 1.22e+03 & -0.825 & -18.8 & -1.39 & 11.2 \\
-0.0402 & -0.158 & 0.113 & -0.811 & 0.0039 & 0.586 & -0.764 & -7.37 & 1.3 & 0.485 & -0.264 & -0.235 & -0.185 & -0.0831 & -0.141 & 0.0433 & -0.336 & -6.4 & -0.324 \\
-0.782 & -4.62 & 16.4 & -18.8 & 21.3 & -0.0063 & -30 & 4.18 & 7.87 & 94.3 & -0.235 & 6.27 & 2.57 & 1.19 & 9.19 & -51.8 & 11.5 & -1.26 & -0.718 \\
1.04 & 1.47 & 2.45 & 6.54 & -0.302 & -3.76 & 2.72 & 10 & 0.645 & 1.09 & -0.185 & 2.57 & -1.92 & -0.619 & 0.0321 & -0.63 & 2.46 & -13.5 & -1.98 \\
-0.0071 & -0.007 & -3.58 & -1.09 & 0.0043 & -0.671 & 0.0895 & 24.3 & 77.3 & -0.313 & -0.0831 & 1.19 & -0.619 & -0.692 & -22.2 & -7.27 & -0.0854 & 3.75 & -0.518 \\
0.713 & -3.21 & -38.6 & -346 & 16.3 & -0.497 & 83.3 & -55.2 & -9.41 & 1.22e+03 & -0.141 & 9.19 & 0.0321 & -22.2 & 1.27e+03 & 31.8 & -3.77 & -22.3 & 3.65 \\
-0.253 & -0.766 & 17.1 & 23.8 & -0.467 & -3.09 & -2.56 & 6.59 & 10.1 & -0.825 & 0.0433 & -51.8 & -0.63 & -7.27 & 31.8 & 0.158 & 5.62 & -2.4 & -43.1 \\
0.209 & -0.617 & -0.382 & -4.27 & -3.54 & 6.61 & 1.25 & -7.84 & 9.7 & -18.8 & -0.336 & 11.5 & 2.46 & -0.0854 & -3.77 & 5.62 & -11.2 & 0.298 & 1.37 \\
-0.557 & -4.54 & -1.64 & 8.92 & -4.69 & 4.33 & 27.6 & 8.16 & 0.467 & -1.39 & -6.4 & -1.26 & -13.5 & 3.75 & -22.3 & -2.4 & 0.298 & -72.6 & 2.91 \\
0.132 & -5.39 & 7.62 & -0.728 & -0.028 & -0.116 & -1.81 & 4.64 & -1.95 & 11.2 & -0.324 & -0.718 & -1.98 & -0.518 & 3.65 & -43.1 & 1.37 & 2.91 & 2.83
\end{pmatrix}$$

Then, the 1-level set $\Omega_1 \subset \mathcal{X}$ of function V is determined, which constitutes a positively invariant domain for system (2.2). The approximated volume of Ω_1 is 89.767. The shape

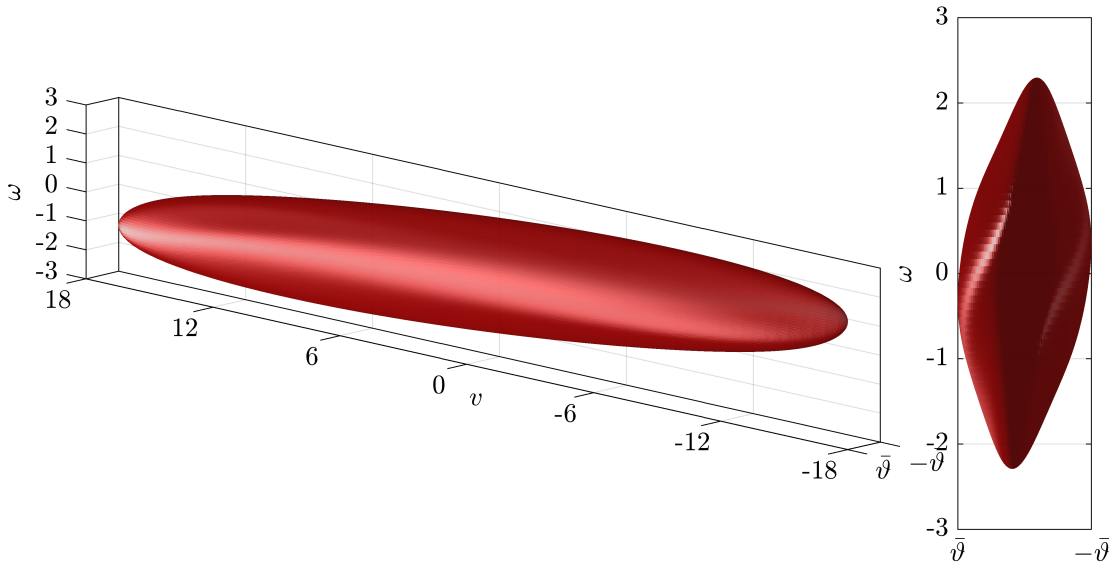

Figure 6.21: Invariant level set Ω_1 of function $V = W \circ \Phi$ computed for the nonlinear inverted pendulum balancing system (2.2). In the figure, $\overline{\vartheta} = \frac{\pi}{4} \simeq 0.7854$.

of Ω_1 is illustrated in Figure 6.21.

The propose computational framework of Chapter 5 and the DOA computational method of this chapter are originally proposed for rational nonlinear (possibly uncertain) dynamical models. However, the embedding allowed us to adapt the proposed approach for a dynamical system with both rational and trigonometrical terms (and their composition). Also observe that the computed Lyapunov $V = W \circ \Phi$ is also a highly nonlinear rational-trigonometrical function with an unstructured matrix P. With this example, we aimed to demonstrate the applicability of the proposed approach for an even broader class of dynamical models than that with rational state (or parameter) dependence.

6.5 Summary

In this chapter, I have proposed a computational method to estimate the domain of attraction (DOA) of uncertain nonlinear (rational) continuous- or discrete-time systems based on Lyapunov's theorem. The proposed DOA computation framework has similar elements to the techniques proposed in [154] (DT case) or [16] (CT case), where the authors used affine annihilators to construct polytopic LMI conditions for stability. The new contributions compared to these references are as follows. I presented automatic numerical techniques to build up a system representation required for DOA computation, whereas, [16; 154] give the theoretical and methodological bases of the polytopic approach for DOA computation. Differently from [154], I allow time-varying uncertainties for both CT and DT cases. In [154], the boundary conditions for the Lyapunov function is formulated by the S-procedure and the volume of the DOA is enlarged by a trace minimization method. Differently from [154], I follow the techniques of [16], where the DOA is enlarged by using slack variables and prescribing additional boundary conditions, which are formulated with Finsler's lemma. Supplementing [16; 154], I propose reductive LMI projections for both Lyapunov conditions and the boundary conditions. To reduce the solutions conservatism I used algorithmically generated maximal annihilators, which, to the best of our knowledge is a new concept in the literature.

10.15774/PPKE.ITK.2021.004

Chapter 7

Induced $\mathcal{L}_2$-gain computation

Alongside the internal stability of a dynamical system, the input-output behaviour of the system is another major attribute, and the induced $\mathcal{L}_2$-gain is its most popular quantitative descriptor. The induced $\mathcal{L}_2$-gain computation for a general nonlinear uncertain system is not covered yet. In this chapter, I propose a novel approach to compute a tight upper bound γ on the induced $\mathcal{L}_2$ norm of a rational nonlinear uncertain model.

7.1 Motivating example

Consider a waste fermenting bioreactor modeled by the continuous fermentation process introduced in Section 2.2. Suppose that the substrate concentration of the inlet waste flow is rapidly changing due to the inhomogeneous substrate concentration of the organic waste mixture to be processed. For a sustainable compost (P) production, the mass of bacteria culture (X) in the bioreactor should be maintained within a relatively tight interval irrespectively of the small substrate concentration perturbations (u_S) of the inlet feed flow.

The induced $\mathcal{L}_2$-gain analysis allows us to obtain quantitative information about the input-output behaviour of the nonlinear process model. In Figure 7.1, we demonstrate two possible system responses to a small inlet substrate concentration perturbation. First, suppose that the system has a small $\mathcal{L}_2$-gain from signal u_S to signal $x_1 = X - X_0$. Then, the system weakens the input perturbation on the output signal and the system remains close to the operating point (X_0, S_0). If the process model has a high $\mathcal{L}_2$-gain (larger than 1), then, the input perturbation is amplified on the output signal. In this case, the system state may leave the domain of attraction of the operating equilibrium point and the bacteria culture might even be washed out. In the knowledge of an upper bound γ on the induced $\mathcal{L}_2$-gain, we can forecast, which of the previous two cases is more likely to occur.

7.2 Convex conditions for induced $\mathcal{L}_2$-gain analysis

7.2.1 System class and storage function

We consider MIMO uncertain nonlinear state-space models in the following form:

$$\Sigma : \begin{cases} \dot{x} = f(x,u,p) = A(x,p)x + B(x,p)u, \text{ with } x(0) = 0, \\ y = h(x,u,p) = C(x,p)x + D(x,p)u, \end{cases} \tag{7.1}$$

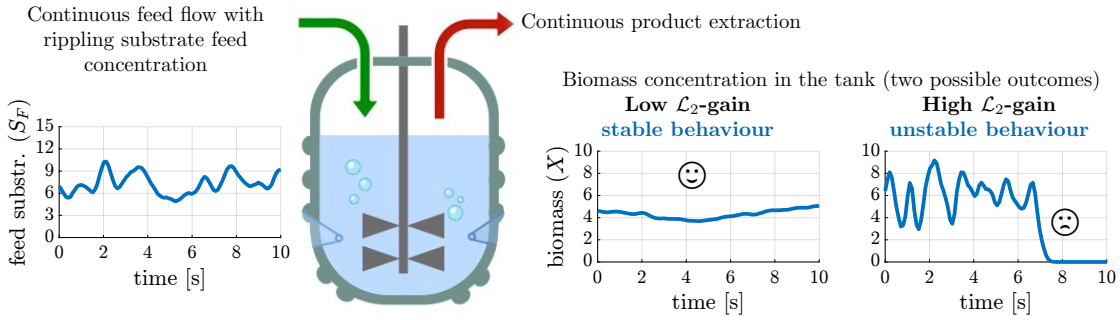

Figure 7.1: Small $\mathcal{L}_2$-gain (typically lower than 1) provides a higher disturbance attenuation, and hence a stable behaviour. Large $\mathcal{L}_2$-gain implies a higher sensitivity to the disturbance signal, which results in the unstable behaviour.

where x, u, y, and p are the state, input, output, and the scheduling parameter signals, respectively, with p satisfying Assumption 3.1. Furthermore, A, B, C, D are well-defined rational functions on $\mathcal{X} \times \mathcal{P}$, where $\mathcal{P}, \mathcal{R} \subset \mathbb{R}^{n_p}$ are compact polytopes, and $\mathcal{X} \subseteq \mathbb{R}^{n_x}$ is a compact polytope (for local analysis) or the whole state-space (for global analysis).

The storage function candidate is constructed in the same form (5.9), as a Lyapunov function was searched for DOA estimation in Chapter 6, namely:

$$V(x,p) = x^\top \mathbf{Q}(x,p)x = \pi^\top(x,p)\, Q(p)\, \pi(x,p), \text{ with } Q(p) = Q_0 + \textstyle\sum_{i=1}^{n_p} Q_i\, p_i, \tag{7.2}$$

where $\pi : \mathcal{X} \times \mathcal{P} \to \mathbb{R}^m$ is a minimal generator, and $Q_0, \dots, Q_{n_p}$ are free symmetric matrices. Note that the Lyapunov matrix of V is $\mathbf{Q}(x,p) = \Pi^\top(x,p)\, Q(p)\, \Pi(x,p)$, where generator $\Pi : \mathcal{X} \times \mathcal{P} \to \mathbb{R}^{m \times n_x}$ satisfies $\pi(x,p) = \Pi(x,p)x$ for all $(x,p) \in \mathcal{X} \times \mathcal{P}$.

Similarly to the DOA computation problem in Chapter 6, we have three source of freedom in the LMI formulation. First, we have to select the minimal generator, which constructs the candidate storage function. Secondly, we need to give a possible quadratic reformulation of the dissipation inequality (3.14b) with the appropriate supply rate (in Corollary 3.13), namely:

$$\begin{aligned} &\tfrac{\partial V}{\partial x}(x,p) f(x,u,p) + \tfrac{\partial V}{\partial p}(x,p)\varrho - \gamma^2 u^\top u + y^\top y \\ &\quad = \left(\begin{smallmatrix}1\\u\end{smallmatrix}\right)^\top \pi_\ell^\top(x,p,\varrho)\, Q_\ell(p,\varrho)\, \pi_\ell(x,p,\varrho) \left(\begin{smallmatrix}1\\u\end{smallmatrix}\right) \le -\alpha_0 \|x\|^2, \end{aligned} \tag{7.3}$$

$$\text{for all } (x,u,p,\varrho) \in \mathcal{X} \times \mathbb{R}^{n_u} \times \mathcal{P} \times \mathcal{R}. \tag{7.3a}$$

where π_ℓ is a minimal generator. Thirdly, we have to select affine annihilators N and N_ℓ for the generators π and π_ℓ.

7.2.2 Model representation

As a first step, a structured LFR is fixed for the dynamic equations of Σ. The equations and the block diagram of the proposed model representation are the following:

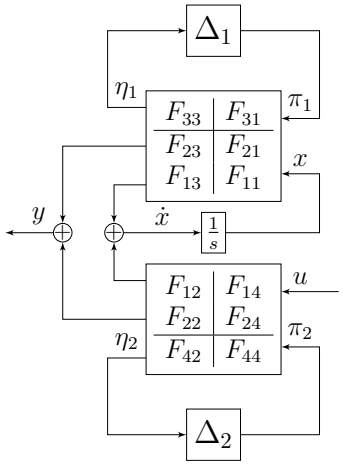

$$\mathcal{F}(\Sigma):\ \left(\begin{array}{c}\dot{x}\\ y\\ \hline \eta_1\\ \eta_2\end{array}\right) = \underbrace{\left(\begin{array}{cc|cc} F_{11} & F_{12} & F_{13} & F_{14}\\ F_{21} & F_{22} & F_{23} & F_{24}\\ \hline F_{31} & 0 & F_{33} & 0\\ 0 & F_{42} & 0 & F_{44}\end{array}\right)}_{F_{::}} \left(\begin{array}{c}x\\ u\\ \hline \pi_1\\ \pi_2\end{array}\right), \tag{7.4}$$

where $\pi_1 = \Delta_1\eta_1$, $\pi_2 = \Delta_2\eta_2$, and constant matrices F_{ij} are determined through the LFRs

$$\begin{pmatrix} A(x,p)\\ C(x,p)\end{pmatrix} = \mathcal{F}_l\left\{\left(\begin{array}{c|c} F_{11} & F_{13}\\ F_{21} & F_{23}\\ \hline F_{31} & F_{33}\end{array}\right), \Delta_1\right\}, \tag{7.4a}$$

$$\begin{pmatrix} B(x,p)\\ D(x,p)\end{pmatrix} = \mathcal{F}_l\left\{\left(\begin{array}{c|c} F_{12} & F_{14}\\ F_{22} & F_{24}\\ \hline F_{42} & F_{44}\end{array}\right), \Delta_2\right\}. \tag{7.4b}$$

Pairs $\pi_1, \eta_1 : [0,\infty) \to \mathbb{R}^{m_1}$, and $\pi_2, \eta_2 : [0,\infty) \to \mathbb{R}^{m_2}$ are the feedback signals through the uncertain blocks Δ_1 and Δ_2, respectively. In the block diagram of $\mathcal{F}(\Sigma)$, the matrices F_{11}, F_{13}, F_{21}, F_{23}, F_{31}, F_{33} are reordered to match the modified order of input and output signals. The coefficient matrices of Σ can also be given in a single equation as follows:

$$\left(\begin{smallmatrix} A(x,p) & B(x,p)\\ C(x,p) & D(x,p)\end{smallmatrix}\right) = \mathcal{F}_l\left\{F_{::}, \left(\begin{smallmatrix}\Delta_1 & \\ & \Delta_2\end{smallmatrix}\right)\right\}. \tag{7.5}$$

To construct a storage function candidate, we derive a generator from (7.4) by eliminating signals η_1 and η_2 as follows[1]:

$$\Pi_1 = \mathcal{F}_l\left\{\left(\begin{smallmatrix} 0 & I_{m_1}\\ F_{31} & F_{33}\end{smallmatrix}\right), \Delta_1\right\},\ \Pi = \left(\begin{smallmatrix} I_{n_x}\\ \Pi_1\end{smallmatrix}\right) : \mathcal{X}\times\mathcal{P} \to \mathbb{R}^{m\times n_x}, \tag{7.6a}$$

$$\Pi_2 = \mathcal{F}_l\left\{\left(\begin{smallmatrix} 0 & I_{m_2}\\ F_{42} & F_{44}\end{smallmatrix}\right), \Delta_2\right\},\ \Pi_b = \left(\begin{smallmatrix} I_{n_u}\\ \Pi_2\end{smallmatrix}\right) : \mathcal{X}\times\mathcal{P} \to \mathbb{R}^{m_b\times n_u}, \tag{7.6b}$$

$$\pi_1 = \Pi_1 x,\ \pi_2 = \Pi_2 u,\ \pi = \Pi x = \left(\begin{smallmatrix} x\\ \pi_1\end{smallmatrix}\right),\ \pi_b = \Pi_b u = \left(\begin{smallmatrix} u\\ \pi_2\end{smallmatrix}\right), \tag{7.6c}$$

where $m = n_x + m_1$, $m_b = n_u + m_2$. From now on Δ_1, Δ_2, Π_1, Π_2, Π, Π_b, π_1, and π are considered as of (x,p), whereas, π_2 and π_b are functions of (x,u,p). The generator form realization of the (7.1) corresponding to LFR $\mathcal{F}(\Sigma)$ is the following:

$$\mathcal{G}(\Sigma):\ \left(\begin{smallmatrix}\dot{x}\\ y\end{smallmatrix}\right) = \left(\begin{smallmatrix} F_{11} & F_{13}\\ F_{21} & F_{23}\end{smallmatrix}\right)\pi(x,p) + \left(\begin{smallmatrix} F_{12} & F_{14}\\ F_{22} & F_{24}\end{smallmatrix}\right)\pi_b(x,u,p). \tag{7.7}$$

***Remark* 7.1.** For simplicity and transparency but without the loss of generality, we assume that functions π and π_b are minimal generators, i.e., $\mathcal{G}(\Sigma)$ is a minimal generator form realization for Σ. Otherwise, let $\left(\begin{smallmatrix}\dot{x}\\ y\end{smallmatrix}\right) = \left(\begin{smallmatrix} G_{11} & G_{13}\\ G_{21} & G_{23}\end{smallmatrix}\right)\widehat{\pi} + \left(\begin{smallmatrix} G_{12} & G_{14}\\ G_{22} & G_{24}\end{smallmatrix}\right)\widehat{\pi}_b$, where

$$\left(\begin{smallmatrix} G_{11} & G_{13}\\ G_{21} & G_{23}\end{smallmatrix}\right) = \left(\begin{smallmatrix} F_{11} & F_{13}\\ F_{21} & F_{23}\end{smallmatrix}\right)S, \text{ and } \left(\begin{smallmatrix} G_{12} & G_{14}\\ G_{22} & G_{24}\end{smallmatrix}\right) = \left(\begin{smallmatrix} F_{12} & F_{14}\\ F_{22} & F_{24}\end{smallmatrix}\right)S_b, \tag{7.8}$$

and the minimal generators $\widehat{\pi}$ and $\widehat{\pi}_b$ satisfy $\pi = S\widehat{\pi}$ and $\pi_b = S_b\widehat{\pi}_b$. To compute $\widehat{\pi}$ with S and $\widehat{\pi}_b$ with S_b, we refer back to Procedure 5.15. ◇

7.2.3 Reformulating the dissipation inequality

As a second step, we need to find an appropriate quadratic factorization of the dissipation inequality as suggested in (7.3). In the following proposition, we present one possible

[1]Subscript b in Π_b, π_b suggests that generator Π_b is related to matrix $B(x,p) = (F_{12}\ F_{14})\Pi_b$.

form of the dissipativity relation.

Proposition 7.1. *Let Σ be given in representation (7.4) with a storage function (7.2). Furthermore, let Q_ℓ and the corresponding generator π_ℓ be given as follows:*

$$Q_\ell(p,\varrho) = \begin{pmatrix} \mathrm{He}\{E_d^\top Q(p) A_d\} + E_d^\top \check{Q}(\varrho) E_d + C_d^\top C_d & E_d^\top Q(p) B_e + C_d^\top D_e \\ B_e^\top Q(p) E_d + D_e^\top C_d & D_e^\top D_e - \gamma^2 E_e^\top E_e \end{pmatrix}, \tag{7.9}$$

$$\pi_\ell(x,p,\varrho) = \begin{pmatrix} \pi_d(x,p,\varrho) & 0 \\ 0 & \Pi_e(x,p) \end{pmatrix} : \mathcal{X} \times \mathcal{P} \times \mathcal{R} \to \mathbb{R}^{(m_d+m_e)\times(1+n_u)}, \tag{7.9a}$$

where $m_d = n_x + 4m_1$, $m_e = n_u + 2m_1 + m_2$, furthermore,

$$\check{Q}(\varrho) = \frac{\mathrm{d}Q}{\mathrm{d}t} = \sum_{i=1}^{n_p} Q_i \varrho_i, \;\; \pi_d = \begin{pmatrix} \pi \\ \frac{\partial \pi_1}{\partial x} F_{11} x \\ \frac{\partial \pi_1}{\partial x} F_{13} \pi_1 \\ \frac{\partial \pi_1}{\partial p} \varrho \end{pmatrix}, \;\; \Pi_e = \begin{pmatrix} \Pi_b \\ \frac{\partial \pi_1}{\partial x} F_{12} \\ \frac{\partial \pi_1}{\partial x} F_{14} \Pi_2 \end{pmatrix}, \tag{7.9b}$$

$$A_d = \begin{pmatrix} F_{11} & F_{13} & 0 & 0 & 0 \\ 0 & 0 & I_{m_1} & I_{m_1} & I_{m_1} \end{pmatrix}, \quad B_e = \begin{pmatrix} F_{12} & F_{14} & 0 & 0 \\ 0 & 0 & I_{m_1} & I_{m_1} \end{pmatrix}, \tag{7.9c}$$

$$C_d = \begin{pmatrix} F_{21} & F_{23} & 0_{n_y \times 3m_1} \end{pmatrix}, \qquad D_e = \begin{pmatrix} F_{22} & F_{24} & 0_{n_y \times 2m_1} \end{pmatrix}, \tag{7.9d}$$

$$E_d = \begin{pmatrix} I_{n_x} & 0 & 0_{n_x \times 3m_1} \\ 0 & I_{m_1} & 0_{m_1 \times 3m_1} \end{pmatrix}, \qquad E_e = \begin{pmatrix} I_{n_u} & 0_{n_u \times m_2} & 0_{n_u \times 2m_1} \end{pmatrix}. \tag{7.9e}$$

Then, a possible quadratic factorization form for the dissipation inequality (7.3) can be given by Q_ℓ and generator π_ℓ. ◇

Proof. The left hand side of (7.3) can be evaluated as follows:

$$\begin{aligned} &\mathrm{He}\Big\{\pi^\top(x,p) Q(p) \Big(\tfrac{\partial \pi}{\partial x}(x,p) A(x,p) x + \tfrac{\partial \pi}{\partial x}(x,p) B(x,p) u + \tfrac{\partial \pi}{\partial p}(x,p) \varrho\Big)\Big\} + \pi^\top(x,p) \check{Q}(\varrho) \pi(x,p) \\ &\quad + \begin{pmatrix} 1 \\ u \end{pmatrix}^\top \Big(C(x,p)x \quad D(x,p)\Big)^\top \Big(C(x,p)x \quad D(x,p)\Big) \begin{pmatrix} 1 \\ u \end{pmatrix} - \gamma^2 u^\top u \le 0. \end{aligned} \tag{7.10}$$

Using the notations in (7.9b)-(7.9e), we can observe the following identities:

$$\tfrac{\partial \pi}{\partial x}(x,p) A(x,p) x + \tfrac{\partial \pi}{\partial p}(x,p) \varrho = \begin{pmatrix} F_{11}x + F_{13}\pi_1(x,p) \\ \frac{\partial \pi_1}{\partial x}(x,p)(F_{11}x + F_{13}\pi_1(x,p)) + \frac{\partial \pi_1}{\partial p}(x,p)\varrho \end{pmatrix} = A_d \pi_d(x,p,\varrho), \tag{7.11a}$$

$$\tfrac{\partial \pi}{\partial x}(x,p) B(x,p) = \begin{pmatrix} F_{12} + F_{14}\Pi_2(x,p) \\ \frac{\partial \pi_1}{\partial x}(x,p)(F_{12} + F_{14}\Pi_2(x,p)) \end{pmatrix} = B_e \Pi_e(x,p), \tag{7.11b}$$

$$C(x,p)x = F_{21}x + F_{23}\pi_1(x,p) = C_d \pi_d(x,p,\varrho), \tag{7.11c}$$

$$D(x,p) = F_{22} + F_{24}\Pi_2(x,p) = D_e \Pi_e(x,p), \tag{7.11d}$$

$$\pi(x,p) = E_d \pi_d(x,p,\varrho), \text{ and } I_{n_u} = E_e \Pi_e(x,p). \tag{7.11e}$$

Accordingly, (7.10) can be altered as follows:

$$\begin{aligned} &\mathrm{He}\{\pi_d^\top(x,p,\varrho) E_d^\top Q(p) (A_d \; B_e) \pi_\ell(x,p,\varrho) \begin{pmatrix} 1 \\ u \end{pmatrix}\} + \pi_d^\top(x,p,\varrho) E_d^\top \check{Q}(\varrho) E_d \pi_d(x,p,\varrho) \\ &\qquad + \begin{pmatrix} 1 \\ u \end{pmatrix}^\top \pi_\ell^\top(x,p,\varrho) \begin{pmatrix} C_d^\top C_d & C_d^\top D_e \\ D_e^\top C_d & D_e^\top D_e - \gamma^2 E_e^\top E_e \end{pmatrix} \pi_\ell(x,p,\varrho) \begin{pmatrix} 1 \\ u \end{pmatrix} \end{aligned} \tag{7.12}$$

$$\begin{aligned} &= \begin{pmatrix} 1 \\ u \end{pmatrix}^\top \pi_\ell^\top(x,p,\varrho) \mathrm{He}\left\{ \begin{pmatrix} E_d^\top Q(p) A_d & E_d^\top Q(p) B_e \\ 0 & 0 \end{pmatrix} \right\} \pi_\ell(x,p,\varrho) \begin{pmatrix} 1 \\ u \end{pmatrix} \\ &\qquad + \begin{pmatrix} 1 \\ u \end{pmatrix}^\top \pi_\ell^\top(x,p,\varrho) \begin{pmatrix} E_d^\top \check{Q}(\varrho) E_d + C_d^\top C_d & C_d^\top D_e \\ D_e^\top C_d & D_e^\top D_e - \gamma^2 E_e^\top E_e \end{pmatrix} \pi_\ell(x,p,\varrho) \begin{pmatrix} 1 \\ u \end{pmatrix} \le 0. \end{aligned} \tag{7.13}$$

Finally, it is already visible from (7.13) that it gives back the right hand side of (7.3) with Q_ℓ and π_ℓ as defined in (7.9). □

7.2.4 Global performance analysis for LPV systems

Let us consider the linear parameter varying subclass of system (7.1):

$$\Sigma_{\mathrm{LPV}} : \begin{cases} \dot{x} = A(p)x + B(p)u, \;\; \text{with } x(0) = 0, \\ y = C(p)x + D(p)u, \end{cases} \tag{7.14}$$

where A, B, C, D are well-defined rational functions of the scheduling parameter only, and $p : [0,\infty) \to \mathcal{P}$ is again a function of the time. System Σ_{LPV} is said to be an LPV

model with rational parameter dependence.

We assume that Σ_{LPV} is globally asymptotically stable for $u \equiv 0$, for all $x(0) \in \mathbb{R}^{n_x}$, and all p satisfying Assumption 3.1. Consequently, the $\mathcal{L}_2$-gain analysis can be executed without any "special" restrictions on the input signal, it only has to belong to $\mathcal{L}_2^{n_u}[0,\infty)$. Furthermore, it is natural to set $\mathcal{X} = \mathbb{R}^{n_x}$, namely, the analysis is performed "globally" over the whole state-space.

Observe that generators Π and Π_b in (7.6) computed for system Σ_{LPV} are functions of p only, as well as, matrix $\mathbf{Q}(p) = \Pi^\top(p)\, Q(p)\, \Pi(p)$ is consequentially independent of the state. Therefore, an equivalent formulation of the dissipation inequality for system Σ_{LPV} can be given as follows:

$$\mathbf{Q}_\ell(p,\varrho) = \Pi_\ell^\top(p,\varrho) Q_\ell(p,\varrho) \Pi_\ell(p,\varrho) = \begin{pmatrix} \mathrm{He}\{\mathbf{Q}(p)A(p)\} + \check{\mathbf{Q}}(p,\varrho) + C^\top(p)\, C(p) & \mathbf{Q}(p)B(p) \\ B^\top(p)\mathbf{Q}(p) & D^\top(p)\, D(p) - \gamma^2 I \end{pmatrix}$$
$$\preceq -\begin{pmatrix} \alpha_0 I_{n_x} & 0 \\ 0 & 0_{n_u \times n_u} \end{pmatrix} \text{ for all } (p,\varrho) \in \mathcal{P} \times \mathcal{R}, \tag{7.15}$$

where Q_ℓ is given in (7.9) and

$$\Pi_\ell = \begin{pmatrix} \Pi_d & \\ & \Pi_e \end{pmatrix} : \mathcal{P} \times \mathcal{R} \to \mathbb{R}^{(m_d+m_e)\times(n_x+n_u)}. \tag{7.16}$$

Differently from π_ℓ in (7.9a), generator Π_ℓ is independent of x as generators Π_d and Π_e simplifies to

$$\Pi_d = \begin{pmatrix} \Pi \\ \Pi_1 F_{11} \\ \Pi_1 F_{13} \Pi_1 \\ \sum_{i=1}^{n_p} \frac{\partial \Pi_1}{\partial p_i} \varrho_i \end{pmatrix} : \mathcal{P} \times \mathcal{R} \to \mathbb{R}^{m_d \times n_x}, \ \Pi_e = \begin{pmatrix} \Pi_b \\ \Pi_1 F_{12} \\ \Pi_1 F_{14} \Pi_2 \end{pmatrix} : \mathcal{P} \to \mathbb{R}^{m_e \times n_u}. \tag{7.17}$$

It is worth mentioning that generator Π_ℓ is typically not minimal.

Finally, as all the "ingredients" are introduced, we present a semidefinite program to compute a tight upper bound γ on the induced $\mathcal{L}_2$-gain of system Σ_{LPV}. The following corollary is a direct consequence of Corollary 3.13, Lemma 3.22, and Proposition 7.1.

Corollary 7.2 [P1] (SDP for global $\mathcal{L}_2$-gain analysis)**.** *Consider system* Σ_{LPV} (7.14) *with storage function* $V : \mathbb{R}^{n_x} \times \mathcal{P} \to \mathbb{R}$ *in the quadratic form*

$$V(x,p) = x^\top \mathbf{Q}(p) x, \ \mathbf{Q}(p) = \Pi^\top(p)\, Q(p)\, \Pi(p), \ Q(p) = Q_0 + \textstyle\sum_{i=1}^{n_p} Q_i\, p_i, \tag{7.18}$$

where Π *is a minimal generator, and consider the quadratic factorization* (7.15) *of* $\mathbf{Q}_\ell$*. Compute*

1. *full column-rank matrix* $S_\ell \in \mathbb{R}^{(m_d+m_e)\times m'_\ell}$ *and minimal generator* $\widehat{\Pi}_\ell : \mathcal{P} \times \mathcal{R} \to \mathbb{R}^{m'_\ell \times (n_x+n_u)}$*, such that* $\Pi_\ell = S_\ell \widehat{\Pi}_\ell$*,*
2. *affine functions* $N : \mathcal{P} \to \mathbb{R}^{s\times m}$ *and* $N_\ell : \mathcal{P} \times \mathcal{R} \to \mathbb{R}^{s_\ell \times m'_\ell}$*, such that* $N\pi \equiv 0$ *and* $N_\ell \widehat{\Pi}_\ell \equiv 0$*.*

Then, Σ_{LPV} *is dissipative with respect to the supply rate* $s(u,y) = \gamma^2\|u\|^2 + \|y\|^2$*, and has a finite* $\mathcal{L}_2$*-gain* $\|\Sigma\|_{\mathcal{L}_2} \le \gamma$ *if there exist* $L \in \mathbb{R}^{m\times s}$ *and* $L_\ell \in \mathbb{R}^{m'_\ell \times s_\ell}$ *such that*

$$Q(p) - \underline{\alpha}_0 I_a + \mathrm{He}\{LN(p)\} \succeq 0, \qquad \text{for all } p \in \mathbf{Ve}(\mathcal{P}), \tag{7.19a}$$
$$S_\ell^\top (Q_\ell(p,\varrho) + \alpha_0 I_\ell) S_\ell + \mathrm{He}\{L_\ell N_\ell(p,\varrho)\} \preceq 0, \quad \text{for all } (p,\varrho) \in \mathbf{Ve}(\mathcal{P} \times \mathcal{R}), \tag{7.19b}$$

for $\alpha_0 = 0$*, and some* $\underline{\alpha}_0 > 0$*, where* $I_a = \mathrm{diag}\{I_{n_x}, 0_{m_1}\}$*,* $I_\ell = \mathrm{diag}\{I_{n_x}, 0_{n_u+m_2+6m_1}\}$*.*

Symmetric matrices $Q_0, \dots, Q_{n_p}$*, and full matrices* L*, and* L_ℓ *are free decision variables and are meant to be found such that they minimize* γ *(appearing in* Q_ℓ*).* ◇

Proof. Condition (7.19a) implies (3.14b). Then, pre- and post-multiply (7.19b) by $(x^\top \ u^\top)\widehat{\Pi}_\ell^\top(p,\varrho)$ and by its transpose, respectively. Considering the proof of Proposition 7.1, we observe that obtained expression resembles the dissipation inequality. □

***Remark* 7.2.** System Σ_{LPV} is strictly dissipative with respect to the supply rate $s(u,y) = \gamma^2\|u\|^2 + \|y\|^2$, and system $\dot{x} = A(p)x$ is globally asymptotically stable with the Lyapunov function (7.18) if (7.19) are satisfied for some $\underline{\alpha}_0, \alpha_0 > 0$. ◇

7.2.5 Induced $\mathcal{L}_2$-gain and local stability

Let us consider a locally asymptotically stable nonlinear (possibly uncertain) system Σ as it is given in (7.1). If we prescribe an upper energy bound on the input signal ($\|u\|_2 \leq \bar{M}_2$), it is possible to compute a *local* upper bound on the induced $\mathcal{L}_2$ norm of Σ. Moreover, it can be shown that the state trajectory of Σ will evolve inside a compact set $\mathcal{X}$. The strong relationship between local stability and induced $\mathcal{L}_2$-gain is already addressed by El Ghaoui and Scorletti [89; 90], and Coutinho et al. [155; 156]. In Section 4.2, we presented in brief both local analyses approaches. We although revisit these concepts, and investigate them in the foreground of the *generalized H_2 nominal performance* [62, Section 3.3.4] of dynamical systems.

In the following theorem, we give a slight generalization of Theorem 4.3, with a different proof compared to that presented by Coutinho et al. [156]. Although it is substantially based on the clever arguments of [62, proof of Proposition 3.12], the proposed derivations have not yet been written, to the best of our knowledge, for uncertain nonlinear systems.

Theorem 7.3. *Let $\mathcal{X} \subset \mathbb{R}^{n_x}$ be a compact subset of the state-space. Assume that function $V : \mathcal{X} \times \mathcal{P} \to \mathbb{R}$ in (7.2) satisfies the dissipativity relations (3.14) on $\mathcal{X} \times \mathcal{P} \times \mathcal{R}$ and for some $\gamma > 0$. Let function $\alpha > 0$ be the highest value satisfying*

$$\Omega_\alpha = \{x \in \mathbb{R}^{n_x} \,|\, \exists\, p \in \mathcal{P} \text{ such that } V(x,p) \leq \alpha\} \subset \mathcal{X}^\circ. \tag{7.20}$$

Assume that system Σ is excited by an input $u \in \mathfrak{U}_\gamma = \{u \in \mathcal{L}_2^{n_u}[0,\infty) \,|\, \|u\|_2 \leq \gamma^{-1}\sqrt{\alpha}\}$. Then, the solution of Σ starting from $x(0) = 0$ will not leave Ω_α and $\|y\|_2 \leq \gamma\|u\|_2$, independently of the parameter signal p satisfying Assumption 3.1. ◇

Note that Ω_α is the "projection" of $\Psi_\alpha = \{(x,p) \in \mathcal{X} \times \mathcal{P} \mid V(x,p) \leq \alpha\}$ onto the state space as it is illustrated in Figure 6.1. Furthermore, $\mathfrak{U}_\gamma$ constitutes the set of admissible input signals.

Proof. Inequality (7.3) implies

$$\begin{aligned} &\tfrac{\partial V}{\partial x}(x(t),u(t))\, f(x(t),u(t),p(t)) + \tfrac{\partial V}{\partial p}(x(t),u(t))\, \dot{p}(t) \\ &\quad \leq \gamma^2\|u(t)\|^2 - \|y(t)\|^2 \leq \gamma^2\|u(t)\|^2 \text{ for all } t \geq 0, \end{aligned} \tag{7.21}$$

with $y = h(x,u,p)$. An equivalent integral formulation of (7.21) is the following:

$$V(x(t),p(t)) \leq \gamma^2 \int_0^t \|u(\tau)\|^2 \mathrm{d}\tau \leq \gamma^2 \int_0^\infty \|u(\tau)\|^2 \mathrm{d}\tau = \gamma^2\|u\|_2^2. \tag{7.22}$$

Remember that the storage function is given in a quadratic form (7.2) with $\mathbf{Q}(x,p) \succ 0$. Consequently, for all (x,p), there exists a symmetric matrix $\sqrt{\mathbf{Q}(x,p)} = R(x,p)$ such that $\mathbf{Q}(x,p) = R(x,p)R(x,p)$. Let $z = R(x,p)x$, therefore,

$$V(x(t),p(t)) = \|R(x(t),p(t))x(t)\|^2 = \|z(t)\|^2 \leq \gamma^2\|u\|_2^2 \text{ for all } t \geq 0, \tag{7.23}$$

Taking the supremum of the left hand side of inequality (7.23) over $t \geq 0$ yields

$$\|z\|_\infty \leq \gamma\|u\|_2 \text{ for all } u \in \mathcal{L}_2. \tag{7.24}$$

Dividing (7.24) by $\|u\|_2$ and taking the supremum over all $u \in \mathcal{L}_2$, we obtain that the induced norm (i.e., the generalized H_2 nominal performance) of the system operator

$\Sigma_z : \mathcal{L}_2 \to \mathcal{L}_\infty$ is smaller than or equal to $\gamma > 0$, where

$$\Sigma_z : \begin{cases} \dot{x} = f(x,u,p), \text{ with } x(0) = 0, \\ z = R(x,p)x. \end{cases} \tag{7.25}$$

The prescribed $\gamma^{-1}\sqrt{\alpha}$ energy bound for u implies that $\|z(t)\|^2 \leq \alpha$ for all $t \geq 0$, thus, $x(t) \in \Omega_\alpha$ for all $t \geq 0$ if $x(0) = 0$. As the state trajectory remains inside $\mathcal{X}$, the dissipation inequality (7.3) ensures that $\|y\|_2 \leq \gamma \|u\|_2$ for all admissible input signal $u \in \mathfrak{U}_\gamma$. □

With a few slight modifications of Corollary 7.2, we give a semidefinite program for the local $\mathcal{L}_2$-gain analysis. For the sake of clarity and completeness, the equations of Corollary 7.2 are presented again adopted for a nonlinear model. A proof for Corollary 7.4 resembles that for Corollary 7.2.

Corollary 7.4 (SDP for local stability and $\mathcal{L}_2$-gain analysis)**.** *Consider system* Σ (7.1) *with storage function* (7.2)*, and the quadratic factorization* $(\pi_\ell{}^\top Q_\ell \pi_\ell \prec 0)$ *of the dissipation inequality* (7.3) *as proposed in Proposition 7.1. Compute*

1. *full column-rank matrix* $S_\ell \in \mathbb{R}^{(m_d+m_e)\times m'_\ell}$ *and minimal generator* $\widehat{\pi}_\ell : \mathcal{X} \times \mathcal{P} \times \mathcal{R} \to \mathbb{R}^{m'_\ell \times (1+n_u)}$*, such that* $\pi_\ell = S_\ell \widehat{\pi}_\ell$*,*
2. *affine functions* $N : \mathcal{X} \times \mathcal{P} \to \mathbb{R}^{s\times m}$ *and* $N_\ell : \mathcal{X} \times \mathcal{P} \times \mathcal{R} \to \mathbb{R}^{s_\ell \times m'_\ell}$*, such that* $N\pi \equiv 0$ *and* $N_\ell \widehat{\pi}_\ell \equiv 0$*.*

Then, system Σ *has a finite* $\mathcal{L}_2$*-gain* $\|\Sigma\|_{\mathcal{L}_2} \leq \gamma$ *for all admissible input* $u \in \mathfrak{U}_\gamma$ *if there exist* $L \in \mathbb{R}^{m\times s}$ *and* $L_\ell \in \mathbb{R}^{m'_\ell \times s_\ell}$*, such that the following LMIs*

$$Q(p) - \underline{\alpha}_0 I_a + \mathrm{He}\{LN(x,p)\} \succeq 0, \qquad \text{for all } (x,p) \in \mathbf{Ve}(\mathcal{X}\times\mathcal{P}), \tag{7.26a}$$

$$S_\ell^\top (Q_\ell(p,\varrho) + \alpha_0 I_\ell) S_\ell + \mathrm{He}\{L_\ell N_\ell(x,p,\varrho)\} \preceq 0, \text{ for all } (x,p,\varrho) \in \mathbf{Ve}(\mathcal{X}\times\mathcal{P}\times\mathcal{R}), \tag{7.26b}$$

are satisfied for $\alpha_0 = 0$ *and some* $\underline{\alpha}_0 > 0$*. Functions* Q_ℓ *and* π_ℓ *are given in* (7.9)*, matrices* I_a *and* I_ℓ *are the same as in* (7.19)*.*

Symmetric matrices $Q_0, \ldots, Q_{n_p}$ *in* (7.2)*, full matrices* L*, and* L_ℓ*, are free decision variables of the SDP and are meant to be found to minimize* γ*.* ◇

Differently from the global analysis in Corollary 7.2, annihilators N and N_d in Corollary 7.4 are functions of the state too.

As we presented in Section 4.2.2, Coutinho et al. [156, Section 3.3] proposed to shape the unitary level set Ω_1 of the storage function to fit into $\mathcal{X}$. However, forcing $\Omega_1 \subset \mathcal{X}^\circ$ may result in a conservative solution. To demonstrate this fact, assume that V satisfies (7.3) and $\Omega_\alpha \in \mathcal{X}^\circ$, $\alpha < 1$. Let

$$\widetilde{V}(x,p) = \alpha^{-1} V(x,p) \geq V(x,p) \text{ on } \mathcal{X}\times\mathcal{P}. \tag{7.27}$$

Then, $\widetilde{V}$ will not necessarily satisfy (7.3). In Section 7.3.1, we demonstrate through a numerical example, that enforcing $1 \leq V(x,p)$ on $\mathcal{F}_k \times \mathcal{P}$ or $1 \leq V(x,p) \leq \tau_k$ on $\mathcal{F}_k \times \mathcal{P}$, $k = 1, \ldots, n_\mathcal{X}$ and minimizing $\gamma + \sum_{k=1}^{m_\mathcal{X}} \tau_k$ may result in a very conservative γ. Consequently, we propose to neglect the boundary LMIs and let the storage function *be shaped completely by the optimal value of* γ. After that the storage function is computed, the value of α corresponding to the maximal level set Ω_α can be determined through a simple optimization:

$$\max \alpha, \text{ s.t. } \alpha \leq V(x,p) \text{ for all } (x,p) \in \mathcal{F}_k \times \mathcal{P}, \text{ where } k = 1, \ldots, n_\mathcal{X}. \tag{7.28}$$

Note that the optimization (7.28) returns the largest level set Ω_α if the storage function is radially nondecreasing (at least with respect to x on $\mathcal{X}$).

Alongside γ, the optimization procedure provides a second important descriptor of the input-output dynamics Σ. The value of $\bar{M}_2 = \gamma^{-1}\alpha$ gives a lower energy bound for the input signal. If the input satisfies $\|u\|_2 \leq \bar{M}_2$, the state trajectory starting from $x(0) = 0$ is asymptotically stable if p satisfies Assumption 3.1. A higher value for $\bar{M}_2$ gives a less conservative bound for the input and provides a more robust input-to-state behaviour.

7.3 Computational examples

In this section, we illustrate the operations of the proposed $\mathcal{L}_2$-gain computation method through some illustrative computational examples.

7.3.1 Forced mass-spring-damper system with a nonlinear stiffness

Let us consider a mass-spring-damper system

$$m\ddot{y} = F - F_k(y) - F_b(\dot{y}). \tag{7.29}$$

with a nonlinear stiffness function [203]:

$$F_k(y) = k_1 y + k_3 y^3 \tag{7.29a}$$

In (7.29), y denotes the displacement of mass m, b is the damping coefficient, $F_b(\dot{y}) = by$ is the force of the damper applied to the mass, F is an external force applied to m. If k_3 is positive, the spring is said to be a hardening spring. A typical mechanical example for such force-deflection relationship in (7.29a), is the highly deflected beam.

Let $m = 1\,\mathrm{kg}$, $b = 1\,\frac{\mathrm{N}}{\mathrm{m/s}}$, $k_1 = 1\,\frac{\mathrm{N}}{\mathrm{m}}$, $k_3 = 2\,\frac{\mathrm{N}}{\mathrm{m}^3}$. Furthermore, we denote $x_1 = y$, $x_2 = \dot{y}$, and $u = F$. Then, the state-space dynamics are given as follows:

$$\begin{cases} \dot{x}_1 = x_2, \\ \dot{x}_2 = -k_1 x_1 - b x_2 - k_3 x_1^3 + u. \end{cases} \tag{7.30}$$

Note that (7.30) is also a variant of the Duffing oscillator model [203]. The coefficient matrices of the state-space model (7.30) and their possible LFR realization $\mathcal{F}(\Sigma)$ are given as follows:

$$\left(\begin{array}{c|c} A(x) & B \\ \hline C & D \end{array}\right) = \left(\begin{array}{cc|c} 0 & 1 & 0 \\ -2x_1^2 - 1 & -1 & 1 \\ \hline 1 & 0 & 0 \end{array}\right), \; F_{::} = \left(\begin{array}{cc|c|cc|c} 0 & 1 & 0 & 0 & 0 & \\ -1 & -1 & 1 & 2 & 0 & \\ \hline 1 & 0 & 0 & 0 & 0 & \\ \hline -0 & 0 & 0 & 0 & 1 & \\ -1 & 0 & 0 & 0 & 0 & \\ \hline & & & & & \end{array}\right), \; \left(\begin{array}{c|c} \Delta_1(x) & \\ \hline & \Delta_2(x) \end{array}\right) = \left(\begin{array}{cc|c} I_3 x_1 & & \\ & x_2 & \\ \hline & & \end{array}\right). \tag{7.31}$$

The empty spaces in block matrix $F_{::}$ highlight that matrices F_{4j} and F_{i4} are empty as the matrix $\left(\begin{smallmatrix} B \\ D \end{smallmatrix}\right)$ is constant and π_2, η_2 are $m_2 = 0$-dimensional feedback signals in the feedback interconnection system $\mathcal{F}(\Sigma)$. Correspondingly, generator Π_2 does not exist (or it is empty) in this model. Furthermore, generator Π, π from (7.6) are determined by

$$\Pi_1(x) = \begin{pmatrix} -x_1^2 & 0 \\ -x_1 & 0 \end{pmatrix}. \tag{7.32}$$

The matrices (7.9) for the dissipation LMI are computed from the LFR realization (7.31). Their values are the following:

$$A_d = \left(\begin{array}{cc|cc|cc|cc|cc} 0 & 1 & 0 & 0 & 0 & 0 & 0 & 0 & 0 & 0 \\ -1 & -1 & 2 & 0 & 0 & 0 & 0 & 0 & 0 & 0 \\ 0 & 0 & 0 & 0 & 1 & 0 & 1 & 0 & 1 & 0 \\ 0 & 0 & 0 & 0 & 0 & 1 & 0 & 1 & 0 & 1 \end{array}\right), \qquad B_e = \left(\begin{array}{c|c|cc|cc} 0 & & 0 & 0 & 0 & 0 \\ 1 & & 0 & 0 & 0 & 0 \\ 0 & & 1 & 0 & 1 & 0 \\ 0 & & 0 & 1 & 0 & 1 \end{array}\right), \tag{7.33}$$

$$C_d = \left(\begin{array}{cc|cc|cc|cc|cc} 1 & 0 & 0 & 0 & 0 & 0 & 0 & 0 & 0 & 0 \end{array}\right), \qquad D_e = \left(\begin{array}{c|c|cc|cc} 0 & & 0 & 0 & 0 & 0 \end{array}\right), \tag{7.34}$$

$$E_d = \left(\begin{array}{cc|cc|cc|cc|cc} 1 & 0 & 0 & 0 & 0 & 0 & 0 & 0 & 0 & 0 \\ 0 & 1 & 0 & 0 & 0 & 0 & 0 & 0 & 0 & 0 \\ 0 & 0 & 1 & 0 & 0 & 0 & 0 & 0 & 0 & 0 \\ 0 & 0 & 0 & 1 & 0 & 0 & 0 & 0 & 0 & 0 \end{array}\right), \qquad E_e = \left(\begin{array}{c|c|cc|cc} 1 & & 0 & 0 & 0 & 0 \end{array}\right). \tag{7.35}$$

Similarly to matrix $F_{::}$, the empty blocks in matrices B_e, D_e, E_e are due to the 0-dimensional feedback signals π_2, η_2. The generators (7.9) corresponding to the dissipation LMIs are as follows:

$$\frac{\partial \pi_1}{\partial x}(x) = \begin{pmatrix} -3x_1^2 & 0 \\ -2x_1 & 0 \end{pmatrix}, \ \frac{\partial \Pi_1}{\partial p} \equiv O_{2\times 2}, \tag{7.36}$$

$$\Pi_d(x) = \begin{pmatrix} 1 & 0 \\ 0 & 1 \\ -x_1^2 & 0 \\ -x_1 & 0 \\ 0 & -3x_1^2 \\ 0 & -2x_1 \\ 0 & 0 \\ 0 & 0 \\ 0 & 0 \\ 0 & 0 \end{pmatrix}, \ \Pi_e \equiv \begin{pmatrix} 1 \\ 0 \\ 0 \\ 0 \\ 0 \end{pmatrix}, \ \pi_\ell(x) = \begin{pmatrix} \Pi_d(x)x & 0 \\ 0 & \Pi_e \end{pmatrix} = \begin{pmatrix} x_1 & 0 \\ x_2 & 0 \\ -x_1^3 & 0 \\ -x_1^2 & 0 \\ -3x_1^2x_2 & 0 \\ -2x_1x_2 & 0 \\ 0 & 0 \\ 0 & 0 \\ 0 & 0 \\ 0 & 0 \\ 0 & 1 \\ 0 & 0 \\ 0 & 0 \\ 0 & 0 \\ 0 & 0 \end{pmatrix}. \tag{7.37}$$

Obviously, generator π_ℓ is not minimal, therefore, we compute S_ℓ and $\widehat{\pi}_\ell$ as requested in Corollary 7.4:

$$S_L = \begin{pmatrix} 1&0&0&0&0&0&0 \\ 0&1&0&0&0&0&0 \\ 0&0&1&0&0&0&0 \\ 0&0&0&1&0&0&0 \\ 0&0&0&0&1&0&0 \\ 0&0&0&0&0&1&0 \\ 0&0&0&0&0&0&0 \\ 0&0&0&0&0&0&0 \\ 0&0&0&0&0&0&0 \\ 0&0&0&0&0&0&0 \\ 0&0&0&0&0&0&1 \\ 0&0&0&0&0&0&0 \\ 0&0&0&0&0&0&0 \\ 0&0&0&0&0&0&0 \\ 0&0&0&0&0&0&0 \end{pmatrix}, \ \widehat{\pi}_\ell(x) = \begin{pmatrix} x_1 & 0 \\ x_2 & 0 \\ -x_1^3 & 0 \\ -x_1^2 & 0 \\ -3x_1^2x_2 & 0 \\ -2x_1x_2 & 0 \\ 0 & 1 \end{pmatrix}. \tag{7.38}$$

Finally the two annihilators N and N_ℓ are computed for generators π and π_ℓ

$$N(x) = \begin{pmatrix} 0 & 0 & 1 & -x_1 \\ x_1 & 0 & 0 & 1 \\ -x_2 & x_1 & 0 & 0 \end{pmatrix}, \ N_\ell(x) = \begin{pmatrix} 0 & 0 & 1 & -x_1 & 0 & 0 & 0 \\ x_1 & 0 & 0 & 1 & 0 & 0 & 0 \\ 0 & 0 & 0 & -3x_2 & 1 & 0 & 0 \\ 2x_2 & 0 & 0 & 0 & 0 & 1 & 0 \\ -x_2 & x_1 & 0 & 0 & 0 & 0 & 0 \\ 0 & 0 & -3x_2 & 0 & x_1 & 0 & 0 \\ 0 & 0 & 0 & -2x_2 & 0 & x_1 & 0 \end{pmatrix}. \tag{7.39}$$

During the analysis, we considered six different rectangular polytopes:

$$\begin{aligned} \mathcal{X}_1 &= [-0.4, 0.4] \times [-0.4, 0.4], & \mathcal{X}_2 &= [-0.9, 0.9] \times [-0.9, 0.9], \\ \mathcal{X}_3 &= [-1.2, 1.2] \times [-1.2, 1.2], & \mathcal{X}_4 &= [-1, 1] \times [-1.5, 1.5], \\ \mathcal{X}_5 &= [-5, 5] \times [-20, 20], & \mathcal{X}_6 &= [-20, 20] \times [-200, 200]. \end{aligned} \tag{7.40}$$

Finally, solving the PD-LMIs (7.26) on the corner points of the actual polytope $\mathcal{X}$, we obtain a value for γ.

To compute an upper bound γ on the induced $\mathcal{L}_2$ norm of system (7.30), we solve the SDP (7.26) as proposed in Corollary 7.2. In Corollary 6.8, we presented additional boundary constraints to shape the Lyapunov function and expand the positively invariant level set appropriately inside polytope $\mathcal{X}$. Though these constraints were designed for RSD shaping, they can be used combined with the $\mathcal{L}_2$-gain analysis. The role of the boundary constraints in (6.33) are similar to the PS constraints (4.11) and (4.34) of [89; 90] and [156], respectively. Namely, they guarantee that the unitary level set Ω_1 of the storage function is closed inside $\mathcal{X}$. In this example, we demonstrate that the performance analysis in combination with the shaping constraints may result in a conservative solution.

$\mathcal{X}$	Method	γ	α	$\bar{M}_2$	vol(Ω_α)	t [sec]
1: $\mathcal{X}_1$	El Ghaoui and Scorletti [89; 90]	2.0411	1	0.48993	0.47918	0.1009
2: $\mathcal{X}_1$	[89; 90], without PS constraint	1.2643	0.1671	0.32331	0.40916	0.0957
3: $\mathcal{X}_1$	Coutinho et al. [156]	3.8116	1	0.26236	0.47546	0.2247
4: $\mathcal{X}_1$	[156], without PS constraint	1.2595	0.13157	0.28799	0.40888	0.1750
5: $\mathcal{X}_1$	Our method, no boundary LMIs	**1.1548**	0.16475	0.35149	0.40641	0.1379
6: $\mathcal{X}_1$	Our method, $1 \leq V(x)$ on $\partial\mathcal{X}$	1.8566	1	**0.53861**	0.4819	0.1426
7: $\mathcal{X}_1$	Our method, $1 \leq V(x) \leq \tau_k$ on $\mathcal{F}_k$	1.8706	1	**0.53460**	0.48989	0.1705
8: $\mathcal{X}_2$	El Ghaoui and Scorletti [89; 90]	2.2859	1.2825	0.49543	1.7386	0.0892
9: $\mathcal{X}_2$	[89; 90], without PS constraint	2.2859	1.2825	0.49543	1.7386	0.1084
10: $\mathcal{X}_2$	Coutinho et al. [156]	2.5895	1	0.38618	1.8286	0.2329
11: $\mathcal{X}_2$	[156], without PS constraint	2.2779	0.55896	0.32821	1.7375	0.1754
12: $\mathcal{X}_2$	Our method, no boundary LMIs	**1.1548**	0.86361	**0.80474**	1.8404	0.1398
13: $\mathcal{X}_2$	Our method, $1 \leq V(x)$ on $\partial\mathcal{X}$	1.158	1	**0.86353**	1.7857	0.1402
14: $\mathcal{X}_2$	Our method, $1 \leq V(x) \leq \tau_k$ on $\mathcal{F}_k$	1.1895	1	**0.84067**	2.0632	0.1618
15: $\mathcal{X}_3$	El Ghaoui and Scorletti [89; 90]	25.169	22.057	0.1866	2.7127	0.1129
16: $\mathcal{X}_3$	[89; 90], without PS constraint	25.169	22.057	0.1866	2.713	0.0984
17: $\mathcal{X}_3$	Coutinho et al. [156]	7.4801	1	0.13369	2.5167	0.2380
18: $\mathcal{X}_3$	[156], without PS constraint	5.8217	0.45954	0.11644	2.3638	0.1528
19: $\mathcal{X}_3$	Our method, no boundary LMIs	**1.1548**	1.5556	**1.0801**	3.0703	0.1282
20: $\mathcal{X}_3$	Our method, $1 \leq V(x)$ on $\partial\mathcal{X}$	**1.1548**	1.5546	**1.0797**	3.1036	0.1402
21: $\mathcal{X}_3$	Our method, $1 \leq V(x) \leq \tau_k$ on $\mathcal{F}_k$	1.294	1	0.77281	3.1313	0.1837
22: $\mathcal{X}_4$	El Ghaoui and Scorletti [89; 90]				*Infeasible problem*	
23: $\mathcal{X}_4$	[89; 90], without PS constraint				*Infeasible problem*	
24: $\mathcal{X}_4$	Coutinho et al. [156]	3.0972	1.3229	0.37137	4.1129	0.1929
25: $\mathcal{X}_4$	[156], without PS constraint	3.0972	1.3229	0.37137	4.1129	0.1823
26: $\mathcal{X}_4$	Our method, no boundary LMIs	**1.1548**	2.4944	**1.3677**	4.5294	0.1304
27: $\mathcal{X}_4$	Our method, $1 \leq V(x)$ on $\partial\mathcal{X}$	**1.1548**	2.4969	**1.3683**	4.525	0.1511
28: $\mathcal{X}_4$	Our method, $1 \leq V(x) \leq \tau_k$ on $\mathcal{F}_k$	1.5772	1	0.63402	4.097	0.1549
29: $\mathcal{X}_5$	El Ghaoui and Scorletti [89; 90]				*Infeasible problem*	
30: $\mathcal{X}_5$	[89; 90], without PS constraint				*Infeasible problem*	
31: $\mathcal{X}_5$	Coutinho et al. [156]				*Infeasible problem*	
32: $\mathcal{X}_5$	[156], without PS constraint				*Infeasible problem*	
33: $\mathcal{X}_5$	Our method, no boundary LMIs	**1.1548**	504.74	**19.455**	292.4	0.1495
34: $\mathcal{X}_5$	Our method, $1 \leq V(x)$ on $\partial\mathcal{X}$	**1.1548**	505.47	**19.469**	293.45	0.1500
35: $\mathcal{X}_5$	Our method, $1 \leq V(x) \leq \tau_k$ on $\mathcal{F}_k$	5.6544	177.18	2.3541	296.77	0.1805
36: $\mathcal{X}_6$	El Ghaoui and Scorletti [89; 90]				*Infeasible problem*	
37: $\mathcal{X}_6$	[89; 90], without PS constraint				*Infeasible problem*	
38: $\mathcal{X}_6$	Coutinho et al. [156]				*Infeasible problem*	
39: $\mathcal{X}_6$	[156], without PS constraint				*Infeasible problem*	
40: $\mathcal{X}_6$	Our method, no boundary LMIs	**1.1548**	52635	**198.67**	9681.7	0.1414
41: $\mathcal{X}_6$	Our method, $1 \leq V(x)$ on $\partial\mathcal{X}$	**1.1548**	52647	**198.69**	9678.6	0.1543
42: $\mathcal{X}_6$	Our method, $1 \leq V(x) \leq \tau_k$ on $\mathcal{F}_k$				*Infeasible problem*	

Table 7.1: Comparative computational results obtained for model (7.30). During the analysis, we considered multiple polytopes $\mathcal{X}_1, \ldots, \mathcal{X}_6$, which correspond to the six blocks of the table. In the first four rows of each block, we present the obtained results for the two reference approaches [89; 90] and [156] with and without the PS conditions (4.11) and (4.34), respectively. The results of our proposed approach is presented in three different setup. First, we used no boundary conditions for the storage function (third row of each block). Secondly, the unitary level set Ω_1 is enforced to lay inside polytope $\mathcal{X}$ (each fourth rows). Finally, the value of the storage function is additionally minimized along the facets of $\mathcal{X}$ (each fifth rows). γ denotes the computed upper bound on the induced $\mathcal{L}_2$-gain of the system. The value of α corresponds to the largest level set Ω_α of the storage function, which lies completely inside of $\mathcal{X}$. $\bar{M}_2 = \sqrt{\alpha}\gamma^{-1}$ is the upper energy bound on the input signal u, which ensures that the state signal will evolve inside Ω_α. vol(Ω_α) denotes the volume of level set Ω_α. t denotes the SDP solver's processing time.

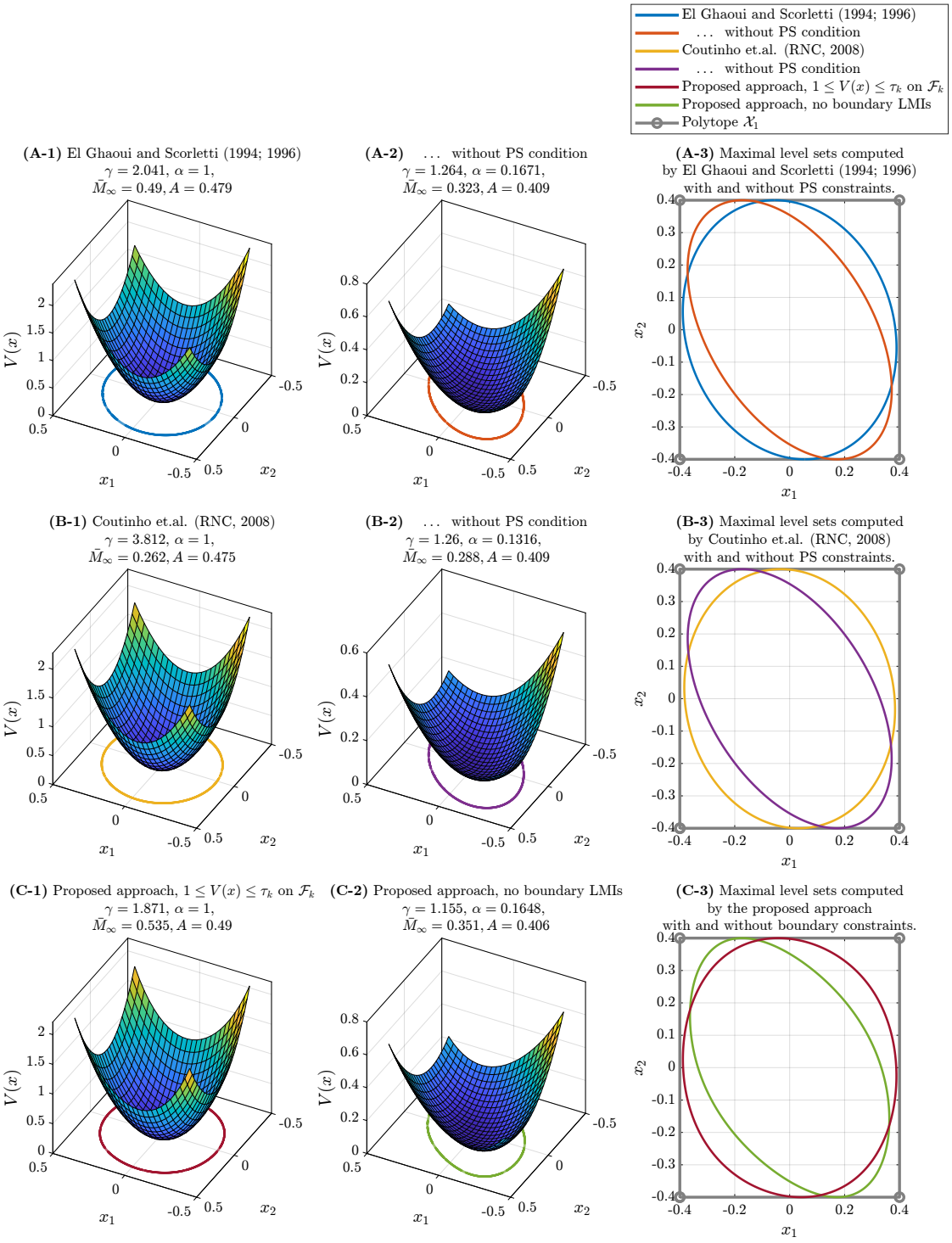

Figure 7.2: Shape of the storage function and its maximal level set Ω_α obtained through the different approaches for model (7.30) with polytope $\mathcal{X}_1$. The storage functions in subplots (A-1), (A-2), (B-1), (B-2), (C-1), (C-2) correspond to Lines 1, 2, 3, 4, 7, 5 of Table 7.1, respectively.

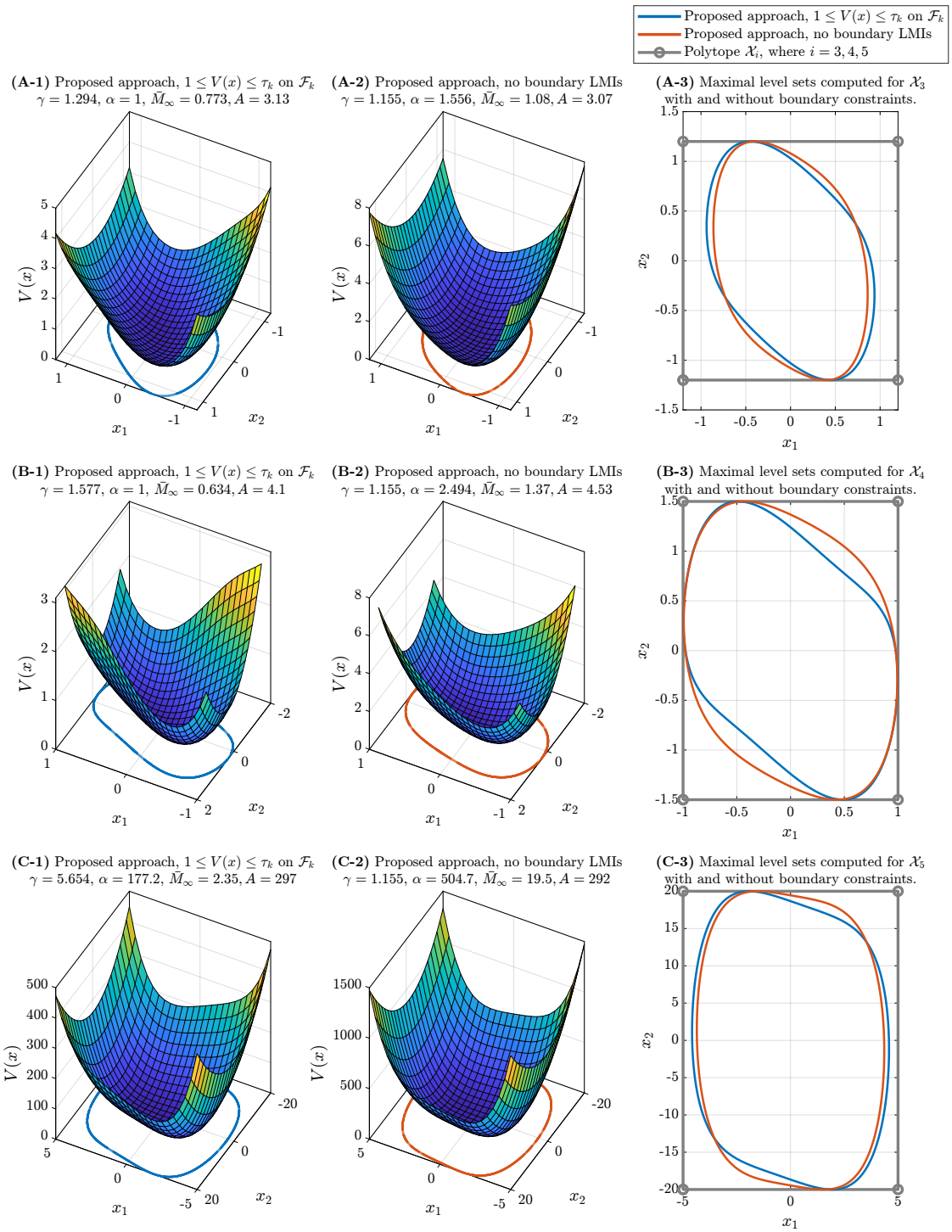

Figure 7.3: Shape of the storage function and its maximal level set Ω_α obtained through the proposed approach for model (7.30) with and without boundary LMIs. The figures illustrate the results obtained for polytopes $\mathcal{X}_3$, $\mathcal{X}_4$, and $\mathcal{X}_5$. The storage functions in subplots (A-1), (A-2), (B-1), (B-2), (C-1), (C-2) correspond to Lines 21, 19, 28, 26, 35, 33 of Table 7.1, respectively.

Through the comparative analysis, we considered two nonlinear solutions of the literature presented in [89; 90] and [156], respectively. For both nonlinear techniques, we execute the analysis with the corresponding PS constraint, then, we perform the analysis without any shaping constraint. Afterwards, we apply our proposed $\mathcal{L}_2$-gain approach in three different setup. First, we neglect the boundary constraints (as proposed in Corollary 7.4). Secondly, we enforce an upper bound boundary constraint (6.33a) on V as follows: $1 \leq V(x)$ on $\partial\mathcal{X}$. Thirdly, we considered both boundary LMIs in (6.33) to force $1 \leq V(x,p) \leq \tau_k$ for all $x \in \partial\mathcal{X}$, and we minimized $\gamma + \sum_{k=1}^{m_\mathcal{X}} \tau_k$.

The numerical results of the comparative evaluation are presented in detail in Table 7.1 for all polytopes in (7.40). Table 7.1, we collected the obtained values for the upper bound γ, the level α of the maximal level set, the input energy bound $\bar{M}_2 = \gamma^{-1}\sqrt{\alpha}$, the volume of the maximal level set Ω_α, and the processing time. For instance, Line 40 of Table 7.1 presents that the system is asymptotically stable with $x(0) = 0$ and $\|u\|_2 \leq 198.7$ and the energy of the output is less than $1.1541 \cdot \|u\|$.

In order to demonstrate the effect of the shaping constraints, we present the storage functions generated by the different approaches in Figure 7.3. In Figure 7.3, we illustrate the storage function obtained by our proposed approach for polytopes $\mathcal{X}_3$, $\mathcal{X}_4$, and $\mathcal{X}_5$.

We observed that the upper bounding boundary constraint (6.33a) is conservative when polytope $\mathcal{X}_1$ or $\mathcal{X}_2$ is considered (Lines 6 and 13 of Table 7.1). Note that in both cases, the unitary level set obtained through neglecting the shaping constraints (Lines 5 and 12 of Table 7.1) are not located inside $\mathcal{X}$. Moreover, enforcing the lower bounding constraint (6.33b) and minimizing the values of $\tau_1, \ldots, \tau_k$ alongside with γ, may result in an unreasonably conservative solution (e.g., Line 35 of Table 7.1).

The numerical values suggest that the upper bound γ, generated by [89; 90] and [156], can also be significantly decreased by neglecting the PS conditions.

For each polytope selection, our approach computes a less conservative value for both the upper bound γ and the input energy limit $\bar{M}_2$ compared to the considered reference solutions.

7.3.2 Continuous fermentation process

In section 6.4.5, we analysed the stability of the closed-loop dynamics of the continuous fermentation process model (2.20) with an uncertain maximal growth rate $\mu_{\max}$, a constant substrate feed concentration ($S_F(t) = S_{F,0} + u_S(t)$, $u_S \equiv 0$), and without actuator noise ($u_F \equiv 0$). Here, we revisit this problem with the same model constants ($V_0 = 4\,\mathrm{l}$, $K_1 = 0.03\,\mathrm{g/l}$, $K_2 = 0.5\,\mathrm{l/g}$, $Y = 0.5$, $S_{F,0} = 10\,\mathrm{g/l}$) and a maximal growth rate $\mu_{\max} = 1$, but we analyse the effect of signals u_F and u_S on the centered state variables $x_1 = X - X_0$ and $x_2 = S - S_0$. Note that X_0 and S_0 are the optimal equilibrium point concentrations of the biomass and the substrate in the tank, and they are computed as presented in Paragraph 2.2.0.1

The state-space equations of the closed-loop model is

$$\begin{cases} \dot{X} = \mu(S)X - \dfrac{X(F_0 - k(S - S_0) + u_F)}{V_0}, \\ \dot{S} = -\dfrac{\mu(S)X}{Y} + \dfrac{(S_{F,0} + u_S - S)(F_0 - k(S - S_0) + u_F)}{V_0}. \end{cases} \tag{7.41}$$

If we collect the terms in (7.41) with respect to the input signals, we obtain the following

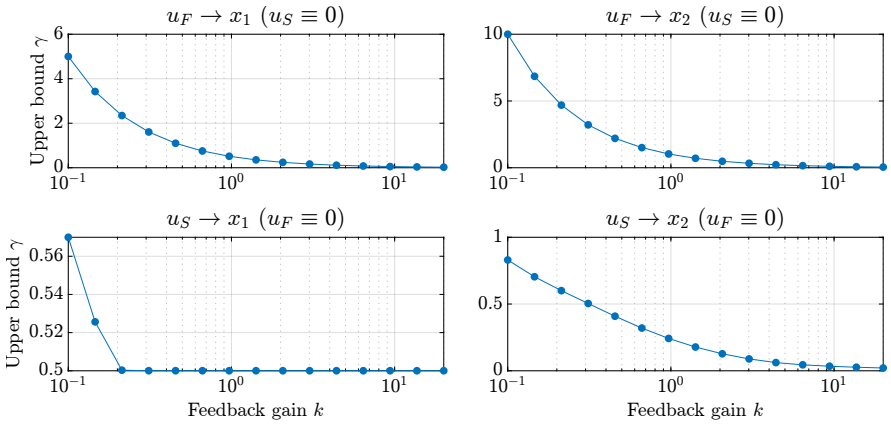

Figure 7.4: Computed upper bound γ on the induced $\mathcal{L}_2$ norm of nonlinear system (7.42) with different input/output configurations and different feedback gain values.

"input-*multi*-affine" model:

$$\begin{cases} \dot{X} = \mu(S)X - \frac{XF_0}{V_0} + \frac{kX(S-S_0)}{V_0} - \frac{X}{V_0}u_F, \\ \dot{S} = -\frac{\mu(S)X}{Y} + \frac{(S_{F,0}-S)F_0}{V_0} - \frac{k(S_{F,0}-S)(S-S_0)}{V_0} + \frac{S_{F,0}-S}{V_0}u_F + \frac{F_0-k(S-S_0)}{V_0}u_S + \frac{1}{V_0}u_F u_S, \end{cases}$$

Finally, the centered input-output model can be written in the following form:

$$\dot{x} = f(x, \mu_{\max}) - k\, g(x)\, x_2 + g(x)\, u_F + g_1(x)\, u_S + g_2(x)\, u_F u_S, \tag{7.42}$$

$$\text{with } f(x, \mu_{\max}) = A_1(x, \mu_{\max})\, x, \text{ and } x = \begin{pmatrix} x_1 \\ x_2 \end{pmatrix} = \begin{pmatrix} X - X_0 \\ S - S_0 \end{pmatrix}, \tag{7.42a}$$

where functions f, g, and A_1 are defined in (6.51)-(6.52), furthermore,

$$g_1(x) = \frac{1}{V_0}\begin{pmatrix} 0 \\ F_0 - k\, x_2 \end{pmatrix},\ g_2(x) = \frac{1}{V_0}\begin{pmatrix} 0 \\ 1 \end{pmatrix}. \tag{7.42b}$$

The centered nonlinear model (7.42) is multi-affine in the input signals u_F and u_S as their product appear in the system equation. Therefore, we analyse the actuator noise effect first, assuming no substrate feed concentration perturbation ($u_S \equiv 0$). Then, we assume no actuator noise ($u_F \equiv 0$), and analyse the effect of u_S on the state variables. For both input signals, we consider (separately) both the centered biomass concentration (x_1) and the centered substrate concentration (x_2) as outputs. The computed γ for each case can be seen in Figure 7.4 in the function of the feedback gain k.

The analysis points out that the disturbance attenuation from u_S to x_1 cannot be decreased below 0.5 with $k \leq 20$. At the same time, the effect of the actuator noise can be reduced arbitrarily with a sufficiently high feedback gain. In Figure 7.6, we present the simulation results of the translated closed-loop system (7.42) with no actuator noise but a smoothed random substrate feed concentration perturbation. In Part (A) and Part (B) of Figure 7.6, the system trajectories are illustrated for two different feedback gain values ($k = 3$ and $k = 10$, respectively) but applying the same input signal (black line in Part (C) of Figure 7.6). The computed trajectories confirms of the results of the $\mathcal{L}_2$-gain analysis, namely, the effect of u_S on x_1 is practically independent of the feedback gain value within $k \in [2, 20]$.

Through the comparative evaluation, we considered again the two significant nonlinear induced $\mathcal{L}_2$-gain approach of [89; 90] and [156]. The numerical results and the positively invariant domains obtained through the different approaches are collected in Table 7.2 and Figure 7.5, respectively. In this example, our approach results in the lower computed γ compared to the considered reference solutions. However, the computational cost of our approach is almost two order of magnitude higher than that of the reference solutions.

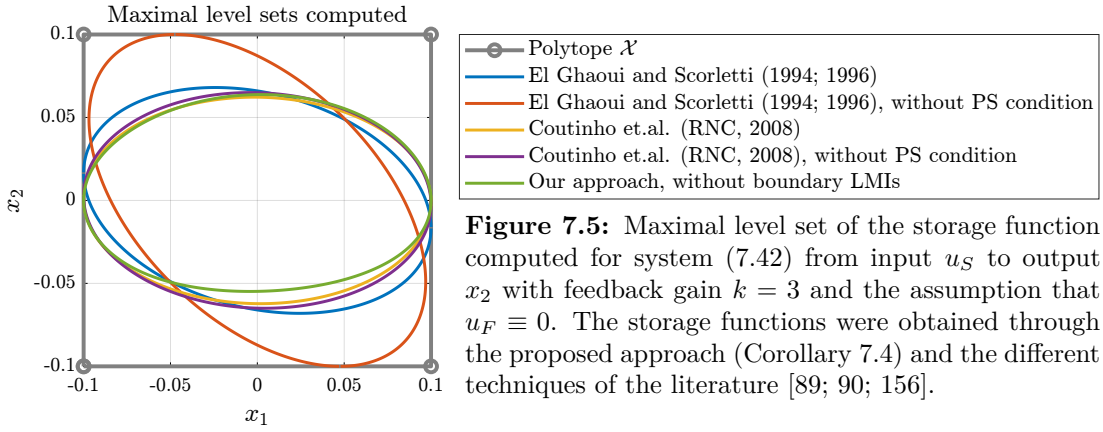

Figure 7.5: Maximal level set of the storage function computed for system (7.42) from input u_S to output x_2 with feedback gain $k = 3$ and the assumption that $u_F \equiv 0$. The storage functions were obtained through the proposed approach (Corollary 7.4) and the different techniques of the literature [89; 90; 156].

Method	γ	α	$\widetilde{M}_2$	vol(Ω_α)	t [s]
El Ghaoui and Scorletti [89; 90]	3.4416	1.0001	0.2906	0.0205	0.1
[89; 90], without PS constraint	0.3496	0.0047	0.1958	0.0263	0.1
Coutinho et al. [156]	9.3969	1.0000	0.1064	0.0194	0.2
[156], without PS constraint	0.0917	0.0058	0.8274	0.0202	0.2
Our method, no boundary LMIs	0.0894	0.0005	0.2463	0.0185	8.8

Table 7.2: Comparative numerical results of the $\mathcal{L}_2$-gain analysis for system (7.42) from input u_S to output x_2 with feedback gain $k = 3$ and the assumption that $u_F \equiv 0$.

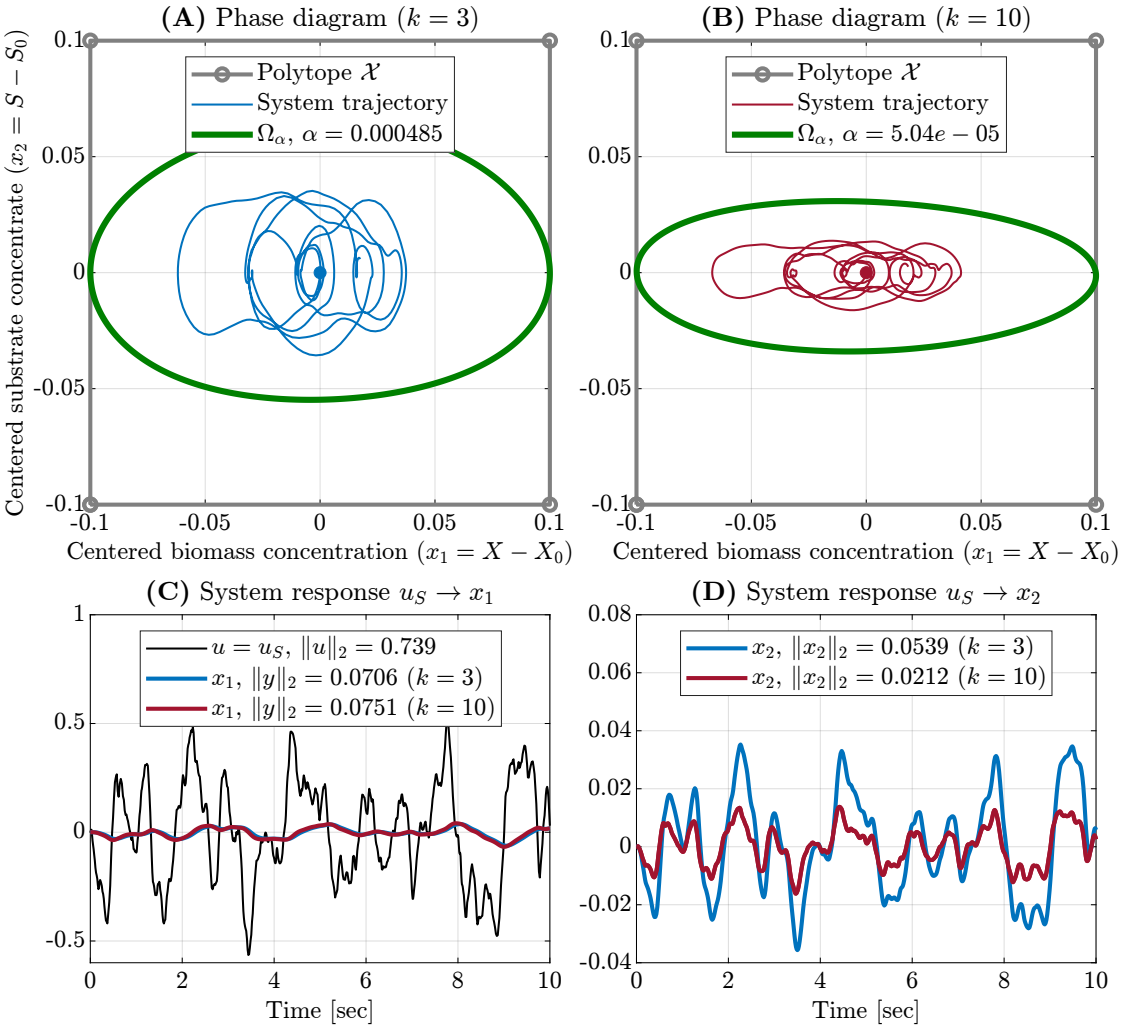

Figure 7.6: Comparative simulation results of system (7.42) with two different feedback gain values ($k = 3$ and $k = 10$), with zero actuator noise ($u_F \equiv 0$), and a smoothed random perturbation (u_S) on the substrate feed concentration.

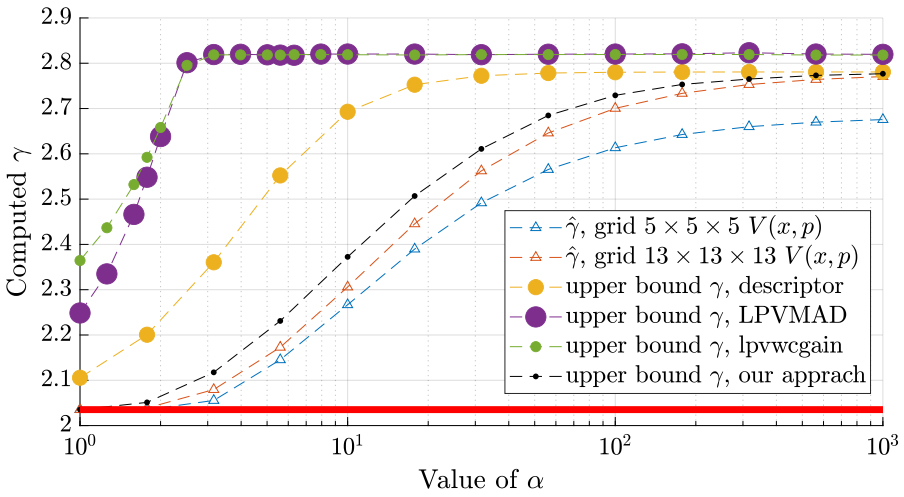

Figure 7.7: Computed upper bound γ for system (7.43) with different values of α considering the descriptor approach of [125] (orange dots), IQC/LFT approach of [113] (small green dots) and [104] (large purple dots), and the proposed approach based on Finsler's lemma (small black dots). The empty triangles illustrate the approximated value for γ using the grid-based approach of [73] and considering two different grid densities. The horizontal red line illustrates the worst-case LTI $\mathcal{H}_\infty$ gain obtained for the frozen parameter values $p_1 = p_2 = p_3 = 2$. This value is a guaranteed lower bound on the induced $\mathcal{L}_2$-gain of system (7.43).

	Method ($\alpha = 100$)	Upper b. γ	Solver [s]	Overall [s]
1:	IQC (Cor. 4.16), LPVMAD [112]	2.8203	37	38
2:	IQC (Cor. 4.16), LPVTools [113]	2.8192	80	101
3:	Descr.-approach (Thm. 4.8, Cor. 4.11)	2.7800	240	250
4:	Our approach (Cor. 7.2)	2.7270	748	807
5:	Grid-based (Thm. 4.1) ($13\times13\times13$)	$\simeq$ 2.7000	531	633
6:	Grid-based (Thm. 4.1) ($5\times5\times5$)	$\simeq$ 2.6134	19	30

Table 7.3: Computational results of our approach compared to other known solutions in the literature obtained for model (7.43). Symbol "$\simeq$" in lines nr. 5-6 highlight that the grid-based approach returns an approximated (not guaranteed) upper bound on the induced $\mathcal{L}_2$ norm.

7.3.3 Global performance analysis of a fourth-order LPV model

We consider an LPV system Σ with matrices [P1]:

$$\left(\begin{array}{c|c} A(p) & B(p) \\ \hline C(p) & D(p) \end{array}\right) = \left(\begin{array}{ccccc|cc} p_1-3 & \frac{2p_1}{2p_3^2+p_1+2}+3 & 0.1p_3 & p_2p_3^2 & & 0 & 0 \\ 0 & -p_2^2-1 & 5 & 0 & & p_2^2+1 & 0 \\ \frac{1}{p_2-5} & 0 & p_1-4 & 0 & & 0 & 0 \\ 0 & 0.1 & 0 & \frac{1}{p_1+2}-5 & & 0 & \frac{p_1}{p_1+2}+2 \\ \hline -\frac{1}{p_2-5} & 0 & 0 & 0 & & 0 & 0 \\ 0 & 0 & p_1+1 & 0 & & 0 & 0 \end{array}\right). \quad (7.43)$$

The values of the parameters and of their derivatives are bounded and belong to the following intervals:

$$\begin{aligned} p_1 &\in [-1,2], & p_2 &\in [-1,2], & p_3 &\in [0,2], \\ \dot{p}_1 &\in [-10\alpha, 10\alpha], & \dot{p}_2 &\in [-\alpha,\alpha], & \dot{p}_3 &\in [-5\alpha, 5\alpha], \end{aligned} \quad (7.44)$$

where $\alpha \geq 1$. During the analysis, we considered multiple values for $\alpha \in [1, 1000]$.

After computing the recursive LFT realization (Section 3.6.2) of matrices $\left(\begin{smallmatrix} A(p) \\ C(p) \end{smallmatrix}\right)$ and $\left(\begin{smallmatrix} B(p) \\ D(p) \end{smallmatrix}\right)$, the corresponding generators π and π_b in (7.6) are not minimal and have $m = 20$ and $m_b = 6$ coordinates, respectively. According to Remark 7.1, and using the proposed

approach of Section 5.4, we obtained

$$\widehat{\pi}(x,p) = \left(\begin{smallmatrix} x \\ \hat{\pi}_1(x,p) \end{smallmatrix}\right) \in \mathbb{R}^{17}, \text{ and } \widehat{\pi}_b(u,p) = \left(\begin{smallmatrix} u \\ \hat{\pi}_2(u,p) \end{smallmatrix}\right) \in \mathbb{R}^5, \text{ where}$$

$$\widehat{\pi}_1^\top(x,p) = \Big(p_1x_1 \ \tfrac{2p_1x_2}{2p_3^2+p_1+2} \ p_1x_3 \ \tfrac{p_1x_4}{p_1+2} \ p_2p_3^2x_4 \ p_2^2x_2 \ p_2x_2 \ \tfrac{p_2x_1}{p_2-5} \ \tfrac{2p_3^2x_2}{2p_3^2+p_1+2} \ \tfrac{2p_3x_2}{2p_3^2+p_1+2} \ p_3x_3 \ p_3^2x_4 \ p_3x_4 \Big),$$

$$\widehat{\pi}_2^\top(u,p) = \begin{pmatrix} p_2u_1 & p_2^2u_1 & \tfrac{2p_1u_2}{p_1+2} \end{pmatrix}. \tag{7.45}$$

Thus, a storage function is computed in the form $V(x,p) = \widehat{\pi}^\top(x,p)\, Q(p)\, \widehat{\pi}(x,p)$.

When $\alpha = 1$ our computed upper bound is very close to the guaranteed lower bound obtained through an LTI $\mathcal{H}_\infty$ analysis of (7.43) for a frozen parameter configuration ($p_1(t) = p_2(t) = p_3(t) = 2$ for all $t \geq 0$). Therefore, we gradually increased the parameter rate variations up to $\alpha = 1000$. The computed upper bound is illustrated for different values of α in Figure 7.7, in which the horizontal red line illustrates the guaranteed lower bound on the induced $\mathcal{L}_2$-gain.

The results obtained by the proposed approach are compared to the results of two IQC/LFT implementations [112; 113], grid- [73] and descriptor-based [125] approaches. These approaches are all outlined in brief in Chapter 3. The comparative computational results are presented in Table 7.3 (for $\alpha = 100$) and in Figure 7.7 (for $\alpha \in [1, 1000]$).

The IQC approach for nominal $\mathcal{L}_2$ performance analysis is outlined in Corollary 4.16. The implementation details related to the IQC software tools [112; 113] are given in Paragraph 4.4.0.1.

The approach of Masubuchi and Suzuki [125] is detailed in Theorem 4.8 alongside with the cross-corner evaluation technique of Masubuchi [126], which is presented in details in Corollary 4.11. First, a descriptor model for system Σ is derived from a relative-minimal LFR realization of Σ as presented in (4.25). Then, we considered the bilinear (in p) linear (in the free variables) matrix inequality (blPD-LMI) (4.76) of Theorem 4.8 with the multi-affine parameter-dependent free matrix variables in (4.75). The resulting blPD-LMI can be solved in an SDP framework as presented in Corollary 4.11.

The grid-based approach of Wu [73] is summarized in Theorem 4.1. In this case, a rational storage function candidate is considered:

$$V(x,p) = x^\top \Big(\textstyle\sum_i Q_i \varpi_i(p) \Big) x, \tag{7.46}$$

where Q_i are free symmetric matrices, and the basis functions in $\varpi_i(p) \in \Big\{ 1;\ p_1,\ p_2,\ p_3;\ p_1^2,\ p_1p_2,\ p_2^2,\ p_1p_3,\ p_2p_3,\ p_3^2;\ p_1^3,\ p_1^2p_2,\ p_1p_2^2,\ p_2^3,\ p_1^2p_3,\ p_1p_2p_3,\ p_2^2p_3,\ p_1p_3^2,\ p_2p_3^2,\ p_3^3;\ \frac{1}{5-p_2},\ \frac{p_1}{p_1+2},\ \frac{p_1}{p_3^2+\frac{p_1}{2}+1} \Big\}$ were selected by considering the generator form realization (7.7) of system (7.43). In order to reduce the solutions conservatism, we used $\delta = 0$ and $T = \infty$ (as proposed in Remark 4.2), and we considered two finite gridding of $\mathcal{P}$ with different density. Accordingly, the computed values for γ are not guaranteed upper bounds on the induced $\mathcal{L}_2$-gain of system (7.43). First, we considered a coarse grid $\mathbf{Gr}(\mathcal{P}, 5 \times 5 \times 5)$ (blue triangles in Figure 7.7), then, we refined the subdivision to $\mathbf{Gr}(\mathcal{P}, 13 \times 13 \times 13)$ (red triangles in Figure 7.7).

It is worth mentioning that the $5 \times 5 \times 5$ gridded solution gives a value 2.6134 for γ. Then, we practically inserted two additional intermediate grid points between every two consecutive grid points (in each dimension). This refined $13 \times 13 \times 13$ gridding resulted in a higher value for γ, namely, 2.7000. This suggests that the actual induced $\mathcal{L}_2$ norm of (7.43) is possibly higher that 2.6134, but it may also be higher than 2.7000.

Compared to the gridded solution, our approach as well as the IQC- and the descriptor-based approaches, provide a guaranteed upper bound on the induced norm. Though, it is computationally more demanding than the IQC- and the descriptor-based approaches,

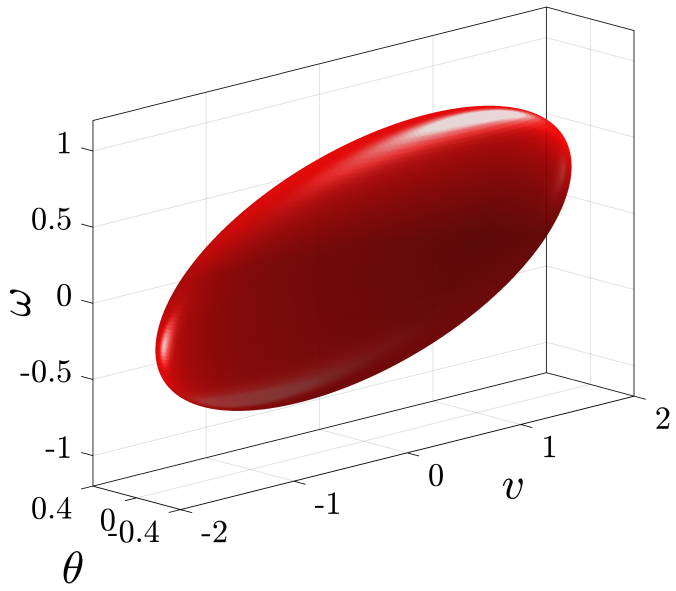

Figure 7.8: Maximal level set $\Omega_c \subset \mathcal{X}^\circ$, of the computed storage function $W(x) = V(x, p(x))$, where $c = 2.1271$. The required energy bound for the input signal is $\|u\|_2 \leq 1.6879$. The approximated volume of Ω_c is 1.886.

our method gives the lowest guaranteed upper bound.

7.3.4 The pendulum-cart system – a qLPV approach

Here, we consider the qLPV model (2.18) of the open-loop down rising pendulum-car system (2.1) introduced in Section 2.1.2, in Remark 2.1. In this model, the locally asymptotically stable equilibrium point $x^* = 0$ corresponds to the state, when the pendulum is at rest, and it points downwards.

In Theorem 7.3, we have already revisited the relation between local stability and finite $\mathcal{L}_2$-gain property. However, qLPV model (2.18) requires even more attention. Remember that the parameter bounds and the parameter rate bounds were determined in Paragraph 2.1.2.1 in the function of the operating domain (polytope $\mathcal{X}$) and the upper bound $\bar{M}_\infty$ on the $\mathcal{L}_\infty$ norm of the input signal.

First of all, we selected the model constants: $m = 1\,\text{kg}$, $M = 2\,\text{kg}$, $\ell = 1\,\text{m}$, $g = 10\,\text{m/s}^2$, $b = 5\,\text{kg/s}$, and $\bar{M}_\infty = 1$. Through a few numerical simulations of system (2.17) with different admissible input signals $u : \|u\|_\infty \leq \bar{M}_\infty$, we fixed the following bounding polytope for the state vector:

$$\mathcal{X} = [-2, 2] \times [-0.4, 0.4] \times [-1.2, 1.2].$$

Then, the corresponding bounding polytopes for p and $\dot{p}$ are

$$\begin{aligned} p \in \mathcal{P} &= [0.9735, 1] \times [0.9211, 1] \times [-0.4673, 0.4673], \\ \dot{p} \in \mathcal{R} &= [-0.1575, 0.1575] \times [-0.4673, 0.4673] \times [-4, 4]. \end{aligned} \tag{7.47}$$

7.3.4.1 $\mathcal{L}_2$-gain and local stability. Suppose that there exists an appropriately small value $\bar{M}_2 < \infty$ such that the state trajectory x from $x(0) = 0$ does not leave the preliminarily selected compact subset $\mathcal{X}$ of the state-space $\mathbb{R}^{n_x}$ for all $t \geq 0$ and all

$$u \in \mathfrak{U} = \left\{ u \in \mathcal{L}_2[0, \infty) \,\middle|\, \|u\|_\infty \leq \bar{M}_\infty,\ \|u\|_2^2 \leq \bar{M}_2 \right\}, \tag{7.48}$$

According to Paragraph 2.1.2.1, polytopes $\mathcal{P}$ and $\mathcal{R}$ in (7.47) were determined such that

$$p(x) \in \mathcal{P},\ \tfrac{\partial p}{\partial x}(x)(f(x) + g(x)u) \in \mathcal{R},\ \forall x \in \mathcal{X},\ \forall u \in \mathbb{R}^{n_u} : \|u\| \leq \bar{M}_\infty. \tag{7.49}$$

	Method	γ	solver [s]	preproc [s]	total [s]
1:	LPVMAD	1.1444	22	1	23
2:	LPVTools	1.1388	61	17	78
3:	Descriptor	0.8741	107	14	121
4:	Proposed approach	0.8641	231	34	265
5:	Grid:15	$\simeq 0.8634$	141	139	280
6:	Grid:5	$\simeq 0.8630$	4	10	14

Table 7.4: Computed upper bound γ for the nominal $\mathcal{L}_2$ performance of LPV system (2.13) using different approaches.

Let $W : \mathcal{X} \times \mathcal{P} \to \mathbb{R}$ be a storage function for the qLPV model (2.18). Then, function $V : \mathcal{X} \to \mathbb{R}$ with $V(x) = W(x, p(x))$ is a storage function for the (translated) nonlinear system (2.17) and it satisfies the dissipation inequality

$$V(x(t)) \leq \int_0^t \gamma^2 \|u(\tau)\|^2 - \|y(\tau)\|^2 \mathrm{d}\tau, \tag{7.50}$$

for all $t \geq 0$, all $u \in \mathfrak{U}$, and for $x(0) = 0$, where the output y is the angle of the pendulum $x_2 = \theta$. Following the reasoning (7.22) of the proof of Theorem 7.3, the left hand side of (7.50) can be upper estimated as follows:

$$V(x(t)) \leq \gamma^2 \int_0^t \|u(\tau)\|^2 \mathrm{d}\tau \leq \gamma^2 \|u\|_2^2 \leq \gamma^2 \bar{M}_2, \tag{7.51}$$

for all $t \geq 0$, $x(0) = 0$. Let $c > 0$ be selected such that the level set

$$\Omega_c = \{x \in \mathcal{X} \,|\, V(x) \leq c\} \subset \mathcal{X}^\circ \tag{7.52}$$

is contained by $\mathcal{X}^\circ$. Finally, let $\bar{M}_2 = c\,\gamma^{-2}$. Then, (7.51) implies $x(t) \in \mathcal{X}$ for all $t \geq 0$ and all $u \in \mathfrak{U}$. ▲

Before the nonlinear analysis, it is worth mentioning that $\underline{\gamma} = 0.5548$ is a guaranteed lower bound on the induced $\mathcal{L}_2$-gain of model (2.18), which is the LTI $\mathcal{H}_\infty$ norm of system (2.18) for the frozen worst-case parameter values $p_1(t) = 0.9735$, $p_2(t) = 0.9211$, $p_3(t) = -0.4673$ for all $t \geq 0$.

The model representation for (2.18), as proposed in Section 7.2.2, is constructed through the recursive LFT realization of Section 3.6.2. First, we computed an LFR of both matrices $A(p)$ and $B(p)$ in (2.18). Then, we obtained representation (7.4), with

$$A(p) = \mathcal{F}_l\left\{\left(\begin{array}{c|c} F_{11} & F_{13} \\ \hline F_{31} & F_{33} \end{array}\right), \Delta_1(p)\right\}, \; B(p) = \mathcal{F}_l\left\{\left(\begin{array}{c|c} F_{12} & F_{14} \\ \hline F_{42} & F_{44} \end{array}\right), \Delta_2(p)\right\}, \tag{7.53}$$

$$F_{21} = C = (0\ 1\ 0), \; F_{22} = D = 0, \; F_{23} = 0, \; F_{24} = 0. \tag{7.54}$$

The sizes of the blocks in Δ_1 are $r = \{2, 11, 2\}$. Whereas, the blocks of Δ_2 have the dimensions $r = \{0, 3, 0\}$. Therefore, the number of rows in $\Pi(p)$ and $\Pi_b(p)$ of (7.6) are $m = 18$ and $m_b = 4$, respectively. After the proposed minimal generator computation of Section 5.4.1, we obtained $\widehat{\Pi}(p) = \begin{pmatrix} 1 \\ \widehat{\Pi}_1(p) \end{pmatrix} \in \mathbb{R}^{13\times 3}$ and $\widehat{\Pi}_b(p) = \begin{pmatrix} I_3 \\ \widehat{\Pi}_2(p) \end{pmatrix} \in \mathbb{R}^{3\times 1}$. Although the proposed approach (Section 5.4) does not necessarily use symbolical operations, the obtained LFRs of $\widehat{\Pi}_1(p)$ and $\widehat{\Pi}_2(p)$ can be evaluated symbolically as:

$$\widehat{\Pi}_1(p) = \begin{pmatrix} 0 & -p_1p_2\sigma_5 & 0 \\ 0 & -p_1\sigma_5 & 0 \\ 0 & -p_2\sigma_5 & 0 \\ 0 & 0 & p_2^2\sigma_5 \\ 0 & 0 & p_2\sigma_5 \\ -p_2\sigma_5 & 0 & 0 \\ 0 & 0 & -p_2p_3\sigma_5 \\ p_2^2\sigma_5 & 0 & 0 \\ 0 & p_2^2\sigma_5 & 0 \\ 0 & 0 & -p_3\sigma_5 \end{pmatrix}, \; \widehat{\Pi}_2(p) = \begin{pmatrix} -p_2\sigma_5 \\ p_2^2\sigma_5 \end{pmatrix}, \; \sigma_5 = \frac{1}{p_2^2 - 7}. \tag{7.55}$$

Using this model, an upper bound $\gamma = 0.8641$ is computed for system (2.18) as

presented in Corollary 7.2. The maximal level set of the computed storage function $W(x)$ is presented in Figure 7.8. In order to keep the state trajectory (staring from $x(0) = 0$) inside $\Omega_c \subset \mathcal{X}^\circ$, $c = 2.1271$, the required energy bound for the input signal u is $\bar{M}_2 = \sqrt{c\gamma^{-2}} = 1.6879$.

The values of matrices F_{ij}, Δ_1, Δ_2 of (7.4), $\Pi(p)$, $\Pi_\ell(p) \in \mathbb{R}^{46\times 4}$, $\widehat{\Pi}(p)$, $\widehat{\Pi}_\ell(p,\varrho) \in \mathbb{R}^{36\times 4}$, S, S_ℓ, $N(p) \in \mathbb{R}^{14\times 13}$, $N_\ell(p,\varrho) \in \mathbb{R}^{50\times 36}$ from Corollary 7.2, and the final optimal value of $Q(p)$ are available on-line [206].

7.3.4.2 Comparative discussion of the results. First, we considered for comparison the grid-based approach of [73, Theorem 3.3.1] using the rational storage function candidate (7.46) with $\varpi_i(p) \in \Big\{1;\ p_1,\ p_2,\ p_3;\ p_1p_2\sigma_5,\ p_1\sigma_5,\ p_2\sigma_5,\ p_2^2\sigma_5,\ p_2p_3\sigma_5,\ p_3\sigma_5\Big\}$. The nonlinear terms $\varpi_i(p)$, were selected from generator $\widehat{\Pi}_1(p)$ in (7.55). We considered both a coarse ($5\times5\times5$) grid on $\mathcal{P}$ (Line 6 of Table 7.4), and a fine ($15\times15\times15$) grid on $\mathcal{P}$ (Line 5 of Table 7.4) to *approximate* an upper bound γ on the induced $\mathcal{L}_2$-gain.

After computing a relative-minimal LFR of $(A(p)\ B(p))$, a descriptor representation was derived as presented in (4.25). Then, we solved the blPD-LMI of Theorem 4.8 using the cross corner evaluation technique of Corollary 4.11. The obtained guaranteed upper bound is presented in Line 3 of Table 7.4.

For the next comparison, we consider the LPVMAD [112] and the LPVTools [113] implementations of the IQC approach (Corollary 4.16). In the computations we considered LPVMAD's default value for $a(s) = (\frac{1}{s+1})$. Compared to LPVMAD, LPVTools generates algorithmically a set of poles for the basis transfer functions as follows: $a(s) = \Big((s+3.844)^{-1}\ (s+167.37)^{-1}\ (s+7288.15)^{-1}\Big)^\top$. The IQC results are presented in Line 1 and Line 2 of Table 7.4. The frequency grid considered by LPVTools consisted of 144 logarithmically spaced discrete values in $[0.0883, 317360.6]$ rad/s. ▲

In this example, our proposed approach has given a more that 20% lower upper estimate for the induced $\mathcal{L}_2$ norm, than the IQC/LFT approach [103; 104; 107], and a more than 1% lower upper bound than the descriptor-based approach of [125]. The complexity of the proposed computation is comparable to the descriptor-approach [125] and the grid-based approach [73].

7.4 Summary

In this chapter, I proposed a systematic procedure to compute a guaranteed upper bound for the induced $\mathcal{L}_2$-gain of qLPV state-space system models with rational state- and parameter-dependent nonlinearities. The proposed method is based on the ideas of [16; 156]. The storage function was searched in a general quadratic form of a rational state- and parameter-dependent vector generated from the LFR realization of the system equation. To formulate convex PD-LMI conditions for stability I used Finsler's lemma with minimal generators and maximal annihilators (Chapter 5).

By the means of an upper energy bound for the input signal, I give convex boundary conditions to obtain a positively invariant level set of the storage function as a guaranteed domain for local asymptotic stability and induced $\mathcal{L}_2$ norm smaller than or equal to $\gamma > 0$.

The proposed method is compared to other state-of-the-art LPV [103; 104; 112; 113] solutions of the literature through a 4th order 2-input 2-output LPV system. Compared to these solutions in the literature, our method results in a convex optimization problem, that scales better with the model and parameter dimension, while systematically using an efficient parameter-dependent storage function.

Differently from the grid-based approach [73], our method theoretically guarantees the correctness of the obtained upper bound, and the storage function is constructed systematically. Compared to the IQC/LFT approaches [103; 104; 107] where dynamic multipliers are used to involve rate bounds in the optimization, our approach is based on the classical dissipation theory, the LMI constraints are transparent, and the rate bounds are involved through the parameter-dependence in the storage function. Differently from the descriptor-based method [125], our approach computes a storage function, which is rational in the parameters.

10.15774/PPKE.ITK.2021.004

Chapter 8

Passivity of LPV systems

In this chapter, I revisit the kidnapped scientist's problem (Problem 2.1). Our ambition is to design dynamical filters, to reconstruct an unknown input (e.g., fault signal) applied to a dynamical system. Here, I address this problem in the foreground of the passivity theory. We propose a novel LMI method for output selection for rational LPV systems.

8.1 Passivity analysis for LPV systems

In this section, the strict passivity property for LPV systems and its relation to the zero dynamics and stable input reconstruction is discussed. We extend the results of [25; 39] to LPV systems with time-varying parametric uncertainty.

We consider MIMO LPV systems of the form:

$$\Sigma : \begin{cases} \dot{x} = f(x,u,p) = A(p)x + B(p)u, \\ y = h(x,p) = C(p)x. \end{cases} \tag{8.1}$$

where x, u, y, and p are the state, input, output, and the scheduling parameter signals, respectively, with p satisfying Assumption 3.1, furthermore, A, B, and C are well-defined rational functions of p.

Assume that system Σ has as many output signals as input signals ($n_y = n_u$). Then, consider a parameter-dependent quadratic storage function candidate defined as follows:

$$V(x,p) = x^\top \mathbf{Q}(p) x, \tag{8.2}$$

where $\mathbf{Q}$ is continuously differentiable on $\mathcal{P}$ with respect to each parameter variable, and $\mathbf{Q}(p) = \mathbf{Q}^\top(p)$ is positive definite for all $p \in \mathcal{P}$. For V to be a storage function, we can formulate the following sufficient and necessary conditions[1] for strict passivity of Σ.

Theorem 8.1 [P1]**.** *System Σ is strictly passive with the storage function* (8.2) *and for $\alpha(\|x\|) = \alpha_0 \|x\|^2$ with some $\alpha_0 > 0$ if and only if Σ has the Kalman-Yakubovich-Popov (KYP) property, namely:*

$$\mathrm{He}\{\mathbf{Q}(p)A(p)\} + \check{\mathbf{Q}}(p,\varrho) + \alpha_0 I_{n_x} \preceq 0, \qquad \text{for all } (p,\varrho) \in \mathcal{P}\times\mathcal{R}, \tag{8.3a}$$

$$\mathbf{Q}(p)B(p) = C^\top(p), \qquad \text{for all } p \in \mathcal{P}, \tag{8.3b}$$

are satisfied, where $\check{\mathbf{Q}}(p,\varrho) = \sum_{i=1}^{n_p} \frac{\partial \mathbf{Q}}{\partial p_i}(p)\varrho_i$. ◇

Proof. Assume that system Σ is strictly passive with (8.2). Then, (3.17) expands to

$$\mathrm{He}\Big\{x^\top \mathbf{Q}(p)\big(A(p)x + B(p)u\big)\Big\} + x^\top \check{\mathbf{Q}}(p,\varrho)x \le \mathrm{He}\Big\{u^\top C(p)x\Big\} - \alpha(\|x\|). \tag{8.4}$$

[1] based on [39, Proposition 4.1.2, Lemma 4.1.3, Corollary 4.1.5]

Scalar inequality (8.4) can be equivalently formulated as the following matrix inequality

$$\begin{pmatrix} x^\top \Big(\mathrm{He}\{\mathbf{Q}(p)A(p)\} + \check{\mathbf{Q}}(p,\varrho) \Big) x + \alpha_0 \|x\|^2 & x^\top (\mathbf{Q}(p)B(p) - C^\top(p)) \\ (B^\top(p)\mathbf{Q}(p) - C(p))x & 0_{n_u \times n_u} \end{pmatrix} \preceq 0. \tag{8.5}$$

According to [39, proof of Corollary 4.1.5], $(n+1)\times(n+1)$ matrix $\left(\begin{smallmatrix} \alpha & \beta^\top \\ \beta & 0_{n\times n} \end{smallmatrix}\right)$ is negative semidefinite if and only if $\beta = 0_{n\times 1}$ and $\alpha \leq 0$. Therefore, (8.5) is equivalent to

$$x^\top \Big(\mathrm{He}\{\mathbf{Q}(p)A(p)\} + \check{\mathbf{Q}}(p,\varrho) + \alpha_0 I_{n_x} \Big) x \leq 0, \tag{8.6a}$$

$$x^\top \Big(\mathbf{Q}(p)B(p) - C^\top(p) \Big) = 0. \tag{8.6b}$$

Inequalities in (8.4), (8.5), and (8.6) should be satisfied for all $x \in \mathbb{R}^{n_x}$ and for all $(p,\varrho) \in \mathcal{P}\times\mathcal{R}$. Conditions (8.6) are equivalent to (8.3). □

8.1.1 Consequences of passivity for LPV systems

In the following, we analyze a few important consequences of strict passivity, which will be exploited later for stable dynamic inversion.

Lemma 8.2. *Assume that* Σ *is passive with storage function* (8.2) *and* $\mathrm{rank}(B(p)) = n_u$ *for all* $p \in \mathcal{P}$. *Then,* $\mathrm{rank}\, C(p)B(p) = n_u$ *for all* $p \in \mathcal{P}$. ◇

Proof. Suppose that $\mathrm{rank}(C(p_0)B(p_0)) < n_u$ for some p_0. Then, there exists a non-zero vector $v \in \mathbb{R}^{n_u}$ such that $C(p_0)B(p_0)v = 0$. From Theorem 8.1, we have that $C(p_0) = B^\top(p_0)\mathbf{Q}(p_0)$, which implies the following identity:

$$0 = v^\top C(p_0)B(p_0)v = v^\top B^\top(p_0)\mathbf{Q}(p_0)B(p_0)v$$

Since $\mathrm{rank}(B(p_0)) = n_u$ and $\mathbf{Q}(p_0)$ is positive definite symmetric, $v = 0$ follows, which is a contradiction. □

***Remark* 8.1.** We say that system Σ has (vector) relative degree 1, if $C(p)B(p)$ is invertible for all $p \in \mathcal{P}$. A more general definition for the vector relative degree is present by Isidori [27, Section 5.1]. ◇

8.1.1.1 Normal form. With reference to [25, Section 4], the non-singularity of $C(p)B(p)$ implies the existence of a well-defined mapping $z = T_2(p)x \in \mathbb{R}^{n_x - n_u}$, which together with $y = C(p)x$ qualify as a new set of local coordinates for Σ. The state variables of Σ in the new coordinates system are:

$$\left(\begin{smallmatrix} y \\ z \end{smallmatrix}\right) = T(p)x, \text{ with } T(p) = \left(\begin{smallmatrix} C(p) \\ T_2(p) \end{smallmatrix}\right) \in \mathbb{R}^{n_x \times n_x}. \tag{8.7}$$

The dynamic equation of Σ in the new coordinates has a special *normal form* [30, Eq. (9.17), Section 9.2]:

$$\Sigma_{y,z} : \begin{cases} \dot{y} = A_{yy}(p,\dot{p})\, y + A_{yz}(p,\dot{p})\, z + B_y(p)u, \\ \dot{z} = A_{zy}(p,\dot{p})\, y + A_{zz}(p,\dot{p})\, z, \end{cases} \tag{8.8}$$

$$\text{where } \left(\begin{smallmatrix} A_{yy}(p,\varrho) & A_{yz}(p,\varrho) \\ A_{zy}(p,\varrho) & A_{zz}(p,\varrho) \end{smallmatrix}\right) = (\check{T}(p,\varrho) + T(p)A(p))T^{-1}(p), \tag{8.8a}$$

$$\text{and } B_y(p) = C(p)B(p),\ \check{T}(p,\varrho) = \textstyle\sum_{i=1}^{n_p} \frac{\partial T}{\partial p_i}(p)\, \varrho_i. \tag{8.8b}$$

Note that the transformed state transition matrix in (8.8a) is partitioned correspondingly to the transformed state variables in y and in z as follows:

$$\begin{aligned} A_{yy} &= (\check{C} + CA)T_1', \quad & A_{yz} &= (\check{C} + CA)T_2', \\ A_{zy} &= (\check{T}_2 + T_2A)T_1', \quad & A_{zz} &= (\check{T}_2 + T_2A)T_2', \end{aligned} \tag{8.9}$$

where $\check{C}(p,\varrho) = \sum_{i=1}^{n_p} \frac{\partial C}{\partial p_i}(p)\, \varrho_i$, $\check{T}_2(p,\varrho) = \sum_{i=1}^{n_p} \frac{\partial T_2}{\partial p_i}(p)\, \varrho_i$, and $T^{-1}(p) = \Big(T_1'(p)\ T_2'(p) \Big)$. ▲

For a rational parameter dependence in the system equations, a possible numeric construction of the transformation matrix $T(p)$ is given in the following Lemma 8.3.

Lemma 8.3. *Assume that system Σ is strictly passive, and functions A, B, C are rational well-defined functions on $\mathcal{P}$. Then, there exists an invertible state transformation* (8.7)*, such that the system equation in the new coordinates has the normal form* (8.8). $\diamond$

Proof. By assumption, $B_y(p) = C(p)B(p)$ is non-singular, therefore, both matrices $C(p)$ and $B(p)$ are full-rank matrices for all $p \in \mathcal{P}$. Due to the fact that $B(p)$ is well-defined on the compact set $\mathcal{P}$ (in a well-posed LFR form), there exists a well-defined matrix $T_2(p)$ in a well-posed LFR form [207] with $\operatorname{rank}(T_2(p)) = n_x - n_u$ and with a bounded norm for all $p \in \mathcal{P}$, such that $T_2(p)B(p) = 0$, namely, $T_2^\top(p)$ is a basis for the kernel space $\operatorname{Ker}(B^\top(p))$ of $B^\top(p)$. The non-singularity of matrix $C(p)B(p)$ implies that the rows of $C(p)$ are are not in $\operatorname{Ker}(B^\top(p))$, additionally, $C(p) \in \mathbb{R}^{n_u \times n_x}$ contains linearly independent rows. Therefore, the square matrix $T(p) = \left(\begin{smallmatrix} C(p) \\ T_2(p) \end{smallmatrix}\right)$ is invertible $\forall p \in \mathcal{P}$. If we apply the state transformation $\left(\begin{smallmatrix} y \\ z \end{smallmatrix}\right) = T(p)x$ to Σ, we obtain the transformed and partitioned dynamics $\Sigma_{y,z}$. $\square$

8.1.1.2 Output zeroing input. In this normal form, the invertibility of $B_y(p)$ makes also possible to compute the *output-zeroing input* u^* for system $\Sigma_{y,z}$, which can force the output y to be identically zero for $y(0) = 0$, any $z(0) \in \mathbb{R}^{n_x - n_y}$, and any parameter trajectory satisfying Assumption 3.1. If we enforce $\dot{y} \equiv 0$, we can express u^* algebraically from the first equation of (8.8) as follows:

$$u^* = -B_y^{-1}(p)\Big(A_{yy}(p,\dot{p})y + A_{yz}(p,\dot{p})z\Big) = -B_y^{-1}(p)\Big(A_{yy}(p,\dot{p}) \;\; A_{yz}(p,\dot{p})\Big)\left(\begin{smallmatrix} y \\ z \end{smallmatrix}\right). \quad (8.10)$$

Considering $y(0) = 0$ and $\dot{y} \equiv 0$ (i.e., $y \equiv 0$), the output zeroing input in the transformed state-space is the following:

$$u^* = -B_y^{-1}(p)A_{yz}(p,\dot{p})z. \quad (8.11)$$

Note that in the original system of coordinates, the closed form for u^* can be derived from the time-derivative of the output equation $y = C(p)x$ of system Σ:

$$\dot{y} = \check{C}(p,\dot{p})x + C(p)\Big(A(p)x + B(p)u^*\Big) \equiv 0, \quad (8.12)$$

Then, the output zeroing input in the terms of the original state vector x is

$$u^* = -\Big(C(p)B(p)\Big)^{-1}\Big(\check{C}(p,\dot{p}) + C(p)A(p)\Big)T^{-1}(p)\left(\begin{smallmatrix} y \\ z \end{smallmatrix}\right). \quad (8.13)$$

Considering (8.10) in the light of (8.8a), (8.8b), and (8.9), we can conclude that the two closed form for u^* are equivalent. ▲

8.1.1.3 Zero dynamics. The so-called *zero dynamics* of system Σ describes the internal behaviour of Σ, when the output zeroing input u^* is applied to it. The *zero dynamics* of system Σ in the new coordinates are characterized by

$$\dot{z} = A_{zz}(p,\dot{p})z. \quad (8.14)$$

In the original system of coordinates the zero dynamics can be described by the closed-loop system driven by the output zeroing input (8.13) as follows:

$$\Sigma_0 : \dot{x} = A(p)x + B(p)u^* = \Big(A(p) - \big(C(p)B(p)\big)^{-1}\Big(\check{C}(p,\dot{p}) + C(p)A(p)\Big)\Big)x, \quad (8.15)$$

with $x(0) \in \operatorname{Ker}\{C(p(0))\}$. ▲

The strong relation between the passivity property and the zero dynamics first was addressed in [25] for nonlinear *time-invariant* systems, and it was generalized to a class of (time-varying) uncertain nonlinear systems in [26]. In the following theorem, we adapt these results for rational LPV systems.

Theorem 8.4. *Assume that p is continuously differentiable and system Σ is strictly passive with a proper positive definite storage function* (5.9)*. Then, the zero dynamics* (8.14) *is asymptotically stable.* ◇

Proof. We follow the derivations of [39, Section 5.1]. Assume that $x(0) \in \mathrm{Ker}\{C(p(0))\}$ and the dissipation inequality $\dot{V} \leq y^\top u + u^\top y - \alpha(\|x\|)$ (3.17) holds. Apply the output zeroing input u^* (8.13) to system Σ. Then, $y \equiv 0$ implies $\dot{V} < -\alpha(\|x\|)$ along the solution $x : t \mapsto x(t) \in \mathrm{Ker}(C(p(t)))$ of the closed-loop dynamics Σ_0 (8.15). Due to the quadratic form (5.9) of the PDSF, $\dot{V} < -\alpha(\|x\|)$ implies the asymptotic stability of (8.15).

As it is shown in Lemma 8.3, mapping $z = T_2(p)x$ can be chosen such that the parameter-dependent (non-singular) transformation matrix $T(p)$ is a well-defined rational function of p, and hence it is also continuously differentiable in p_i [94, Section 7.1.14] and $\check{T}(p, \varrho)$ has a bounded norm for all $p \in \mathcal{P}$ and all $\varrho \in \mathcal{R}$. If p is continuously differentiable, function T in (8.7) is a time-varying Lyapunov transformation in the sense of Definition 3.11, and T preserves the internal stability of system $\Sigma_{y,z}$.

Finally, the asymptotic stability of (8.15) implies the asymptotic stability of the zero dynamics (8.14). □

8.1.1.4 Unknown input reconstruction. A stable zero dynamics (Theorem 8.4) implies the existence of a stable dynamic inversion filter. Additionally, passivity provides the invertibility of matrix $C(p)B(p)$ as stated by Lemma 8.2. Therefore, the unknown input applied to a strictly passive LPV system can be reconstructed asymptotically in the knowledge of the output y and the parameter signals p and their derivatives $(\dot{y}, \dot{p})$. The equations of the dynamic inverse are the following

$$\Sigma_{y,z}^{-1} : \begin{cases} \dot{\hat{z}} = A_{zz}(p, \dot{p})\hat{z} + A_{zy}(p, \dot{p})y, & \text{where } \hat{z}(0) = 0, \\ \hat{u} = B_y^{-1}(p)(\dot{y} - A_{yy}(p, \dot{p})y - A_{yz}(p, \dot{p})\hat{z}). \end{cases} \tag{8.16}$$

Observe that the input is algebraically expressed from the first equation of (8.8), where signal z is hidden (i.e., it represents the unobservable modes of system Σ). Therefore, we simulate the zero dynamics driven by the output y and starting from the initial state $z(0) = 0$. ▲

***Remark* 8.2.** If it is reasonable to assume that $y(0) = 0$, a dynamic inversion filter can be design without the knowledge of the state transformation matrix $T(p)$. The equations of the dynamic inverse in the original system of coordinates are:

$$\Sigma^{-1} : \begin{cases} \dot{\hat{x}} = \Big(A(p) - (C(p)B(p))^{-1}\Big(\check{C}(p, \dot{p}) + C(p)A(p)\Big)\Big)\hat{x} + (C(p)B(p))^{-1}\dot{y}, \\ \hat{u} = (C(p)B(p))^{-1}\Big(\dot{y} - \Big(\check{C}(p, \dot{p}) + C(p)A(p)\Big)\hat{x}\Big), \end{cases} \tag{8.17}$$

where $\hat{x}(0) = 0$. ◇

8.1.2 Feedback equivalence to a passive LPV system

Generally, we can say that (strict) passivity is a conservative property as it requires internal stability and a special input-output relationship, which are abstracted by the KYP properties (8.3). According to Byrnes et al. [25], a weaker property, the *feedback (strict) passivity* of Σ is a sufficient condition for an asymptotically stable zero dynamics.

Definition 8.5. *We say that Σ with $n_u = n_y$ is feedback (strictly) passive with a storage function $V = x^\top \mathbf{Q}\, x$* (8.2) *if Σ is feedback equivalent to a (strictly) passive system, namely, there exists a state feedback $u = -\mathbf{K}(p)x + \mathbf{G}(p)v$ with well-defined functions $\mathbf{K} : \mathcal{P} \to \mathbb{R}^{n_u \times n_x}$, $\mathbf{G} : \mathcal{P} \to \mathbb{R}^{n_u \times n_u}$ and $G(p)$ non-singular, such that the closed-loop*

system

$$\Sigma_{K,G}: \begin{cases} \dot{x} = (A(p) - B(p)\mathbf{K}(p))x + B(p)\mathbf{G}(p)v \\ y = C(p)x \end{cases} \tag{8.18}$$

is strictly passive from input v to output y with a storage function (8.2). ◇

***Remark* 8.3.** According to Theorem 8.1, system $\Sigma_{K,G}$ is strictly passive with a storage function (8.2) if it has the KYP property, namely,

$$\mathrm{He}\{\mathbf{Q}(p)(A(p) - B(p)\mathbf{K}(p))\} + \check{\mathbf{Q}}(p,\varrho) + \alpha_0 I \preceq 0 \quad \text{for all } (p,\varrho) \in \mathcal{P}\times\mathcal{R}, \tag{8.19a}$$

$$\mathbf{Q}(p)B(p)\mathbf{G}(p) = C^\top(p) \quad \text{for all } p \in \mathcal{P}, \tag{8.19b}$$

where $\alpha_0 > 0$. ◇

In the following two theorem, we show an important relationship between feedback passivity, stable zero dynamics, and relative degree 1. In Theorem 8.6, we adapt the results of [25, Theorem 4.7] and [26, Theorem 1] to LPV models.

Theorem 8.6. *Assume that Σ has a same number of input and output signals ($n_u = n_y$), and it is feedback strictly passive. Then, the zero dynamics of Σ is asymptotically stable, and $C(p)B(p)$ is non-singular for all $p \in \mathcal{P}$.* ◇

Proof. Assume that the closed-loop system $\Sigma_{K,G}$ is passive and x is the solution of $\Sigma_{K,G}$ with output zeroing input v^*, a parameter trajectory satisfying Assumption 3.1, and $x(0) \in \mathrm{Ker}\{C(p(0))\}$. Obviously, the same trajectory x is the solution of the open-loop system Σ with output zeroing input $u^* = -\mathbf{K}(p)x + \mathbf{G}(p)v^*$, the same parameter trajectory, and the same initial condition $x(0) \in \mathrm{Ker}\{C(p(0))\}$.

(Zero dynamics) Assume that Σ is feedback equivalent to a passive system with storage function V. Then, $y \equiv 0$ implies $\dot{V} \le 0$ along the solutions of the closed-loop system $\Sigma_{K,G}$. Let (x,p,u^*) denote the solution of the zero dynamics Σ_0 (8.15) with output zeroing input u^* in (8.10) and parameter trajectory p. Then, (x,p,v^*) is the solution of system $\Sigma_{K,G}$ with the output zeroing input $v^* = \mathbf{G}^{-1}(p)(u^* + \mathbf{K}(p)x)$. Therefore, $\dot{V} \le 0$ along the solution x of Σ_0 with p.

(Relative degree) Assume that Σ is feedback equivalent to a passive system. Then, according to Lemma 8.2, $C(p)B(p)\mathbf{G}(p)$ has rank n_u. Since $\mathbf{G}(p)$ is a full-rank matrix, we obtain that $C(p)B(p)$ has rank n_u. □

In the following theorem, we present an interesting sufficient condition for feedback equivalence to a strictly passive LPV system. Theorem (8.7) first was formulated by Moreno [60] for linear time-invariant systems. Here, we extend and prove the result of Moreno for general (well-posed) LPV systems.

Theorem 8.7. *Consider system Σ with $n_u = n_y$. Assume that there exist functions $\mathbf{Q}: \mathcal{P} \to \mathbb{R}^{n_x \times n_x}$, $\mathbf{K}: \mathcal{P} \to \mathbb{R}^{n_u \times n_x}$, such that $\mathbf{Q}(p)$ is symmetric positive definite for all $p \in \mathcal{P}$ and system Σ satisfies the following criteria*

$$\begin{aligned} &\mathrm{He}\Big\{\mathbf{Q}(p)A(p) - \mathbf{K}^\top(p)C(p)\Big\} + \check{\mathbf{Q}}(p,\varrho) + \alpha_0 I_{n_x} \preceq 0, \quad \textit{for all } (p,\varrho) \in \mathcal{P}\times\mathcal{R}, \\ &\mathbf{Q}(p)B(p) = C^\top(p), \qquad\qquad \textit{for all } p \in \mathcal{P}. \end{aligned} \tag{8.20}$$

Then, Σ is feedback equivalent to a strictly passive LPV system with $u = \mathbf{K}(p)x + v$. ◇

Proof. Let us rewrite the KYP conditions (8.20) into a single matrix inequality as follows:

$$\mathrm{He}\left\{\begin{pmatrix} I & \mathbf{K}^\top(p) \\ 0 & I \end{pmatrix}\begin{pmatrix} \mathbf{Q}(p) & 0 \\ 0 & I \end{pmatrix}\begin{pmatrix} A(p) & B(p) \\ -C(p) & 0 \end{pmatrix}\right\} + \begin{pmatrix} \check{\mathbf{Q}}(p,\dot{p}) + \alpha_0 I & 0 \\ 0 & 0 \end{pmatrix} \preceq 0. \tag{8.21}$$

Then, multiply (8.21) by $\left(\begin{smallmatrix} I & -\mathbf{K}^\top(p) \\ 0 & I \end{smallmatrix}\right)$ from the left and by $\left(\begin{smallmatrix} I & 0 \\ -\mathbf{K}(p) & I \end{smallmatrix}\right)$ from the right:

$$\mathrm{He}\left\{\begin{pmatrix} \mathbf{Q}(p) & 0 \\ 0 & I \end{pmatrix}\begin{pmatrix} A(p)-B(p)\mathbf{K}(p) & B(p) \\ -C(p) & 0 \end{pmatrix}\right\} + \begin{pmatrix} \check{\mathbf{Q}}(p,\dot{p})+\alpha_0 I & 0 \\ 0 & 0 \end{pmatrix} \preceq 0. \tag{8.22}$$

Evaluating (8.22), we obtain

$$\begin{pmatrix} \mathrm{He}\{\mathbf{Q}(p)(A(p)-B(p)\mathbf{K}(p))\}+\check{\mathbf{Q}}(p,\dot{p})+\alpha_0 I & \mathbf{Q}(p)B(p)-C^\top(p) \\ B^\top(p)\mathbf{Q}(p)-C(p) & 0 \end{pmatrix} \preceq 0. \tag{8.23}$$

Condition (8.22) is equivalent to the KYP criteria (8.19) for $\Sigma_{K,G}$ with $\mathbf{G} \equiv I_{n_u}$. Finally, we got that system Σ is feedback equivalent to

$$\Sigma_{K,I} : \begin{cases} \dot{x} = \big(A(p)-B(p)\mathbf{K}(p)\big)x + B(p)v \\ y = C(p)x \end{cases} \tag{8.24}$$

that is strictly passive system with $V(x,p) = x^\top \mathbf{Q}(p)\, x$. □

***Remark* 8.4.** The parameter-dependent conditions in (8.20) are convenient as they are linear in the unknown functions $\mathbf{Q}$ and $\mathbf{K}$. On the other hand, the assumption that $\mathbf{G} \equiv I_{n_u}$ makes these conditions conservative. In section 8.3, we present an equivalent condition for feedback passivity. ◇

8.2 Passivating structured output selection

In this section, we consider an asymptotically stable LPV system. We assume that we are able to place sensors assembling more independent measurements (y) than the number of the emerging fault signals (u), namely, $n_y > n_u$. Naturally, in this situation, we have more information to reconstruct the unknown input from the measurements. Here, we propose a specific parameter-dependent output projection transformation that provides strict passivity (and hence stable dynamic inversion) for system Σ.

We are looking for a parameter-dependent quadratic storage function $V = x^\top \mathbf{Q}\, x$ (7.18) and a parameter-dependent output mapping $\mathbf{G} : \mathcal{P} \to \mathbb{R}^{n_y \times n_u}$, such that Σ with the combined output

$$\bar{y} = \mathbf{G}^\top(p) y = \mathbf{G}^\top(p) C(p) x, \tag{8.25}$$

is strictly passive with respect to V.

***Remark* 8.5.** Notation for function $\mathbf{G}$ was already used in Section 8.1.2, to nominate a parameter-dependent feed-forward gain $\mathbf{G}(p)$ in the feedback rule $u = -\mathbf{K}(p)x + \mathbf{G}(p)v$. Later, in Section 8.3, it will turn out that the role of the parameter-dependent output mapping $\mathbf{G}(p)$ is similar to that of the feed-forward gain $\mathbf{G}(p)$. This abuse of notation is consider for the sake of reusability. ◇

The second KYP condition (8.3b) for system Σ with output $\bar{y}$ is the following:

$$\mathbf{Q}(p)B(p) = C^\top(p)\mathbf{G}(p) \text{ for all } p \in \mathcal{P}. \tag{8.26}$$

Note that (8.26) is a matrix equality condition with nonlinear (rational) parameter dependence, where $\mathbf{G}$ and $\mathbf{Q}$ are unknown functions. Therefore, the algebraic structure of $\mathbf{G}$ and $\mathbf{Q}$ should be defined carefully, such that the same set of rational terms appear on both sides of equality (8.26). The rational terms of function B should be contained by function $\mathbf{G}$. Similarly, function $\mathbf{Q}$ should inherit the rational terms of function C.

In the following subsection, we give a possible LFR realization for the system equation, which will generate an advantageous structure for $\mathbf{Q}$ and $\mathbf{G}$.

8.2.0.1 Dynamical model representation. We consider a well-posed LFR realization

of the model matrices of Σ as follows:

$$\begin{pmatrix} A(p) \\ C(p) \end{pmatrix} = \mathcal{F}_l\left\{ \left(\begin{array}{c|c} F_{11} & F_{13} \\ F_{21} & F_{23} \\ \hline F_{31} & F_{33} \end{array}\right), \Delta_1(p) \right\},\ B(p) = \mathcal{F}_l\left\{ \left(\begin{array}{c|c} F_{12} & F_{14} \\ \hline F_{42} & F_{44} \end{array}\right), \Delta_2(p) \right\}. \tag{8.27}$$

The equations of Σ can be written in the following structured LFR:

$$\mathcal{F}(\Sigma):\ \begin{pmatrix} \dot{x} \\ y \\ \hline \eta_1 \\ \eta_2 \end{pmatrix} = \underbrace{\left(\begin{array}{cc|cc} F_{11} & F_{12} & F_{13} & F_{14} \\ F_{21} & 0 & F_{23} & 0 \\ \hline F_{31} & 0 & F_{33} & 0 \\ 0 & F_{42} & 0 & F_{44} \end{array}\right)}_{F_{::}} \begin{pmatrix} x \\ u \\ \hline \pi_1 \\ \pi_2 \end{pmatrix}, \qquad \begin{array}{c} \text{with } \pi_1 = \Delta_1\eta_1, \\ \text{and } \pi_2 = \Delta_2\eta_2, \end{array} \tag{8.28}$$

where F_{ij} are constant matrices and $\pi_1, \eta_1 \in \mathbb{R}^{m_1}$, respectively $\pi_2, \eta_2 \in \mathbb{R}^{m_2}$ are the feedback signals through the parameter-dependent blocks Δ_1 and Δ_2 corresponding to the two LFRs in (8.27).

Observe that representation (8.28) is a special case of (7.4) written for LPV systems without a direct feedthrough term ($D \equiv 0$). Due to the same dynamical input-output model representation, a few variables will be reused from Chapter 7. Compared to (7.6), generators

$$\Pi = \left(\begin{smallmatrix} I_{n_x} \\ \Pi_1 \end{smallmatrix}\right) : \mathcal{P} \to \mathbb{R}^{m \times n_x},\ \Pi_b = \left(\begin{smallmatrix} I_{n_u} \\ \Pi_2 \end{smallmatrix}\right) : \mathcal{P} \to \mathbb{R}^{m_b \times n_u}, \tag{8.29}$$

as well as, Π_1, Π_2 are functions of the parameter p only. ▲

To formulate sufficient convex conditions for strict passivity, we need again to find an appropriate factorization for the nonlinear KYP properties. The KYP inequality conditions (8.3a) is rewritten as presented in Proposition 6.4. However, the KYP *equality* condition (8.26) requires a special attention. To factorize (8.26), we need to presume a particular algebraic structure for mapping $\mathbf{G}$. In the following proposition, we propose a possible reformulation for the KYP properties.

Proposition 8.8. *Let Σ be given in representation* (8.28) *with a quadratic storage function $V = x^\top \mathbf{Q}\, x$* (7.18)*, and a parameter-dependent output mapping $\bar{y} = \mathbf{G}^\top(p) y$* (8.25)*. Consider generators Π_d, Π_e, which are defined in* (7.17)*. Let $\mathbf{G}$ be given in the following form:*

$$\mathbf{G}(p) = G(p)\Pi_e(p) \text{ with } G(p) = G_0 + \sum_{i=0}^{n_p} G_i p_i \in \mathbb{R}^{n_y \times m_e}, \tag{8.30}$$

where $G_0, \dots, G_{n_p}$ are constant matrices. Then, the KYP properties (8.3a) *and* (8.26) *can be written in the following factorized form:*

$$\mathrm{He}\{\mathbf{Q}(p)A(p)\} + \check{\mathbf{Q}}(p,\varrho) = \Pi_d^\top(p,\varrho)\, Q_d(p,\varrho)\, \Pi_d(p,\varrho) \preceq -\alpha_0 I_{n_x}, \tag{8.31a}$$

$$\mathbf{Q}(p)B(p) - C^\top(p)\mathbf{G}(p) = \Pi^\top(p)\left(Q(p)B_e - C_a^\top G(p)\right)\Pi_e(p) = 0, \tag{8.31b}$$

where

$$Q_d(p,\varrho) = \mathrm{He}\Big\{E_d^\top Q(p) A_d\Big\} + E_d^\top \check{Q}(\varrho) E_d \text{ with } \check{Q}(\varrho) = \textstyle\sum_{i=1}^{n_p} Q_i\, \varrho_i, \tag{8.32}$$

and $C_a = (F_{21}\ F_{23})$. Matrices A_d, B_e, E_d are defined in (7.9c)-(7.9e). ◇

Proof. (KYP inequality property) Following the proof of Proposition 7.1, the left hand side of (8.31a) can be written as follows:

$$\mathrm{He}\Big\{\Pi^\top(p)Q(p)\Pi(p)(F_{11}\ F_{13})\Pi(p)\Big\} + \mathrm{He}\Big\{\Pi^\top(p)Q(p)\check{\Pi}(p,\varrho)\Big\} + \Pi^\top(p)\check{Q}(\varrho)\Pi(p). \tag{8.33}$$

Observe that $\Pi(p) = E_d\Pi_d(p,\varrho)$, furthermore, similarly to (7.11a), we have that

$$\Pi(p)\,(F_{11}\ F_{13})\,\Pi(p) = \left(\begin{smallmatrix} F_{11}+F_{13}\,\Pi_1(p) \\ \Pi_1(p)\,(F_{11}+F_{13}\,\Pi(p))+\check{\Pi}_1(p,\varrho) \end{smallmatrix}\right) = A_d\,\Pi_d(p,\varrho) \tag{8.34}$$

$$\text{where } \check{\Pi}(p,\varrho) = \sum_{i=1}^{n_p} \frac{\partial \Pi}{\partial p_i}(p)\varrho_i,\ \check{\Pi}_1(p,\varrho) = \sum_{i=1}^{n_p} \frac{\partial \Pi_1}{\partial p_i}(p)\varrho_i. \tag{8.34a}$$

Finally, (8.33) can be written in the form:

$$\Pi_d^\top(p,\varrho)\left(\mathrm{He}\{E_d\,Q(p)\,A_d\} + E_d^\top\,\check{Q}(\varrho)\right)\Pi_d(p,\varrho). \tag{8.35}$$

(KYP equality property) First, we expand the left hand side of (8.31b) as follows:

$$\Pi^\top(p)\,Q(p)\,\Pi(p)\,(F_{12}\ F_{14})\,\Pi_b(p) - \Pi^\top(p)\,(F_{11}\ F_{13})^\top\,G(p)\,\Pi_e(p). \tag{8.36}$$

As observed in (7.11b), we write the following:

$$\Pi(p)\,(F_{12}\ F_{14})\,\Pi_b(p) = \begin{pmatrix} F_{12}+F_{14}\,\Pi_2(p) \\ \Pi_1(p)\,(F_{12}+F_{14}\,\Pi_2(p)) \end{pmatrix} = B_e\,\Pi_e(p). \tag{8.37}$$

Finally, (8.36) can be altered as presented in (8.31b). □

In the following corollary, we present one of the major contributions of this chapter, namely, we give sufficient convex conditions that imply the KYP properties for strict passivity of system Σ with output (8.25).

Corollary 8.9 (SDP for passivating structured output selection)**.** *Consider LPV system* (8.1) *with a quadratic storage function* $V = x^\top \mathbf{Q}\,x$ (7.18)*, and the minimal generator* $\Pi : \mathcal{P} \to \mathbb{R}^{m\times n_x}$*. Compute*

1. *full column-rank matrix* $S_d \in \mathbb{R}^{m_d\times m_d'}$ *and minimal generator* $\widehat{\Pi}_d : \mathcal{P}\times\mathcal{R} \to \mathbb{R}^{m_d'\times n_x}$*, such that* $\Pi_d = S_d\widehat{\Pi}_d$*,*
2. *full column-rank matrix* $S_e \in \mathbb{R}^{m_e\times m_e'}$ *and minimal generator* $\widehat{\Pi}_e : \mathcal{P}\times\mathcal{R} \to \mathbb{R}^{m_e'\times n_u}$*, such that* $\Pi_e = S_e\widehat{\Pi}_e$*,*
3. *affine functions* $N : \mathcal{P} \to \mathbb{R}^{s\times m}$*,* $N_d : \mathcal{P}\times\mathcal{R} \to \mathbb{R}^{s_d\times m_d'}$*, and* $N_e : \mathcal{P} \to \mathbb{R}^{s_e\times m_e'}$*, such that* $N\Pi \equiv 0$*,* $N_d\widehat{\Pi}_d \equiv 0$*, and* $N_e\widehat{\Pi}_e \equiv 0$*.*

Then, system (8.28) *is strictly passive from input* u *to output* $\bar{y}$ (8.25) *if there exist* $L \in \mathbb{R}^{m\times s}$*,* $L_d \in \mathbb{R}^{m_d'\times s_d}$*,* $L_a \in \mathbb{R}^{m_e'\times s}$*, and* $L_e \in \mathbb{R}^{m\times s_e}$*, such that*

$$Q(p) + \mathrm{He}\{LN(p)\} - \underline{\alpha}_0 I_a \succeq 0, \qquad \text{for all } p \in \mathbf{Ve}(\mathcal{P}), \tag{8.38a}$$

$$S_d^\top\,(Q_d(p,\varrho) + \alpha_0 I_d)\,S_d + \mathrm{He}\{L_d N_d(p,\varrho)\} \preceq 0, \qquad \text{for all } (p,\varrho) \in \mathbf{Ve}(\mathcal{P}\times\mathcal{R}), \tag{8.38b}$$

$$\big(Q(p)B_e - C_a^\top G(p)\big)\,S_e + N^\top(p)L_a^\top + L_e N_e(p) = 0, \qquad \text{for all } p \in \mathbf{Ve}(\mathcal{P}), \tag{8.38c}$$

for some $\alpha_0, \underline{\alpha}_0 > 0$*, and* $I_a = \mathrm{diag}\,\{I_{n_x}, 0_{m_1}\}$*,* $I_d = \mathrm{diag}\,\{I_{n_x}, 0_{4m_1}\}$*.*

Symmetric matrices $Q_0, \ldots, Q_{n_p}$*, and full matrices* $G_0, \ldots, G_{n_p}$*,* L*,* L_d*,* L_a*, and* L_e *are free decision variables of the semidefinite program.* ◇

Proof. (Geometry of V*)* Obviously, (8.38a) implies that $\mathbf{Q}(p) = \Pi^\top p\,Q(p)\,\Pi(p)$ is positive definite for all $p \in \mathcal{P}$, and that $V(x,p) = x^\top\,\mathbf{Q}(p)\,x$ is positive and radially unbounded for all $p \in \mathcal{P}$.

(KYP inequality property) Pre- and post-multiplying (8.38b) by $\Pi_d^\top(p,\varrho)$ and $\Pi_d(p,\varrho)$, respectively, the Lagrange multiplier terms $\mathrm{He}\{L_d N_d(p,\varrho)\}$ vanish. Therefore, we retain the KYP inequality (8.31a).

(KYP equality property) In the same fashion, we pre- and post-multiply (8.38c) by $\Pi^\top(p)$ and $\Pi_e(p)$, respectively, then, we get back the KYP equality (8.31b). □

The computed passivating output projection $\bar{y} = \mathbf{G}(p)y$ provides a stable zero dynamics and an invertible $C(p)B(p)$ for system (8.28).

***Remark* 8.6.** In order to solve the nonlinear PD-LME $\mathbf{Q}B - C^\top\mathbf{G} \equiv 0$ (8.26), the equality conditions between the coefficients of the identical rational terms in each element

of the matrix identity have to be extracted, which requires computationally demanding symbolic operations. However, the computationally more tractable affine PD-LME $QB_e - C_a^\top G \equiv 0$ is only a sufficient condition for (8.26). In order to make it less conservative, we use again affine annihilators, which introduce new degrees of freedom into $QB_e - C_a^\top G + N^\top L_a^\top + L_e N_e \equiv 0$ (8.38c). ⋄

8.3 Stability analysis for the zero dynamics

In this section, we consider a (possibly unstable) *square* system Σ ($n_u = n_y$) and formulate sufficient convex conditions to test whether the zero dynamics are globally asymptotically stable. These conditions are rendered through the KYP properties formulated for the closed-loop system to test feedback equivalence to a strictly passive LPV system. For the sake of reusability, we intentionally redefine a few notations.

We are looking for a state feedback law

$$u = -\mathbf{K}(p)x + \mathbf{G}(p)v \tag{8.39}$$

with well-defined rational functions $\mathbf{K} : \mathcal{P} \to \mathbb{R}^{n_u \times n_x}$ and $\mathbf{G} : \mathcal{P} \to \mathbb{R}^{n_u \times n_u}$, such that $\det(\mathbf{G}(p)) \neq 0$ and the closed-loop system $\Sigma_{K,G}$ in (8.18) is strictly passive with a quadratic storage function $V : \mathbb{R}^{n_x} \times \mathcal{P} \to \mathbb{R}$,

$$V(x,p) = x^\top \mathbf{P}(p)\, x, \tag{8.40}$$

$$\text{where } \mathbf{P}^{-1}(p) = \mathbf{Q}(p) = \Pi^\top(p)\, Q(p)\, \Pi(p), \tag{8.40a}$$

$$\text{and } Q(p) = Q_0 + \textstyle\sum_{i=1}^{n_p} Q_i\, p_i \in \mathbb{R}^{m \times m}. \tag{8.40b}$$

For generator Π in (8.40a), a possible formula will be given soon.

According to Theorem 8.1, the KYP properties for the strict passivity of Σ with feedback (8.39) and storage function (8.40) are the following:

$$\operatorname{He}\{\mathbf{P}(p)(A(p) - B(p)\mathbf{K}(p))\} + \check{\mathbf{P}}(p,\varrho) + \alpha_0 I_{n_x} \preceq 0, \quad \text{for all } (p,\varrho) \in \mathcal{P} \times \mathcal{R}, \tag{8.41a}$$

$$\mathbf{P}(p)B(p)\mathbf{G}(p) = C^\top(p), \quad \text{for all } p \in \mathcal{P}, \tag{8.41b}$$

where, as previously, $\check{\mathbf{P}}(p,\varrho) = \sum_{i=1}^{n_p} \frac{\partial \mathbf{P}}{\partial p_i}(p)\varrho_i$. Observe that the matrix-valued constraints in (8.41) are not linear in the unknown functions functions $\mathbf{P}$, $\mathbf{K}$, and $\mathbf{G}$. In order to make condition (8.41a) convex, we multiply both sides of (8.41a) and the left hand side of (8.41b) by the positive definite symmetric matrix $\mathbf{Q}(p)$. We note that this technique is commonly used in the literature (see, e.g., [62; 63]). Keeping in mind that $\frac{\mathrm{d}(\mathbf{PQ})}{\mathrm{d}t} = \mathbf{P}\dot{\mathbf{Q}} + \dot{\mathbf{P}}\mathbf{Q} \equiv 0$, we obtain the following constraints:

$$\operatorname{He}\{A(p)\mathbf{Q}(p) - B(p)\mathbf{H}(p))\} - \check{\mathbf{Q}}(p,\varrho) + \alpha_0 I_{n_x} \preceq 0, \quad \text{for all } (p,\varrho) \in \mathcal{P} \times \mathcal{R}, \tag{8.42a}$$

$$B(p)\mathbf{G}(p) = \mathbf{Q}(p)C^\top(p), \quad \text{for all } p \in \mathcal{P}, \tag{8.42b}$$

where $\mathbf{H}(p) = \mathbf{K}(p)\mathbf{Q}(p)$ for all $p \in \mathcal{P}$. Also observe that the first term in (8.42) can be altered as follows:

$$\operatorname{He}\{A(p)\mathbf{Q}(p) - B(p)\mathbf{H}(p))\} = \operatorname{He}\Big\{\mathbf{Q}(p)A^\top(p) - B(p)\mathbf{H}(p))\Big\}. \tag{8.43}$$

Finally, we obtain an equivalent formulation of the KYP constraints, which are advantageous for the polytopic convexification. The final "pseudo-dual" formalization of the KYP properties for the strict passivity of the closed-loop system $\Sigma_{K,G}$ is given in the following proposition.

Proposition 8.10. *Assume that there exist functions* $\mathbf{H} : \mathcal{P} \to \mathbb{R}^{n_u \times n_x}$, $\mathbf{Q} : \mathcal{P} \to \mathbb{R}^{n_x \times n_x}$, *and* $\mathbf{G} : \mathcal{P} \to \mathbb{R}^{n_u \times n_y}$ *with* $\mathbf{Q}^\top(p) = \mathbf{Q}(p)$ *and* $\operatorname{rank}(\mathbf{G}(p)) = n_y$ *for all* $p \in \mathcal{P}$,

such that

$$\mathbf{Q}(p) - \underline{\alpha}_0 I_{n_x} \succeq 0, \qquad \text{for all } p \in \mathcal{P}, \tag{8.44a}$$

$$\mathrm{He}\Big\{\mathbf{Q}(p)A^\top(p) - B(p)\mathbf{H}(p))\Big\} - \check{\mathbf{Q}}(p,\varrho) + \alpha_0 I_{n_x} \preceq 0, \quad \text{for all } (p,\varrho) \in \mathcal{P}\times\mathcal{R}, \tag{8.44b}$$

$$\mathbf{Q}(p)C^\top(p) - B(p)\mathbf{G}(p) = 0, \qquad \text{for all } p \in \mathcal{P}, \tag{8.44c}$$

are satisfied for some $\underline{\alpha}_0, \alpha_0 > 0$. *Then,* Σ *with* (8.39) *is feedback equivalent to a strictly passive LPV system* $(\Sigma_{K,G})$ *with the quadratic storage function* $V = x^\top \mathbf{P}\, x$ (8.40), *where* $\mathbf{P}(p) = \mathbf{Q}^{-1}(p)$ *and* $\mathbf{K}(p) = \mathbf{H}(p)\mathbf{P}(p)$ *for all* $p \in \mathcal{P}$. ◇

Proof. The derivations were presented in (8.41)-(8.43). □

From the computational point of view, again, it is not obvious how to select appropriate generators for unknown functions $\mathbf{Q}$, $\mathbf{H}$, and $\mathbf{G}$ such that a solution for the matrix equality (8.44c) can be found. In the following, we give a specific model representation for LPV system Σ, which generates a possible algebraic structure for the unknown matrices of (8.44). Compared to LFR (8.27), now, we consider the transposed realization of system Σ as follows:

$$\begin{pmatrix} A^\top(p) \\ B^\top(p) \end{pmatrix} = \mathcal{F}_l\left\{ \left(\begin{array}{c|c} F_{11} & F_{13} \\ F_{21} & F_{23} \\ \hline F_{31} & F_{33} \end{array}\right), \Delta_1 \right\}, \; C^\top(p) = \mathcal{F}_l\left\{ \left(\begin{array}{c|c} F_{12} & F_{14} \\ \hline F_{42} & F_{44} \end{array}\right), \Delta_2 \right\}. \tag{8.45}$$

We call (8.45) the transposed LFR realization relatively to (8.27), due to the fact that the transposition of constant matrices F_{ij} gives back the system dynamics, namely:

$$\mathcal{F}^\top(\Sigma): \; \left(\begin{array}{c} \dot{x} \\ y \\ \hline \bar{\eta}_1 \\ \bar{\eta}_2 \end{array}\right) = \underbrace{\left(\begin{array}{cc|cc} F_{11}^\top & F_{21}^\top & F_{31}^\top & 0 \\ F_{12}^\top & 0 & 0 & F_{42}^\top \\ \hline F_{13}^\top & F_{23}^\top & F_{33}^\top & 0 \\ F_{14}^\top & 0 & 0 & F_{44}^\top \end{array}\right)}_{\bar{F}_{::} = F_{::}^\top} \left(\begin{array}{c} x \\ u \\ \hline \bar{\pi}_1 \\ \bar{\pi}_2 \end{array}\right), \quad \begin{array}{c} \text{with } \bar{\pi}_1 = \Delta_1 \bar{\eta}_1, \\ \text{and } \bar{\pi}_2 = \Delta_2 \bar{\eta}_2, \end{array} \tag{8.46}$$

Observe that (8.46) holds as a direct consequence of the transposition rule for LFRs (Lemma 3.29):

$$\left(\begin{smallmatrix} A(p) & B(p) \\ C(p) & 0 \end{smallmatrix}\right) = \left(\begin{smallmatrix} A^\top(p) & C^\top(p) \\ B^\top(p) & 0 \end{smallmatrix}\right)^\top = \mathcal{F}_l\Big\{F_{::}, \left(\begin{smallmatrix} \Delta_1(p) & \\ & \Delta_2(p) \end{smallmatrix}\right)\Big\}^\top = \mathcal{F}_l\Big\{F_{::}^\top, \left(\begin{smallmatrix} \Delta_1(p) & \\ & \Delta_2(p) \end{smallmatrix}\right)\Big\}. \tag{8.47}$$

Since $n_u = n_y$, we can reuse the definitions for generators Π_1, Π (7.6a), Π_2, Π_b (7.6b), Π_d, Π_e (7.17), matrices A_d, B_e, E_d (7.9c)-(7.9e), and $C_a = (F_{21}\ F_{23})$ of Proposition 8.8, where the corresponding matrices F_{ij} are now defined by the transposed LFR (8.45).

Function $\mathbf{Q}$ was preliminarily defined in (8.40a), furthermore, let $\mathbf{H}$ and $\mathbf{G}$ be rational functions in the following forms:

$$\mathbf{H}(p) = H(p)\Pi_d(p) \text{ and } \mathbf{G}(p) = G(p)\Pi_e(p), \tag{8.48}$$

$$\text{with } H(p) = H_0 + \textstyle\sum_{i=1}^{n_p} H_i p_i \in \mathbb{R}^{m\times m_d}, \tag{8.48a}$$

$$G(p) = G_0 + \textstyle\sum_{i=1}^{n_p} G_i p_i \in \mathbb{R}^{m\times m_e}, \tag{8.48b}$$

where matrices Q_i in (8.40b), H_i in (8.48a), and G_i in (8.48b) are free matrix variables of the appropriate size.

Then, following the arguments of Proposition 8.8, the KYP constraints (8.44b) and (8.44c) for the closed-loop system $\Sigma_{K,G}$ can be written as follows:

$$\mathrm{He}\Big\{\mathbf{Q}(p)A^\top(p) - B(p)\mathbf{H}(p))\Big\} - \check{\mathbf{Q}}(p,\varrho) = \Pi_d^\top(p)\, Q_d(p,\varrho)\, \Pi_d(p) \preceq -\alpha_0 I_{n_x}, \tag{8.49a}$$

$$\mathbf{Q}(p)C^\top(p) - B(p)\mathbf{G}(p) = \Pi^\top(p)\Big(Q(p)B_e - C_a^\top G(p)\Big)\Pi_e(p) = 0, \tag{8.49b}$$

where

$$Q_d(p,\varrho) = \mathrm{He}\Big\{E_d^\top\, Q(p)\, A_d - E_d^\top\, C_a^\top\, H(p)\Big\} - E_d^\top\, \check{Q}(\varrho)\, E_d. \tag{8.50}$$

Observe that inequality (8.49a) is ensured by (8.38b), the equality (8.49b) is implied by (8.38c), finally, the positivity and the radially unbounded nature of storage function (8.40) is guaranteed by (8.38a). Practically, we can "reuse" Corollary 8.9 but with $Q_d(p)$ defined in (8.50). Full column rank matrices S_d, S_e, and affine annihilators N, N_d, and N_e in Corollary 8.9 are to be computed the same, furthermore, all variables and constants in (8.38) together with the Lagrange multipliers L, L_d, L_a, and L_e have the same dimensions.

The results of Section 8.3 are concluded in the following corollary.

Corollary 8.11. *The feasibility of convex conditions* (8.38) *in Corollary 8.9 with* $Q_d(p)$ (8.50) *imply a globally asymptotically stable zero dynamics for the (possibly unstable) LPV system* Σ *in the transposed LFR realization* (8.46). ◇

***Remark* 8.7.** It worth remarking that the simultaneous structured output selection (Section 8.2) together with the feedback passivity analysis (Section 8.3) results in matrix-valued constraints, which are nonlinear in the parameters and bilinear in the free variables. Practically, we would be looking for an output $\bar{y} = \mathbf{M}^\top(p)C(p)x$ such that system Σ with the output $\bar{y}$ is feedback equivalent to a strictly passive LPV system with $u = -\mathbf{K}(p)x + \mathbf{G}(x)v$. The factorization of the highly nonlinear KYP constraints

$$\mathrm{He}\{\mathbf{Q}(A(p) - B(p)\,\mathbf{K}(p))\} + \check{Q}(p,\varrho) + \alpha_0 I_{n_x} \preceq 0 \qquad \text{for all } (p,\varrho) \in \mathcal{P}\times\mathcal{R}, \tag{8.51}$$

$$\mathbf{Q}(p)\, C^\top(p)\, \mathbf{M}(p) = B(p)\, \mathbf{G}(p) \qquad \text{for all } p \in \mathcal{P}, \tag{8.52}$$

are not obvious here. Therefore, it is not straightforward how we can formulate a system of sufficient (even) bilinear matrix (in)equality constraints for the resulting KYP conditions. ◇

8.4 Illustrative examples

In this section, we illustrate the operations of the proposed passivity analysis procedure through two illustrative LPV system model. First, the LPV model of the pendulum-cart system is considered. Then, an artificial example is presented to demonstrate a passivating output selection and dynamic inversion for a multiple-input multiple-output LPV system.

8.4.1 The problem of the kidnapped scientist revisited

In this section, we revisit Problem 2.1 raised in Section 2.1. Suppose that a pendulum is forced to the ceiling of a van, in which a scientist is captured. For simplicity, we consider a van, which is traveling along a straight highway, accordingly, we can assume that the pendulum is moving along the plane spanned by the longitudinal and vertical axes of the van. We assume that the kidnapped scientist can precisely measure the angle $\theta(t)$ and angular velocity $\omega(t)$ of the pendulum, furthermore, he knows the mass of the pendulum (m), the length of the pendulum (2ℓ), and the gravitational acceleration (g). The scientist aims to reconstruct the velocity $v(t)$ of the van.

Note that the first Euler-Lagrange equation in (2.1) formulates a strong relationship between all the three state variables (v,θ,ω), although, the differential equation does not contain the mass of the cart (M, i.e., mass of the van), the friction coefficient (b), nor the

external force applied to the cart (F). Therefore, our ambition is that the information available for the scientist are sufficient to asymptotically observe the velocity of van.

First, consider the LPV model (2.18) of the pendulum-cart system centered around the stable equilibrium point with the following constants and assumptions:

$$\begin{aligned}
\text{constants}: &\quad m = 1\,\text{kg},\ \ell = 2\,\text{m},\ g = 10\,\text{m/s}^2,\ M = 1\,\text{kg},\ b = 1\,\text{kg/s},\ I = \tfrac{4}{3}m\ell^2,\\
\text{assumptions}: &\quad |v(t)| \le 2\,\text{m/s},\ |\theta(t)| \le 0.4\,\text{rad},\ |\omega(t)| \le 1.2\,\text{rad/s},\ |F(t)| \le 1\,\text{N},\ \forall t \ge 0,\\
\text{polytopes}: &\quad \begin{cases} p(t) \in \mathcal{P} = [0.974, 1] \times [0.921, 1] \times [-0.467, 0.467], \\ \dot{p}(t) \in \mathcal{R} = [-0.158, 0.158] \times [-0.467, 0.467] \times [-3, 3],\ \forall t \ge 0, \end{cases}
\end{aligned} \tag{8.53}$$

Polytopes $\mathcal{P}$ and $\mathcal{R}$ were computed as presented in (2.15) and (2.16) by considering the assumed bounds for the state and input signals.

System (2.18) has two output functions (θ and ω) and a single input function F. Therefore, we have the possibility to find a passivating output square down transformation $\mathbf{G}^\top(p)$, such that system (2.18) is strictly passive from input F to output $\bar{y} = \mathbf{G}^\top(p)y$. Finally, the strict passivity property allows us to reconstruct the unknown input F as well as, to observe the unknown state v (without the knowledge of F).

To compute the passivating output function, we considered (2.18) in the LFR form (8.27). Using the object-oriented LFT realization, we obtained a 15-dimensional LFR for $\left(\begin{smallmatrix} A(p) \\ C(p) \end{smallmatrix}\right)$ with $r_1 = 2$, $r_2 = 11$, $r_3 = 2$, and a 3-dimensional LFR for $B(p)$ with $r_1 = 0$, $r_2 = 3$, $r_3 = 0$. We found that the corresponding matrices $\Pi(p) \in \mathbb{R}^{18\times 3}$, $\Pi_b(p) \in \mathbb{R}^{4\times 1}$ and $\Pi_e(p) \in \mathbb{R}^{34\times 1}$ are not minimal. Using the proposed minimal generator computation technique of Section 5.4, we obtained

$$\widehat{\Pi}(p) = \begin{pmatrix} I_3 \\ \widehat{\Pi}_1(p) \end{pmatrix},\ \widehat{\Pi}_b(p) = \begin{pmatrix} 1 \\ 3p_2\zeta_1(p) \\ 3p_2^2\zeta_1(p) \end{pmatrix},\ \text{and} \tag{8.54}$$

$$\Pi_e(p) = \begin{pmatrix} 1 \\ 3p_2\zeta_1(p) \\ 3p_2^2\zeta_1(p) \\ 9p_2^3\zeta_1^2(p) \\ 9p_2^2\zeta_1^2(p) \\ 9p_2^2p_3\zeta_1^2(p) \\ 9p_2p_3\zeta_1^2(p) \end{pmatrix},\ \widehat{\Pi}_1(p) = \begin{pmatrix} 0 & 3p_1p_2\zeta_1(p) & 0 \\ 0 & 3p_1\zeta_1(p) & 0 \\ 0 & 3p_2\zeta_1(p) & 0 \\ 0 & 0 & 3p_2^2\zeta_1(p) \\ 0 & 0 & 3p_2\zeta_1(p) \\ 3p_2\zeta_1(p) & 0 & 0 \\ 0 & 0 & 3p_2p_3\zeta_1(p) \\ 3p_2^2\zeta_1(p) & 0 & 0 \\ 0 & 3p_2^2\zeta_1(p) & 0 \\ 0 & 0 & 3p_3\zeta_1(p) \end{pmatrix}.$$

where

$$\zeta_1(p) = -\frac{1}{3\sigma_4(p)} = \frac{1}{3m^2\ell^2p_2^2 - 3(I + m\ell^2)(m + M)} = \frac{1}{3p_2^2 - 14}. \tag{8.55}$$

We are looking for a storage function $V = x^\top \mathbf{Q}\, x$ (8.40), with $\mathbf{Q}(p) = \Pi^\top(p)Q(p)\Pi(p)$ and an output square down function $\mathbf{G}$, with $\mathbf{G}(p) = G(p)\Pi_e(p)$, where Q and G are affine functions of p, furthermore, the coefficient matrices of Q and G are free decision variables. We evaluate the (affine) parameter-dependent LMI and LME conditions (8.38) in each vertex of polytope $\mathcal{P} \times \mathcal{X}$. Solving the resulting SDP problem, we obtained:

$$G(p) = G_0 + G_1p_1 + G_2p_2 + G_3p_3, \tag{8.56}$$

where

$$\begin{aligned}
G_0 &= \left(\begin{smallmatrix} -0.1786 & 0 & -0.2723 & -0.0933 & 0.1542 & 1.3733 & -0.2468 \\ -0.027 & 0 & 0.395 & 0.5825 & 4.4238 & -1.3558 & -0.2727 \end{smallmatrix}\right), \\
G_1 &= \left(\begin{smallmatrix} 0.009 & -0.4422 & -0.009 & 0.4327 & 0.0619 & 0.0513 & -0.0366 \\ 0 & 0.0036 & 0 & 0 & 0 & 0 & 0 \end{smallmatrix}\right), \\
G_2 &= \left(\begin{smallmatrix} 0.0901 & 0.3875 & -0.0901 & -0.0597 & -0.8727 & 0.0077 & -2.4576 \\ 0.0606 & 1.3281 & -0.0606 & -4.8588 & 10.922 & 0.0363 & 2.3375 \end{smallmatrix}\right), \\
G_3 &= \left(\begin{smallmatrix} 0.0039 & -0.0518 & -0.0039 & 0.1294 & 1.1296 & 0.0016 & 0.0017 \\ 0 & -0.0526 & 0 & 0.0143 & -0.9547 & 0.2845 & 0.2255 \end{smallmatrix}\right).
\end{aligned}$$

The coefficient matrices of $Q(p)$ are not included in this document due to their large size.

Unknown input and state reconstruction for the hypothetical model. First of all, we derive the normal form (8.8) and the inverse dynamics (8.16) for system (2.18) with parameters (8.53). We simulated the nonlinear model (2.17) with the *same parameters* (8.53) and with a non-trivial input function. Using the simulated values of $\theta(t)$ and $\omega(t)$, we computed the parameter signals according to (2.12). Finally, we reconstructed the velocity of the cart and the input function as presented in (8.16) by using the output $y = \left(\begin{smallmatrix}\theta\\ \omega\end{smallmatrix}\right)$ and the parameter signals and their time-derivative. Note that in this case study, we assumed a complete knowledge of the model. The plot of the input function, the resulting state, output and parameter signals, and the reconstructed signals are illustrated in Figure 8.1.

Unknown state reconstruction with a limited knowledge of the model parameters. Let the actual mass of the van be $M = 2000\,\mathrm{kg}$ and the friction coefficient be $b = 5\,\mathrm{kg/s}$. Simultaneously, we consider the inverse dynamics derived for the scientist's pendulum-cart model (8.53), with some freely selected values for M and b. Although that the measured values of $\theta(t)$ and $\omega(t)$ correspond to the actual parameter values of the pendulum-cart model, we try to reconstruct both the unknown input and state signals with the scientist's hypothetical model. We found that the velocity function can be asymptotically observed, but the input signal is not reconstructible. The results of this case study are illustrated in Figure 8.2.

8.4.2 Output projection synthesis to a fourth-order LPV model

Consider the following rational LPV system with 2 inputs and 3 outputs and with two time-varying parameters p_1 and p_2:

$$\left(\begin{array}{c|c} A(p) & B(p) \\ \hline C(p) & 0 \end{array}\right) = \left(\begin{array}{cccc|cc} -p_2^2-1 & 5 & 0 & 0 & \frac{p_1+1}{p_2^2+1}+1 & 1 \\ 0 & p_1-4 & 0 & 0 & p_1 & 0 \\ \frac{1}{10} & 0 & \frac{-5p_1-9}{p_1+2} & 0 & 0 & 0 \\ 0 & \frac{p_1}{p_2-5} & 0 & -1 & 0 & 4-2p_2 \\ \hline 1 & \frac{1}{p_2-5} & 2 & 0 & 0 & 0 \\ 2 & 0 & 1 & 0 & 0 & 0 \\ 0 & 0 & 1 & 1 & 0 & 0 \end{array}\right)$$

$$\mathcal{P} = [-1,2] \times [-1,2],\ \mathcal{R} = [-1,1] \times [-3,3]. \tag{8.57}$$

The computed minimal generators are

$$\widehat{\Pi}(p) = \begin{pmatrix} I_4 \\ \widehat{\Pi}_1(p) \end{pmatrix}, \qquad \widehat{\Pi}_b(p) = \begin{pmatrix} I_2 \\ \widehat{\Pi}_2(p) \end{pmatrix}, \qquad \text{where } \Pi_1(p) = \begin{pmatrix} 0 & p_1 & 0 & 0 \\ 0 & 0 & \frac{p_1}{p_1+2} & 0 \\ 0 & \frac{p_1 p_2}{p_2-5} - p_1 & 0 & 0 \\ p_2^2 & 0 & 0 & 0 \\ p_2 & 0 & 0 & 0 \\ 0 & \frac{p_2}{p_2-5} & 0 & 0 \end{pmatrix},\ \Pi_2(p) = \begin{pmatrix} p_1 - \frac{p_1 p_2^2}{p_2^2+1} & 0 \\ p_1 & 0 \\ \frac{p_2^2}{p_2^2+1} & 0 \\ \frac{p_2}{p_2^2+1} & 0 \\ 0 & -p_2 \end{pmatrix}.$$

The closed form of affine function $Q : \mathcal{P} \to \mathbb{R}^{10\times 10}$, $G : \mathcal{P} \to \mathbb{R}^{10\times 14}$ alongside with $\Pi : \mathcal{P} \to \mathbb{R}^{10\times 4}$, $\Pi_d : \mathcal{P} \times \mathcal{R} \to \mathbb{R}^{24\times 4}$, $\Pi_e : \mathcal{P} \to \mathbb{R}^{14\times 2}$, with their affine annihilators $N : \mathcal{P} \to \mathbb{R}^{7\times 10}$, $N_d : \mathcal{P} \times \mathcal{R} \to \mathbb{R}^{29\times 24}$, $N_e : \mathcal{P} \to \mathbb{R}^{16\times 14}$, and other variables are available on-line at [208].

The feasibility problem (8.38) includes a 10×10 PDLMI (8.38a), a 24×24 PDLMI (8.38b), and 10×14 PDLME (8.38c), which were evaluated in 4, 16, and 4 corner points, respectively. The number of free decision variables in functions Q, G, and in the matrix Lagrange multipliers L, L_d, L_a, and L_e is 1315. The LMI computations last 3 seconds.

The computed function $\mathbf{G}$ and $\mathbf{Q}$ satisfy the KYP equality (8.3b) with a 10^{-10} tolerance, namely for some $p^{(i)} \in \mathcal{P}$ (including the corner points) the absolute value of the worst nonzero element of matrix $\mathbf{Q}(p^{(i)})B(p^{(i)}) - C^\top(p^{(i)})\mathbf{G}(p^{(i)})$ was less than 10^{-10}.

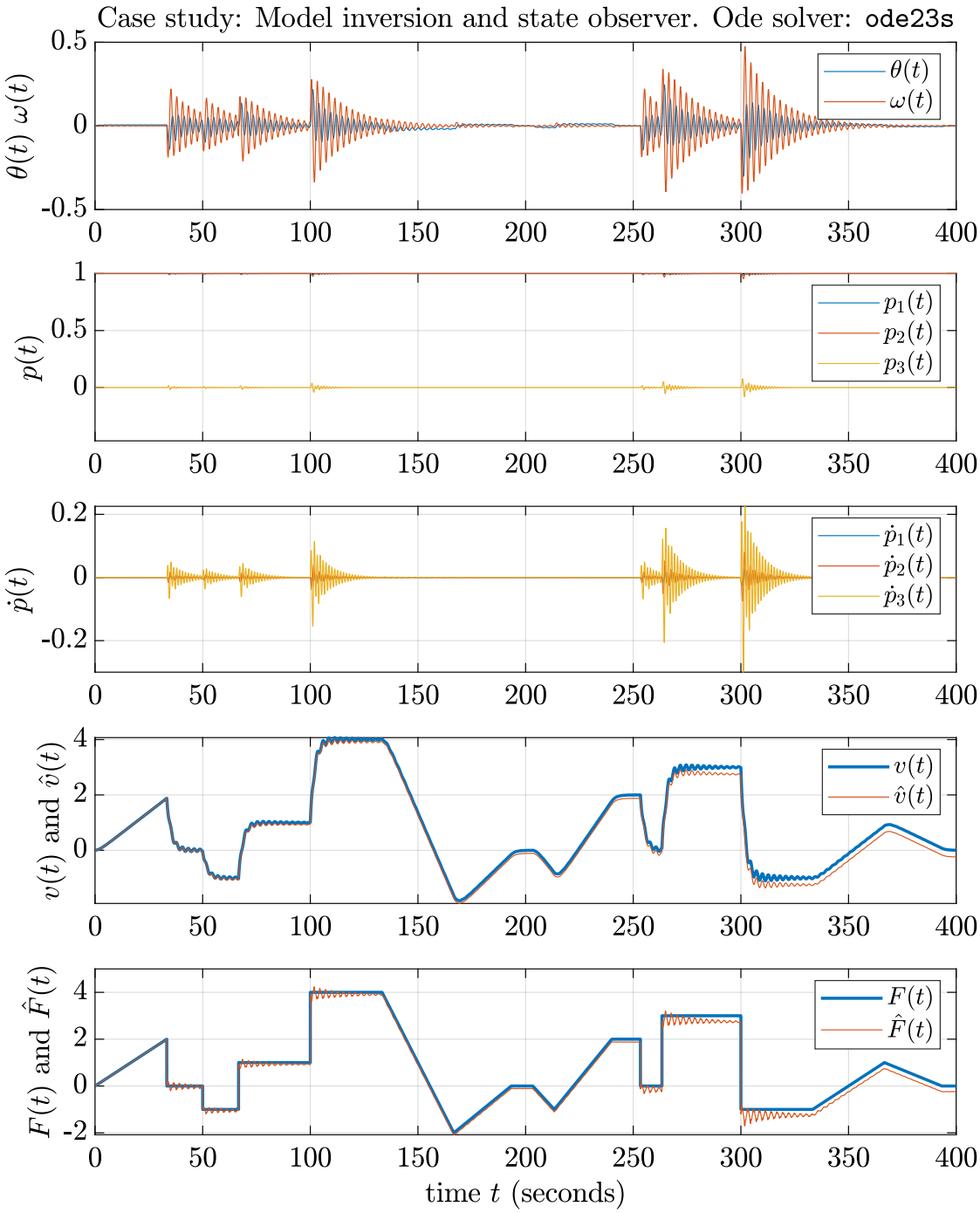

Figure 8.1: Input and state reconstruction for the LPV model (2.18) of the inverted pendulum system (2.17). The first subplot illustrates the measured state variables θ and ω. In the second subplot the parameter signals are presented, which are the functions of the measured state variables. The thirds subplot, illustrates the time-derivative of the parameter signals. Last two subplots illustrate the unknown state and input signals, respectively, and their reconstructed values.

10.15774/PPKE.ITK.2021.004

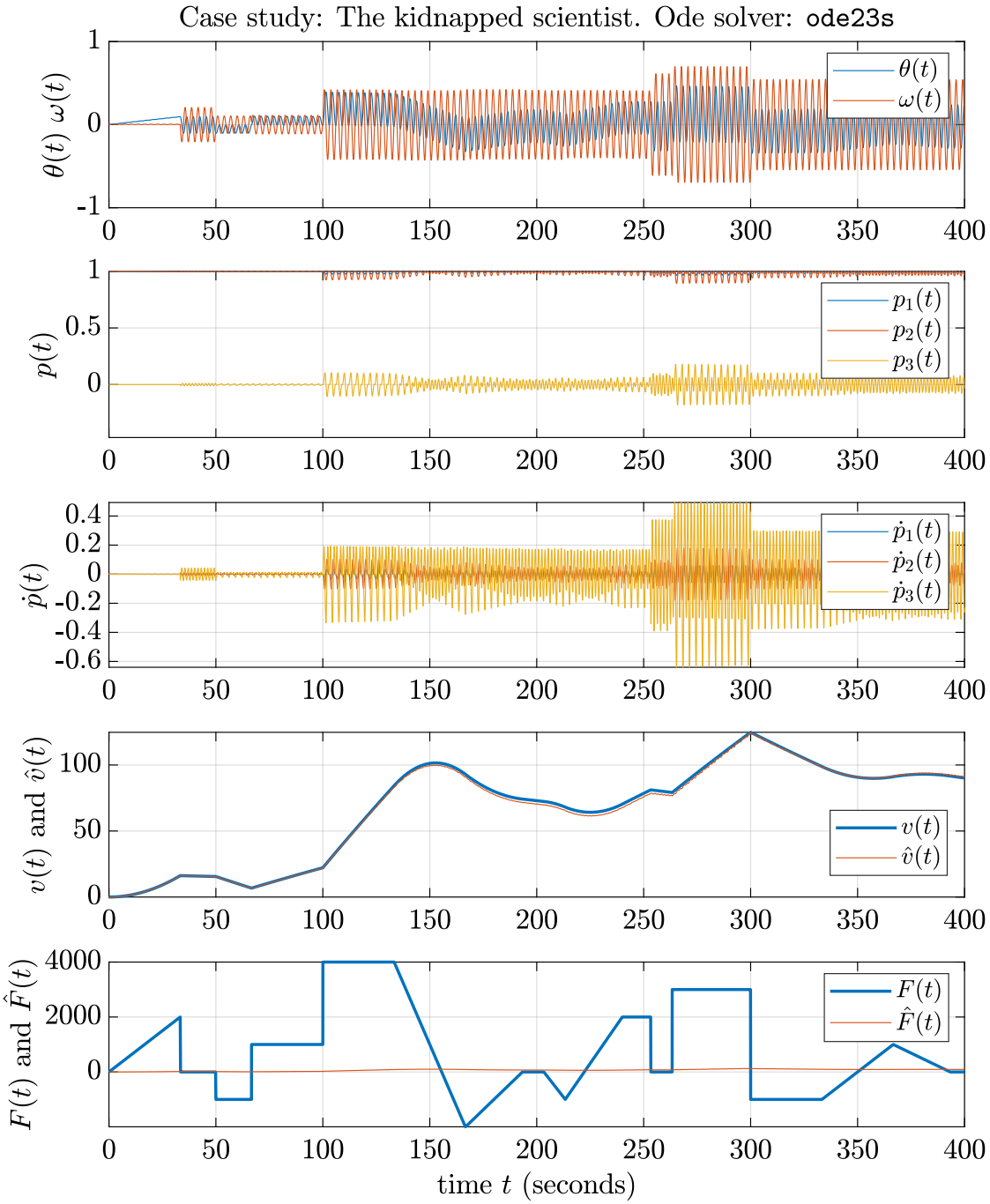

Figure 8.2: State reconstruction for the LPV model (2.18) of the inverted pendulum system (2.17) without the knowledge of the cart's actual mass and the friction coefficient. The first subplot illustrates the measured state variables θ and ω. In the second subplot the parameter signals are presented, which are the functions of the measured state variables. The thirds subplot, illustrates the time-derivative of the parameter signals. Last two subplots illustrate the unknown state and input signals, respectively, and their reconstructed values. Note that the unknown input signal is not reconstructed successfully.

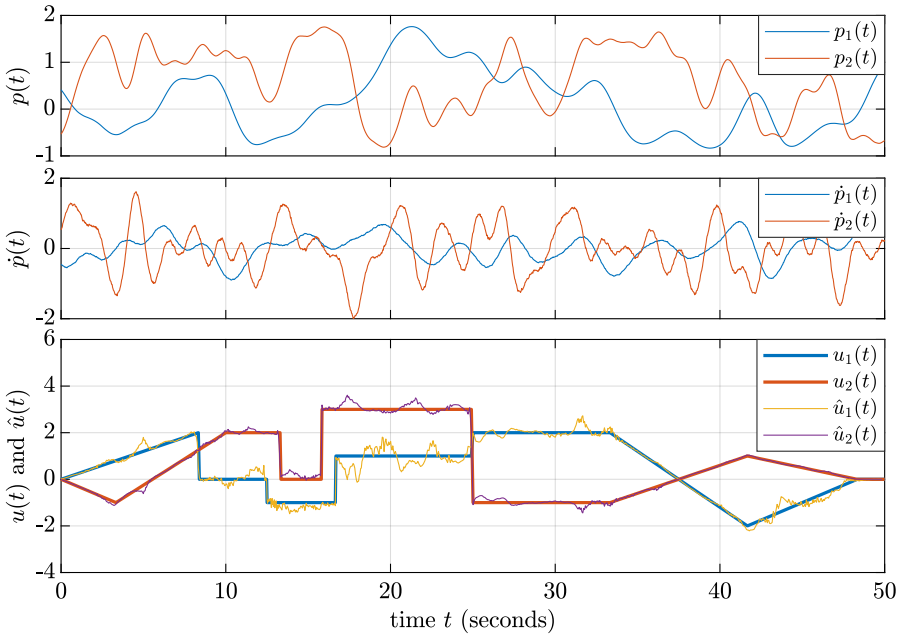

Figure 8.3: Dynamic inversion for system in Example 8.4.2.

Using $\mathbf{G}^\top(p)y$ as the new output vector, a stable dynamic inverse was computed as presented in Paragraph 8.1.1.4. The results of the dynamic inversion of system Σ are illustrated in Figure 8.3.

8.5 Summary

An efficient systematic procedure is proposed in this chapter for the passivity analysis and passivating output synthesis of rational LPV systems. For the dissipativity relations, I used a parameter-dependent proper quadratic storage function. In order to relax the KYP equality condition, a rational parameter-dependent output projection is co-designed through LMI computations, which also allows the handling of non-square systems. The LPV system equation is given in a structured LFR form, from which I generate the rational algebraic structure of the storage function and of the output projection matrix. To reduce the conservatism, maximal annihilators are used as proposed in Section 5.3. In comparison with [149; 150; 156], the main contributions in the field of dissipativity analysis of nonlinear systems with Finsler's lemma relaxation is that I gave an automatic procedure to generate a fixed rational structure for the storage function candidate with free coefficient variables and then systematically formulate sufficient convex LMI conditions for strict passivity. As presented in Theorem 8.4, I proposed a new way to use affine annihilators with matrix Lagrange multipliers to solve a matrix-valued equality condition, which was applied to handle the KYP equality condition (8.38c).

10.15774/PPKE.ITK.2021.004

Chapter 9

Conclusions

The main contributions and the proposed theses of this work are summarized in this chapter, then the possible directions of further research are given. The relevant chapter of the dissertation and the related publications are highlighted at the end of each thesis point.

9.1 New scientific contributions

I. Based on the linear fractional transformation (LFT) and Finsler's lemma, I have proposed a novel computational framework to model and solve a parameter-dependent matrix (in)equality constraint, which is affine in the *unknown variables* and rational in the *parameters*. I formulated sufficient linear matrix inequality (LMI) or equality (LME) constraints to find a possibly conservative solution for the rationally parameter-dependent inequality or equality condition, respectively.

A) I proposed both a symbolical and a numerical method to compute a basis for the parameter independent (i.e., constant) kernel space of a so-called generator, which constitutes a well-defined rational matrix-valued function of the parameters appearing in the rational parameter-dependent matrix (in)equality constraint. The algorithm is also applicable if the parameter values are restricted to a subset of the parameter space [P1].

B) I have introduced the notion of a maximal annihilator to reduce the conservatism of the formulated sufficient LMI/LME constraints. I have proved the existence of a non-unique maximal annihilator for a fixed generator. I have shown that the maximal annihilator provides the largest possible degree of freedom for the sufficient convex condition. Based on the constant kernel computation technique, I proposed a numerical method to compute a maximal annihilator for a generator [P1; P3].

C) I have introduced the notion of a minimal generator to reduce the dimensionality of the generated sufficient convex conditions. The minimal generator determines the minimum size of the LMI/LME that can be attained by a projection transformations without affecting the solution set of the sufficient convex constraint [P1].

D) To compute a minimal generator and the corresponding LMI dimension reduction transformation, I proposed an efficient numerical method based on the constant kernel computation technique [P1; P2; P4].

The results are described in detail in Chapter 5.

Related publications: [P1; P2; P3; P4].

II. I have designed a systematic procedure to compute robust stability domain (RSD) for nonlinear rational uncertain systems.

A) I have proposed a general quadratic structure for Lyapunov function candidates obtained from the LFR realization of the nonlinear system model. For model dimension reduction, I used the technique proposed in thesis point I.D. I have shown that this technique results in a significant dimension reduction of the optimization problem compared to other known solutions in the literature [P3].

B) I extended the proposed RSD computation method to discrete-time nonlinear systems [P2].

The results are described in detail in Chapter 6.

Related publications: [P2; P3; P4; P5; P6; P8; P13; P16].

III. I have introduced new computational methods for induced $\mathcal{L}_2$-gain and passivity analysis of linear parameter-varying (LPV) and nonlinear state-space models in a quasi-LPV form.

A) I proposed a novel method to compute an upper bound on the induced $\mathcal{L}_2$ norm of a nonlinear rational uncertain system [P1; P14]. Through numerical examples, I have demonstrated that the proposed approach is able to provide a tighter upper bound than the state-of-the-art IQC approach with parameter-dependent storage functions and swapping lemma (Köroğlu and Scherer, 2006; Scherer et al., 2008; Pfifer and Seiler, 2016), the descriptor approach (Masubuchi and Suzuki, 2008), or the method of (Coutinho et al., 2008) for nonlinear systems.

B) I have shown that a feedback (strictly) passive LPV model has relative degree 1 and an (asymptotically) stable zero dynamics. I proposed an LFT-based approach to compute a parameter-dependent state transformation, which leads the LPV state-space model into a special normal form advantageous for dynamic inversion and input reconstruction [P7].

C) I formulated sufficient LMI and LME constraints to guarantee strict passivity or feedback strict passivity of a rational LPV system [P7].

D) I proposed a passivating structured output selection method for an asymptotically stable rational LPV system. I developed a method to perform stable dynamic inversion for rational LPV systems [P7].

The results are described in detail in Chapters 7 and 8.

Related publications: [P1; P7; P14].

10.15774/PPKE.ITK.2021.004

9.2 Suggestions for future research

We would like to extend the results presented in this thesis in the following directions.

Dynamic invariants. The maximal annihilator selection algorithm of Section 5.3 could be extended in a fairly straightforward way to find polynomial/rational maximal annihilators with a fixed (but parameterized) structure. Using such a (not necessarily affine) maximal annihilator, we could be able to compute dynamic invariants (i.e., functions of the state and parameter that do not change their value along the system trajectories). Dynamic invariants make room to compute analytically the controllable manifold of a partially controllable system.

Input-to-state stability. In [P16], we have presented some preliminary results on computational input-to-state stability (ISS) analysis. We have shown that a Lyapunov function computed for DOA estimation is also an ISS-Lyapunov function satisfying the ISS inequalities [40, Lemma 10.4.2]. We found that for $\|u\|_\infty \leq M$ the estimated domain where the disturbed motion of the state is taking place is fairly large compared to the actual disturbance region. Namely, the computed local upper-estimate for the induced $\mathcal{L}_\infty$ norm of system Σ with $y^2 = V(x)$ is unreasonably large (conservative). An interesting question is, how ISS certificates can be relaxed to obtain a tighter upper bound for the induced $\mathcal{L}_\infty$ norm.

Local passivity analysis. We aim to formulate local passivity certificates to perform passivity analysis/output synthesis with certain constraints on the input signal. We will investigate the following two possibilities to start with:

1. We can start from the tight relationship of strict passivity and ISS property. It is well-known, that for any strictly passive system there exists a static output feedback law such that the closed-loop is ISS. Future work in this area will be directed towards finding a strictly passive system that is output-feedback equivalent to the actual system.
2. It is also known that strict output passivity implies finite $\mathcal{L}_2$-gain [39]. The next step is to find a technique to inject the disturbance attenuation level into the KYP properties and tie it down as much as possible.

Output selection. Future work in inversion-based fault detection will be devoted to passivating output selection by considering physical or technological sensor placement constraints.

Positivstellensatz. Finsler's lemma and maximal annihilators can be used to solve Positivstellensatz (PS) conditions locally over a polytope, which may result in a less conservative solution compared to a global solution obtained by SOS approach.

10.15774/PPKE.ITK.2021.004

Appendix A

Partitioning of $\mathcal{I}_n \times \mathcal{I}_n$ – Examples

The partitions of $\mathcal{I}_1 \times \mathcal{I}_1$ is

$$\mathscr{P}_{1,1} = \{((0),(0))\}, \mathscr{P}_{1,2} = \{((1),(1))\}, \mathscr{P}_{1,3} = \{((0),(1)),((1),(0))\},$$

The partitions of $\mathcal{I}_2 \times \mathcal{I}_2$ is

- 4 partitions with a single element:

  $\mathscr{P}_{2,1} = \{((0,0),(0,0))\}$,
  $\mathscr{P}_{2,2} = \{((0,1),(0,1))\}$,
  $\mathscr{P}_{2,3} = \{((1,0),(1,0))\}$,
  $\mathscr{P}_{2,4} = \{((1,1),(1,1))\}$,

- 4 partitions with 2 elements:

  $\mathscr{P}_{2,5} = \{((0,0),(0,1)),((0,1),(0,0))\}$,
  $\mathscr{P}_{2,6} = \{((1,0),(1,1)),((1,1),(1,0))\}$,
  $\mathscr{P}_{2,7} = \{((0,0),(1,0)),((1,0),(0,0))\}$,
  $\mathscr{P}_{2,8} = \{((0,1),(1,1)),((1,1),(0,1))\}$,

- a single partition with 4 elements:

  $\mathscr{P}_{2,9} = \{((0,0),(1,1)),((0,1),(1,0)),((1,0),(0,1)),((1,1),(0,0))\}$,

The partitions of $\mathcal{I}_3 \times \mathcal{I}_3$ is

- 8 partitions with a single element:

  $\mathscr{P}_{3,1} = \{((0,0,0),(0,0,0))\}$,
  $\mathscr{P}_{3,2} = \{((0,0,1),(0,0,1))\}$,
  $\mathscr{P}_{3,3} = \{((0,1,0),(0,1,0))\}$,
  $\mathscr{P}_{3,4} = \{((0,1,1),(0,1,1))\}$,
  $\mathscr{P}_{3,5} = \{((1,0,0),(1,0,0))\}$,
  $\mathscr{P}_{3,6} = \{((1,0,1),(1,0,1))\}$,
  $\mathscr{P}_{3,7} = \{((1,1,0),(1,1,0))\}$,
  $\mathscr{P}_{3,8} = \{((1,1,1),(1,1,1))\}$,

- 12 partitions with 2 elements:

  $\mathscr{P}_{3,9} = \{((0,0,0),(0,0,1)),((0,0,1),(0,0,0))\}$,
  $\mathscr{P}_{3,10} = \{((0,1,0),(0,1,1)),((0,1,1),(0,1,0))\}$,

$$\mathscr{P}_{3,11} = \{((0,0,0),(0,1,0)),((0,1,0),(0,0,0))\},$$
$$\mathscr{P}_{3,12} = \{((0,0,1),(0,1,1)),((0,1,1),(0,0,1))\},$$
$$\mathscr{P}_{3,13} = \{((1,0,0),(1,0,1)),((1,0,1),(1,0,0))\},$$
$$\mathscr{P}_{3,14} = \{((1,1,0),(1,1,1)),((1,1,1),(1,1,0))\},$$
$$\mathscr{P}_{3,15} = \{((1,0,0),(1,1,0)),((1,1,0),(1,0,0))\},$$
$$\mathscr{P}_{3,16} = \{((1,0,1),(1,1,1)),((1,1,1),(1,0,1))\},$$
$$\mathscr{P}_{3,17} = \{((0,0,0),(1,0,0)),((1,0,0),(0,0,0))\},$$
$$\mathscr{P}_{3,18} = \{((0,0,1),(1,0,1)),((1,0,1),(0,0,1))\},$$
$$\mathscr{P}_{3,19} = \{((0,1,0),(1,1,0)),((1,1,0),(0,1,0))\},$$
$$\mathscr{P}_{3,20} = \{((0,1,1),(1,1,1)),((1,1,1),(0,1,1))\},$$

- 6 partitions with 4 elements:

$$\mathscr{P}_{3,21} = \{((0,0,0),(0,1,1)),((0,0,1),(0,1,0)),((0,1,0),(0,0,1)),((0,1,1),(0,0,0))\},$$
$$\mathscr{P}_{3,22} = \{((1,0,0),(1,1,1)),((1,0,1),(1,1,0)),((1,1,0),(1,0,1)),((1,1,1),(1,0,0))\},$$
$$\mathscr{P}_{3,23} = \{((0,0,0),(1,0,1)),((0,0,1),(1,0,0)),((1,0,0),(0,0,1)),((1,0,1),(0,0,0))\},$$
$$\mathscr{P}_{3,24} = \{((0,1,0),(1,1,1)),((0,1,1),(1,1,0)),((1,1,0),(0,1,1)),((1,1,1),(0,1,0))\},$$
$$\mathscr{P}_{3,25} = \{((0,0,0),(1,1,0)),((0,1,0),(1,0,0)),((1,0,0),(0,1,0)),((1,1,0),(0,0,0))\},$$
$$\mathscr{P}_{3,26} = \{((0,0,1),(1,1,1)),((0,1,1),(1,0,1)),((1,0,1),(0,1,1)),((1,1,1),(0,0,1))\},$$

- a single partition with 8 element:

$$\mathscr{P}_{3,27} = \{((0,0,0),(1,1,1)),((0,0,1),(1,1,0)),((0,1,0),(1,0,1)),((0,1,1),(1,0,0)),$$
$$((1,0,0),(0,1,1)),((1,0,1),(0,1,0)),((1,1,0),(0,0,1)),((1,1,1),(0,0,0))\}.$$

The author's publications

SCI journal papers

[P1] P. Polcz, T. Péni, B. Kulcsár, and G. Szederkényi. Induced L2-gain computation for rational LPV systems using Finsler's lemma and minimal generators. *Systems & Control Letters*, 142:104738, 2020. ISSN: 0167-6911. DOI: 10.1016/j.sysconle.2020.104738.

[P2] P. Polcz, T. Péni, and G. Szederkényi. Computational method for estimating the domain of attraction of discrete-time uncertain rational systems. *European Journal of Control*, 49:68–83, 2019. ISSN: 0947-3580. DOI: 10.1016/j.ejcon.2018.12.004.

[P3] P. Polcz, T. Péni, and G. Szederkényi. Improved algorithm for computing the domain of attraction of rational nonlinear systems. *European Journal of Control*, 39:53–67, 2017. ISSN: 0947-3580. DOI: 10.1016/j.ejcon.2017.10.003.

Other journal papers

[P4] P. Polcz, T. Péni, and G. Szederkényi. Reduced linear fractional representation of nonlinear systems for stability analysis. *IFAC-PapersOnLine*, 51(2):37–42, 2018. 9th Vienna International Conference on Mathematical Modelling. ISSN: 2405-8963. DOI: 10.1016/j.ifacol.2018.03.007.

[P5] P. Polcz and G. Szederkényi. Computational stability analysis of Lotka-Volterra systems. *Hungarian Journal of Industry and Chemistry*, 44(2):113–120, 2016. DOI: 10.1515/hjic-2016-0014.

[P6] P. Polcz, G. Szederkényi, and T. Péni. An improved method for estimating the domain of attraction of nonlinear systems containing rational functions. *Journal of Physics: Conference Series*, 659(1):012038, Nov. 2015. DOI: 10.1088/1742-6596/659/1/012038.

Conference papers

[P7] P. Polcz, B. Kulcsár, T. Péni, and G. Szederkényi. Passivity analysis of rational LPV systems using Finsler's lemma. In: *2019 IEEE 58th Conference on Decision and Control (CDC)*. Nice, France, Dec. 2019, 3793–3798. DOI: 10.1109/CDC40024.2019.9029877.

[P8] P. Polcz, G. Szederkényi, and K. M. Hangos. Computational stability analysis of an uncertain bioreactor model. In: *13th International Symposium on Stability, Vibration, and Control of Machines and Structures - SVCS 2016, June 16-18, Budapest, Hungary*. 2016, 21–32.

[P9] P. Polcz, G. Szederkényi, and B. Kulcsár. Computation of rational parameter dependent Lyapunov functions for LPV systems. In: *Swedish Control Conference (Reglermöte) 2018*. Link: https://easychair.org/publications/preprint/8Td4. 2018. DOI: 10.29007/9m7r.

[P10] P. Polcz and G. Szederkényi. On the use of Finsler's lemma - technical notes. In: *15th International PhD Workshop on Systems and Control (PhD Workshop 2018)*. 2018.

Other papers and research reports

[P11] P. Polcz, G. Szederkényi, and B. Kulcsár. Observer based dynamic output design for linear time-invariant systems ensuring stable zero dynamics. *Jedlik Laboratories Reports*, VI.(1):3–14, 2018.

[P12] P. Polcz, G. Szederkényi, and T. Péni. An improved method for estimating the domain of attraction of uncertain rational nonlinear systems by using LMI stability conditions. *Jedlik Laboratories Reports*, III.(4):7–33, 2015.

[P13] P. Polcz and G. Szederkényi. Domain of attraction computation of a unique non-zero equilibrium point of a Lotka-Volterra system. In: *PhD Proceedings Annual Issues of the Doctoral School Pázmány Péter Catholic University, Faculty of Information Technology and Bionics - 2020*. Ed. by P. S. G. Prószéky. 50/a Práter street, 1083 Budapest, Hungary: Pázmány University ePress, 2020, in press.

[P14] P. Polcz and G. Szederkényi. Local performance estimation of nonlinear rational systems in a convex computational framework using Finsler's lemma and affine annihilators. In: *PhD Proceedings Annual Issues of the Doctoral School Pázmány Péter Catholic University, Faculty of Information Technology and Bionics - 2019*. Ed. by P. S. G. Prószéky. 50/a Práter street, 1083 Budapest, Hungary: Pázmány University ePress, 2019, in press.

[P15] P. Polcz and G. Szederkényi. Global stability analysis of linear parameter varying systems via quadratic separator for uncertain constrained systems. In: *PhD Proceedings Annual Issues of the Doctoral School Pázmány Péter Catholic University, Faculty of Information Technology and Bionics - 2018*. Ed. by P. S. G. Prószéky. 50/a Práter street, 1083 Budapest, Hungary: Pázmány University ePress, 2018, 34–34.

[P16] P. Polcz and G. Szederkényi. Computational stability analysis of an uncertain Van der Pol system. In: *PhD Proceedings Annual Issues of the Doctoral School Pázmány Péter Catholic University, Faculty of Information Technology and Bionics - 2017*. Ed. by P. S. G. Prószéky. 50/a Práter street, 1083 Budapest, Hungary: Pázmány University ePress, 2017, 41–41.

[P17] P. Polcz and (supervisor Gábor Szederkényi). An improved method for estimating the domain of attraction of uncertain nonlinear systems. In: *National Students' Scientific Conference*. 2017. URL: http://polcz.itk.ppke.hu/files/palyamunka_40192_0181.pdf.

[P18] P. Polcz and (supervisor Gábor Szederkényi). Stability analysis of uncertain nonlinear systems using optimization. MSc thesis. Pázmány Péter Catholic University Faculty of Information Technology and Bionics, 2016.

References

[1] J. L. Massera. On Liapounoff's conditions of stability. *The Annals of Mathematics*, 50(3):705, July 1949. DOI: 10.2307/1969558.

[2] C. M. Kellett. Classical converse theorems in Lyapunov's second method. *Discrete and Continuous Dynamical Systems - Series B*, 20(8):2333–2360, Aug. 2015. DOI: 10.3934/dcdsb.2015.20.2333.

[3] S. F. Hafstein. An algorithm for constructing Lyapunov functions. *Electronic Journal of Differential Equations*, 2007, 2007.

[4] J. Björnsson, P. Giesl, S. Hafstein, C. M. Kellett, and H. Li. Computation of continuous and piecewise affine Lyapunov functions by numerical approximations of the Massera construction. In: *53rd IEEE Conference on Decision and Control*. Dec. 2014, 5506–5511. DOI: 10.1109/CDC.2014.7040250.

[5] J. Björnsson, P. Giesl, S. F. Hafstein, C. M. Kellett, and and. Computation of Lyapunov functions for systems with multiple local attractors. *Discrete & Continuous Dynamical Systems - A*, 35(9):4019–4039, 2015. DOI: 10.3934/dcds.2015.35.4019.

[6] J. Björnsson and S. F. Hafstein. Efficient Lyapunov function computation for systems with multiple exponentially stable equilibria. *Procedia Computer Science*, 108:655–664, 2017. International Conference on Computational Science, ICCS 2017, 12-14 June 2017, Zurich, Switzerland. ISSN: 1877-0509. DOI: 10.1016/j.procs.2017.05.285.

[7] A. I. Doban and M. Lazar. Computation of Lyapunov functions for nonlinear differential equations via a Massera-type construction. *IEEE Transactions on Automatic Control*, 63(5):1259–1272, May 2018. ISSN: 2334-3303. DOI: 10.1109/TAC.2017.2736961.

[8] R. Bobiti and M. Lazar. Automated-sampling-based stability verification and DOA estimation for nonlinear systems. *IEEE Transactions on Automatic Control*, 63(11):3659–3674, Nov. 2018. ISSN: 2334-3303. DOI: 10.1109/TAC.2018.2797196.

[9] V. I. Zubov and L. F. Boron. *Methods of A. M. Lyapunov and their application*. Noordhoff Groningen, 1964.

[10] F. Camilli, L. Grüne, and F. Wirth. A generalization of Zubov's method to perturbed systems. *SIAM Journal on Control and Optimization*, 40(2):496–515, 2001. DOI: 10.1137/S036301299936316X.

[11] F. Camilli, L. Grüne, and F. Wirth. Control Lyapunov functions and Zubov's method. *SIAM Journal on Control and Optimization*, 47(1):301–326, 2008.

[12] A. Vannelli and M. Vidyasagar. Maximal Lyapunov functions and domains of attraction for autonomous nonlinear systems. *Automatica*, 21(1):69–80, Jan. 1985. ISSN: 0005-1098. DOI: 10.1016/0005-1098(85)90099-8.

[13] S. Rozgonyi, K. M. Hangos, and G. Szederkényi. Determining the domain of attraction of hybrid non-linear systems using maximal Lyapunov functions. *Kybernetika*, 46:19–37, 2010. DOI: 10338.dmlcz/140048.

[14] A. Papachristodoulou. Scalable analysis of nonlinear systems using convex optimization. PhD thesis. California Institute of Technology, 2005.

[15] U. Topcu, A. K. Packard, and P. Seiler. Local stability analysis using simulations and sum-of-squares programming. *Automatica*, 44(10):2669–2675, 2008. DOI: 10.1016/j.automatica.2008.03.010.

[16] A. Trofino and T. J. M. Dezuo. LMI stability conditions for uncertain rational nonlinear systems. *International Journal of Robust and Nonlinear Control*, 24(18):3124–3169, 2013. cited By 14. DOI: 10.1002/rnc.3047.

[17] P. Giesl and S. Hafstein. Construction of Lyapunov functions for nonlinear planar systems by linear programming. *Journal of Mathematical Analysis and Applications*, 388:463–479, 2012. DOI: 10.1016/j.jmaa.2011.10.047.

[18] H. A. Poonawala. Stability analysis via refinement of piece-wise linear Lyapunov functions. In: *2019 IEEE 58th Conference on Decision and Control (CDC)*. 2019, 1442–1447.

[19] R. Bouyekhf and L. T. Gruyitch. An alternative approach for stability analysis of discrete time nonlinear dynamical systems. *Journal of Difference Equations and Applications*, 24(1):68–81, 2018. DOI: 10.1080/10236198.2017.1391239.

[20] D. P. Mandic and J. Chambers. *Recurrent neural networks for prediction: learning algorithms, architectures and stability*. New York, NY, USA: John Wiley & Sons, Inc., 2001. ISBN: 0471495174.

[21] H. L. Smith and H. R. Thieme. Persistence and global stability for a class of discrete time structured population models. *Discrete and Continous Dynamtical Systems Series A (DCDS-A)*, 2013. DOI: 10.3934/dcds.2013.33.xx.

[22] A. R. Heravi and G. A. Hodtani. A new robust fixed-point algorithm and its convergence analysis. *Journal of Fixed Point Theory and Applications*, 19(4):3191–3215, Dec. 2017. ISSN: 1661-7746. DOI: 10.1007/s11784-017-0474-5.

[23] J. Kapinski, J. V. Deshmukh, S. Sankaranarayanan, and N. Arechiga. Simulation-guided Lyapunov analysis for hybrid dynamical systems. In: *Proceedings of the 17th international conference on Hybrid systems: computation and control*. ACM. 2014, 133–142.

[24] J. Kapinski and J. Deshmukh. Discovering forward invariant sets for nonlinear dynamical systems. In: *Springer Proceedings in Mathematics and Statistics*. Vol. 117. cited By 1. 2015, 259–264. DOI: 10.1007/978-3-319-12307-3_37.

[25] C. I. Byrnes, A. Isidori, and J. C. Willems. Passivity, feedback equivalence, and the global stabilization of minimum phase nonlinear systems. *IEEE Transactions on Automatic Control*, 36(11):1228–1240, 1991. cited By 873. DOI: 10.1109/9.100932.

[26] W. Lin and T. L. Shen. Robust passivity and feedback design for minimum-phase nonlinear systems with structural uncertainty. *Automatica*, 35(1):35–47, 1999. ISSN: 0005-1098. DOI: 10.1016/s0005-1098(98)00120-4.

[27] A. Isidori. *Nonlinear control systems*. Ed3. Springer-Verlag London, 1995. ISBN: 978-1-4471-3909-6. DOI: 10.1007/978-1-84628-615-5.

[28] Z. Szabo, J. Bokor, and G. Balas. Inversion of LPV systems and its application to fault detection. *In Proc. IFAC Safeprocess, Washington, DC*, 1:235–240, 2003.

[29] J. Bokor and Z. Szabó. Fault detection and isolation in nonlinear systems. *Annual Reviews in Control*, 33(2):113–123, 2009. ISSN: 1367-5788. DOI: 10.1016/j.arcontrol.2009.09.001.

[30] Z. Szabó. A geometric approach for the control of switch and LPV systems. A dissertation submitted in partial fufillment of the requirements for the degree of D.Sc. at Hungarian Academy of Sciences. PhD thesis. 2010.

[31] B. Kulcsar, J. Bokor, and J. Shinar. Unknown input reconstruction for LPV systems. *International Journal of Roboust and Nonlinear Control*, 20(5):579–595, 2010.

[32] J. Dong and M. Verhaegen. Identification of fault estimation filter from I/O data for systems with stable inversion. *IEEE Transactions on Automatic Control*, 57(6):1347–1361, 2012.

[33] B. Kulcsar and M. Verhaegen. Robust inversion based fault estimation for discrete-time LPV systems. *IEEE Transactions on Automatic Control*, 57(6):1581–1586, 2012.

[34] H. K. Khalil. *Nonlinear systems*. Pearson Education. Prentice Hall, 2002. ISBN: 9780130673893.

[35] A. Dabiri, B. Kulcsár, and H. Köroğlu. Distributed LPV state-feedback control under control input saturation. *IEEE Transactions on Automatic Control*, 62(5):2450–2456, May 2017. DOI: 10.1109/TAC.2016.2598967.

[36] T. Péni, B. Vanek, G. Lipták, Z. Szabó, and J. Bokor. Nullspace-based input reconfiguration architecture for overactuated aerial vehicles. *IEEE Transactions on Control Systems Technology*, 26(5):1826–1833, Sept. 2018. DOI: 10.1109/TCST.2017.2737622.

[37] K. Z. Østergaard, J. Stoustrup, and P. Brath. Linear parameter varying control of wind turbines covering both partial load and full load conditions. *International Journal of Robust and Nonlinear Control*, 19(1):92–116, Jan. 2009. DOI: 10.1002/rnc.1340.

[38] S. Wang and P. Seiler. Gridded-based LPV control of a Clipper Liberty Wind Turbine. *Wind Energy*, 21(11):1106–1120, 2018.

[39] A. Van der Schaft. *L2-gain and passivity techniques in nonlinear control*. 3rd. Secaucus, NJ, USA: Springer-Verlag New York, Inc., 2017. ISBN: 978-3-319-49992-5. DOI: 10.1007/978-3-319-49992-5.

[40] A. Isidori. *Nonlinear control systems II*. London, UK, UK: Springer-Verlag London, 1999. ISBN: 978-1-4471-1160-3,1852331887. DOI: 10.1007/978-1-4471-0549-7.

[41] R. Sepulchre, M. Jankovic, and P. V. Kokotovic. *Constructive nonlinear control*. Communications and Control Engineering. Springer, 1997. ISBN: 978-1-4471-0967-9.

[42] R. Sepulchre, M. Janković, and P. V. Kokotović. Recursive designs and feedback passivation. In: *Systems and Control in the Twenty-First Century*. Ed. by C. I. Byrnes, B. N. Datta, C. F. Martin, and D. S. Gilliam. Boston, MA: Birkhäuser Boston, 1997, 313–326. ISBN: 978-1-4612-4120-1.

[43] A. Loria, E. Panteley, and H. Nijmeijer. A remark on passivity-based and discontinuous control of uncertain nonlinear systems. *Automatica*, 37(9):1481–1487, 2001. ISSN: 0005-1098. DOI: 10.1016/s0005-1098(01)00097-8.

[44] B. Brogliato, R. Lozano, B. Maschke, and O. Egeland. *Dissipative systems analysis and control*. Vol. 2. Springer, 2007.

[45] J. R. Forbes and C. J. Damaren. Passive linear time-varying systems: state-space realizations, stability in feedback, and controller synthesis. In: *Proceedings of the 2010 American Control Conference*. June 2010, 1097–1104. DOI: 10.1109/ACC.2010.5530792.

[46] C. S. Li and J. Zhao. Robust passivity-based H-infinity control for uncertain switched nonlinear systems. *International Journal of Robust and Nonlinear Control*, 26(14):3186–3206, 2016. ISSN: 1049-8923. DOI: 10.1002/rnc.3499.

[47] A. Astolfi, R. Ortega, and R. Sepulchre. Stabilization and disturbance attenuation of nonlinear systems using dissipativity theory. *European Journal of Control*, 8(5):408–431, 2002. ISSN: 0947-3580. DOI: 10.3166/ejc.8.408-431.

[48] G. Szederkényi, K. M. Hangos, J. Bokor, and T. Vámos. Linear output selection for feedback linearization. *IFAC Proceedings Volumes*, 35(1):109–114, 2002. 15th IFAC World Congress. ISSN: 1474-6670. DOI: 10.3182/20020721-6-ES-1901.00268.

[49] G. Basile and G. Marro. *Controlled and conditioned invariants in linear system theory*. Prentice Hall Englewood Cliffs, 1992.

[50] J. C. Willems. Dissipative dynamical systems part I: General theory. *Archive for Rational Mechanics and Analysis*, 45(5):321–351, Jan. 1972. ISSN: 1432-0673. DOI: 10.1007/BF00276493.

[51] A. Van Der Schaft. Port-Hamiltonian systems: an introductory survey. In: *Proceedings of the international congress of mathematicians*. Vol. 3. Citeseer. 2006, 1339–1365.

[52] C. Arghir. Transverse feedback passivation in control of multi-machine and multi-converter power networks. PhD thesis. ETH Zurich, 2019.

[53] J. Travieso-Torres, M. Duarte-Mermoud, and P. Zagalak. Passivity based stabilization of non-minimum phase nonlinear systems. *Kybernetika*, 45(3):417–426, 2009.

[54] H. Pang and J. Zhao. Robust passivity, feedback passification and global robust stabilisation for switched non-linear systems with structural uncertainty. *IET Control Theory & Applications*, 9(11):1723–1730, July 2015. DOI: 10.1049/iet-cta.2014.1273.

[55] D. Yang and J. Zhao. Feedback passification for switched LPV systems via a state and parameter-triggered switching with dwell time constraints. *Nonlinear Analysis-Hybrid Systems*, 29:147–164, 2018. ISSN: 1751-570X. DOI: 10.1016/j.nahs.2018.01.005.

[56] H. F. los Reyes, A. Schaum, T. Meurer, and J. Alvarez. Passivity-based output-feedback control for a class of 1-D semilinear PDE models. In: *2019 16th International Conference on Electrical Engineering, Computing Science and Automatic Control (CCE)*. Sept. 2019, 1–6. DOI: 10.1109/ICEEE.2019.8884530.

[57] T. Binazadeh and H. Gholami. Finite-time robust passive control of uncertain discrete time-delay systems using output feedback: application on Chua's circuit. *Circuits, Systems, and Signal Processing*, 39(5):2349–2375, Oct. 2019. DOI: 10.1007/s00034-019-01275-y.

[58] T. Sangpet and S. Kuntanapreeda. Finite-time synchronization of hyperchaotic systems based on feedback passivation. *Chaos, Solitons & Fractals*, 132:109605, 2020. ISSN: 0960-0779. DOI: 10.1016/j.chaos.2020.109605.

[59] S. Zhang and H. Nie. Asynchronous feedback passification for discrete-time switched systems under state-dependent switching with dwell time constraint. *International Journal of Adaptive Control and Signal Processing*, 34(4):427–443, 2020. DOI: 10.1002/acs.3090. eprint: https://onlinelibrary.wiley.com/doi/pdf/10.1002/acs.3090. URL: https://onlinelibrary.wiley.com/doi/abs/10.1002/acs.3090.

[60] J. Moreno. Existence of unknown input observers and feedback passivity for linear systems. In: *Proceedings of the 40th IEEE Conference on Decision and Control (Cat. No.01CH37228)*. Vol. 4. Orlando, FL, USA, Dec. 2001, 3366–3371 vol.4. DOI: 10.1109/CDC.2001.980353.

[61] E. Rocha-Cózatl and J. Moreno. Passivity and unknown input observers for nonlinear systems. *IFAC Proceedings Volumes*, 35(1):345–350, 2002. 15th IFAC World Congress. ISSN: 1474-6670. DOI: 10.3182/20020721-6-ES-1901.00219.

[62] C. W. Scherer and S. Weiland. *Linear matrix inequalities in control*. Technical University of Delft, The Netherlands, Delft, 2000.

[63] S. Boyd, L. El Ghaoui, E. Feron, and V. Balakrishnan. *Linear matrix inequalities in system and control theory*. Vol. 15. Studies in Applied Mathematics. Philadelphia, PA: SIAM, June 1994. ISBN: 0-89871-334-X.

[64] S. Boyd and L. Vandenberghe. *Convex optimization*. New York, NY, USA: Cambridge University Press, 2004. ISBN: 0521833787.

[65] J. Doyle. Analysis of feedback systems with structured uncertainties. *IEE Proceedings D - Control Theory and Applications*, 129(6):242–250, Nov. 1982. ISSN: 0143-7054. DOI: 10.1049/ip-d.1982.0053.

[66] J. Doyle and A. Packard. Uncertain multivariable systems from a state space perspective. In: *1987 American Control Conference*. 1987, 2147–2152.

[67] J. Doyle, A. Packard, and K. Zhou. Review of LFTs, LMIs, and μ. In: *Proceedings of the 30th IEEE Conference on Decision and Control*. 1991, 1227–1232 vol.2.

[68] K. Zhou and J. Doyle. *Essentials of robust control*. Prentice Hall Modular Series for Eng. Prentice Hall, Upper side river, New Jersey, 1998. ISBN: 9780135258330.

[69] D.-W. Gu, P. H. Petkov, and M. M. Konstantinov. *Robust control design with MATLAB*. 2nd ed. Springer Publishing Company, Incorporated, 2013. ISBN: 1447146816, 9781447146810.

[70] L. A. Zadeh. On stability of linear varying-parameter systems. *Journal of Applied Physics*, 22(4):402–405, 1951.

[71] J. S. Shamma. Analysis and design of gain scheduled control systems. PhD thesis. Massachusetts Institute of Technology, 1988.

[72] J. S. Shamma and J. R. Cloutier. Gain-scheduled missile autopilot design using linear parameter varying transformations. *Journal of Guidance, Control, and Dynamics*, 16(2):256–263, Mar. 1993. DOI: 10.2514/3.20997.

[73] F. Wu. Control of linear parameter varying systems. PhD thesis. University of California at Berkeley, 1995.

[74] F. Wu, X. H. Yang, A. Packard, and G. Becker. Induced L2-norm control for LPV systems with bounded parameter variation rates. *International Journal of Robust and Nonlinear Control*, 6(9-10):983–998, 1996. DOI: 10.1002/(SICI)1099-1239(199611)6:9/10<983::AID-RNC263>3.0.CO;2-C.

[75] W. J. Rugh and J. S. Shamma. Research on gain scheduling. *Automatica*, 36(10):1401–1425, 2000. ISSN: 0005-1098. DOI: 10.1016/S0005-1098(00)00058-3.

[76] J. S. Shamma. An overview of LPV systems. In: *Control of linear parameter varying systems with applications*. Springer, 2012, 3–26.

[77] J. Mohammadpour and C. W. Scherer. *Control of linear parameter varying systems with applications*. Springer Science & Business Media, 2012.

[78] P. Apkarian, J.-M. Biannic, and P. Gahinet. Self-scheduled H-infinity control of missile via linear matrix inequalities. *Journal of Guidance, Control, and Dynamics*, 18(3):532–538, 1995.

[79] E. Feron, P. Apkarian, and P. Gahinet. Analysis and synthesis of robust control systems via parameter-dependent Lyapunov functions. *IEEE Transactions on Automatic Control*, 41(7):1041–1046, 1996.

[80] P. Gahinet, P. Apkarian, and M. Chilali. Affine parameter-dependent Lyapunov functions and real parametric uncertainty. *IEEE Transactions on Automatic Control*, 41(3):436–442, Mar. 1996. ISSN: 1558-2523. DOI: 10.1109/9.486646.

[81] G. Balas, J. Bokor, and Z. Szabo. Invariant subspaces for LPV systems and their applications. *IEEE Transactions on Automatic Control*, 48(11):2065–2069, Nov. 2003. ISSN: 0018-9286. DOI: 10.1109/TAC.2003.819647.

[82] R. C. L. F. Oliveira and P. L. D. Peres. Stability of polytopes of matrices via affine parameter-dependent Lyapunov functions: asymptotically exact LMI conditions. *Linear algebra and its applications*, 405:209–228, 2005.

[83] P. B. Cox, S. Weiland, and R. Tóth. Affine parameter-dependent Lyapunov functions for LPV systems with affine dependence. *IEEE Transactions on Automatic Control*, 63(11):3865–3872, Nov. 2018. ISSN: 0018-9286. DOI: 10.1109/TAC.2018.2824982.

[84] A. Walsh and J. R. Forbes. Very strictly passive controller synthesis with affine parameter dependence. *IEEE Transactions on Automatic Control*, 63(5):1531–1537, 2018. ISSN: 0018-9286. DOI: 10.1109/tac.2017.2748928.

[85] M. K. H. Fan, A. L. Tits, and J. C. Doyle. Robustness in the presence of mixed parametric uncertainty and unmodeled dynamics. *IEEE Transactions on Automatic Control*, 36(1):25–38, Jan. 1991. ISSN: 0018-9286. DOI: 10.1109/9.62265.

[86] P. Lambrechts, J. Terlouw, S. Bennani, and M. Steinbuch. Parametric uncertainty modeling using LFTs. In: *American Control Conference*. cited By 53. 1992, 267–272.

[87] D. Peaucelle and D. Arzelier. Robust performance analysis with LMI-based methods for real parametric uncertainty via parameter-dependent Lyapunov functions. *IEEE Transactions on Automatic Control*, 46(4):624–630, Apr. 2001. ISSN: 0018-9286. DOI: 10.1109/9.917664.

[88] E. Prempain and I. Postlethwaite. L2 and H2 performance analysis and gain-scheduling synthesis for parameter-dependent systems. *Automatica*, 44(8):2081–2089, 2008. ISSN: 0005-1098. DOI: 10.1016/j.automatica.2007.12.008.

[89] L. El Ghaoui and G. Scorletti. Performance control of rational systems using linear-fractional representations and LMIs. In: *Proceedings of 1994 33rd IEEE Conference on Decision and Control*. Vol. 3. Dec. 1994, 2792–2797 vol.3. DOI: 10.1109/CDC.1994.411377.

[90] L. El Ghaoui and G. Scorletti. Control of rational systems using linear-fractional representations and linear matrix inequalities. *Automatica*, 32(9):1273–1284, 1996. ISSN: 0005-1098. DOI: 10.1016/0005-1098(96)00071-4.

[91] J. C. Cockburn and B. G. Morton. Linear fractional representations of uncertain systems. *Automatica*, 33(7):1263–1271, 1997.

[92] R. D'Andrea and S. Khatri. Kalman decomposition of linear fractional transformation representations and minimality. In: *Proceedings of the 1997 American Control Conference (Cat. No.97CH36041)*. Vol. 6. Albuquerque, New Mexico, USA, June 1997, 3557–3561 vol.6. DOI: 10.1109/ACC.1997.609484.

[93] S. Hecker and A. Varga. Symbolic techniques for low order LFT-modelling. *IFAC-PapersOnline*, 16(1):523–528, Mar. 2005. 16th IFAC World Congress. ISSN: 1474-6670. DOI: 10.3182/20050703-6-CZ-1902.01032.

[94] J.-F. Magni. *User manual of the Linear Fractional Representation Toolbox: version 2.0*. Jan. 2006.

[95] S. Hecker, A. Varga, and J.-F. Magni. Enhanced LFR-toolbox for MATLAB. In: *IEEE International Symposium on Computer Aided Control Systems Design*. 2004, 25–29. DOI: 10.1109/CACSD.2004.1393845.

[96] J.-M. Biannic and C. Roos. *Generalized state space: A new Matlab class to model uncertain and nonlinear systems as linear fractional representations*. available with the SMAC Toolbox at http://w3.onera.fr/smac/gss. 2016-2019.

[97] J.-M. Biannic, L. Burlion, F. Demourant, G. Ferreres, G. Hardier, T. Loquen, and C. Roos. *The SMAC toolbox: A collection of libraries for systems modeling, analysis and control*. online available at http://w3.onera.fr/smac/. June 2016.

[98] V. Yakubovich. Frequency conditions for the absolute stability of control systems with several nonlinear or linear nonstationary blocks. *Avtomatika i telemekhanika*, 6:5–30, 1967.

[99] A. Megretski and A. Rantzer. System analysis via integral quadratic constraints. *IEEE Transactions on Automatic Control*, 42(6):819–830, 1997. ISSN: 0018-9286. DOI: 10.1109/9.587335.

[100] C. W. Scherer. LPV control and full block multipliers. *Automatica*, 37(3):361–375, 2001. ISSN: 0005-1098. DOI: 10.1016/S0005-1098(00)00176-X.

[101] C. Scherer. LMI relaxations in robust control. *European Journal of Control*, 12(1):3–29, 2006. ISSN: 0947-3580. DOI: 10.3166/ejc.12.3-29.

[102] U. Jönsson. Robustness analysis of uncertain and nonlinear systems. eng. PhD thesis. Department of Automatic Control, Lund Institute of Technology (LTH), 1996, 183.

[103] A. Helmersson. An IQC-based stability criterion for systems with slowly varying parameters. *IFAC Proceedings Volumes*, 32(2):3183–3188, 1999. 14th IFAC World Congress 1999, Beijing, China, 5-9 July. ISSN: 1474-6670. DOI: 10.1016/S1474-6670(17)56543-X.

[104] H. Köroğlu and C. W. Scherer. Robust stability analysis against perturbations of smoothly time-varying parameters. In: *45th IEEE Conference on Decision and Control*. San Diego, CA, USA, Dec. 2006, 2895–2900. DOI: 10.1109/CDC.2006.376805.

[105] H. Köroğlu and C. W. Scherer. Robust performance analysis for structured linear time-varying perturbations with bounded rates-of-variation. *IEEE Transactions on Automatic Control*, 52(2):197–211, Feb. 2007. ISSN: 1558-2523. DOI: 10.1109/TAC.2006.890482.

[106] C.-Y. Kao and A. Rantzer. Stability analysis of systems with uncertain time-varying delays. *Automatica*, 43(6):959–970, 2007.

[107] J. Veenman and C. W. Scherer. IQC-synthesis with general dynamic multipliers. *International Journal of Robust and Nonlinear Control*, 24(17):3027–3056, 2014. DOI: 10.1002/rnc.3042.

[108] H. Pfifer and P. Seiler. Robustness analysis of linear parameter varying systems using integral quadratic constraints. *International Journal of Robust and Nonlinear Control*, 25(15):2843–2864, 2015. DOI: 10.1002/rnc.3240.

[109] H. Pfifer and P. Seiler. Less conservative robustness analysis of linear parameter varying systems using integral quadratic constraints. *International Journal of Robust and Nonlinear Control*, 26(16):3580–3594, 2016. DOI: 10.1002/rnc.3521.

[110] J. Veenman, C. W. Scherer, and H. Köroğlu. Robust stability and performance analysis based on Integral Quadratic Constraints. *European Journal of Control*, 31:1–32, 2016. ISSN: 0947-3580. DOI: 10.1016/j.ejcon.2016.04.004.

[111] P. Seiler. Stability analysis with dissipation inequalities and integral quadratic constraints. *IEEE Transactions on Automatic Control*, 60(6):1704–1709, June 2015. ISSN: 1558-2523. DOI: 10.1109/TAC.2014.2361004.

[112] C. W. Scherer, H. Köroğlu, and M. Farhood. LPVMAD–The IQC analysis tool. *Tech. Report, TU Delft for ESA*, 2008.

[113] A. Hjartarson, P. Seiler, and A. Packard. LPVTools: a toolbox for modeling, analysis, and synthesis of parameter varying control systems. *IFAC-PapersOnLine*, 48(26):139–145, 2015. 1st IFAC Workshop on Linear Parameter Varying Systems LPVS 2015, Grenoble, FRANCE. ISSN: 2405-8963. DOI: 10.1016/j.ifacol.2015.11.127.

[114] T. Iwasaki and G. Shibata. LPV system analysis via quadratic separator for uncertain implicit systems. *IEEE Transactions on Automatic Control*, 46(8):1195–1208, Aug. 2001. ISSN: 0018-9286. DOI: 10.1109/9.940924.

[115] D. Luenberger. Dynamic equations in descriptor form. *IEEE Transactions on Automatic Control*, 22(3):312–321, June 1977. ISSN: 1558-2523. DOI: 10.1109/TAC.1977.1101502.

[116] H.-S. Wang, C.-F. Yung, and F.-R. Chang. Bounded real lemma and H∞ control for descriptor systems. In: *Proceedings of the 1997 American Control Conference (Cat. No.97CH36041)*. Vol. 3. June 1997, 2115–2119 vol.3. DOI: 10.1109/ACC.1997.611064.

[117] K. Takaba, N. Morihira, and T. Katayama. A generalized Lyapunov theorem for descriptor system. *Systems & Control Letters*, 24(1):49–51, 1995. ISSN: 0167-6911. DOI: 10.1016/0167-6911(94)00041-S.

[118] T. Asai and S. Hara. Robust stabilization of the uncertain linear systems based on descriptor form representation. *Transactions of the Society of Instrument and Control Engineers*, 31(8):1037–1046, 1995. DOI: 10.9746/sicetr1965.31.1037.

[119] I. Masubuchi, Y. Kamitane, A. Ohara, and N. Suda. H∞ control for descriptor systems: a matrix inequalities approach. *Automatica*, 33(4):669–673, 1997. ISSN: 0005-1098. DOI: 10.1016/S0005-1098(96)00193-8.

[120] K. Takaba. Robust H2 control of descriptor system with time-varying uncertainty. *International Journal of Control*, 71(4):559–579, 1998. DOI: 10.1080/002071798221678.

[121] A. Bouali, M. Yagoubi, and P. Chevrel. New LMI-based conditions for stability, H∞ performance analysis and state-feedback control of rational LPV systems. In: *2007 European Control Conference (ECC)*. July 2007, 5411–5417. DOI: 10.23919/ECC.2007.7068588.

[122] P. Bliman, R. C. L. F. Oliveira, V. F. Montagner, and P. L. D. Peres. Existence of homogeneous polynomial solutions for parameter-dependent linear matrix inequalities with parameters in the simplex. In: *45th IEEE Conference on Decision and Control*. San Diego, CA, USA, Dec. 2006, 1486–1491. DOI: 10.1109/CDC.2006.377429.

[123] I. Masubuchi, T. Akiyama, and M. Saeki. Synthesis of output feedback gain-scheduling controllers based on descriptor LPV system representation. In: *42th IEEE Conference on Decision and Control*. Vol. 6. Maui, HI, USA, Dec. 2003, 6115–6120 Vol.6. DOI: 10.1109/CDC.2003.1272243.

[124] I. Masubuchi. Dissipativity inequalities for continuous-time descriptor systems with applications to synthesis of control gains. *Systems & Control Letters*, 55(2):158–164, 2006. ISSN: 0167-6911. DOI: 10.1016/j.sysconle.2005.06.007.

[125] I. Masubuchi and A. Suzuki. Gain-scheduled controller synthesis based on new LMIs for dissipativity of descriptor LPV systems. *IFAC Proceedings Volumes*, 41(2):9993–9998, 2008. 17th IFAC World Congress. ISSN: 1474-6670. DOI: 10.3182/20080706-5-KR-1001.01691.

[126] I. Masubuchi. An exact solution to parameter-dependent convex differential inequalities. In: *1999 European Control Conference (ECC)*. Aug. 1999, 1043–1048. DOI: 10.23919/ECC.1999.7099445.

[127] I. Masubuchi. On numerical solution of parameter-dependent convex differential inequalities. In: *38th IEEE Conference on Decision and Control*. Vol. 1. Phoenix, AZ, USA, Dec. 1999, 305–309 vol.1. DOI: 10.1109/CDC.1999.832793.

[128] J. Lasserre. Global optimization with polynomials and the problem of moments. *SIAM Journal on Optimization*, 11(3):796–817, 2001. DOI: 10.1137/S1052623400366802.

[129] C. W. Scherer and C. W. J. Hol. Matrix sum-of-squares relaxations for robust semi-definite programs. *Mathematical Programming*, 107(1):189–211, June 2006. ISSN: 1436-4646. DOI: 10.1007/s10107-005-0684-2.

[130] P. Seiler and G. J. Balas. Quasiconvex sum-of-squares programming. In: *49th IEEE Conference on Decision and Control*. Atalanta, USA, Dec. 2010, 3337–3342. DOI: 10.1109/CDC.2010.5717672.

[131] G. Chesi. LMI techniques for optimization over polynomials in control: A survey. *IEEE Transactions on Automatic Control*, 55(11):2500–2510, Nov. 2010. ISSN: 0018-9286. DOI: 10.1109/TAC.2010.2046926.

[132] G. Chesi. *Domain of attraction: analysis and control via SOS programming*. Vol. 415. Springer Science & Business Media, 2011. DOI: 10.1007/978-0-85729-959-8.

[133] G. Chesi. Rational Lyapunov functions for estimating and controlling the robust domain of attraction. *Automatica*, 49(4):1051–1057, 2013.

[134] G. Valmorbida and J. Anderson. Region of attraction estimation using invariant sets and rational Lyapunov functions. *Automatica*, 75:37–45, 2017. ISSN: 0005-1098. DOI: 10.1016/j.automatica.2016.09.003.

[135] D. Han and M. Althoff. On estimating the robust domain of attraction for uncertain non-polynomial systems: an LMI approach. In: *2016 IEEE 55th Conference on Decision and Control*. cited By 0. 2016, 2176–2183. DOI: 10.1109/CDC.2016.7798586.

[136] G. Chesi, A. Garulli, A. Tesi, and A. Vicino. Polynomially parameter-dependent Lyapunov functions for robust stability of polytopic systems: an LMI approach. *IEEE Transactions on Automatic Control*, 50(3):365–370, Mar. 2005. ISSN: 0018-9286. DOI: 10.1109/TAC.2005.843848.

[137] R. C. L. F. Oliveira and P. L. D. Peres. Parameter-dependent LMIs in robust analysis: characterization of homogeneous polynomially parameter-dependent solutions via LMI relaxations. *IEEE Transactions on Automatic Control*, 52(7):1334–1340, July 2007. ISSN: 0018-9286. DOI: 10.1109/TAC.2007.900848.

[138] G. Chesi. Robust stability of time-varying uncertain systems with rational dependence on the uncertainty. *IEEE Transactions on Automatic Control*, 55(10):2353–2357, Oct. 2010. ISSN: 0018-9286. DOI: 10.1109/TAC.2010.2053470.

[139] G. Chesi. Sufficient and necessary LMI conditions for robust stability of rationally time-varying uncertain systems. *IEEE Transactions on Automatic Control*, 58(6):1546–1551, June 2013. ISSN: 0018-9286. DOI: 10.1109/TAC.2012.2229840.

[140] P. A. Parrilo. Structured semidefinite programs and semialgebraic geometry methods in robustness and optimization. PhD thesis. California Institute of Technology, 2000.

[141] F. Wu and S. Prajna. SOS-based solution approach to polynomial LPV system analysis and synthesis problems. *International Journal of Control*, 78(8):600–611, 2005. DOI: 10.1080/00207170500114865.

[142] E. Summers, A. Chakraborty, W. Tan, U. Topcu, P. Seiler, G. Balas, and A. Packard. Quantitative local $\mathcal{L}_2$-gain and reachability analysis for nonlinear systems. *International Journal of Robust and Nonlinear Control*, 23(10):1115–1135, 2013.

[143] J. Löfberg. Pre- and post-processing sum-of-squares programs in practice. *IEEE Transactions on Automatic Control*, 54(5):1007–1011, May 2009. ISSN: 0018-9286. DOI: 10.1109/TAC.2009.2017144.

[144] A. Papachristodoulou, J. Anderson, G. Valmorbida, S. Prajna, P. Seiler, and P. A. Parrilo. *SOSTOOLS: sum of squares optimization toolbox for MATLAB*. Available from http://www.eng.ox.ac.uk/control/sostools. http://arxiv.org/abs/1310.4716, 2013.

[145] S. Yang and F. Wu. Control of polynomial nonlinear systems using higher degree Lyapunov functions. *Journal of Dynamic Systems, Measurement and Control, Transactions of the ASME*, 136(3), 2014. cited By 4. DOI: 10.1115/1.4026172.

[146] M. Vatani and M. Hovd. Lyapunov stability analysis and controller design for rational polynomial systems using sum of squares programming. In: *56nd IEEE Conference on Decision and Control*. Melbourne, Australia, Dec. 2017, 4266–4271. DOI: 10.1109/CDC.2017.8264288.

[147] S. Pirkelmann, D. Angeli, and L. Grüne. *Approximate computation of storage functions for discrete-time systems using sum-of-squares techniques*. Major parts of this work were conducted during a visit of the first author at Imperial College in London, UK. Bayreuth, Jan. 2019. URL: https://eref.uni-bayreuth.de/47444/.

[148] D. S. De Madeira and J. Adamy. Asymptotic stabilization of nonlinear systems using passivity indices. In: *2016 American Control Conference (ACC)*. July 2016, 1154–1159. DOI: 10.1109/ACC.2016.7525073.

[149] D. S. De Madeira. Contributions to passivity theory and dissipative control synthesis. PhD thesis. Technische Universität, 2018.

[150] D. S. De Madeira and J. Adamy. Output feedback control of rational nonlinear systems: a new approach based on passivity indices. In: *2016 IEEE 55th Conference on Decision and Control (CDC)*. Las Vegas, NV, USA, Dec. 2016, 3880–3885. DOI: 10.1109/CDC.2016.7798855.

[151] D. Angeli, R. Amrit, and J. B. Rawlings. On average performance and stability of economic model predictive control. *IEEE Transactions on Automatic Control*, 57(7):1615–1626, July 2012. ISSN: 0018-9286. DOI: 10.1109/TAC.2011.2179349.

[152] L. Grüne and M. Stieler. Asymptotic stability and transient optimality of economic MPC without terminal conditions. *Journal of Process Control*, 24(8):1187–1196, 2014. Economic nonlinear model predictive control. ISSN: 0959-1524. DOI: 10.1016/j.jprocont.2014.05.003.

[153] G. Stengle. A nullstellensatz and a positivstellensatz in semialgebraic geometry. *Mathematische Annalen*, 207(2):87–97, June 1974. ISSN: 1432-1807. DOI: 10.1007/BF01362149.

[154] D. F. Coutinho, M. Fu, and A. Trofino. Regional stability and performance analysis for a class of nonlinear discrete-time systems. In: *41th IEEE Conference on Decision and Control*. Vol. 3. Las Vegas, NV, USA, 2002, 2675–2680.

[155] D. F. Coutinho, A. Trofino, and M. Fu. Nonlinear H-infinity control: an LMI approach. *IFAC Proceedings Volumes*, 35(1):91–96, 2002. 15$^{\text{th}}$ IFAC World Congress. ISSN: 1474-6670. DOI: 10.3182/20020721-6-ES-1901.00350.

[156] D. F. Coutinho, M. Fu, A. Trofino, and P. Danès. L2-gain analysis and control of uncertain nonlinear systems with bounded disturbance inputs. *International Journal of Robust and Nonlinear Control*, 18(1):88–110, 2008. DOI: 10.1002/rnc.1207.

[157] D. F. Coutinho, C. E. de Souza, and A. Trofino. Stability analysis of implicit polynomial systems. *IEEE Transactions on Automatic Control*, 54(5):1012–1018, 2009. cited By 20. DOI: 10.1109/TAC.2009.2017145.

[158] D. Peaucelle and Y. Ebihara. Robust stability analysis of discrete-time systems with parametric and switching uncertainties. *IFAC Proceedings Volumes*, 47(3):724–729, 2014. 19th IFAC World Congress. ISSN: 1474-6670. DOI: 10.3182/20140824-6-ZA-1003.00282.

[159] Y. Ebihara, D. Peaucelle, and D. Arzelier. *S-variable approach to LMI-based robust control*. Springer, 2015.

[160] M. C. de Oliveira and R. E. Skelton. Perspectives in robust control. In: ed. by S. O. R. Moheimani. Springer, 2001. Chap. Stability tests for constrained linear systems, 241–257.

[161] B. Bhiri, C. Delatre, M. Zasadzinski, and K. Abderrahim. Finite-time stability via polynomial Lyapunov function of nonlinear quadratic systems. In: *American Control Conference (ACC)*. Vol. 2016-July. cited By 0. 2016, 1142–1147. DOI: 10.1109/ACC.2016.7525069.

[162] U. Topcu. Quantitative local analysis of nonlinear systems. PhD thesis. University Of California, Berkeley, 2008.

[163] J.-F. Magni. *Linear fractional representation toolbox (version 2.0) for use with Matlab*. 2006.

[164] J. Löfberg. YALMIP : a toolbox for modeling and optimization in MATLAB. In: *Proceedings of the CACSD Conference*. Taipei, Taiwan, 2004. DOI: 10.1109/CACSD.2004.1393890. URL: http://users.isy.liu.se/johanl/yalmip.

[165] MOSEK ApS. *The MOSEK optimization toolbox for MATLAB manual. version 7.1 (revision 28)*. 2015. URL: http://docs.mosek.com.

[166] J. F. Sturm. Using SeDuMi 1.02, a Matlab toolbox for optimization over symmetric cones. *Optimization Methods and Software*, 11(1-4):625–653, Jan. 1, 1999. DOI: 10.1080/10556789908805766.

[167] Y. Labit, D. Peaucelle, and D. Henrion. SEDUMI INTERFACE 1.02: a tool for solving LMI problems with SEDUMI. In: *Proceedings, IEEE International Symposium on Computer Aided Control System Design*. Jan. 1, 2002, 272–277.

[168] W.-S. Lu. SeDuMi: remarks and examples. Mar. 13, 2012.

[169] K. C. Toh, M. J. Todd, and R. H. Tütüncü. SDPT3 – A Matlab software package for semidefinite programming, Version 1.3. *Optimization Methods and Software*, 11(1-4):545–581, 1999. DOI: 10.1080/10556789908805762.

[170] L. F. Shampine and M. W. Reichelt. The MATLAB ODE suite. *SIAM Journal on Scientific Computing*, 18(1):1–22, Jan. 1997. DOI: 10.1137/s1064827594276424.

[171] H. Kajiwara, P. Apkarian, and P. Gahinet. Wide-range stabilization of an arm-driven inverted pendulum using linear parameter-varying techniques. In: *Guidance, Navigation, and Control Conference and Exhibit*. American Institute of Aeronautics and Astronautics, Aug. 1998. DOI: 10.2514/6.1998-4503.

[172] K. Ling, P Falugi, J. Maciejowski, and L Chisci. Robust predictive control of the Furuta pendulum. In: *IFAC 15th Triennial World Congress, Barcelona, Spain*. 2002.

[173] D. Angeli. Almost global stabilization of the inverted pendulum via continuous state feedback. *Automatica*, 37(7):1103–1108, 2001. ISSN: 0005-1098. DOI: 10.1016/S0005-1098(01)00064-4.

[174] J. Acosta, R. Ortega, A. Astolfi, and I. Sarras. A constructive solution for stabilization via immersion and invariance: The cart and pendulum system. *Automatica*, 44(9):2352–2357, 2008. ISSN: 0005-1098. DOI: 10.1016/j.automatica.2008.01.006.

[175] I. Sarras, H. B. Siguerdidjane, and R. Ortega. Stabilization of the experimental cart-pendulum system with proven domain of attraction. *European Journal of Control*, 4:329–340, 2010. DOI: 10.3166/ejc.16.329-340.

[176] N. J. Mathew, K. K. Rao, and N. Sivakumaran. Swing up and stabilization control of a rotary inverted pendulum. *IFAC Proceedings Volumes*, 46(32):654–659, 2013. 10th IFAC International Symposium on Dynamics and Control of Process Systems. ISSN: 1474-6670. DOI: 10.3182/20131218-3-IN-2045.00128.

[177] M. Magdy, A. E. Marhomy], and M. A. Attia. Modeling of inverted pendulum system with gravitational search algorithm optimized controller. *Ain Shams Engineering Journal*, 10(1):129–149, 2019. ISSN: 2090-4479. DOI: 10.1016/j.asej.2018.11.001.

[178] H. Gritli and S. Belghith. Robust feedback control of the underactuated inertia wheel inverted pendulum under parametric uncertainties and subject to external disturbances: LMI formulation. *Journal of the Franklin Institute*, 355(18):9150–9191, 2018. Special Issue on Control and Signal Processing in Mechatronic Systems. ISSN: 0016-0032. DOI: 10.1016/j.jfranklin.2017.01.035.

[179] M. Ciężkowski. Method for determination of interaction between a two-wheeled self-balancing vehicle and its rider. *Mechanics*, 22(5), Nov. 2016. DOI: 10.5755/j01.mech.22.5.13315.

[180] R. Ferrante. A robust control approach for rocket landing. MSc thesis. Artificial Intelligence School of Informatics University of Edinburgh, 2017.

[181] M. A. Savageau and E. O. Voit. Recasting nonlinear differential equations as S-systems: A canonical nonlinear form. *Mathematical Biosciences*, 87(1):83–115, 1987. ISSN: 0025-5564. DOI: 10.1016/0025-5564(87)90035-6.

[182] A. Papachristodoulou and S. Prajna. Analysis of non-polynomial systems using the sum of squares decomposition. In: *Positive Polynomials in Control*. Springer Berlin Heidelberg, Aug. 2005, 23–43. DOI: 10.1007/10997703_2.

[183] D. Qian and J. Yi. *Hierarchical sliding mode control for under-actuated cranes*. Springer Berlin Heidelberg, 2015. DOI: 10.1007/978-3-662-48417-3.

[184] G. Bastin and D. Dochain. *On-line estimation and adaptive control of bioreactors*. 1990.

[185] G. Szederkényi, N. R. Kristensen, K. M. Hangos, and S. B. Jorgensen. Nonlinear analysis and control of a continuous fermentation process. *Computers and Chemical Engineering*, 26:659–670, 2002. DOI: 10.1016/S0098-1354(01)00793-1.

[186] T. Kailath. *Linear systems*. Information and System Sciences Series. Prentice-Hall, 1980. ISBN: 9780135369616.

[187] K. Zhou, J. C. Doyle, K. Glover, et al. *Robust and optimal control*. Vol. 40. Prentice hall New Jersey, 1996.

[188] J. von zur Gathen. Irreducibility of multivariate polynomials. *Journal of Computer and System Sciences*, 31(2):225–264, 1985. ISSN: 0022-0000. DOI: 10.1016/0022-0000(85)90043-1.

[189] A. Varga and G. Looye. Symbolic and numerical software tools for LFT-based low order uncertainty modeling. In: *Computer Aided Control System Design, 1999. Proceedings of the 1999 IEEE International Symposium on*. IEEE. 1999, 1–6.

[190] G. H. Golub and C. F. van Loan. *Matrix computations 4th ed.* 4th. Baltimore, MD, USA: Johns Hopkins University Press, 2013. ISBN: 1421407949 9781421407944.

[191] T. Iwasaki and S. Hara. Generalized KYP lemma: unified frequency domain inequalities with design applications. *IEEE Transactions on Automatic Control*, 50(1):41–59, 2005.

[192] I. Masubuchi. Matrix inequality conditions for dissipativity of continuous-time descriptor systems and its application to synthesis of control gains. In: vol. 16. 2005, 272–277.

[193] A. Rantzer. On the Kalman-Yakubovich-Popov lemma. *Systems & Control Letters*, 28(1):7–10, 1996. ISSN: 0167-6911. DOI: 10.1016/0167-6911(95)00063-1.

[194] R. Wallin, C.-Y. Kao, and A. Hansson. A cutting plane method for solving KYP-SDPs. *Automatica*, 44(2):418–429, 2008. ISSN: 0005-1098. DOI: 10.1016/j.automatica.2007.06.026.

[195] B. van der Pol. On relaxation-oscillations. *The London, Edinburgh, and Dublin Philosophical Magazine and Journal of Science*, 2(11):978–992, 1926. DOI: 10.1080/14786442608564127.

[196] W. Adkins. *Algebra: An approach via module theory*. New York, NY: Springer New York, 1992. ISBN: 9781461269489.

[197] Q. Liu, H. S. Abbas, J. M. Velni, and H. Werner. Distributed controller design for LPV/LFT distributed systems in input-output form. *IFAC-PapersOnLine*, 50(1):11409–11414, 2017. 20th IFAC World Congress. ISSN: 2405-8963. DOI: 10.1016/j.ifacol.2017.08.1803.

[198] G. Chesi. Estimating the domain of attraction for uncertain polynomial systems. *Automatica*, 40(11):1981–1986, 2004. cited By 65. DOI: 10.1016/j.automatica.2004.06.014.

[199] P. Grinfeld. *Introduction to tensor analysis and the calculus of moving surfaces*. Springer-Verlag New York, 2013. ISBN: 978-1-4939-5505-3. DOI: 10.1007/978-1-4614-7867-6.

[200] N. Qian. On the momentum term in gradient descent learning algorithms. *Neural networks*, 12(1):145–151, 1998.

[201] Z. Xu, Q. Song, and D. Wang. Recurrent neural tracking control based on multivariable robust adaptive gradient-descent training algorithm. *Neural Computing and Applications*, 21(7):1745–1755, 2012. cited By 3. DOI: 10.1007/s00521-011-0618-2.

[202] F. Moon and P. Holmes. A magnetoelastic strange attractor. *Journal of Sound and Vibration*, 65(2):275–296, 1979. ISSN: 0022-460X. DOI: 10.1016/0022-460X(79)90520-0.

[203] M. J. Brennan and I. Kovacic. Examples of physical systems described by the Duffing equation. *The Duffing Equation: Nonlinear Oscillators and their Behaviour (eds. I. Kovacic and MJ Brennan), Wiley, ISBN*, 830182507:25–53, 2011.

[204] S. Lenci and G. Rega. Forced harmonic vibration in a Duffing oscillator with negative linear stiffness and linear viscous damping. *The Duffing Equation: Nonlinear Oscillators and their Behaviour (eds. I. Kovacic and MJ Brennan), Wiley, ISBN*, 830182507:219–276, 2011.

[205] T. Berge, J.-S. Lubuma, G. Moremedi, N. Morris, and R. Kondera-Shava. A simple mathematical model for Ebola in Africa. *Journal of Biological Dynamics*, 11(1):42–74, 2017. DOI: 10.1080/17513758.2016.1229817.

[206] P. Polcz. *Induced $\mathcal{L}_2$-gain analysis of LPV systems*. GitHub repository, https://github.com/ppolcz/LPV_L2. 2020.

[207] J.-F. Magni. Computation of the kernel of linear fractional representations. In: *42th IEEE Conference on Decision and Control*. Vol. 2. Maui, HI, USA, June 2003, 1058–1063 vol.2. DOI: 10.1109/CCA.2003.1223157.

[208] http://polcz.itk.ppke.hu/files/results/CDC-2019-Ex1. [Online; accessed 20-March-2019]. 2019.